Mechanisms of hemolysin A Type 1 secretion in *Escherichia coli*

Inaugural-Dissertation

zur Erlangung des Doktorgrades
der Mathematisch-Naturwissenschaftlichen Fakultät
der Heinrich-Heine-Universität Düsseldorf

vorgelegt von

Michael Hubert Horst Lenders

aus Düsseldorf

Düsseldorf, Dezember 2015

aus dem Institut für Biochemie
der Heinrich-Heine-Universität Düsseldorf

Gedruckt mit der Genehmigung der
Mathematisch-Naturwissenschaftlichen Fakultät der
Heinrich-Heine-Universität Düsseldorf

Referent: Prof. Dr. Lutz Schmitt
Koreferent: Prof. Dr. Karl-Erich Jaeger

Tag der mündlichen Prüfung: 16.12.2015

Für meine Familie

Zusammenfassung

Eine der essentiellen Nanomaschinerien in Gram-negativen Bakterien sind die Typ I Sekretionssysteme (T1SS). Sie sekretieren ein breites Spektrum an Substraten aus dem Cytoplasma, über die innere und äußere Membran, direkt in den extrazellulären Raum. Der Transportprozess erfolgt ungefalten und in einen Schritt ohne ein periplasmatisches Intermediat. Die Vielfalt der sekretierten Proteine reicht von 78 bis 8682 Aminosäuren in der Görße und umfasst Hämophore, Lipasen, Hüllproteine, Nodulations- und Adhäsionsproteine sowie Toxine. Allen Substraten gemein ist das C-terminale Sekretionssignal, welches weder während noch nach der Sekretion abgeschnitten wird. Eines der am besten charakterisierten T1SS Substrate ist das Zellen-lysierende Toxin Hämolysin A (HlyA). HlyA gehört zu der *repeats in toxin* (RTX) Proteinfamilie. Sein Sekretionssystem besteht aus dem äußeren Membranprotein (OMP) TolC, das eine Pore durch die äußere Membran bildet, dem ABC-Transporter Hämolysin B (HlyB) in der inneren Membran, der den Transportprozess antreibt und das Substrat erkennt, und dem Membranfusionsprotein (MFP) Hämolysin D (HlyD), das TolC und HlyB miteinander verbindet und den periplasmatischen Raum überbrückt. Zusammen bilden diese Proteine das HlyA T1SS.

Während dieser Doktorarbeit wurde die Direktionalität und die Rolle des Sekretionssignals des HlyA Transportes charakterisiert. Die Fusion des gesteigerten grün fluoreszierenden Proteins (eGFP) an den N-Terminus von HlyA bzw. HlyAc (C-terminale 218 Aminosäuren von HlyA) resultierte in einer Verstopfung des gesamten HlyA T1SS. Markierungen der Termini und Fluoreszenzmikroskopie bestätigten, dass der C-Terminus als erstes an die Zelloberfläche gelangt. Ferner legten Deletionen des Sekretionssignals nahe, dass das Sekretionssignal essentiell für die Einführung des Substrates in den Translokator ist. Außerden erlaubten die verstopfen und markierten Transporter die Quantifizierung der aktiven HlyA T1SS pro Bakterienzelle. Dadurch konnte die Sekretionsrate bezogen auf sekretierte Aminosäuren pro Sekunde und Sekretionssystem quantifiziert werden. Die Sekretionsrate ist nicht beeinflusst von der Proteinlänge, der Anzahl an Glycin-reichen Wiederholungen und der extrazellulären Kalziumkonzentration. Zusätzlich konnten HlyB Mutanten und die Fusionsproteine zeigen, dass die ATP-Hydrolyse essential für das Einfädeln des Substrates in das HlyA T1SS ist.

Abstract

One of the most essential nanomachineries in Gram-negative bacteria are the Type I secretion system (T1SS). They secrete a broad range of substrates from the cytoplasm across the inner and outer membrane directly into the extracellular space. The transport process occur unfolded in one step without any periplasmic intermediate. The variety of secreted proteins range in size from 78 to 8682 amino acids and contain hemophores, lipases, S-layer proteins, nodulation and adhesion factors as well as toxins. All substrate in common is the C-terminal secretion signal which is not cleaved during or after secretion. One of the best characterized T1SS substrates is the cell lysing toxin hemolysin A (HlyA). HlyA belongs to the repeats in toxin (RTX) protein family. Its secretion system consists of the outer membrane protein (OMP) TolC that builds a pore through the outer membrane, the inner membrane ABC transporter hemolysin B (HlyB) that energizes the transport process and recognizes the substrate and the membrane fusion protein (MFP) hemolysin D (HlyD) that connects TolC and HlyB and bridges the periplasmic space. Together these proteins build up the fully assembled HlyA T1SS.

During this doctoral research, the role of the secretion signal and the directionality of the HlyA transport was characterized. An enhanced Green Fluorescence Protein (eGFP) fusion to the N-terminus of HlyA respectively HlyAc (C-terminal 218 amino acids of HlyA) results in stalling of the HlyA T1SS. Different labeling of the termini and fluorescence microscopy confirm that the C-terminus appears first at the cell surface. Further, secretion signal deletions of this fusions indicated that the secretin signal is essential for threading the substrate inside the translocator.

Moreover, stalled and labeled transporters allow the quantification of active HlyA T1SS per bacterial cell. As a consequence, the rate of secreted substrate amino acids per second and secretion system can be quantified. The secretion rate is unaffected by the length of the protein, the amount of glycine rich repeats and the extracellular calcium concentration.

Additionally, fluorescence microscopy with HlyB mutant and the fusion proteins determines that ATP hydrolyzes is essential for substrate threading into the HlyA T1SS as well.

Contents

1. Introduction

1.1. Protein-mediated transport

Eukaryotic, prokaryotic and archaeal cells are surrounded by a membrane that separates the cell interior form the extracellular environment. Bacterial cell membranes are typically 6 to 10 nm thick and are impermeable for ions and less permeable for hydrophilic molecules [Singer and Nicolson, 1972]. Transport of essential nutrients, ions or small hydrophilic molecules like sugars or peptides across the membrane is highly regulated and controlled. Embedded in the cellular membrane are membrane proteins that enable the transport of ionic and hydrophilic substances across the membrane in both directions. They allow passive diffusion across the membrane by building a hydrophilic channel that allow specific substrate passage along their concentration gradient (membrane channels) [Gouaux and Mackinnon, 2005]. Membrane transporters catalyze transport against a concentration gradient. This active transport process can energized by consumption of energy (primary transport) or by coupling to transport movement of a second substrate along a concentration gradient (secondary transport). Energy can provided by light or ATP hydrolysis [Boyer, 1997, Lanyi, 2004]. Further, the passage of substrates across the cell membrane is highly controlled. In Gram-negative bacteria, transport of secretory proteins without influencing the protein structure or function is mediated by the general secretory (Sec) pathway, by the twin arginine translocation (Tat) pathway or by a broad range of secretion systems (see Chapter 1.2) [Wickner et al., 1991, Berks et al., 2005, Osborne et al., 2005].

1.2. Secretion systems in Gram-negative bacteria

Gram-negative bacteria have a broad range of nanomachineries for substrate secretion into the extracellular space respectively the into a target cell [Costa et al., 2015]. Substrates of the systems are small molecules, proteins and deoxyribonucleic acid (DNA). They can have tasks in adhesion, pathogenicity, adaption or in survival. Depending on the secretion system, the substrates remain associated with the outer membrane (OM),

are released in the extracellular space or injected into a target cell [Costa et al., 2015].

These complex systems span both membranes or only the OM. Nanomachineries spanning both membranes are the Type 1-4 and 6 secretion system whereas Type V secretion system (T5SS) span the OM (see Figure 1.1) [Costa et al., 2015]. The secretion process itself occurs in one- or two-steps. In case of an one-step mechanism, substrates are secreted from the cytoplasm directly into the extracellular space respectively into the target cell [Costa et al., 2015]. Type I secretion system (T1SS), T3SS, T4SS and T6SS use this kind of mechanism. A two-step mechanism, like for the double membrane spanning T2SS and for the OM spanning T5SS, transports the substrates from the periplasmic space in the extracellular space respectively into the target cell [Costa et al., 2015]. In a first step, these substrates are translocated by the Sec or the Tat pathway into the periplasm [Costa et al., 2015]. Substrate secretion occurs unfolded or partially folded in most of the systems. T2SS and T6SS can secret completely or partially folded substrates [Costa et al., 2015]. Activity of the secretion systems is highly regulated. It is proposed that the secretion activation of the secretion system is initialized by target cell receptors via adhesion [Gerlach and Hensel, 2007].

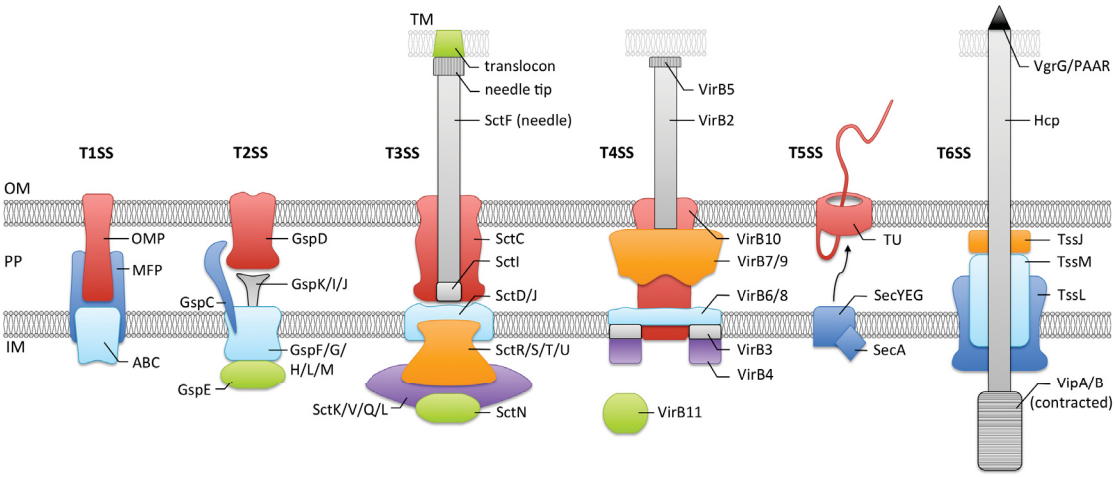

Figure 1.1.: **Structural organization of the secretion systems of Gram-negative bacteria**
Figure is taken and modified from Chapter 3.2.

1.2.1. Type I secretion system (T1SS)

T1SS transport a broad range of substrates that varies in size and function. Substrates size can vary greatly in size between 78 (uncharacterized protein from *Sinorhizobium*

meliloti) and 8682 amino acids [Delepelaire, 2004]. Substrates are, for example, the 188 amino acid hemophore HasA from *Serratia marcescens*, the 8682 amino acids adhesion factor LapA from *Pseudomonas fluorescens* or the 1024 amino acid pore forming toxin hemolysin A (HlyA) from *Escherichia coli* [Arnoux et al., 1999, Hinsa et al., 2003, Delepelaire, 2004]. resistance-nodulation-division (RND) efflux pumps like the Acr system from *Escherichia coli* [Du et al., 2014] are close related to the T1SS. They transport small molecules, like antibacterial compounds for antibiotic resistance mechanism [Piddock, 2006]. RND pumps consists of an inner membrane (IM) component, a periplasmic adapter protein that is similar to membrane fusion protein (MFP) of T1SS and the outer membrane protein (OMP) TolC [Du et al., 2014, Costa et al., 2015]. They form together a continuous tunnel across both membranes with a length of approximately 320 Å [Du et al., 2014]. In comparison to the transport energized by ATP hydrolysis, the energy for the transport process of RND efflux pumps is generated by proton transport [Costa et al., 2015]. Substrate binding to the IM components induces the complex assembly whereby the substrate is transported from the periplasm or the IM leaflet to the MFP cavity. Together with recruited TolC, the translocator allow the substrate release from the cavity into the extracellular space [Costa et al., 2015]. Compared to RND efflux pumps, the IM component of T1SS consists of an ATP binding cassette (ABC) transporter. ABC transporter of T1SS can harbor an additional N-terminal domain. This domain could be a C39 protease domain or a C39-like domain (CLD). The domains are involved in substrate recognition (see Chapter 1.3.1) [Kanonenberg et al., 2013, Costa et al., 2015]. Together with a MFP and the OMP, they form a continuous channel for substrate translocation. ATP hydrolyzes is energizing the secretion [Thanabalu et al., 1998].

1.2.2. Type II secretion system (T2SS)

T2SS transport a diverse number of hydrolyzing enzyme and toxins [Nivaskumar and Francetic, 2014]. The system consists of 12-15 different proteins and this proteins are called General secretion pathway proteins in *Escherichia coli* (see Figure 1.1) [Korotkov et al., 2012]. The proteins build a complex consisting of four different parts. Inside the cell, the cytosolic ATPase is localized, followed by the IM platform, the periplasmic 'pseudopilus' and the OM complex (reviewed in [Costa et al., 2015]) [Campos et al., 2010]. The cytosolic ATPase interacts with the proteins of the IM platform whereas these proteins are additionally interacting with the OM complex [Py et al., 2001, Gray et al., 2011, Korotkov et al., 2011, McLaughlin et al., 2012, Lu et al., 2013]. Together

they assemble to a continuous channel with a cylindrical shaped structure and an 155 Å outer diameter and a length of 200 Å [Reichow et al., 2010]. The 'pseudopilus' of the T2SS is localized in the periplasm and involved in substrate extrusion through the OM channel [Nivaskumar et al., 2014]. The substrates for T2SS are first transported unfolded by the Sec pathway or folded by the Tat pathway into the periplasmic space [Nivaskumar et al., 2014]. In the periplasm, the substrates are pushed through the pore [Costa et al., 2015]. Assembly of the 'pseudopilus' and protein translocation are energized by ATP hydrolyzes (reviewed in [Costa et al., 2015]).

1.2.3. Type III secretion system (T3SS)

Substrates of T3SS are mainly bacterial effector proteins that are transported to the cytoplasm or the plasma membrane of eukaryotic target cells [Costa et al., 2015]. The proteins promote bacterial invasion by modulation of the target cell function [Cornelis, 2006, Büttner, 2012]. An example is the *Salmonella typhimurium* T3SS [Kubori et al., 1998]. The secretion system consists of a 3.5 MDa multiprotein complex of 25 different proteins [Kubori et al., 1998]. The complex has a syringe-like shape and is organized in two subdomains, a double-membrane spanning base and a needle-like filament [Marlovits et al., 2004, Marlovits et al., 2006, Schraidt and Marlovits, 2011]. Furthermore, additional cytosolic proteins are involved in substrate recruitment, in keeping the substrate unfolded or are transport associated [Eichelberg et al., 1994, Akeda and Galán, 2005, Kawamoto et al., 2013]. The double-membrane spanning base consists of two concentric inner rings, which are inserted in the IM [Kubori et al., 1998, Yip et al., 2005, Schraidt and Marlovits, 2011]. The outer ring is localized above the inner rings and inserted in the OM. A periplasmic neck of the outer ring connecting it with the inner rings [Schraidt and Marlovits, 2011, Costa et al., 2015]. The needle-like filament has a length of 30-70 nm and a width of 10-13 nm [Marlovits et al., 2006]. The filament has an extracellular tube-like structure and consist of multiple copies of a single protein. These proteins are oriented in a right-handed helical torsion [Poyraz et al., 2010, Loquet et al., 2012]. *In vitro* experiments show that the inner diameter of the needle-like tube is roughly 25 Å which only allows transport of unfolded substrates [Loquet et al., 2012]. Cryo-electron microscopy (cryo-EM) analyses confirm the unfolded secretion of the substrate and that the base and the needle-like tube work together as a continuous channel [Radics et al., 2014]. Host-cell contact initiates substrate secretion with the N-terminus ahead [Radics et al., 2014, Costa et al., 2015]. Secretion of translocator and effector proteins proceed in a strict hierarchical and coordinated manner that is encoded in the first

100 residues of the substrate [Büttner, 2012, Galán et al., 2014]. This region is stabilized by chaperons and guided to the T3SS recognition site [Parsot et al., 2003, Costa et al., 2015]. Substrate engagement with a sorting mechanism (sorting platform) at the needle complex base results in ATP-dependent translocation [Lara-Tejero et al., 2011, Costa et al., 2015, Hu et al., 2015].

1.2.4. Type IV secretion system (T4SS)

In comparison to other secretion systems, T4SS are able to transport DNA and proteins (reviewed in [Costa et al., 2015]). T4SS are the most ubiquitous secretion systems that are found in Gram-positive, Gram-negative bacteria and in archaea [Alvarez-Martinez and Christie, 2009]. In these organisms, they are mainly involved to mediate plasmid DNA conjugation (reviewed in [Costa et al., 2015]). Furthermore, T4SS transport pathogens, transforming proteins, toxins and effector proteins [Alvarez-Martinez and Christie, 2009]. The translocation complex consist of 12 different proteins whereby six of this proteins form the scaffold and translocation apparatus [Christie et al., 2014], two form the pilus with extracellular space extension [Trokter et al., 2014], three are ATPases and energize the system by ATP hydrolysis and the last protein is a trans-glycosylases that locally degrades the peptidoglycan of the cell to allow pilus biogenesis [Trokter et al., 2014]. The T4SS can be separated into three different compartments, a core-OM complex that is connected by a central stalk with the bipartite IM complex [Low et al., 2014, Costa et al., 2015]. The core-OM complex has a two-layer structure [Fronzes et al., 2009], which (inner and outer layer; see Figure 1.1, red and orange structures) are connected by a middle platform whereby the outer layer form the OM pore [Chandran et al., 2009, Rivera-Calzada et al., 2013]. The structure of the stalk is elongated whereas the cytoplasmic site of the IM complex consists of two barrels [Low et al., 2014, Costa et al., 2015]. Only the VirB10 protein of the T4SS spans the entire cell envelope and interacts with several different compartments in the IM and OM (reviewed in [Costa et al., 2015]). Additionally, this protein acts as a signal transmitter that release ATP-driven conformational changes in the cytoplasmic ATPases to the gating of the OM channel [Cascales and Christie, 2004, Costa et al., 2015]. Extracellular tubular polymers build the T4SS pilus that establish the cell-cell contact and function as channels to transport single-stranded DNA during conjugation [Bradley, 1980, Dürrenberger et al., 1991, Costa et al., 2015].

1.2.5. Type V secretion system (T5SS)

T5SS are highly diverse secretion systems with different subgroups. In comparison to the other secretion systems, the T5SS Va subgroup belong to the 'classic' autotransporter systems and will be described in more detail [Jose et al., 1995, Desvaux et al., 2009]. Other subgroups are Vb, Vc, Vd and Ve that differs in special characteristics, such as polypeptide-transport-associated domains, oligomerization states and domain arrangements (reviewed in [Gawarzewski et al., 2013]) [Cotter et al., 2005, Clantin et al., 2007, Leo et al., 2012].

Unique feature of the Va T5SS is the fusion of the substrate with its secretion pore (called autotransporter) [Gawarzewski et al., 2013]. Typical substrates for autotransporter are virulence and adhesion factors and factors for biofilm formation [Leo et al., 2012]. The autotransporter polypeptide is first translocated unfolded by the Sec pathway from the cytoplasm into the periplasmic space. The polypeptide itself consists of a secretion domain (called 'passenger' domain, which represent the T5SS substrate) and a transmembrane domain (called 'translocator' or 'β-domain') [Leyton et al., 2012]. The secretion domain is unfolded or partly folded in the periplasm whereas the transmembrane domain inserts into the OM to build a β-barrel pore to allow secretion of the passenger domain. Energized is the secretion process by folding of the passenger domain at the pore exit. Compared to the other systems, the secretion of T5SS is ATP and proton gradient independent [Junker et al., 2009, Costa et al., 2015]. The autotransporter polypeptide is stabilized and kept unfolded by periplasmic chaperones whereas the Bam complex assists in the insertion of the transmembrane domain in the OM [Voulhoux et al., 2003, Wu et al., 2005, Hagan et al., 2010, Ieva et al., 2011, Roman-Hernandez et al., 2014, Costa et al., 2015]. The passenger domain is secreted through the OM with its C-terminus ahead [Ieva and Bernstein, 2009, Junker et al., 2009]. Depending on the function, the passenger domain remain anchored at the extracellular surface or is cleaved autocatalytically or by an additional peptidase domain and released in the environment [Costa et al., 2015]. The final step of passenger domain secretion is realized by conformational changes of the linker region between the secretion and transmembrane domain to an α-helical structure (reviewed in [Costa et al., 2015]). The exact mechanism of passenger domain secretion is not completely understood but crystal structure of some autotransporter support a hairpin-loop-mediated transport [Oomen et al., 2004, Meng et al., 2006, van den Berg, 2010, Gawarzewski et al., 2014]. Other studies implicate a direct link between β-barrel assembly of the transmembrane domain and the initiation of secretion with an active involvement of the Bam complex or an translocation and

assembly model for efficient secretion [Selkrig et al., 2012, Gruss et al., 2013, Pavlova et al., 2013, Costa et al., 2015].

1.2.6. Type VI secretion system (T6SS)

T6SS secrets toxic effector proteins into eukaryotic and prokaryotic cells. They are essential for pathogenesis and bacterial competition (reviewed in [Costa et al., 2015]). The secretion apparatus consist of 13 core and several assisting components [Zheng and Leung, 2007, Boyer et al., 2009, Costa et al., 2015]. The system is build up by two complexes, a membrane complex and a tail complex [Zoued et al., 2014]. The membrane complex contain T4SS homologous IM proteins that anchored the tail complex inside the cell envelope. The tail complex contain evolutionary related contractile bacteriophage tail components. Structures are tail sheath, an inner tube and a baseplate (reviewed in [Costa et al., 2015]). The protein VgrG form a spike in the center of the baseplate and functions as a nucleation platform for T6SS tail tube formation [Leiman et al., 2009, Basler et al., 2012, Brunet et al., 2014, Costa et al., 2015]. Time-lape fluorescence imaging of the tail sheath confirm a highly dynamic substructure that can contract rapidly, dissemble and reassemble. Length of the tail sheath can be close to the width of the cell [Basler et al., 2012]. Its outer diameter is 290 Å and the central channel is 110 Å in diameter [Kube et al., 2014]. Function of the T6SS mechanism is similar to the contraction mechanism of phage tails [Basler et al., 2012, Costa et al., 2015, Kudryashev et al., 2015]. An unknown extracellular signal induces conformational changes in the baseplate complex that results in contraction of the sheath. The inner tube, the VgrG and additional other proteins are translocated out of the cell and across the target cell membrane [Ho et al., 2014, Zoued et al., 2014]. Final contraction leads to translocation of multiple effectors into the target cell (reviewed in [Costa et al., 2015]).

1.2.7. Type VII secretion system (T7SS)

T7SS are a special secretion apparatus for virulence of mycobacteria like *Mycobacterium tuberculosis*. In comparison to Gram-negative bacteria, mycobacteria have a mycomembrane (consisting of a waxy lipid coat of mycolic acids) instead of a OM [Houben et al., 2014]. Conserved T7SS gene clusters are although found in Gram-positiv bacteria [Houben et al., 2014]. The secretion system is a 1.5 MDa protein complex whereby the core channel in the IM consists of four different proteins. One of the proteins form the central channel and an other has an ATPase cytosolic domain [Costa et al., 2015]. The translocation complex is associated with the protease MycP that is important for

substrate processing [Solomonson et al., 2013]. Further, the substrate is cytosolic associated with two other proteins, an ATPase and a protein that chaperone and guiding-like function [Houben et al., 2014, Korotkova et al., 2014]. The overall mechanism of T7SS is poorly understood and a component for OM translocation is yet unknown (reviewed in [Costa et al., 2015]).

1.2.8. Chaperone-usher pathway

Furthermore, other secretion pathways in Gram-negative bacteria are also know. The chaperone-usher pathway is used to assemble and secrete fimbriae. Fimbriae or pili are important for host cell recognition and attachment to contribute pathogenicity and biofilm formation [Wright et al., 2007, Costa et al., 2015]. Subunits of the pilus are transported unfolded by the Sec pathway into the periplasm and stabilized by periplasmic chaperones [Hultgren et al., 1991, Vetsch et al., 2004]. The chaperone-stabilized subunits are transported to the 'usher' OM protein that is essential for pilus assembly by catalyzing subunit polymerization and pilus secretion (reviewed in [Costa et al., 2015]).

1.2.9. Curli biogenesis system

The curli biogenesis system is responsible for curli biogenesis. Curli are extracellular protein fibres that are part of the functional amyloid class. They protect bacteria from hostile environment. This kind of protection is mediated by contributing to biofilm formation or by facibitating interactions with the host immune system [Olsén et al., 1989, Hammar et al., 1995, Costa et al., 2015]. Curli consists of two subunits, the major and the minor curli subunit. The major subunit is secreted unfolded by the Sec pathway into the periplasm and also unfolded across the OM. In a next step, the major curli subunit assembles into curli fibres at the extracellular surface with the help of the minor subunit that nucleates the polymerization [Hammer et al., 2012, Costa et al., 2015]. The OM secretion apparatus consists of three different proteins and build a cage with a 9 Å-diameter channel [Goyal et al., 2014]. It is assumed, that an entropy gradient is created across the membrane by the channel and leads to extrusion of the curli subunits. A similar entropy-driven transport could be observed for the chaperonins GroEL and GroES [Brinker et al., 2001, Takagi et al., 2003]. The secretion apparatus functions as an undated, non-selective, secretion channel that uses a diffusion-based, entropy-driven transport mechanism similar to that of chaperoning [Brinker et al., 2001, Takagi et al., 2003, Costa et al., 2015].

1.3. The hemolysin A (HlyA) T1SS

T1SS are one of the most prominent nanomachineries in Gram-negative bacteria. They transport a broad range of substrates ranging from small molecules to large proteins across both cell membranes. Secreted proteins could be metalloproteases, toxins, S-layer proteins, hemophores, lipases or adhesion factors [Delepelaire, 2004]. T1SSs are able to secrete these substances in one step across both membranes without any periplasmic intermediate [Schatz and Beckwith, 1990].

The T1SS itself consists of three different compartments that interact with each other to build a continuous translocator [Létoffé et al., 1996, Thanabalu et al., 1998]. The ABC transporter and the MFP are localized in the inner membrane. Together, they interact with the OMP and build a pore that spans the periplasmic space and allow transport from the cytoplasm directly into the extracellular space.

One of the most prominent substrate for Type I secretion is the RTX pore building toxin HlyA from *E. coli*. The HlyA T1SS consists of three different proteins. The IM localized dimeric ABC transporter HlyB and the MFP HlyD interacts with the OMP TolC. Together, they assemble into a multi protein complex. This translocation complex allows the recognition and secretion of HlyA (see Figure 1.1) unfolded using ATP hydrolyzes in one step across both membranes without any periplasmic intermediate.

1.3.1. The ABC transporter hemolysin B (HlyB)

One of the most essential compartments of the HlyA T1SS is the ABC transporter HlyB. HlyB consists of a N-terminal CLD, followed by a transmembrane domain (TMD) and a C-terminal localized nucleotide binding domain (NBD). The protein has a length of 707 amino acids. A functional homodimer builds the active ABC transporter (see Figure 1.2 A).

The nucleotide binding domain (NBD)

The NBD of HlyB is localized at the C-terminus between amino acids 468 and 707. Its crucial role during transport is the transformation of chemical stored energy into mechanical movement translocation [Lenders et al., 2013]. The chemical energy is provided by ATP which is hydrolyzed to ADP in presence of Mg^{2+} coordination during the transport process. ATP hydrolysis is essential for completing the HlyA transport and secretion cycle [Thanabalu et al., 1998]. The exact role of ATP hydrolysis during one secretion cycle is unknown but it is assumed that is energizing the transport process.

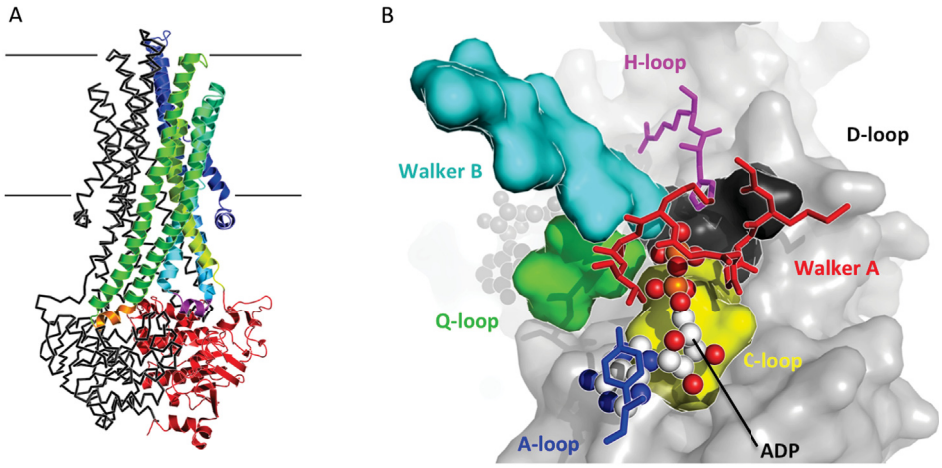

Figure 1.2.: **Spatial arrangement of an ABC exporter and structural features of the ABC exporter NBD**
(A) Structure of Sav1866 from *Staphylococcus aureus* with bound ADP (pdb file 2HYD) and for clarity with one monomer colored dark gray. The other monomer's TMD is colored in blue, cyan, yellow and green, while the corresponding NBD is colored red. Coupling helix 1 (purple helix) is thought to make contact with both NBDs during formation of the nucleotide sandwich. Coupling helix 2 (orange helix) is always domain-swapped to interact with the opposing NBD. (B) Close-up view of the gray NBD and the sandwiched ADP molecule. Directly involved conserved motifs are colored as follows: Walker A, red; Q-loop, green; H-loop, purple; Walker B, cyan; A-loop, blue; C-loop, yellow; D-loop, black. Figure is taken and modified from [Lenders et al., 2013] and highlighted in Chapter 3.1.

The primary sequence of NBDs from ABC transporters chair some highly conserved sequence motifs that are found in ABC transporters in archeae, prokaryotes and eukaryotes [Seeger and van Veen, 2009]. They contain two subdomains. The α-helical subdomain contains the ABC signature motif, called C-loop, that is the unique feature of ABC transporters [Ames et al., 1992] and coordinates the γ-phosphate of ATP [Zaitseva et al., 2005]. It is represented by the sequence motif LSGGQ [Ames et al., 1992]. The catalytic subdomain harbors six additional motifs that are the Walker A, Walker B, Q-loop, A-loop, H-loop and D-loop [Oswald et al., 2006]. The Walker A motif has the sequence motif GXXGXGK(S/T) where X represents any amino acid [Walker et al., 1982], whereas the Walker B motif has the sequence motif $\phi\phi\phi\phi$D where ϕ represents any hydrophobic residue. Together, both motifs form a nucleotide binding groove that coordinates Mg^{2+} and the triphosphate group of ATP [Oswald et al., 2006]. Neighboring NBD interaction is mediated by the D-loop with the sequence motif SALD. Here, the

aspartate interacts with the Walker A of the neighboring NBD [Seeger and van Veen, 2009]. A conserved tyrosine represents the A-loop and stack again the adenine ring of ATP to provide the binding affinity of the NBD [Kim et al., 2006, Carrier et al., 2007]. The Q-loop and the H-loop consists of a conserved glutamine respectively a conserved histidine. Both loops are interacting with the γ-phosphate of ATP. Directly in the case of the H-loop or indirectly via a structured water molecule in the case of the Q-loop (see Figure1.2 B) [Zaitseva et al., 2005]. These interaction is essential for the conformational coupling between the NBDs and TMDs [Oswald et al., 2006].

Furthermore, ABC exporters harbors an additional X-loop with the sequence motif TEVGERG that promotes communication between the NBDs and the TMDs [Dawson and Locher, 2006].

HlyB NBDs acts as a functional dimer [Schmitt et al., 2003, Zaitseva et al., 2006] as described for other ABC transporters like MJ0796 or MalK, the ATPase subunit of the maltose transporter [Smith et al., 2002, Chen et al., 2003]. Both nucleotide binding interfaces are involved in the functional dimer. Together, they build a 'nucleotide sandwich' with a 'head-to-tail' arrangement [Smith et al., 2002, Zaitseva et al., 2005]. Here, the Walker A of the first NBD interacts with the C-loop of the second NBD and the other way round to build two functional nucleotide binding interfaces that enables NBD dimerization and ATP hydrolysis [Jones and George, 1999, Chen et al., 2003, Hollenstein et al., 2007].

Further, the secretion signal of HlyA is interacting with the NBDs of HlyB. Surface plasmon resonance (SPR) studies demonstrate a specific interaction between the HlyB NBDs and the C-terminal 50 amino acids of its substrate HlyA [Benabdelhak et al., 2003].

The transmembrane domain (TMD)

The predicted localization of the HlyB TMD is between the amino acids 154 and 436. ABC exporters like HlyB are predicted to contain typically six transmembrane helices [Zolnerciks et al., 2011], whereas the amount of transmembrane helices for ABC importers various from five [Hollenstein et al., 2007, Oldham et al., 2007] like in the case of MetI [Kadaba et al., 2008] up to ten like in the case of BtuC [Locher et al., 2002, Pinkett et al., 2007]. The transmembrane helices are located antiparallel to each other, span through the IM and, in case of RND pumps, extend as intracellular loops in the cytoplasm. For the multidrug exporter AcrB, extended periplasmic loops could also observed that show direct interaction with TolC [Tamura et al., 2005]. HlyB does not harbor this

extended periplasmic loops and show no direct interaction to TolC [Thanabalu et al., 1998].

A special feature for ABC transporters are 'coupling helices' that are involved in transmitting conformational changes between the TMDs and NBDs of the transporter. In the case of ABC exporters, coupling helix 1 is flanked by transmembrane helices 2 and 3 (see Figure 1.2 A, purple helix), whereas coupling helix 2 is localized between transmembrane helices 4 and 5 (see Figure 1.2 A, orange helix). Coupling helix 1 interacts with both NBDs of the dimer via the Q-loops and neighboring residues and coupling helix 2 interacts only with the opposing NBD [Dawson and Locher, 2006].

Complementation experiments with a secretion-defective mutant of HlyA show that there is a directly interaction between HlyA and the HlyB TMDs. Secretion deficient HlyA lacking the last C-terminal 29 amino acids could complemented with HlyB variants to restore the secretion and the hemolytic activity of HlyA. The mutations of the HlyB variants are all located close to the predicted inner face of the cytoplasmic membrane [Zhang et al., 1993]. In general, it could be show that the substrate recognition and interaction by ABC transporter of T1SS is essential for the secretion process and for the recruitment of the active translocator [Binet and Wandersman, 1995].

ABC transporters are normally oriented in an inward-facing conformation in absence of the substrate and only substrate and ATP binding leads to an outward-facing conformation [Jardetzky, 1966]. In the inward-facing conformation, the ABC transporter is closed and passive diffusion of molecules or salt ions is avoided [Jones et al., 2009].

The C39-like domain (CLD)

The N-terminal localized CLD of HlyB is a 125 amino acids small domain that reaches to position 125 in the protein. The CLD shows 42 % homology to cysteine proteases that belongs to the papain superfamily [Ishii et al., 2010]. These peptidases are normally present in ABC transporters that are involved in the secretion of bacteriocin. The C39 protease domain cleaves the bacteriocin N-terminal precursor peptides C-terminal after a conserved motif of 15 amino acids, the GG motif, to produces the mature protein [Dirix et al., 2004, Håvarstein et al., 1995, Kotake et al., 2008, Wu and Tai, 2004].

In comparison, the C39 domain of HlyB is degenerated (for that reason called CLD) and show no peptidase activity. The cysteine of the catalytic triad is substituted by a tyrosine and even a re-introduction of a cysteine does not restore the protease activity of the CLD [Lecher et al., 2012, Kanonenberg et al., 2013]. The nuclear magnetic resonance (NMR) structure confirm that this is due to the fact that the histidine of the

catalytic triad is flipped out of the active site through π-π stacking with a tryptophan residue [Lecher et al., 2011]. According to this, the function of the CLD is still under speculation.

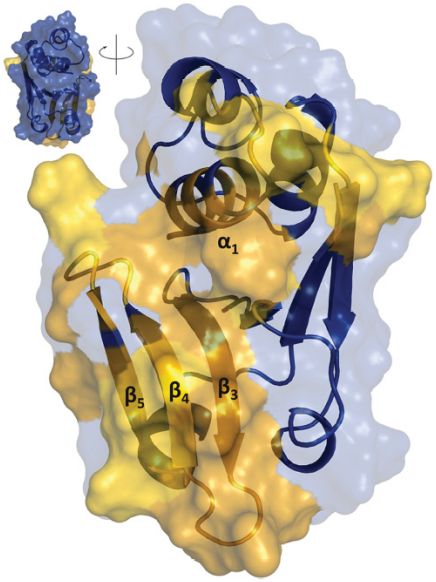

Figure 1.3.: **Surface representation of the nuclear magnetic resonance (NMR) structure of the CLD**
Structure of the CLD (pdb file 3ZUA). Amino acids of the CLD that displayed a GG repeat interaction are shown as yellow surface whereas the rest of the protein surface is highlighted in blue. Downscaled structure in the upper left corner represents the backside of the CLD. Figure is taken from [Lecher et al., 2012].

It is known that the CLD is essential for HlyA secretion. Without the CLD, secretion is completely abolished [Lecher et al., 2012]. Pull-down experiments confirm that the CLD only interacts with the unfolded substrate and that interaction is disturbed after Ca^{2+} induced folding of HlyA. Further, the unfolded substrate interaction is independent of the presence of the secretion signal [Lecher et al., 2012]. NMR chemical shift perturbation experiments highlights an alternative binding groove at the CLD for HlyA (see Figure 1.3) that is localized on the opposite side of the domain compared to fully active C39 proteases [Lecher et al., 2012]. The authors mentioned that the CLD acts as a receptor for HlyA that keeps it intracellular unfolded. No other known chaperone could be observed to be involved in protecting unfolded HlyA inside the cell [Holland et al., 2005]. Further, SecB involvement as described in the case for HasA could be excluded for the HlyA T1SS [Delepelaire and Wandersman, 1998, Bakkes et al., 2010].

The N-terminal extensions of the T1SS ABC transporter allow the categorization into

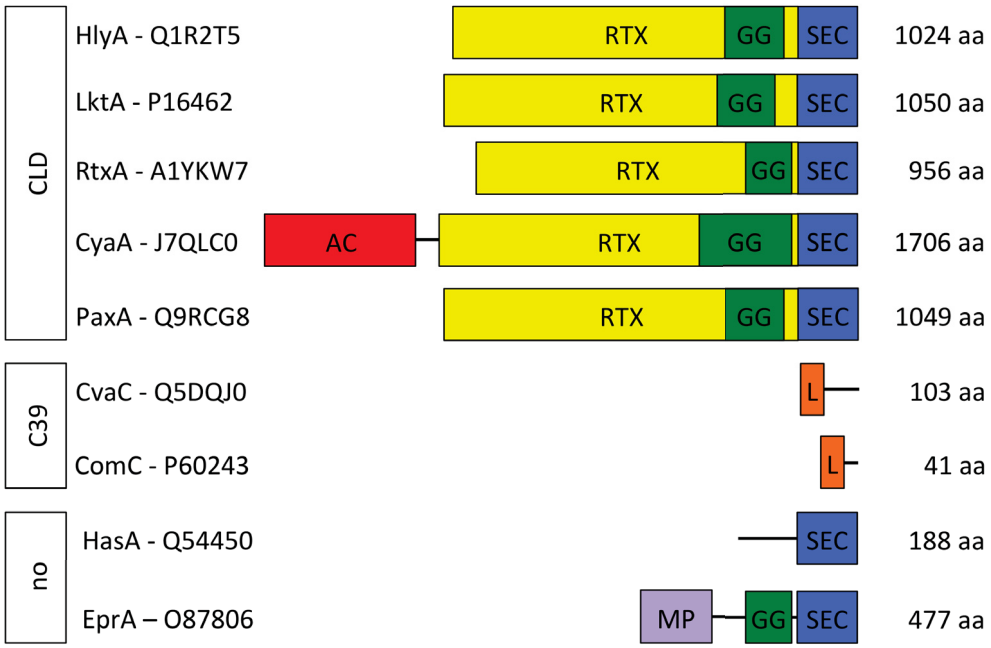

Figure 1.4.: **Domain organization of different T1SS substrates**
Boxes on the left highlight the ABC transporter families involved in the T1SS. "CLD" describes a T1SS with an ABC transporter with an N-terminal CLD extension, contributing defective peptidase, "C39" describes a T1SS with an ABC transporter having an active N-terminal C39 peptidase domain and "no" describes an ABC transporter without additional domains. Proteins are abbreviated as follows and listed with their corresponding UniProtKB entries: HlyA, hemolysin A; LktA, leukotoxin; RtxA, RtxA; CyaA, bifunctional hemolysin/adenylate cyclase; PaxA, exotoxin PaxA; CvaC, colicin V protein; ComC, competence-stimulating peptide type 1; HasA, hemophore HasA; EprA, metalloprotease EprA. Domains of the substrates are labeled as follows: AC, adenylate cyclase domain; RTX, RTX domain; GG, GG repeats; SEC, secretion signal; L, N-terminal leader peptide; MP, metalloprotease domain. Figure is taken and modified from [Lenders et al., 2015] and highlighted in Chapter 3.5.

three distinct groups (see Figure 1.4) [Lecher et al., 2012, Kanonenberg et al., 2013]. The first group contain transporters that harbors an authentic C39 protease domain. This group contains the bacteriocin secretion systems as well as microcins T1SS and T1SS that secretes rather small substrates (<10 kDa) with a cleavable N-terminal leader peptide for secretion. The second group contains the ABC transporters with CLD that transport larger substrates (<55 kDa). The substrates of CLD dependent T1SS are all members of the RTX toxin family [Lecher et al., 2012, Kanonenberg et al., 2013]. ABC transporters of the last group harbors no additional N-terminal domain and secretes

substrates like the hemophore HasA [Lecher et al., 2012, Kanonenberg et al., 2013].

1.3.2. The membrane fusion protein (MFP) hemolysin D (HlyD)

The MFP of the HlyA T1SS is HlyD. HlyD consists of 478 amino acids and can be separated into three different parts. The first 59 amino acids build a small cytosolic domain, followed by a single transmembrane helix (amino acids 60 to 80) and a huge periplasmic domain ranging from amino acid 81 to 478.

Cross-linking experiments with the functional T1SS *in vivo* shows that the presence of HlyD is essential for the secretion process. HlyD co-localized with HlyB in the IM even in absence of the substrate HlyA. HlyA is recognized by HlyB and HlyD and its presence leads to recruitment of TolC by binding to HlyD [Thanabalu et al., 1998].

The N-terminal cytosolic domain of HlyD is essential for secretion and consists of 59 amino acids with a potential amphiphatic helix (residues 2-26) followed by a cluster of charged residues (residues 34-38) with the consensus sequence R(E/K)KDE. Deletion of the proposed amphiphatic helix results in strongly reduced HlyA secretion levels whereas deletion of the charged residues abolished secretion completely [Balakrishnan et al., 2001]. Furthermore, cross-linking experiments revealed the important role of the charged amino acids in TolC recruitment. Without residues 34-38 TolC could not be recruited anymore, although the HlyA/HlyD-interaction and the oligomerization of HlyD were not influenced [Balakrishnan et al., 2001]. The cytosolic domain is only present in MFP that are involved in T1SS and could not be observed in MFPs of other transport systems like RND pumps. Substrate interaction of the cytosolic domain is special for HlyD. Co-precipitation studies of other T1SS involved MFP like HasE or PrtE show no direct MFP-substrate interaction [Létoffé et al., 1996].

In contrast, the periplasmic part of MFP is present in all members of the family [Zgurskaya et al., 2009] and well characterized by various structures. Crystal structures of the MFP AcrA, MacA, CusB, EmrA or MexA are available, but no structure of MFP involved in T1SS is currently revealed [Higgins et al., 2004, Yum et al., 2009, Su et al., 2009, Akama et al., 2004b, Hinchliffe et al., 2014].

It can be assumed that the structure of the periplasmic part of HlyD is similar to the known crystal structures of other MFPs. The central portion of all MFP are the two lipoyl half-motifs that are highly conserved in MFP [Zgurskaya et al., 2009, Johnson and Church, 1999]. The lipoyl half-motifs are interrupted by an α-helical domain with an α-hairpin that differs in length by integer multiples of seven residues depending on the periplasmic bridging distance of the MFP (see Figure 1.5). Both lipoyl half-motifs

consist of four β-strands that are homologous to each other and interact together to form a β-sandwich [Zgurskaya et al., 2009, Johnson and Church, 1999].

For HlyD, it could be shown that point mutation in this part of the protein results in reduced secretion levels and the incorrect folding of the released substrate in the extracellular space [Pimenta et al., 2005]. Further, the α-hairpin is essential for TolC interaction [Kim et al., 2010, Xu et al., 2010]. Mutants in this area results in abolished HlyD-TolC interaction [Lee et al., 2012].

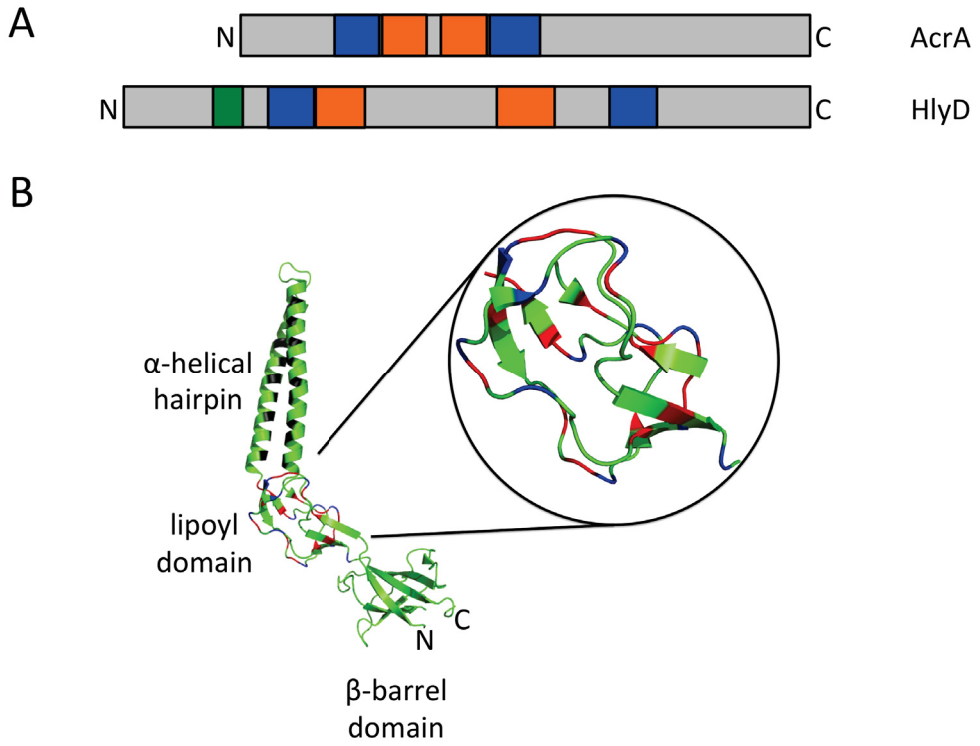

Figure 1.5.: **Structure and domain organization of AcrA and HlyD**
(A) Domain organization of AcrA and HlyD. Grey boxes represent the primary structure of the proteins. Blue boxes highlights the N and C-terminal lipoyl half-motifs whereas the orange boxes represents the the N and C-terminal α-helices of the α-helical domain. (B) Cartoon representation of monomeric AcrA (pdb file 2F1M; left side) and zoom in the lipoyl half-motifs (right side). Blue colored residues represent identical and red colored similar amino acids in the lipoyl half-motifs of MFP in over 50 % of sequences. Figure is taken and modified from Chapter 3.2.

Further, the C-terminus (the last 100 amino acids) represents the most conserved part of all MFP including HlyD. Structures of AcrA or MacA show no resolved C-terminus [Higgins et al., 2004, Yum et al., 2009] due to high flexibility of the region.

The last amino acids are essential for the secretion process. Lacking of the C-terminus or modification by adding a tag results in non functional secretion systems [Ge et al., 2009]. HlyD with a C-terminal fusion to a 10-amino acid c-Myc epitope results in abolished secretion without inhibiting substrate engagement to HlyD or assembly of the translocation complex [Thanabalu et al., 1998].

The oligomeric state of MFP is not consistent and varies strongly between members of this protein family. Cross-linked HlyD, AcrA and MexA show in *in vivo* experiments dimer and trimer formation [Thanabalu et al., 1998, Zgurskaya and Nikaido, 2000, Nehme and Poole, 2007]. Recent publication show higher oligomer formation for AcrA during electron microscopic studies [Xu et al., 2011] and for MacA, which forms stable hexamers in solution and in the crystals [Yum et al., 2009]. A hexameric oligomeric state for HlyD is conceivable because HlyD could act in some case as an adapter to bridge dimeric HlyB and trimeric TolC.

Stable higher oligomers of MacA, EmrA and AcrA could also detect by SPR spectroscopy. It could be observed that oligomer stability correlates with the stability of the MFP-TolC complex [Tikhonova et al., 2009]. Until now, no comparable studies have been performed for HlyD.

1.3.3. The outer membrane protein (OMP) TolC

TolC is the OMP of the HlyA T1SS. It consists of 493 amino acids whereas the first N-terminal 22 amino acids represent the signal peptide responsible for TolC transport that is cleaved off from the mature protein. The mature protein has a length of 471 amino acids [Koronakis et al., 2000]. Trimeric TolC build a continuous channel in the OM which is 140 Å in size whereof nearly 100 Å represent a periplasmic extension (see Figure 1.6 A). Structurally, TolC can be separated in two different parts. The first part is the β-barrel that builds the channel through the OM and the second part is the periplasmic extension building an α-barrel [Koronakis et al., 2000].

The β-barrel has a height of 40 Å including its extracellular loops. It consists of 12 β-strains, 4 β-strains per monomer. In the crystal structure, the barrel has a hollow cylindrical shape [Koronakis et al., 2000]. Molecular dynamic (MD) simulations of TolC suggest that a more hollow triangular prism like shape of the β-barrel is the energetically favorable conformation [Vaccaro et al., 2008]. Such a shape for the β-barrel of an OMP could already be observed in the crystal structure of OprM [Akama et al., 2004a]. According to this the cylindrical shape of TolC could maybe induced by the crystallization environment. Further, it could be shown that the β-barrel of TolC has an influence on

folding of substrates into their native conformation. Amino acid substitutions L42P and S257P in the β-barrel of TolC results in reduced hemolytic activity of secreted HlyA without or even less affecting the transport efficiency [Vakharia et al., 2001].

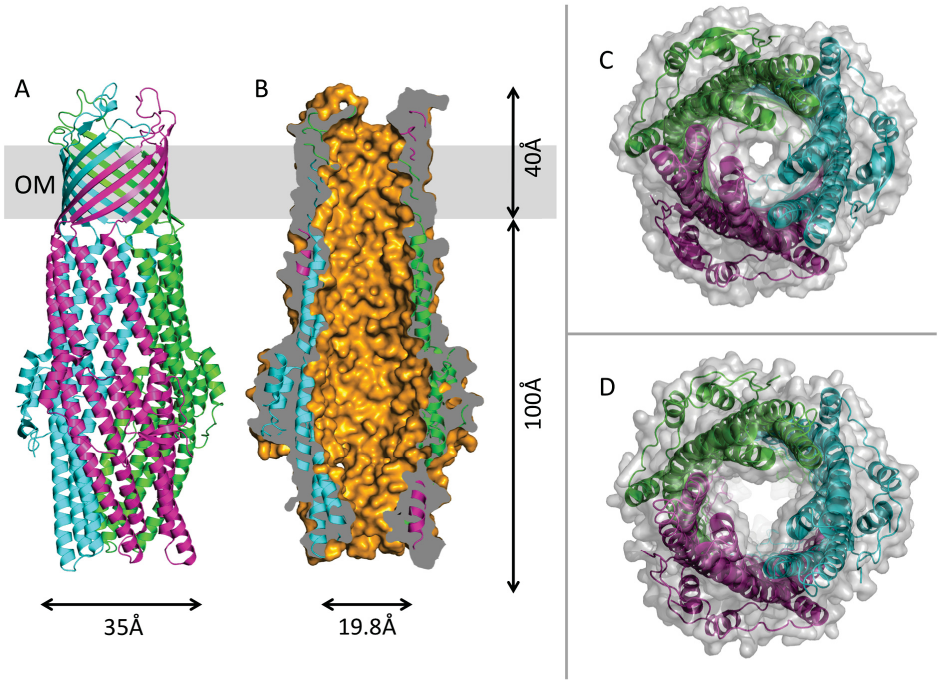

Figure 1.6.: **Structural overview of TolC**
(A) Cartoon representation of the side view of the TolC homotrimer in its closed state. The different monomers of TolC are highlighted in green, cyan and magenta. (B) A cross-section side view of a space-filling model of the TolC trimer shows a near-continuous channel from the β-barrel in the OM to the periplasmic entrance of the β-barrel. The grey surface highlights the cross-sectional area in combination with a cartoon representation of the side view of the TolC homotrimer. The bright orange surface shows the inner and outer surface of the part of TolC (the black arrows indicate the dimensions of TolC). (C) View through the closed pore towards the periplasmic entrance of the β-barrel. Monomers are highlighted in green, cyan and magenta. To illustrate the closed conformation, the shape of the surface of TolC is shown in transparent grey panels (A, B and C are based on pdb file 1EK9). (D) View through a sequential open state of the pore towards the periplasmic entrance of the β-barrel. The monomers are highlighted in green, cyan and magenta. To illustrate the sequential open conformation, the shape of the surface of TolC is shown in transparent grey panels (D is based on pdb file 2XMN). Figure is taken from [Lenders et al., 2013] and highlighted in Chapter 3.1.

The 100 Å α-barrel follows the β-barrel by expanding into the periplasmic space. Its

maximal outer diameter is 35 Å (see Figure 1.6 A). It consists of four α-helices per monomer [Koronakis et al., 2000]. Intermeshing of side chains, so called 'knobs-into-holes' packing, between two neighboring helices, stabilizes the 12 laterally packed helices [Koronakis et al., 2004]. The α-barrel builds a water-filled pore with a inner diameter of 20 Å (see Figure 1.6 B). The pore is limited on one side by the open β-barrel and on the other side at the periplasmic end by densely packed coiled-coils. The coiled-coil structure has a diameter of 3.5 Å and an iris-like shape (see Figure 1.6 C) [Koronakis et al., 2004].

The diameter of 3.5 Å at the end is even to small for passage of ions (see Figure 1.6 C) [Delepelaire, 2004]. This 'periplasmic gate' is stabilized and kept close by salt bridges and hydrogen bonds of the nearby localized amino acids. Especially, amino acids T152, D153, Y362 and R367, which are localized in the coiled coil region, play an important role by keeping the periplasmic end closed. Conductivity experiments with TolC variants leaking these critical amino acids confirm that the periplasmic end is partly open [Andersen et al., 2002]. Crystal structures of the Y362 and R367 alanine double mutant illustrates this partly open conformation (see Figure 1.6 D). Both structures visualize an 'iris-like motion' of the coiled coils at the periplasmic end of the α-barrel [Andersen et al., 2002, Pei et al., 2011].

First evidences for an 'iris-like motion' of the periplasmic coiled coils were observed by *in vitro* and *in vivo* studies of the TolC variants with the partly open end [Eswaran et al., 2003]. Cysteine cross-linking of the α-helical coiled coils combined with conductivity experiments show a recovery of the gating activity of TolC. *In vivo*, the recovery of the gating activity indicates that an untwisting of the α-helical coiled coils is necessary for successful substrate secretion. In case of the HlyA T1SS cysteine cross-linking of the TolC variants abolished secretion but more importantly TolC is still recruited and the T1SS assembles completely [Eswaran et al., 2003]. Upon opening, the inner α-helical coiled coils surround the outer α-helical coiled coils at the periplasmic ends of the α-barrel [Bavro et al., 2008, Pei et al., 2011]. Further, the structures of TolC with the closed and open periplasmic site highlight an increasing distance between the inner α-helical coiled coils that ranged from 12.2 Å in wild type TolC to 18.9 Å and 21.3 Å in the TolC mutants (see Figure 1.6 C and D; reviewed in [Lenders et al., 2013]) [Pei et al., 2011]. The increasing distance resulting in substrate passage like ions trough TolC *in vitro* [Pei et al., 2011].

TolC and other OMP are involved in translocator formation that allows their corresponding secretion systems the successful secretion of their substrates. In T1SS, TolC is only interacting with the MFP but not with the cognate ABC transporters [Létoffé

et al., 1996, Thanabalu et al., 1998]. Direct interaction between TolC and an RND transporter was observed in the case of the Acr multidrug efflux pump system. There, TolC is directly interacting with the transporter AcrB [Tamura et al., 2005]. Cross-linking experiments indicate in this case a tip-to-tip interaction between AcrB and TolC, whereas a additional binding groove for the MFP AcrA could observed. The binding groove enabled TolC a direct interaction with the N-terminal α-helix of the MFP [Bavro et al., 2008, Pei et al., 2011, Tamura et al., 2005].

The function is proposed to be a water-filled channel that allows the passage of substrates across the OM. An energizing aspect or direct active involvement in substrate transport was not observed. MD simulations indicate that TolC undergoes a complex pattern of conformational movements during the 'iris-like motion' that provides a peristaltic motion in the periplasmic domain [Vaccaro et al., 2008].

1.3.4. The substrate HlyA

The substrate of the HlyA T1SS is HlyA, a 1024 amino acids and 110 kDa large toxin. HlyA belongs to the RTX protein family, which is defined by nonapeptide GG repeats with the sequence motive GGXGXGUX. U represents a large or hydrophobic amino acids. Chapter 1.4.1 describes the function of the GG repeats more detailed. The repeats are localized in a cluster close to the C-terminus (see Figure 1.7). The extreme C-terminus followed this cluster. It harbors the HlyA secretion signal that is non-cleaved during secretion and is recognized by the HlyA T1SS (see Chapter 1.4.1 for more detailed information).

HlyA is synthesized as a non-toxic pre-protein (pro-HlyA) and matures via post translational fatty acid acylation into its active form. Acylation is carried out by the acylase hemolysin C (HlyC), which uses the acylated acyl carrier protein (acyl-ACP) for fatty acid transfer [Issartel et al., 1991, Stanley et al., 1994, Ludwig et al., 1996, Stanley et al., 1998]. For that purpose, HlyC transfer the acyl residue of acyl-ACP to itself. The covalent intermediate acyl-HlyC transfers the acyl residue to the ϵ-amino groups of the HlyA lysines K564 and K690 in a following step (see Figure 1.7) [Worsham et al., 2001, Worsham et al., 2005]. Normally, fatty acids with a length of 14, 15 or 17 carbon atoms are transferred [Ludwig et al., 1996, Lim et al., 2000]. Deletion of the HlyC binding domain or substitution of the lysines K564 and K690 abolished acylation and results in fully secreted but non active HlyA [Hardie et al., 1991, Stanley et al., 1994]. The Ca^{2+} binding affinity of HlyA is not influenced by acylation [Nicaud et al., 1985, Boehm et al., 1990, Hughes et al., 1992, Moayeri and Welch, 1997]. It could be shown that

the residues S20, H23, V127, G128 and K129 are involved in the catalysis of HlyC acyl transfer [Guzmán-Verri et al., 1997, Trent et al., 1999b, Trent et al., 1999a, Trent et al., 1999c, Worsham et al., 2001]. The structure of *E. coli* HlyC is not solved but the HlyC homolog ApxC from *Actinobacillus pleuropneumoniae* indicated that HlyC is a dimer in solution via inter monomer interaction by a N-terminal α-helix [Greene et al., 2015]. As reaction mechanism, a complex formation of pro-HlyA, HlyC and acyl-ACP as well as a ping-pong mechanism are proposed [Stanley et al., 1991, Worsham et al., 2001].

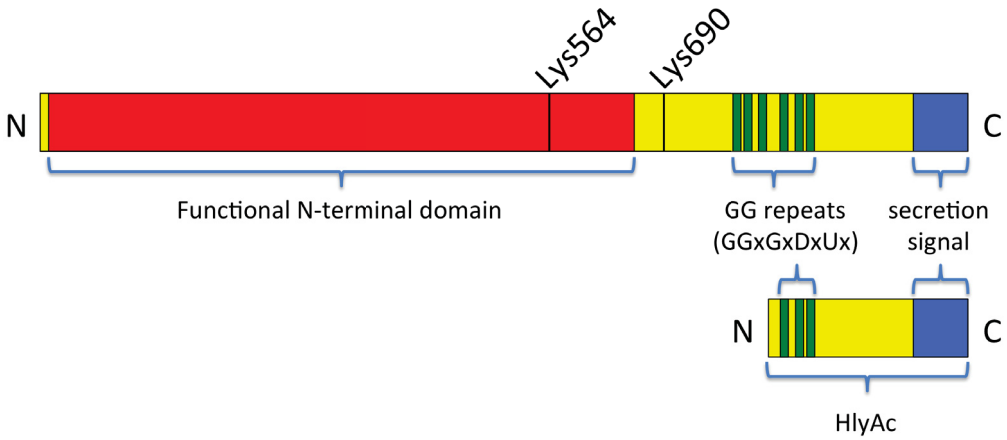

Figure 1.7.: **Domain organization of HlyA and HlyAc**
Upper boxes represent the domain organization of HlyA and the lower one the domain organization of HlyAc. Yellow boxes represent the primary structure. The blue boxes highlights the secretion signal whereas the green boxes represents the GG repeats and the red box the functional N-terminal domain of HlyA. Acylation sites of HlyA are highlighted with the amino acid positions Lys564 and Lys690.

The toxin is secreted by some uropathogenic *Escherichia coli* strains [Ludwig et al., 1991, Welch et al., 1992] and is able to lyse for example erythrocytes or mammalian epithelial cell. Erythrocytes lysis by HlyA could be followed by hemoglobin release [Minshew et al., 1978, Brooks et al., 1980, DeBoy et al., 1980]. The exact interaction mechanism of HlyA with the target membrane that results in erythrocytes lysis is not definitely determined. Different possibilities have been proposed. Cell lysis could be mediated by HlyA pore formation that leads to target cell turgor increase by Ca^{2+} influx and finally to cell death by lyses [Rennie et al., 1974, Bhakdi et al., 1986]. This mechanism can work without and with a receptor. In case of a receptor mediated pore formation, HlyA can interact with a receptor and activate distinct signaling pathway that leads that leads to a destruction of the host immune system by Ca^{2+} influx [Lally et al., 1997]. Furthermore, interaction with outer membrane vesicles with the host membrane

can result in HlyA to host interaction. Gram-negative bacteria harbor outer membrane vesicles [Beveridge, 1999] and HlyA was already observed in this particles [Balsalobre et al., 2006]. In case of the ClyA activity, it could be show that such an interaction is necessary [Wai et al., 2003].

The oliogomeric state of HlyA in solution is known to be a monomer or a dimer [Thomas et al., 2014b]. Monomeric HlyA could at lower concentration prefer receptor recognition whereas at higher concentration oligomerization and pore formation could be induced [Menestrina et al., 1995, Stanley et al., 1998].

The C-terminal 218 amino acids of HlyA (HlyAc) are secreted autonomous in high amounts. It contain the secretion signal and three GG repeats (see Figure 1.7). The fragment is well characterized and sufficient for secretion [Nicaud et al., 1986]. Fusions of other proteins to the HlyAc fragment results in some cases in secretion by the HlyA T1SS [Mackman et al., 1987, Kenny et al., 1991, Blight and Holland, 1994, Gentschev et al., 2002, Bakkes et al., 2010, Schwarz et al., 2012a].

1.4. Secretion process

1.4.1. Signals for secretion

The essential signal for secretion of T1SS substrates is encoded in the C-terminal secretion signal. The signal is localized within the last 50 to 60 amino acids of the substrate and is not cleaved during or after the secretion process [Nicaud et al., 1986, Mackman et al., 1987, Jarchau et al., 1994]. It could be shown that the secretion signal is necessary and sufficient for secretion. Amino acid substitutions in the secretion signal leads to strongly reduced or complete abolished secretion [Gray et al., 1986, Stanley et al., 1991, Kenny et al., 1994]. Furthermore, fusions of non secreted proteins with the secretion signal highlights the role. Some fusion proteins harboring the secretion signal are recognized and secreted by the HlyA T1SS. They become new substrates for the secretion system [Blight and Holland, 1994]. According to this, it is surprising that the sequence motif for substrates of T1SS is not conserved. Only for RTX proteins, a sequence segment at the last 20-30 C-terminal amino acids could identified that contain maybe important information for secretion [Luo et al., 2015]. Nevertheless, it is more likely that the secondary structure of the secretion signal acts as the recognition motif [Wolff et al., 1994, Zhang et al., 1995].

Another important signature motif for the T1SS secretion process are the GG repeats that are found in most of the substrates [Delepelaire, 2004]. The RTX proteins represents

the main family of T1SS substrates and are characterized by these GG repeats. In most of the substrates, the GG repeats are localized close to the secretion signal (see Figure 1.4) [Strathdee and Lo, 1989]. The consensus sequence of the GG repeats is highly conserved and defined by the motif GGxGxDxUx where U represents a large or hydrophobia amino acid [Baumann et al., 1993, Bauche et al., 2006, Linhartová et al., 2010]. The GG repeats containing proteins vary greatly in size and range from 78 to 8682 amino acids as described for LapA from *Pseudomonas fluorescens* [Hinsa et al., 2003, Delepelaire, 2004]. The amount of GG repeats correlates with the protein length and occurs mainly with one repeat for every 6-12 kDa [Delepelaire, 2004, Linhartová et al., 2010]. All GG repeats containing substrates have an acidic isoelectric point [Delepelaire, 2004]. The repeats are involved in protein folding. Binding of calcium ions to the GG repeats induces protein folding [Rose et al., 1995, Rhodes et al., 2001]. The induced structure consists of an embedded Ca^{2+} surrounded by β-roll and β-sandwich [Linhartová et al., 2010]. Folding induced by the GG repeats appears only in the extracellular space due to the higher calcium ion concentration that exceed the K_D for calcium ion binding [Thomas et al., 2014a]. The intracellular calcium ion level is to low for folding initiation [Gangola and Rosen, 1987, Ludwig et al., 1988, Jones et al., 1999].

Furthermore, some T1SS substrates, like HasA [Arnoux et al., 1999], harbors additional regions [Finnie et al., 1998]. The 188 amino acid large hemophore HasA has compared to RTX proteins no GG repeats but additional motifs that are linear distributed over the whole peptide [Masi and Wandersman, 2010] and are not essential for secretion but maximize the secretion level of HasA [Masi and Wandersman, 2010].

1.4.2. Secretion of unfolded substrate

In case of the HlyA T1SS, the inner diameter of TolC is known (see Chapter 1.3.3). It can be assumed that 20 Å of TolC represent a bottleneck in size for substrate translocation [Koronakis et al., 2004]. This diameter is comparable with the size of one α-helix. Compared with the 110 kDa HlyA or the 900 kDa LapA it is very unlikely that T1SS can secrete completely folded substrates [Hinsa et al., 2003, Delepelaire, 2004]. As a consequence, the substrates have to be secreted at least partly or completely unfolded.

For the HlyA and HasA secretion systems, it could be shown that the substrate secretion occurs only in an unfolded state [Debarbieux and Wandersman, 2001, Bakkes et al., 2010]. Furthermore, intracellular folded HasA leads to an inhibition of its own T1SS for secretion [Debarbieux and Wandersman, 2001]. To prevent this, SecB keeps HasA intracellular unfolded or at least in a transport-competent, respectively loosely folded

state [Delepelaire and Wandersman, 1998, Sapriel et al., 2003]. Fusion proteins with maltose binding protein (MBP) and HlyAc (see Figure 1.1) that contains the secretion signal and three GG repeats [Nicaud et al., 1986] results in complete abolished secretion. The secretion ability can be restored by introducing point mutations in the MBP part of the fusion protein that reduces the folding rate [Bakkes et al., 2010]. Thereby it was shown that the folding rate of the fusion protein dictates its secretion level. Slow folding mutants secretes more efficient whereas faster folding mutants secretes less efficient. Binding studies to an amylose resin confirmed that the MBP mutants only influence the folding speed but not the binding capacity of MBP [Bakkes et al., 2010].

Similar experiments were done with an intestinal fatty acid binding protein (IFABP) that was also fused to the HlyAc fragment. IFABP is well characterized and slow folding mutants of the protein have been reported [Kim and Frieden, 1998]. Fusion protein with wild type IFABP could not been secreted whereas the slow folding IFABP mutants G80V and G121V could be secreted in high amounts [Schwarz et al., 2012a]. IFABP function is not influenced by the folding rate. Binding experiments with the fluorescence fatty acid analog 11-(Dansylamino)undecanoic acid (DAUDA) shows the same binding affinity for the IFABP variants as for the wild type [Kim and Frieden, 1998, Schwarz et al., 2012a].

1.4.3. Substrate orientation

Chapter 1.4.1 highlights the important role of the secretion signal for the secretion process. It is essential and sufficient for secretion [Jarchau et al., 1994, Zhang et al., 1995]. Further, it is directly influencing the catalytic cycle of its ABC transporter NBDs [Benabdelhak et al., 2003]. Due to the fact that T1SS substrates are secreted unfolded [Debarbieux and Wandersman, 2001, Bakkes et al., 2010, Schwarz et al., 2012b] the proteins have to enter the translocator with one terminus first. The substrates can enter the T1SS with the secretion signal ahead or at last. Both opportunities leads to two fundamental different working models and roles of the secretion signal for type I secretion [Lenders et al., 2013].

In case of an ‘activating’ T1SS pathway, the secretion signal initiates the transport process (see Figure 1.8). In the first step, HlyB NBD dimerization is initiated by binding of ATP and the secretion signal [Benabdelhak et al., 2003, Zaitseva et al., 2006]. The substrate interaction with the ABC transporter stimulates the TolC recruitment by the MFP [Létoffé et al., 1996, Thanabalu et al., 1998]. Afterwards, the NBD dimerization leads to conformational changes of the TMDs of HlyB and allows binding of the secretion

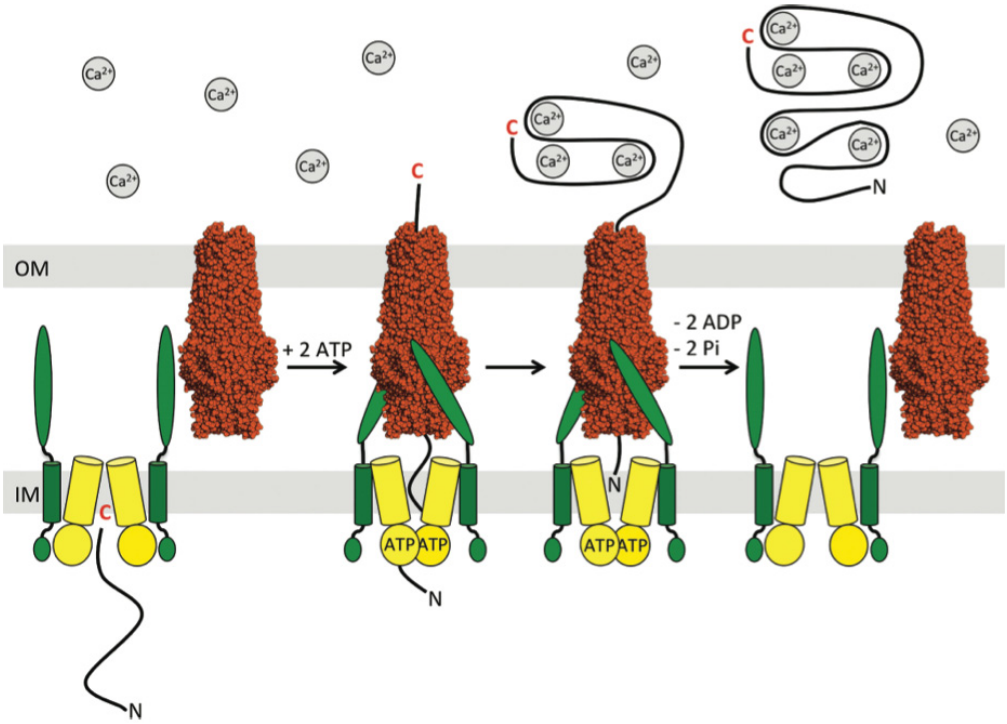

Figure 1.8.: **Possible steps of an activating T1SS pathway**
In the first step the OMP TolC (shown in side view as orange spheres and based on pdb file 1EK9), in the presence of the transport substrate, is recruited by the MFP and the ABC protein (highlighted in green and yellow, respectively) located in the IM. The oligomeric state of the MFP is unknown so far but to ensure a better overview only two MFPs are shown. TolC recruitment is mediated by binding of the substrate secretion signal to the two IM proteins, ABC transporter and MFP. Simultaneously, the binding of the secretion signal initiates ATP binding by the ABC transporter. The resulting conformational changes in the TMDs of the ABC transporter displace the C-terminus of the unfolded substrate into the translocator. Third, the substrate is 'pulled' through the translocator by progressive folding in the calcium-rich extracellular space (calcium ions highlighted as gray dots). When the substrate passes completely through the translocator, it is presumed that this triggers ATP hydrolysis of both ATP molecules and will reset the transporter to its initial state. Finally, the transport complex dissociates and releases ADP and free phosphate into the cytoplasm. The fully folded substrate then diffuses into the extracellular space. Figure is taken and modified from Chapter 3.1.

signal and its entering into the translocation pore. In the next step, the substrate is transported to the extracellular space where folding is induced by the extracellular amount of Ca^{2+} and dissociate from the T1SS takes place. If this process takes place

under continuous ATP hydrolysis, is not analyzed yet. Finally, the substrate release is realized by the translocator and leads to ATP hydrolyzes, conformational changes of the ABC transporter (from an outward to an inward facing conformation) and to the disassembly of the T1SS. The secretion system is restored in the initial state and ready again for a new substrate translocation.

In favor for an activating T1SS pathway, many fusion proteins are secreted by the HlyA T1SS. They harbor the HlyAc fragment that contains the secretion signal [Mackman et al., 1987, Kenny et al., 1991, Blight and Holland, 1994, Gentschev et al., 2002, Bakkes et al., 2010, Schwarz et al., 2012a]. The proteins have nothing to do with type I secretion but they are still recognized and transported with the HlyAc fragment. For that purpose, the secretion can only initiate after translocation of the secretion signal. Nevertheless, the secretion signal alone is still secretable [Jarchau et al., 1994]. For the Prt T1SS could be shown *in vitro* that the ATPase activity of the ABC transporter PrtD is inhibited by the secretion signal of its substrate [Delepelaire, 1994].

In case of a terminating T1SS pathway, the secretion signal terminates the secretion process and leads to a reset of the transporter. For this kind of mechanism, the transport has to be initiate by an unknown factor that leads to ATP and substrate binding. The substrate possess additional N-terminal regions that allows its binding to the ABC transporter [Masi and Wandersman, 2010]. Binding leads to the assembly of the T1SS and to conformational changes of the transporters TMDs (from an inward to an outward facing conformation). Afterwards, secretion to the extracellular space will occur with the N-terminus first.

In a final step, the secretion signal will be secreted at last and induces the ATP hydrolyzes with the release of the substrate. This results in a conformational change of the ABC transporter from its outward to inward facing conformation and to a disassembly of the T1SS.

Arguments for the terminating model are that those proposed additional N-terminal regions (anchor regions) could be found in the primary sequence of HasA [Masi and Wandersman, 2010]. Additionally, it could be shown that the secretion signal is important for dissociation of the translocator by affecting the catalytic cycle of the NBDs [Cescau et al., 2007]. In case of the Has secretion system, the secretion signal of HasA is responsible for the ATP hydrolyzes of its ABC transporter HasD [Masi and Wandersman, 2010]. Such a mechanism is expectable for the HlyA T1SS, too. Here, the GG repeats could act as such anchor regions because its interaction with the CLD of HlyB could be confirmed [Lecher et al., 2012]. Although, stabilization of the ABC transporter by binding of the secretion signal could possible, too. This could lead to the assembly of

the HlyA T1SS and finally to the secretion of HlyA with its N-terminus ahead.

1.5. Transport mechanism

1.5.1. Hierarchy of assembly

The states of assembly for the HlyA T1SS could been highlighted by cross-linking studies and further experiments [Thanabalu et al., 1998]. HlyA is recognized by its ABC transporter HlyB and its MFP HlyD [Thanabalu et al., 1998]. The secretion signal of the substrate binds to the NBDs of HlyB [Benabdelhak et al., 2003] whereas the GG repeats interacts with the CLD [Lecher et al., 2012]. Further, HlyA is interacting with the cytoplasmic part of HlyD [Balakrishnan et al., 2001]. The exact part of HlyA for HlyD interaction has not been determined yet.

The interaction of HlyA with HlyB and HlyD results in recruitment of TolC by the MFP. Substrate and HlyB respectively HlyD presents alone results not in recruitment of TolC [Thanabalu et al., 1998]. The substrate MFP interaction is special for the HlyA T1SS and could not observed for other T1SS like Prt or Has [Létoffé et al., 1996]. Coprecipitation experiments with these secretion systems show a serial assembly of the single compartments. The substrate interacts only with the ABC transporter whereas the ABC transporter interacts with the substrate and the MFP. The MFP itself interact only with the ABC transporter and the OMP but not with the substrate whereas the OMP only interfere with the MFP [Létoffé et al., 1996].

Further, ATP binding leads to the complex assembly whereas ATP hydrolyzes seems only important for completing the secretion process [Thanabalu et al., 1998]. Currently, it is not clear whether ATP binding is essential for the translocator formation or not.

1.5.2. Energizing of translocation

The inherent driving force for energizing the substrate translocation in type I secretion is not know yet. A combination of different factors like ATP hydrolyzes, the proton motive force or diffusion, could be responsible.

ATP hydrolyzes is involved in energizing translocation. Without hydrolyzes the secretion cycle can not completed [Thanabalu et al., 1998]. Nevertheless, the number of ATP that are consumed for one transport cycle is not known. It is know that only two ATP are consumed per transported substrate for the OpuA from *Lactococcus lactis* [Patzlaff et al., 2003], for the glycine-betaine or the maltose importer from *Escherichia coli* [Mimmack et al., 1989]. Energizing by an iterative mechanism where one ATP is hydrolyzed

for a distinct number of transported amino acids could be possible, too. Such a mechanism is described for the Sec pathway with one consumed ATP for 20-30 delocalized amino acids [Schiebel et al., 1991, Uchida et al., 1995].

The proton motive force (PMF) is partly involved in the early stages of HlyA secretion [Koronakis et al., 1991]. For secretion experiments, carbonylcyanide m-chlorophenylhydrazone (CCCP) was used for collapsing the PMF and for inhibiting the membrane potential and results in a complete abolished secretion [Koronakis et al., 1991]. This behavior could only observed in early stages of secretion, in later stages secretion is not influenced by CCCP anymore. CCCP is not inhibiting HlyB and HlyD during this experiments. This confirm that the effect basis on a collapsed PMF respectively the membrane potential [Koronakis et al., 1991].

Further, diffusion could act as the driving force for secretion. Due to this assumption, the translocator act partly as a gating channel without any active transport activity and the proteins are diffusing along their concentration gradient respectively their electrostatic gradient. All T1SS substrates have an acidic isoelectric point that results in a negatively charge of the proteins inside the cells [Delepelaire, 2004]. The proteins can travel along their charge gradient across the membrane. Further, the T1SS substrate concentrations is much higher inside the cell compared with the extracellular space. The proteins can travel along a concentration gradient through the translocator.

The binding affinity of the conformational stages of the ABC transporter could also be involved in energizing the transport process. The transporter can appear in an inward and an outward facing conformation. The conformation have different binding affinities for the substrate [Martin et al., 2001]. The inward facing conformation will have a higher binding affinity compared to the outward facing state. A lower affine outward facing conformation releases the substrate and prevents revers transport. Such binding affinities by the transporter stages could only observed for small protein molecules but not for T1SS substrates [Martin et al., 2001].

Furthermore, the Ca^{2+} binding affinity of the GG repeats could act as the inherent driving force for energizing the substrate translocation. GG repeats are prominent in most of the T1SS substrates [Delepelaire, 2004] and their amount correlates with protein length with one repeat per 6-12 kDa [Delepelaire, 2004, Linhartová et al., 2010]. As mentioned above, the repeats bind Ca^{2+} and induced protein folding [Rose et al., 1995, Rhodes et al., 2001]. Protein folding takes place only in the extracellular space due to the high extracellular Ca^{2+} concentration [Jones et al., 1999]. The GG repeats reach the cell surface and start folding. The folding represents the inherent driving force that 'pulls' the rest of the protein out of the translocator [Linhartová et al., 2010]. In this case,

backsliding of the protein is prevented due to the globular size of the folded substrate that can not enter the translocator anymore.

1.5.3. Function of CLD, MFP and OMP

Chapter 1.3.1 highlights that a chaperone function of the HlyB CLD is likely. In contrast to fully active C39 proteases like ComA from *Streptococcus pneumoniae* [Ishii et al., 2010] the catalytic triad of the HlyB CLD is degenerated [Lecher et al., 2011]. The CLD interacts with the unfolded substrate (the GG repeats) over a binding site that is localized on the opposite site of the protein in comparison to C39 proteases [Lecher et al., 2012]. Other T1SS without CLD prevent degradation by SecB interaction like in the case of HasA [Delepelaire and Wandersman, 1998, Sapriel et al., 2003, Wolff et al., 2003]. How systems without CLD or SecB like the Prt T1SS manage the prevention of substrate degradation is not known [Delepelaire and Wandersman, 1998]. Further, the CLD of HlyB is involved in negative regulation of the ATPase activity of the ABC transporter *in vitro* (Sven Reimann personal communication).

An involvement of MFPs and OMPs in protein folding could be observed for the HlyA and the Cva T1SS. Point mutations in HlyD and TolC leads to incorrect folded and lower levels of substrate with reduced hemolytic activity [Hwang and Tai, 1999, Vakharia et al., 2001, Pimenta et al., 2005]. Hemolytic activity of HlyA could be restored in this cases by de- and renaturating *in vitro*. Furthermore, specific HlyD mutations results in a reduced hemolytic activity by increasing the extracellular Ca^{2+} concentration [Pimenta et al., 2005]. For interpreting this results, it is possible that the formation and stable packing of HlyD is disturbed which results in an aberrant movement of the substrate through the translocation complex [Pimenta et al., 2005]. It is mentionable that MFPs and OMPs work as an isolator for HlyA to prevent Ca^{2+} interaction inside the translocator. MD simulation of TolC indicated a gating activity for its extracellular end that could prevent Ca^{2+} insertion into the T1SS [Vaccaro et al., 2008].

2. Aims

One of the most prominent example for T1SS in Gram-negative bacteria is the HlyA T1SS from *Escherichia coli*. The RTX protein HlyA is one of the major virulence factors of uropathogenic *Escherichia coli* (UPEC) strains that causes gravely diseases in humans [Menestrina et al., 1994].

The HlyA T1SS consists of three different components, the OMP TolC, the ABC transporter HlyB and the MFP HlyD. Together they assemble to the tripartite translocator that catalyze HlyA secretion. Secretion of HlyA occurs unfolded in one step from the cytoplasm directly into the extracellular space [Thanabalu et al., 1998, Bakkes et al., 2010]. The secretion signal of HlyA initiates secretion and is responsible for the assembly of the T1SS complex. It contains all information for successful secretion and can be secreted alone [Jarchau et al., 1994]. Nevertheless, many aspects of the transport process are not fully understood.

One of these aspects is the orientation of the substrate during secretion. An aim of this doctoral thesis was to find out whether directionality of secretion exists and if so, whether the N- or C-terminus of HlyA is translocated first through the T1SS.

Moreover, the role of the secretion signal during initiation of the translocation process is not completely understood and should be studied during this work in more detail.

The rate of HlyA secretion is not characterized yet. The speed of the T1SS is still an open field of discussion. For comparison, the injection speed of the SipA T3SS is within the scope of 4795-41100 amino acids per sec and T3SS, whereas the speed for Sec dependent transport is 152-228 amino acids per sec and transporter [Schlumberger et al., 2005, Robson et al., 2009]. According to this, the influence of protein length, number of GG repeats and the role of external calcium ion concentration on HlyA secretion have to be investigated in this work in more detail.

Furthermore the role of the different states of the cycle for ATP hydrolysis for the HlyA secretion process in unknown. This question was addressed during this doctoral thesis, too.

3. Publications

3.1. Chapter I - Molecular insights into type I secretion systems

Title Molecular insights into type I secretion systems

Authors Michael H.H. Lenders[a], Sven Reimann[a], Sander H. J. Smits and Lutz Schmitt
[a]: These authors contributed equally to this article.

Published in *Biological chemistry* (2013)

Impact factor 2.689

Own proportion of this work 30 %;
Writing of the manuscript.

DE GRUYTER DOI 10.1515/hsz-2013-0171 — Biol. Chem. 2013; 394(11): 1371–1384

Review

Michael H.H. Lenders[a], Sven Reimann[a], Sander H. J. Smits and Lutz Schmitt*

Molecular insights into type I secretion systems

Abstract: Type 1 secretion systems are one of the main machineries in Gram-negative bacteria involved in the secretion of a wide range of substrates from the cytoplasm across the inner and outer membrane in one step to the extracellular space. The range of substrates varies from small proteins up to large surface layer proteins of about 900 kDa. Most of the substrates have a non-cleavable C-terminal secretion signal and so-called GG repeats that are able to bind calcium ions. The translocator complex is composed of a trimeric outer membrane protein that provides a pore in the outer membrane. A multimeric membrane fusion protein spans the periplasm and forms a continuous channel connecting the outer membrane protein with a dimeric ATP-binding cassette transporter in the inner membrane. The ATP-binding cassette-transporter is thought to form a channel through the inner membrane and energizes the transport process. This review will provide a detailed view of the components of the translocator and will summarize structural as well as functional data.

Keywords: ATP-binding cassette (ABC)-transporter; ATPase; haemolysin A; membrane fusion protein; outer membrane protein; type 1 secretion.

[a]These authors contributed equally to this article.
***Corresponding author: Lutz Schmitt,** Institute of Biochemistry, Heinrich Heine University, Universitätsstraße 1, D-40225 Düsseldorf, Germany, e-mail: Lutz.Schmitt@hhu.de
Michael H.H. Lenders, Sven Reimann and Sander H. J. Smits: Institute of Biochemistry, Heinrich Heine University, Universitätsstraße 1, D-40225 Düsseldorf, Germany

Introduction

A broad range of morphologically diverse bacteria are known to secrete proteins to the exterior (Pugsley and Schwartz, 1985). The type 1 secretion system (T1SS) has evolved in Gram-negative bacteria to secrete substances in one step from the cytoplasm across both the inner and outer membrane, without any periplasmic intermediate. This mechanism of secretion is independent of the Sec-mediated pathway (Schatz and Beckwith, 1990).

The transport complex itself contains three specific components, which interact with each other and build up the secretion apparatus (Letoffe et al., 1996; Thanabalu et al., 1998). Two proteins are located in the inner membrane, an ATP-binding cassette (ABC) transporter and a membrane fusion protein (MFP). The third component is a protein residing in the outer membrane, which has therefore been called an outer membrane protein (OMP). This forms a channel from the periplasm to the extracellular medium. Components of T1SSs reside in the membranes of the bacterial envelope. Most substrates of T1SSs contain a non-cleavable C-terminal secretion signal, which upon interaction with their ABC transporter initiates assembly of the whole transport complex (Letoffe et al., 1996; Thanabalu et al., 1998).

The importance of the T1SS is demonstrated by its numerous transport substrates, which vary from small proteins like the hemophore HasA (19 kDa) to huge surface layer proteins up to 900 kDa in size (Letoffe et al., 1994; Hinsa et al., 2003; Satchell, 2011). Other transported substrates include adenylate cyclases, lipases and proteases. One of the best-characterized T1SSs and the first to be identified is the hemolysin A (HlyA) secretion machinery of *Escherichia coli*. HlyA is found in most uropathogenic strains and was discovered in the early 1980s (Springer and Goebel, 1980; Welch et al., 1981, 1983; Mackman and Holland, 1984). Therefore it represents one of the paradigms of T1SSs.

Despite extensive research on the system, many aspects are still controversial. In this review we gather together existing results regarding the following questions:

- Does substrate folding take place prior or after the transport process?
- Which parts of the substrate and the components of the transport complex interact with each other?
- What is the specific function of the components of the translocon during assembly and transport?

Furthermore, we will speculate about the transport mechanism in the light of the questions raised above.

Components of the type 1 secretion system

The outer membrane protein

An OMP is an essential part of the T1SS and knock-out mutants lead to secretion deficient bacterial strains (Wandersman and Delepelaire, 1990). Members of this family include TolC, PrtF, CyaE and LipD (Delepelaire, 2004). TolC is the best-characterized protein of this family, since in addition to biochemical and functional studies, the structure of TolC in the closed and 'sequential open state' is known (Koronakis et al., 2000; Pei et al., 2011). Here, the 'sequential open state' describes the structure of the partially open periplasmic gate of TolC. Furthermore, secretion-deficient mutants were used to identify crucial amino acids, cross-linking studies investigated the closed state of the pore in great detail and conductance experiments of the transition states with a 'sequentially open' state of TolC resulted in a detailed picture of the protein's function (Vakharia et al., 2001; Andersen et al., 2002; Eswaran et al., 2003). TolC is not only involved in protein transport through the T1SS of Cva and Hly but is also an essential part of multiple drug efflux systems in *E. coli* such as Acr, Mac and Emr (Koronakis et al., 2004).

The homotrimeric TolC is 140 Å in length, as shown in Figure 1A, from its periplasmic tip region to the extracellular loops of its β-barrel, and builds a continuous channel that spans the outer membrane and extends to a large extent into the periplasmatic space. The β-barrel measures 40 Å in the outer diameter and consists of four β-strains per monomer, which form a hollow cylindrical shape. A 100 Å tunnel formed by 12 α-helices follows the β-barrel and expands into the periplasm. These helices are packed laterally with two neighboring helices building an α-barrel, see Figure 1A (Koronakis et al., 2000). The interaction between two neighboring helices is stabilized by so called 'knobs-into-holes' packing (Koronakis et al., 2004). Here, the intermeshing of side chains stabilizes the assembly of the 12 laterally packed helices of the α-barrel (Koronakis et al., 2004). The accessible interior diameter of the water-filled pore is 20 Å (35 Å for the outer diameter), see Figure 1A and B. The periplasmic end formed by densely packed coiled coils is closed and only 3.5 Å in diameter. This is too small to allow passage of even ions, see Figure 1C (Delepelaire, 2004). Salt bridges and hydrogen bonds stabilize this closed conformation. The most important amino acids of the closed conformation are T152, D153, Y362 and R367, which are located in the coiled coil region at the periplasmic end of the pore. Conductivity experiments showed that the mutation of these amino acids to alanine resulted in a partly opened conformation of TolC (Andersen et al., 2002). The structure of the Y362F and R367S double mutant showed an enlarged periplasmic entrance of the protein (Figure 1D) due to a weakening of the ionic interactions between the monomers (Pei et al., 2011).

It is proposed that upon opening, TolC undergoes an 'iris-like motion' of the inner α-helical coiled coils around the outer coiled coils at the periplasmic ends of the α-barrel (Eswaran et al., 2003). Cross-linking studies have suggested that an untwisting of the 'entrance helices' is necessary for TolC-dependent substrate secretion (as in the case of the hemolysin T1SS), but not for TolC recruitment (Eswaran et al., 2003). Data from TolC mutants that form only open state structures emphasized this iris-like motion of the inner α-helical coiled coils (helices H7/H8). Helix H7 moves around helix H8 and together they move around the outer coiled coils (helices H3/H4) at the periplasmatic ends (Bavro et al., 2008; Pei et al., 2011). These structures highlight an increasing distance between the inner α-helical coiled coils from 12.2 Å in wild type TolC to 18.9 Å and 21.3 Å in the TolC mutants (Figure 1C and D). This increasing distance results in an increased conductivity ranging from 80 pS in wild type TolC to 370 pS and 1000 pS in the TolC mutants (Pei et al., 2011).

In all T1SSs, TolC or other OMPs in the active pore interact with a membrane fusion protein (Letoffe et al., 1996; Thanabalu et al., 1998). So far, direct interactions between OMPs and the cognate ABC transporter yet to be observed in T1SS and probably do not exist. In contrast, in the Acr multidrug efflux pump system TolC directly interacts with the secondary transporter AcrB (Tamura et al., 2005). Cross-linking experiments of cysteine residues introduced by site-directed mutagenesis showed that the transporter forms a complex by transient tip-to-tip interaction with TolC. In addition, structural data derived from the open state of TolC identified a binding groove for interaction with the membrane fusion protein AcrA (Bavro et al., 2008; Pei et al., 2011). This is also in line with cross-linking studies of site-specific TolC and AcrA cysteine variants (Lobedanz et al., 2007). The binding groove is located between the lower α-helical barrel of TolC and the N-terminal α-helix of the AcrA coiled coil. As mentioned above, the α-helical domain of MFPs, especially the α-hairpin, seems to be essential for interaction with TolC (Stegmeier et al., 2006; Kim et al., 2010). The open state structure of TolC allows us to speculate that a larger interaction interface with the N-terminal α-helix of the MFP could be possible (Pei et al., 2011).

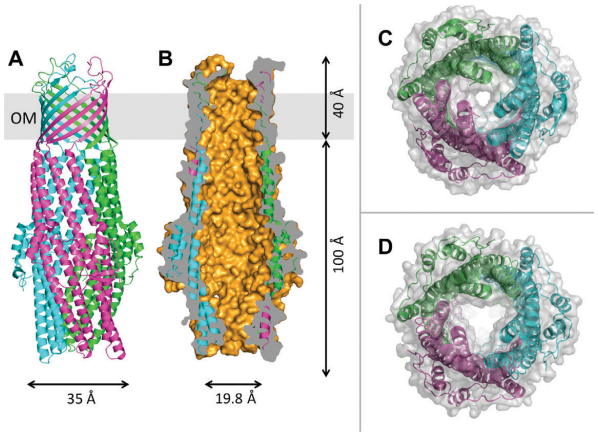

Figure 1 Structural overview of TolC.
(A) Cartoon representation of the side view of the TolC homotrimer in its closed state. The different monomers of TolC are highlighted in green, cyan and magenta. (B) A cross-section side view of a space-filling model of the TolC trimer shows a near-continuous channel from the β-barrel in the outer membrane (OM) to the periplasmic entrance of the α-barrel. The gray surface highlights the cross-sectional area in combination with a cartoon representation of the side view of the TolC homotrimer. The bright orange surface shows the inner and outer surface of the part of TolC (the black arrows indicate the dimensions of TolC). (C) View through the closed pore towards the periplasmic entrance of the α-barrel. Monomers are highlighted in green, cyan and magenta. To illustrate the closed conformation, the shape of the surface of TolC is shown in transparent gray panels (A, B and C are based on Protein Data Bank entry 1EK9). (D) View through a sequential open state of the pore towards the periplasmic entrance of the α-barrel. The monomers are highlighted in green, cyan and magenta. To illustrate the sequential open conformation, the shape of the surface of TolC is shown in transparent gray panels (D is based on Protein Data Bank entry 2XMN).

Molecular dynamic simulation of TolC indicated the possibility of a more complex pattern of conformational movements. In particular, a peristaltic motion in the periplasmatic domain that may facilitate transport of the substrates through the tunnel was proposed. Furthermore, movement was observed in coarse-grained simulations and two putative gate regions, located at either end of the protein, were identified. However, additional simulation of TolC also suggested that the cylindrical shape of the β-barrel represents a crystallographic artifact. After 2 nanoseconds of simulation, the barrel changed its shape to that of a more triangular prism. This conformation was also observed in the crystal structure of the functional TolC homolog OprM (Akama et al., 2004a; Vaccaro et al., 2008).

The membrane fusion protein

Bacterial MFPs are a highly diverse group in terms of structures and mechanisms (Zgurskaya et al., 2009). MFPs are involved in many multicomponent transport systems such as T1SSs or multidrug efflux systems. The transporter components of these systems are members of the resistance-nodulation-cell division, ABC or major facilitator superfamilies. So far, no structures of any MFPs involved in T1SS are available, but structures of analogous proteins involved in multidrug resistance, such as AcrA (Higgins et al., 2004) or MacA, have been reported. Several structures for other MFPs are also available, like CusB or MexA, which will not be discussed in detail here (Akama et al., 2004b; Su et al., 2009). AcrA and MacA are part of tri-partite multidrug efflux pumps. AcrA interacts with a transporter of the resistance-nodulation-cell division family and MacA interacts with an ABC-transporter. All MFPs share a highly conserved C-terminal part, whose structure is not resolved in the crystals. It has however been shown that this part of the molecule is essential for the secretion process of the transport complex (Schulein et al., 1994).

In contrast to the lipid anchor of AcrA and a single transmembrane spanning helix of MacA, MFPs of T1SSs contain a single transmembrane-spanning helix and a cytoplasmic tail (Figure 3 shows this part as a circle). In the case of the hemolysin T1SS, it has been demonstrated that the MFP hemolysin D (HlyD) directly interacts with the transport substrate and that its presence is essential for the assembly of the secretion complex and for the

secretion process itself (Balakrishnan et al., 2001). In contrast, co-precipitation experiments of other T1SSs such as HasE or PrtE indicated no direct interaction of the MFP with the substrate (Letoffe et al., 1996).

Most MFPs, including those of T1SSs, contain an α-helical domain (Johnson and Church, 1999). In the case of AcrA and MacA, this α-helical domain, especially the α-hairpin, is essential for interaction with TolC (Kim et al., 2010; Xu et al., 2010, 2011b). Mutants of the α-hairpin of the α-helical domain in HlyD disturbed this interaction (Lee et al., 2012). The MFPs of T1SSs are also involved in folding substrates into their native conformation. In the case of hemolysin and colicin V, amino acid substitution of MFPs resulted in reduced transport efficiencies associated with incorrectly folded substrates in the extracellular space (Hwang and Tai, 1999; Pimenta et al., 2005).

In vivo experiments showed that AcrA, MexA and HlyD can be cross-linked, resulting in the detection of dimers or trimers (Zgurskaya and Nikaido, 2000; Balakrishnan et al., 2001; Nehme and Poole, 2007; Zgurskaya et al., 2009). These results were obtained in the absence of the transporter and TolC (Zgurskaya et al., 2009). Recent models, however, propose higher-order oligomeric states. Thus, AcrA may form hexamers, as derived from electron microscopic studies (Xu et al., 2011a). MacA forms stable hexamers in solution that were also obtained inside the crystals (Yum et al., 2009). Studies using surface plasmon resonance spectroscopy also showed that MFPs are prone to oligomerization. In the case of MacA, stable oligomers were formed and survived for more than 3 minutes. The oligomers of EmrA were formed with low-micromolar affinity, whereas AcrA oligomerization requires non-physiological protein concentrations (Tikhonova et al., 2009). The data demonstrate decreasing stability of MFP oligomers in the order MacA, EmrA, AcrA. Furthermore, the stability of the MFP–TolC complex was correlated with the same order of stability as MFP oligomers. These authors assumed that the dynamic nature and variations in MFP oligomerization correlates with structural particularities of the respective IM transporters.

The ABC transporter

ABC transporters are ATP-dependent primary transporters. They are found in archeae, prokaryotes and eukaryotes and are able to transport a broad range of substrates across biological membranes (Higgins, 1992). The general ABC transporter blueprint includes two hydrophobic transmembrane domains (TMDs) and two highly conserved hydrophilic nucleotide-binding domains (NBDs, Figure 2). The NBDs supply the energy needed for transport by nucleotide binding, Mg^{2+} coordination and/or hydrolysis (Oswald et al., 2006). All components of the ABC transporter can be found as a four-domain polypeptide or assembled from up to four subunits encoded by different genes into a stable complex (Kerr, 2002; Davidson et al., 2008; Zolnerciks et al., 2011).

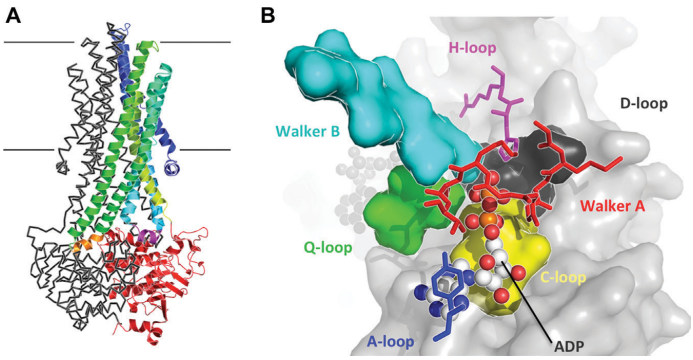

Figure 2 Spatial arrangement of an ATP-binding cassette exporter and structural features of the ATP-binding cassette exporter nucleotide-binding domains (NBDs).
(A) Structure of Sav1866 from *Saccharomyces aureus* with bound ADP (Protein Data Bank entry 2HYD) and for clarity with one monomer colored dark gray. The other monomer's transmembrane domains are colored in blue, cyan, yellow and green, while the corresponding NBD is colored red. Coupling helix 1 (purple helix) is thought to make contact with both NBDs during formation of the nucleotide sandwich. Coupling helix 2 (orange helix) is always domain-swapped to interact with the opposing NBD. (B) Close-up view of the gray NBD and the sandwiched ADP molecule. Directly involved conserved motifs are colored as follows: Walker A, red; Q-loop, green; H-loop, purple; Walker B, cyan; A-loop, blue; C-loop, yellow; D-loop, black.

In consideration of the NBD's crucial role in transforming chemical energy to mechanical movement translocation, it is not surprising that the primary sequence of NBDs is highly conserved (Seeger and van Veen, 2009). Each NBD consists of two subdomains with several highly conserved motifs (Figure 2). Thus, for example, the α-helical subdomain carries the ABC signature motif (also called the C-loop) represented by the sequence motif LSGGQ (Ames et al., 1992). This motif is the hallmark of the ABC transporter superfamily. The catalytic subdomain contains six conserved motifs (Walker A, Walker B, Q-loop, A-loop, H-loop, and D-loop). For detailed reviews on the function of each motif see, Oswald et al. (2006) or Seeger and van Veen (2009). In contrast to these motifs conserved in all ABC transporters (exporters and importers), the X-loop (consensus sequence TEVGERG) is only found in ABC-exporters and appears to be involved in interdomain communication and cross-talk between the NBD and the TMD (Dawson and Locher, 2006).

Several structural studies have shown that NBDs act as functional dimers, such as MJ0796, an uncharacterized ABC transporter (Smith et al., 2002), MalK the ATPase subunit of the maltose transporter (Chen et al., 2003) and the NBD of HlyB (Schmitt et al., 2003; Zaitseva et al., 2006). Furthermore, an oligomeric active conformation was confirmed through the dependence of ATPase activity on HlyB–NBD concentration (Zaitseva et al., 2006). Further analysis suggested an ATP-induced dimerization, emphasizing the role of the dimer as the active form of the enzyme (Zaitseva et al., 2005). Thus, two NBDs form a functional unit, enclosing two nucleotide-binding sites at their interfaces. These cavities form a 'nucleotide sandwich' (Smith et al., 2002) with a 'head-to-tail' arrangement of the NBDs. This arrangement was first predicted by Jones and George (1999), subsequently verified in the MalK structure (Chen et al., 2003) and finally confirmed via the structure of the multidrug ABC transporter Sav1866 by Hollenstein et al. (2007).

In contrast to the NBD, the ABC-TMDs vary greatly in sequence, architecture and the number of transmembrane helices. Most ABC exporters exhibit six α-helices per TMD, which extend as intracellular loops into the cytoplasm. Consequently, the NBD is about 25 Å away from the membrane. The 'coupling helices' are postulated to be involved in the transmission of crucial conformational changes from the NBDs to the TMDs. In the case of ABC exporters, coupling helix 1 is flanked by transmembrane helices 2/3, and is thought to make contact with both NBDs (Figure 2A, purple helix). Coupling helix 2 is flanked by transmembrane helices 4/5, is always domain-swapped, and interacts with the opposing NBD (Figure 2A, orange helix) (Dawson and Locher, 2006). In contrast, ABC importers contain between five (MetI) (Hollenstein et al., 2007; Oldham et al., 2007; Kadaba et al., 2008) and ten (BtuC) (Locher et al., 2002; Pinkett et al., 2007) α-helices per TMD, occasionally containing an additional N-terminal transmembrane helix that is domain swapped to the other TMD. Furthermore, ABC importers possess only one coupling helix, coupling helix 1, while coupling helix 2 is absent.

In the case of T1SS, secretion-defective HlyA mutants with an altered C-terminal secretion signal could be complemented by mutations within the corresponding ABC transporter HlyB (Zhang et al., 1993). These experiments demonstrated that ABC transporters recognize and bind to the cognate transport substrate. Surface plasmon resonance studies of the HlyB-NBD and HlyA provided further evidence for a specific interaction of the C-terminal 50 residues of the substrate with its ABC transporter (Benabdelhak et al., 2003). This highlights the fact that the NBD plays a crucial role in substrate recognition. In this T1SS, functional analysis of hybrid transporters formed by PrtD, PrtE and PrtF with HasD, HasE and TolC, respectively, demonstrated *in vivo* that the ABC transporter is responsible for recognition of the substrate (Binet and Wandersman, 1995). Moreover, the transporter might even be involved in 'protecting' the substrate as shown in the case of HlyB. Here, the canonical composition of four modules (two TMDs and two NBDs) is supplemented by an additional N-terminal extension of 123 amino acids, called the 'C39-like domain' (CLD). The CLD is indispensible for secretion and binds exclusively the unfolded state of the Repeats in Toxins (RTX) domain of HlyA (Lecher et al., 2012). As no known chaperone is likely involved in protecting unfolded HlyA inside the cell (Holland et al., 2005), the CLD of HlyB is thought to fulfill this role (Lecher et al., 2012). In parallel to binding the transport substrate, an ABC transporter seems to play a crucial role in recruitment of the other components of the transport complex, a process that is only initiated in the presence of the signal sequence of the substrate. In the case of HasA lacking the C-terminal secretion signal, the protein – as expected – is not secreted. However, assembly of the transport complex still takes place (Cescau et al., 2007). Further investigations using substrate affinity-chromatography revealed an ordered recruitment of the transport complex. Thus, the substrate initiates this process while interacting with the ABC transporter, which in turn interacts with the membrane fusion protein. Finally, the outer membrane factor is engaged (Letoffe et al., 1996) to complete the transport pathway.

The role of ABC transporters in the assembly of a functional complex also depends on ATP, as shown in the case of HlyB (Thanabalu et al., 1998) and MacB, an ABC transporter and founding member of the macrolide exporter family. MacB interaction with the corresponding membrane fusion protein was also observed in the presence of ATP (Lu and Zgurskaya, 2012), which suggested that binding of ATP initiates transport complex recruitment (Thanabalu et al., 1998). Further ATP hydrolysis energizes substrate transport (Koronakis et al., 1993, 1995; Letoffe et al., 2001). ATP also appears to compete with the secretion signal of HlyA for binding to the HlyB-NBDs complex release, as shown by surface plasmon resonance spectroscopy for the hemolysin system (Benabdelhak et al., 2003). Further studies validate the importance of ATP as they have shown that complex release only occurs in the presence of an intact Walker B motif (Masi and Wandersman, 2010).

Signals affecting secretion

Transport substrates of T1SS share several common denominators. The secretion signal is usually located at the C-terminal end (last 50–60 C-terminal amino acids) and is not cleaved during transport (Nicaud et al., 1986; Mackman et al., 1987; Jarchau et al., 1994). Its presence is necessary and sufficient for secretion (Gray et al., 1986; Stanley et al., 1991; Kenny et al., 1994). Therefore, the secretion signal has been fused to non-secretable proteins, which consequently become substrates of T1SS. Nevertheless, the sequence reveals no clear consensus, suggesting that the secondary structure is the recognition motif (Wolff et al., 1994; Zhang et al., 1995). The secretion signal seems to consist of two α-helices bridged by a linker peptide and followed by an unstructured and flexible region (Hui et al., 2000; Hui and Ling, 2002).

Some transport substrates like HasA are secretion-competent while containing only this secretion signal, whereas other substrates contain additional motifs (Finnie et al., 1998; Delepelaire and Wandersman, 2003). Most secreted proteins of T1SSs belong to the RTX family. These are characterized by glycine-rich repeats located close to the secretion signal and giving rise to the name RTX (Strathdee and Lo, 1989). Nearly all members of this family are secreted by T1SS and have distinctive repeats with the consensus sequence GGxGxDxxx (GG repeat), where x can be any amino acid (Ludwig and Goebel, 1999; Linhartova et al., 2010). A sequence analysis of bacterial genomes revealed that GG repeats containing proteins vary greatly in size (from 78 to 8682 residues), nearly all of them have an acidic isoelectric point (pI) and contain very few or no cysteines (Delepelaire, 2004). The parallel β-roll or β-sandwich structure appears to promote folding into the active conformation by binding of calcium ions to these nonapeptide repeats (Rose et al., 1995; Rhodes et al., 2001). Folding is induced outside of the cell, because of the low intracellular calcium concentration (<100 nM) (Gangola and Rosen, 1987; Ludwig et al., 1988; Jones et al., 1999).

Type 1 secretion occurs in an unfolded state

If we consider that the interior diameter of TolC is 20 Å in size (Koronakis et al., 2004), which is comparable to the width of two α-helices oriented parallel or antiparallel to each other, the question arises of how proteins of up to 900 kDa in size can be secreted through such a small pore. One possibility could be that secretion occurs in an unfolded conformation across both membranes of Gram-negative bacteria. Evidence for translation of unfolded substrates has been obtained, for example, for HlyA (Bakkes et al., 2010) and HasA (Debarbieux and Wandersman, 2001).

At least one T1SS relies on SecB interaction. Research investigating HasA secretion has revealed a direct dependency of HasA secretion on the presence of SecB (Delepelaire and Wandersman, 1998; Sapriel et al., 2003). It has been shown that SecB keeps HasA in transport-competent, unfolded or at least loosely-folded state. However, in the case of the hemolysin T1SS, SecB is not involved in secretion (Bakkes et al., 2010). Furthermore the C-terminal 60 amino acids of T1SS substrates are indispensable for secretion (Mackman et al., 1987; Stanley et al., 1991; Gentschev et al., 1995; Chervaux and Holland, 1996). Second, Bakkes et al. (2010) showed that folding rates dictated secretion level; slow folding proteins, forming unfolded intermediates, resulted in higher secretion levels in contrast to fast folding proteins. Taking this into account, we have been able to impose secretion of non-native T1SS substrates, for example, the maltose binding protein. Slow folding mutations affected the speed of folding but not the refolding velocity or functionality of the mature maltose binding protein (Bakkes et al., 2010). Another example emphasizing the importance of folding rate in the promotion of secretion was a fusion of a C-terminal fragment of HlyA containing the secretion signal with the cytosolic eukaryotic intestinal fatty acid binding protein. Again, only a

slow-folding mutant could be secreted, in contrast to the wild-type protein (Schwarz et al., 2012). Following secretion and folding, the slow folding mutant was biologically active, showing the same binding affinity for DAUDA, a fluorescence fatty acid analog, as the wild type (Schwarz et al., 2012).

Transport mechanism of type 1 secretion system

The exact mechanism and assembly of T1SS is not understood and many questions remain unanswered. For example how do T1SSs transport their substrate in an energetically favorable way? How much ATP is used for one secretion cycle? Are there any other energy sources that favor the secretion process? Is the N-terminal end or the C-terminal part secreted first?

This leads to another question, namely what is the role of the secretion signal? Is the secretion signal responsible for dissociation of the type 1 translocon, its assembly or both? What prevents large substrates like RTX toxins that are secreted in an unfolded form from being degraded in the cell? Finally, do the MFP and OMP also have a direct function during secretion or are they only involved in forming the tunnel-channel that spans both membranes?

We cannot answer these questions in this review but at least we want to summarize possible mechanisms and try to answer the questions based on today's knowledge.

Energizing type 1 secretion system transport

The stoichiometry of ATP consumption during the transport process of an ABC transporter has been characterized. In the case of the ABC importer OpuA from *Lactococcus lactis* (Patzlaff et al., 2003) and the maltose and glycine-betaine import system of *E. coli* (Mimmack et al., 1989), two ATP molecules are hydrolyzed during one transport cycle. In contrast, TAP1/2 or CFTR hydrolyses only one ATP during transport cycle (Chen et al., 2004; Zhou et al., 2006).

In the case of T1SS, the number of ATP molecules consumed per transport cycle is unknown. For proteins of up to 900 kDa such as LapA in *Pseudomonas fluorescens* (Hinsa et al., 2003) it seems, at first glance, impossible that only two ATP molecules are required to energize this process. In comparison, the Sec pathway consumes one ATP per 20–30 amino acids translocated (Schiebel et al., 1991; Uchida et al., 1995). Such an iterative ATP hydrolyzing process for energizing the transport of T1SS has not been confirmed so far.

The question is how T1SSs manage to energize the transport process. It was reported that the proton motive force (PMF) is partly involved in the early stages of HlyA translocation. HlyA secretion was inhibited if the membrane potential and the proton gradient of the PMF collapsed. Furthermore, selective depletion of the proton gradient also blocked successful secretion (Koronakis et al., 1991).

Most of the T1SS substrates have an isoelectric point below 5 (Delepelaire, 2004). This indicates that substrates have an overall negative charge within the cell, resulting in a charge gradient across the membrane. Furthermore, the concentration of the substrate inside the cell is much higher than in the extracellular space. A concentration gradient and the PMF facing outward might allow diffusion across the cell wall and both membranes.

During transport, as deduced from crystal structures of putative intermediates, an ABC transporter occurs in at least two different conformations. The inward-facing conformation represents a state of the ABC transporter open to the cytoplasm, while the outward-facing conformation is open to the periplasm. Some evidence indicates that the alternative conformations have different binding affinities (Martin et al., 2001). The inward facing conformation may have a higher binding affinity in comparison to the outward facing conformation. Therefore, the inward facing conformation binds the substrate, whereas the outward facing conformation promotes the release of the substrate into the extracellular space. Importantly, this mechanism could also prevent the reverse transport of the substrate. This mechanism is effective for small proteins, but the question arises as to how this can be directly transferred to mechanisms of higher polypeptides.

Another driving force for the type 1 secretion process could be linked to the glycine-rich repeats found in most T1SS substrates (Delepelaire, 2004). The amount of the repeats correlates with the size of the protein and occurs mainly with one repeat for every 6–12 kDa (Delepelaire, 2004; Linhartova et al., 2010). As mentioned above, these repeats bind Ca^{2+} ions and induce folding of the protein. Inside bacterial cells, the Ca^{2+} concentration is around 100 nM (Jones et al., 1999), which will prevent folding. After secretion, the proteins start folding in the extracellular space where the Ca^{2+} concentration is much higher. The Ca^{2+}-induced folding of the proteins could involve an inherent driving force, which 'pulls' the protein through the transporter. Such a pulling mechanism is mentioned

by Linhartova et al. (2010) and is supported by various experimental data from the hemolysin T1SS. The folding of the proteins would also prevent transport in the opposite direction, because folded proteins are too large to re-enter the TolC pore.

The role of the secretion signal

As mentioned above, many results concerning different T1SSs demonstrate that the C-terminal secretion signal of the substrates is required for secretion and directly effect the catalytic cycle of the NBDs of the ABC transporter. However, the impact appears to vary depending on the effect of the signal sequence on catalytic activity between different T1SSs. In the case of HasA, the secretion signal seems to be responsible for HasD-driven ATP hydrolysis and dissociation of the translocation complex (Masi and Wandersman, 2010). Data for the T1SS metalloproteases PrtB and PrtG of *Erwinia chrysanthemi* suggest that *in vitro* the secretion signal inhibits the ATPase activity of the ABC transporter PrtD (Delepelaire, 1994). These results lead to two fundamentally different mechanisms of how the secretion signal controls secretion. Does the secretion signal induce ATP binding/dimerization of the NBDs and thus induce secretion by switching the transporter from an inward- to an outward-facing conformation (activating model) concomitant with ATP hydrolysis? Or does the secretion signal trigger ATP-hydrolysis of the ABC transporter only at the last stage, leading to substrate release on the surface and dissociation of the secretion complex (terminating model)?

Figure 3 highlights how an 'activating model' could work. First, binding of ATP and the secretion signal of the substrate induce dimerization of the NBDs and simultaneously trigger recruiting of TolC to the secretion complex. In a second step, the ABC transporter changes the conformation of the TMDs to open up the transport pathway,

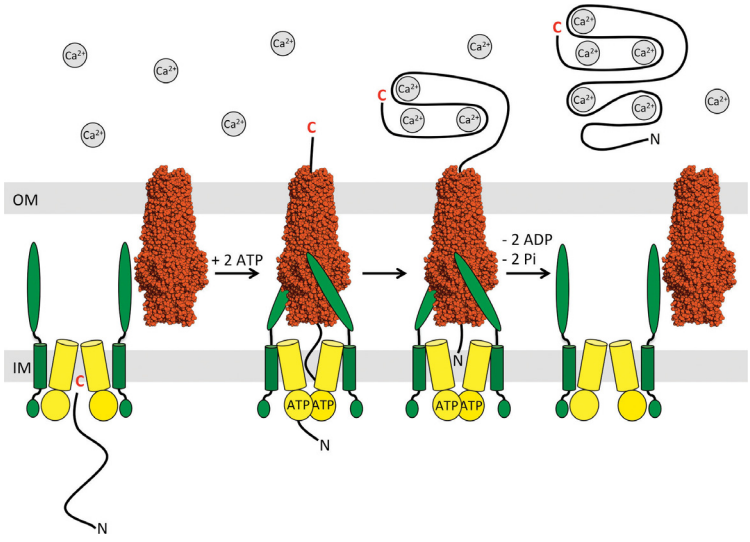

Figure 3 Possible steps of an activating type 1 secretion system pathway.
In the first step the outer membrane (OM) TolC (shown in side view as orange spheres and based on Protein Data Bank entry 1EK9), in the presence of the transport substrate, is recruited by the MFP and the ATP-binding cassette (ABC) protein (highlighted in green and yellow, respectively) located in the inner membrane. The oligomeric state of the membrane fusion protein (MFP) is unknown so far but to ensure a better overview only two MFPs are shown. TolC recruitment is mediated by binding of the substrate secretion signal to the two IM proteins, ATP-binding cassette transporter and MFP. Simultaneously, the binding of the secretion signal initiates ATP binding by the ABC transporter. The resulting conformational changes in the transmembrane domains of the ATP-binding cassette transporter displace the C-terminus of the unfolded substrate into the translocator. Third, the substrate is 'pulled' through the translocator by progressive folding in the calcium-rich extracellular space (calcium ions highlighted as gray dots). When the substrate passes completely through the translocator, it is presumed that this triggers ATP hydrolysis of both ATP molecules and will reset the transporter to its initial state. Finally, the transport complex dissociates and releases ADP and free phosphate into the cytoplasm. The fully folded substrate then diffuses into the extracellular space.

with the secretion signal leading the way into and through the transenvelope channel. In a third step, the substrate translocates progressively to the extracellular space, where folding and finally dissociation from the complex takes place. In a fourth step, the release of the substrate is in some way detected by the transporter and ATP-hydrolysis is triggered, which resets the transporter (switching from an outward- to an inward-facing conformation). This results in the disassembly of the whole secretion complex. Despite this, a detailed mechanism initiating ATP-hydrolysis is so far still unclear.

A 'terminating model' of protein secretion for type 1 secretion of HasA has also been proposed. Transport has to be initiated by a so-far unknown factor and leads to binding of ATP and the substrate. The substrate is bound by N-terminal 'anchors' to the ABC transporter and leads to the recruitment of the other subunits of the transport complex (Masi and Wandersman, 2010). Through ATP-binding, dimerization of the NBDs is induced, which leads to a switch of the transporter from an inward- to an outward-facing conformation. In the following step, the substrate is secreted with its N-terminus first and traverses the transport channel to the extracellular space. Finally, interaction of the C-terminal secretion signal induces ATP hydrolysis, which resets the transporter to an inward-facing conformation, releases the secreted protein and dissembles the translocation complex.

The main difference between the models is the orientation of the substrate during secretion, the C-terminal signal sequence either leading the way through the translocator or being the last to enter the channel. In favor of the activating model is the fact that many fusion proteins are secreted by the hemolysin T1SS (Mackman et al., 1987; Kenny et al., 1991; Blight and Holland, 1994; Gentschev et al., 2002; Bakkes et al., 2010; Schwarz et al., 2012). These proteins are fused at their C-terminus to a fragment of HlyA that contains the secretion signal. The secretion process can therefore only start after translation of the secretion signal. Furthermore, the isolated secretion signal of HlyA can be secreted autonomously by the T1SS (Jarchau et al., 1994) and contains all information for secretion.

In the case of HasA, multiple upstream regions of the primary sequence (anchoring sequences) appear to interact with the ABC transporter HasD (Masi and Wandersman, 2010). Other authors propose that the secretion signal is important for the dissociation of the secretion complex by affecting the catalytic cycle of the NBDs (Cescau et al., 2007). For these reasons, the 'terminating model' would be more appropriate in the case of HasA.

What protects unfolded intracellular type 1 secretion system substrates from degradation?

Several different experiments indicate that T1SS substrates are secreted in an unfolded state (Debarbieux and Wandersman, 2001; Bakkes et al., 2010). As mentioned above, the resulting question is what prevents the unfolded substrates from degradation?

In the case of the hemolysin T1SS, the ABC transporter contains a N-terminal appendix (CLD), with extensive identity to C39 proteases. The structure of the isolated domain was solved by nuclear magnetic resonance spectroscopy (Lecher et al., 2011). In contrast to regular C39 proteases like ComA from *Streptococcus pneumonia* (Ishii et al., 2010), the catalytic triad is degenerated and there is no enzyme activity. The CLD interacts with HlyA and is specifically required for secretion. Pull-down assays have indicated a specific interaction of the CLD with unfolded HlyA but not with its folded conformation (Lecher et al., 2012). Thus, the CLD interacts inside the cell with unfolded HlyA, perhaps acting as a chaperone to protect HlyA from degradation.

The N-terminal CLD is not present in all ABC transporters of T1SSs. How do other systems without a CLD manage to protect the unfolded substrate against degradation? For HasA, a small protein with no GG repeats, SecB was clearly shown to be required for HasA secretion (Delepelaire and Wandersman, 1998; Sapriel et al., 2003; Wolff et al., 2003). However, the question remains as to how other T1SSs that are SecB-independent like Prt (Delepelaire and Wandersman, 1998) and do not contain a CLD manage to stabilize their intracellular substrates.

Function of membrane fusion protein and outer membrane protein components of the translocator

MFPs and OMPs assemble to form a continuous channel together with the ABC transporter, which crosses both membranes and allows secretion of this cognate protein. Nevertheless, studies of random point mutations in MFPs, in particular HlyD (Pimenta et al., 2005) and CvaA (Hwang and Tai, 1999) and in OMPs, notably TolC (Vakharia et al., 2001), resulted in incorrect folding of the substrates, although these were secreted in normal amounts. In the case of TolC, six mutants were identified that had normal secretion levels but reduced hemolytic activity (Vakharia et al., 2001). The activity of secreted HlyA could be restored by de- and renaturating *in vitro*. Time-course experiments

in this study showed that HlyA is secreted more slowly in the mutants. This may point to a role of TolC in interacting with HlyA, thereby altering its correct folding (Delepelaire, 2004).

Specific mutants in MFPs resulted in similar phenotypes. In the case of HlyD, specific mutations in the periplasmic part of the protein resulted in reduced hemolytic activity of secreted HlyA (Pimenta et al., 2005). The amount of HlyD and HlyA in the mutants was similar to that of the wild type and the hemolytic activity of HlyA could be restored as in the case of TolC mutants by de- and renaturating *in vitro* (Pimenta et al., 2005). Another interesting aspect is that the hemolytic activity of these HlyD mutants is reduced by increasing the extracellular Ca^{2+} concentration. The exact role of Ca^{2+} is not completely understood and is highly speculative to the extent that it affects the formation and stable packing of the HlyD molecules and results in an aberrant movement of HlyA through the translocator (Pimenta et al., 2005).

Conclusion

The T1SS is one of the most important systems for the one-step secretion of substrates in Gram-negative bacteria, as shown by their ubiquitous occurrence and wide substrate range. Furthermore, the transport system is fascinating due to its simple arrangement of three components, enabling an energetically-favorable transport process over a huge distance. Current biochemical and structural data from T1SSs allow only an overview of the transport process. One of the most challenging and crucial aspects will be the investigation of the interaction of all translocator components. Further structural analysis will be essential to gain a better understanding of the transport mechanism and especially the key role of the ABC transporter.

Acknowledgments: We thank all members of the Institute of Biochemistry, Heinrich-Heine-Universität Düsseldorf, for helpful and very fruitful discussions. We gratefully acknowledge support (and training) from the International NRW Research School BioStruct, granted by the Ministry of Innovation, Science and Research of the State North Rhine-Westphalia, the Heinrich-Heine-University Düsseldorf, and the Entrepreneur Foundation at the Heinrich-Heine-University of Düsseldorf. Apologies to all our colleagues who contributed to our current understanding of T1SS but were not referenced due to space limitations.

Received May 6, 2013; accepted July 2, 2013; previously published online July 5, 2013

References

Akama, H., Kanemaki, M., Yoshimura, M., Tsukihara, T., Kashiwagi, T., Yoneyama, H., Narita, S., Nakagawa, A., and Nakae, T. (2004a). Crystal structure of the drug discharge outer membrane protein, OprM, of *Pseudomonas aeruginosa*: dual modes of membrane anchoring and occluded cavity end. J. Biol. Chem. *279*, 52816–52819.

Akama, H., Matsuura, T., Kashiwagi, S., Yoneyama, H., Narita, S., Tsukihara, T., Nakagawa, A., and Nakae, T. (2004b). Crystal structure of the membrane fusion protein, MexA, of the multidrug transporter in *Pseudomonas aeruginosa*. J. Biol. Chem. *279*, 25939–25942.

Ames, G.F., Mimura, C.S., Holbrook, S.R., and Shyamala, V. (1992). Traffic ATPases: a superfamily of transport proteins operating from *Escherichia coli* to humans. Adv. Enzymol. Relat. Areas. Mol. Biol. *65*, 1–47.

Andersen, C., Koronakis, E., Bokma, E., Eswaran, J., Humphreys, D., Hughes, C., and Koronakis, V. (2002). Transition to the open state of the TolC periplasmic tunnel entrance. Proc. Nat. Acad. Sci. USA *99*, 11103–11108.

Bakkes, P.J., Jenewein, S., Smits, S.H., Holland, I.B., and Schmitt, L. (2010). The rate of folding dictates substrate secretion by the *Escherichia coli* hemolysin type 1 secretion system. J. Biol. Chem. *285*, 40573–40580.

Balakrishnan, L., Hughes, C., and Koronakis, V. (2001). Substrate-triggered recruitment of the TolC channel-tunnel during type I export of hemolysin by *Escherichia coli*. J. Mol. Bol. *313*, 501–510.

Bavro, V.N., Pietras, Z., Furnham, N., Perez-Cano, L., Fernandez-Recio, J., Pei, X.Y., Misra, R., and Luisi, B. (2008). Assembly and channel opening in a bacterial drug efflux machine. Mol. Cell *30*, 114–121.

Benabdelhak, H., Kiontke, S., Horn, C., Ernst, R., Blight, M.A., Holland, I.B., and Schmitt, L. (2003). A specific interaction between the NBD of the ABC-transporter HlyB and a C-terminal fragment of its transport substrate haemolysin A. J. Mol. Biol. *327*, 1169–1179.

Binet, R. and Wandersman, C. (1995). Protein secretion by hybrid bacterial ABC-transporters: specific functions of the membrane ATPase and the membrane fusion protein. EMBO J. *14*, 2298–2306.

Blight, M.A. and Holland, I.B. (1994). Heterologous protein secretion and the versatile *Escherichia coli* haemolysin translocator. Trends. Biotechnol. *12*, 450–455.

Cescau, S., Debarbieux, L., and Wandersman, C. (2007). Probing the in vivo dynamics of type I protein secretion complex association through sensitivity to detergents. bacteriology Bacteriol. *189*, 1496–1504.

Chen, J., Lu, G., Lin, J., Davidson, A.L., and Quiocho, F.A. (2003). A tweezers-like motion of the ATP-binding cassette dimer in an ABC transport cycle. Mol. Cell *12*, 651–661.

Chen, M., Abele, R., and Tampe, R. (2004). Functional non-equivalence of ATP-binding cassette signature motifs in the transporter associated with antigen processing (TAP). J. Biol. Chem. *279*, 46073–46081.

Chervaux, C. and Holland, I.B. (1996). Random and directed mutagenesis to elucidate the functional importance of helix II and F-989 in the C-terminal secretion signal of *Escherichia coli* hemolysin. J. Bacteriol. *178*, 1232–1236.

Davidson, A.L., Dassa, E., Orelle, C., and Chen, J. (2008). Structure, function, and evolution of bacterial ATP-binding cassette systems. MMBR *72*, 317–364.

Dawson, R.J. and Locher, K.P. (2006). Structure of a bacterial multidrug ABC transporter. Nature *443*, 180–185.

Debarbieux, L. and Wandersman, C. (2001). Folded HasA inhibits its own secretion through its ABC exporter. EMBO J. *20*, 4657–4663.

Delepelaire, P. (1994). PrtD, the integral membrane ATP-binding cassette component of the *Erwinia chrysanthemi* metalloprotease secretion system, exhibits a secretion signal-regulated ATPase activity. J. Biol. Chem. *269*, 27952–27957.

Delepelaire, P. (2004). Type I secretion in gram-negative bacteria. Biochim. Biophys. Acta. *1694*, 149–161.

Delepelaire, P. and Wandersman, C. (1998). The SecB chaperone is involved in the secretion of the *Serratia marcescens* HasA protein through an ABC transporter. EMBO J. *17*, 936–944.

Delepelaire, P. and Wandersman, C. (2003). Protein export and secretion in Gram-negative bacteria. In: Microbial Transport Systems, G. Winkelmann, ed. (Weinheim: Wiley-VCH Verlag GmbH & Co. KGaA), pp. 165–208.

Eswaran, J., Hughes, C., and Koronakis, V. (2003). Locking TolC entrance helices to prevent protein translocation by the bacterial type I export apparatus. J. Mol. Biol. *327*, 309–315.

Finnie, C., Zorreguieta, A., Hartley, N.M., and Downie, J.A. (1998). Characterization of *Rhizobium leguminosarum* exopolysaccharide glycanases that are secreted via a type I exporter and have a novel heptapeptide repeat motif. J. Bacteriol. *180*, 1691–1699.

Gangola, P. and Rosen, B.P. (1987). Maintenance of intracellular calcium in *Escherichia coli*. J. Biol. Chem. *262*, 12570–12574.

Gentschev, I., Dietrich, G., and Goebel, W. (2002). The *E. coli* alpha-hemolysin secretion system and its use in vaccine development. Trends. Microbiol. *10*, 39–45.

Gentschev, I., Sokolovic, Z., Mollenkopf, H.J., Hess, J., Kaufmann, S.H., Kuhn, M., Krohne, G.F., and Goebel, W. (1995). *Salmonella* strain secreting active listeriolysin changes its intracellular localization. Infect. Immun. *63*, 4202–4205.

Gray, L., Mackman, N., Nicaud, J.M., and Holland, I.B. (1986). The carboxy-terminal region of haemolysin 2001 is required for secretion of the toxin from *Escherichia coli*. Mol. Gen. Genet. *205*, 127–133.

Higgins, C.F. (1992). ABC transporters: from microorganisms to man. Ann. Rev. Cell Biol. *8*, 67–113.

Higgins, M.K., Bokma, E., Koronakis, E., Hughes, C., and Koronakis, V. (2004). Structure of the periplasmic component of a bacterial drug efflux pump. Proc. Nat. Sci. USA *101*, 9994–9999.

Hinsa, S.M., Espinosa-Urgel, M., Ramos, J.L., and O'Toole, G.A. (2003). Transition from reversible to irreversible attachment during biofilm formation by *Pseudomonas fluorescens* WCS365 requires an ABC transporter and a large secreted protein. Mol. Microbiol. *49*, 905–918.

Holland, I.B., Schmitt, L., and Young, J. (2005). Type 1 protein secretion in bacteria, the ABC-transporter dependent pathway (review). Mol. Membr. Biol. *22*, 29–39.

Hollenstein, K., Frei, D.C., and Locher, K.P. (2007). Structure of an ABC transporter in complex with its binding protein. Nature *446*, 213–216.

Hui, D. and Ling, V. (2002). A combinatorial approach toward analyzing functional elements of the *Escherichia coli* hemolysin signal sequence. Biochem *41*, 5333–5339.

Hui, D., Morden, C., Zhang, F., and Ling, V. (2000). Combinatorial analysis of the structural requirements of the *Escherichia coli* hemolysin signal sequence. J. Biol. Chem. *275*, 2713–2720.

Hwang, J. and Tai, P.C. (1999). Mutational analysis of CvaA in the highly conserved domain of the membrane fusion protein family. Curr. Microbiol. *39*, 195–199.

Ishii, S., Yano, T., Ebihara, A., Okamoto, A., Manzoku, M., and Hayashi, H. (2010). Crystal structure of the peptidase domain of *Streptococcus* ComA, a bifunctional ATP-binding cassette transporter involved in the quorum-sensing pathway. J. Biol. Chem. *285*, 10777–10785.

Jarchau, T., Chakraborty, T., Garcia, F., and Goebel, W. (1994). Selection for transport competence of C-terminal polypeptides derived from *Escherichia coli* hemolysin: the shortest peptide capable of autonomous HlyB/HlyD-dependent secretion comprises the C-terminal 62 amino acids of HlyA. Mol. Gen. Genet. *245*, 53–60.

Johnson, J.M. and Church, G.M. (1999). Alignment and structure prediction of divergent protein families: periplasmic and outer membrane proteins of bacterial efflux pumps. J. Mol. Biol. *287*, 695–715.

Jones, H.E., Holland, I.B., Baker, H.L., and Campbell, A.K. (1999). Slow changes in cytosolic free Ca2+ in *Escherichia coli* highlight two putative influx mechanisms in response to changes in extracellular calcium. Cell Calcium *25*, 265–274.

Jones, P.M. and George, A.M. (1999). Subunit interactions in ABC transporters: towards a functional architecture. FEMS Micriobiol. Lett. *179*, 187–202.

Kadaba, N.S., Kaiser, J.T., Johnson, E., Lee, A., and Rees, D.C. (2008). The high-affinity *E. coli* methionine ABC transporter: structure and allosteric regulation. Science *321*, 250–253.

Kenny, B., Chervaux, C., and Holland, I.B. (1994). Evidence that residues -15 to -46 of the haemolysin secretion signal are involved in early steps in secretion, leading to recognition of the translocator. Mol. Microbiol. *11*, 99–109.

Kenny, B., Haigh, R., and Holland, I.B. (1991). Analysis of the haemolysin transport process through the secretion from *Escherichia coli* of PCM, CAT or beta-galactosidase fused to the Hly C-terminal signal domain. Mol. Microbiol. *5*, 2557–2568.

Kerr, I.D. (2002). Structure and association of ATP-binding cassette transporter nucleotide-binding domains. Biochim. Biophys. Acta *1561*, 47–64.

Kim, H.M., Xu, Y., Lee, M., Piao, S., Sim, S.H., Ha, N.C., and Lee, K. (2010). Functional relationships between the AcrA hairpin tip region and the TolC aperture tip region for the formation of the bacterial tripartite efflux pump AcrAB-TolC. J. Bacteriol. *192*, 4498–4503.

Koronakis, E., Hughes, C., Milisav, I., and Koronakis, V. (1995). Protein exporter function and in vitro ATPase activity are correlated in ABC-domain mutants of HlyB. Mol. Microbiol. *16*, 87–96.

Koronakis, V., Eswaran, J., and Hughes, C. (2004). Structure and function of TolC: the bacterial exit duct for proteins and drugs. Ann. Rev. Biochem. *73*, 467–489.

Koronakis, V., Hughes, C., and Koronakis, E. (1991). Energetically distinct early and late stages of HlyB/HlyD-dependent secretion across both *Escherichia coli* membranes. EMBO J. *10*, 3263–3272.

Koronakis, V., Hughes, C., and Koronakis, E. (1993). ATPase activity and ATP/ADP-induced conformational change in the soluble domain of the bacterial protein translocator HlyB. Mol. Microbiol. *8*, 1163–1175.

Koronakis, V., Sharff, A., Koronakis, E., Luisi, B., and Hughes, C. (2000). Crystal structure of the bacterial membrane protein TolC central to multidrug efflux and protein export. Nature *405*, 914–919.

Lecher, J., Schwarz, C.K., Stoldt, M., Smits, S.H., Willbold, D., and Schmitt, L. (2012). An RTX transporter tethers its unfolded substrate during secretion via a unique N-terminal domain. Structure *20*, 1778–1787.

Lecher, J., Stoldt, M., Schwarz, C.K., Smits, S.H., Schmitt, L., and Willbold, D. (2011). 1H, 15N and 13C resonance assignment of the N-terminal C39 peptidase-like domain of the ABC transporter Haemolysin B (HlyB). Biomol. NMR Assign. *5*, 199–201.

Lee, M., Jun, S.Y., Yoon, B.Y., Song, S., Lee, K., and Ha, N.C. (2012). Membrane fusion proteins of type I secretion system and tripartite efflux pumps share a binding motif for TolC in gram-negative bacteria. PloS One *7*, e40460.

Letoffe, S., Delepelaire, P., and Wandersman, C. (1996). Protein secretion in gram-negative bacteria: assembly of the three components of ABC protein-mediated exporters is ordered and promoted by substrate binding. EMBO J. *15*, 5804–5811.

Letoffe, S., Deniau, C., Wolff, N., Dassa, E., Delepelaire, P., Lecroisey, A., and Wandersman, C. (2001). Haemophore-mediated bacterial haem transport: evidence for a common or overlapping site for haem-free and haem-loaded haemophore on its specific outer membrane receptor. Mol. Microbiol. *41*, 439–450.

Letoffe, S., Ghigo, J.M., and Wandersman, C. (1994). Secretion of the *Serratia marcescens* HasA protein by an ABC transporter. J. Bacteriol. *176*, 5372–5377.

Linhartova, I., Bumba, L., Masin, J., Basler, M., Osicka, R., Kamanova, J., Prochazkova, K., Adkins, I., Hejnova-Holubova, J., Sadilkova, L., et al. (2010). RTX proteins: a highly diverse family secreted by a common mechanism. FEMS Microbiol. Rev. *34*, 1076–1112.

Lobedanz, S., Bokma, E., Symmons, M.F., Koronakis, E., Hughes, C., and Koronakis, V. (2007). A periplasmic coiled-coil interface underlying TolC recruitment and the assembly of bacterial drug efflux pumps. Proc. Nat. Acad. Sci. USA *104*, 4612–4617.

Locher, K.P., Lee, A.T., and Rees, D.C. (2002). The *E. coli* BtuCD structure: a framework for ABC transporter architecture and mechanism. Science *296*, 1091–1098.

Lu, S., and Zgurskaya, H.I. (2012). Role of ATP binding and hydrolysis in assembly of MacAB-TolC macrolide transporter. Mol. Microbiol. *86*, 1132–1143.

Ludwig, A. and Goebel, W. (1999). The family of the multigenic encoded RTX toxin. In: The Comprehensive Sourcebook of Bacterial Protein Toxins, J.E. Alouf, and J.H. Freer, eds. (Amsterdam: Academic Press), pp. 330–348.

Ludwig, A., Jarchau, T., Benz, R., and Goebel, W. (1988). The repeat domain of *Escherichia coli* haemolysin (HlyA) is responsible for its Ca2+-dependent binding to erythrocytes. Mol. Gen. Genet. *214*, 553–561.

Mackman, N., Baker, K., Gray, L., Haigh, R., Nicaud, J.M., and Holland, I.B. (1987). Release of a chimeric protein into the medium from *Escherichia coli* using the C-terminal secretion signal of haemolysin. EMBO J. *6*, 2835–2841.

Mackman, N. and Holland, I.B. (1984). Functional characterization of a cloned haemolysin determinant from *E. coli* of human origin, encoding information for the secretion of a 107K polypeptide. Mol. Gen. Genet. *196*, 129–134.

Martin, C., Higgins, C.F., and Callaghan, R. (2001). The vinblastine binding site adopts high- and low-affinity conformations during a transport cycle of P-glycoprotein. Biochem. *40*, 15733–15742.

Masi, M. and Wandersman, C. (2010). Multiple signals direct the assembly and function of a type 1 secretion system. J. Bacteriol. *192*, 3861–3869.

Mimmack, M.L., Gallagher, M.P., Pearce, S.R., Hyde, S.C., Booth, I.R., and Higgins, C.F. (1989). Energy coupling to periplasmic binding protein-dependent transport systems: stoichiometry of ATP hydrolysis during transport in vivo. Proc. Nat. Acad. Sci. USA *86*, 8257–8261.

Nehme, D. and Poole, K. (2007). Assembly of the MexAB-OprM multidrug pump of *Pseudomonas aeruginosa*: component interactions defined by the study of pump mutant suppressors. J. Bacteriol. *189*, 6118–6127.

Nicaud, J.M., Mackman, N., Gray, L., and Holland, I.B. (1986). The C-terminal, 23 kDa peptide of *E. coli* haemolysin 2001 contains all the information necessary for its secretion by the haemolysin (Hly) export machinery. FEBS Lett. *204*, 331–335.

Oldham, M.L., Khare, D., Quiocho, F.A., Davidson, A.L., and Chen, J. (2007). Crystal structure of a catalytic intermediate of the maltose transporter. Nature *450*, 515–521.

Oswald, C., Holland, I.B., and Schmitt, L. (2006). The motor domains of ABC-transporters. What can structures tell us? Naunyn-Schmiedeberg's archives of pharmacology *372*, 385–399.

Patzlaff, J.S., van der Heide, T., and Poolman, B. (2003). The ATP/substrate stoichiometry of the ATP-binding cassette (ABC) transporter OpuA. J. Biol. Chem. *278*, 29546–29551.

Pei, X.Y., Hinchliffe, P., Symmons, M.F., Koronakis, E., Benz, R., Hughes, C., and Koronakis, V. (2011). Structures of sequential open states in a symmetrical opening transition of the TolC exit duct. Proc. Nat. Sci. USA *108*, 2112–2117.

Pimenta, A.L., Racher, K., Jamieson, L., Blight, M.A., and Holland, I.B. (2005). Mutations in HlyD, part of the type 1 translocator for hemolysin secretion, affect the folding of the secreted toxin. J. Bacteriol. *187*, 7471–7480.

Pinkett, H.W., Lee, A.T., Lum, P., Locher, K.P., and Rees, D.C. (2007). An inward-facing conformation of a putative metal-chelate-type ABC transporter. Science *315*, 373–377.

Pugsley, A.P. and Schwartz, M. (1985). Export and secretion of proteins by bacteria. FEMS Microbiol. Lett. *32*, 3–38.

Rhodes, C.R., Gray, M.C., Watson, J.M., Muratore, T.L., Kim, S.B., Hewlett, E.L., and Grisham, C.M. (2001). Structural

consequences of divalent metal binding by the adenylyl cyclase toxin of *Bordetella pertussis*. Arch. Biochem. Biophys. *395*, 169–176.

Rose, T., Sebo, P., Bellalou, J., and Ladant, D. (1995). Interaction of calcium with *Bordetella pertussis* adenylate cyclase toxin. Characterization of multiple calcium-binding sites and calcium-induced conformational changes. J. Biol. Chem. *270*, 26370–26376.

Sapriel, G., Wandersman, C., and Delepelaire, P. (2003). The SecB chaperone is bifunctional in *Serratia marcescens*: SecB is involved in the Sec pathway and required for HasA secretion by the ABC transporter. J. Bacteriol. *185*, 80–88.

Satchell, K.J. (2011). Structure and function of MARTX toxins and other large repetitive RTX proteins. Ann. Rev. Microbiol. *65*, 71–90.

Schatz, P.J. and Beckwith, J. (1990). Genetic analysis of protein export in *Escherichia coli*. Ann. Rev. Genet. *24*, 215–248.

Schiebel, E., Driessen, A.J., Hartl, F.U., and Wickner, W. (1991). Delta mu H+ and ATP function at different steps of the catalytic cycle of preprotein translocase. Cell *64*, 927–939.

Schmitt, L., Benabdelhak, H., Blight, M.A., Holland, I.B., and Stubbs, M.T. (2003). Crystal structure of the nucleotide-binding domain of the ABC-transporter haemolysin B: identification of a variable region within ABC helical domains. J. Mol. Biol. *330*, 333–342.

Schulein, R., Gentschev, I., Schlor, S., Gross, R., and Goebel, W. (1994). Identification and characterization of two functional domains of the hemolysin translocator protein HlyD. Mol. Gen. Genet. *245*, 203–211.

Schwarz, C.K., Landsberg, C.D., Lenders, M.H., Smits, S.H., and Schmitt, L. (2012). Using an *E. coli* Type 1 secretion system to secrete the mammalian, intracellular protein IFABP in its active form. J. Biotechnol. *159*, 155–161.

Seeger, M.A. and van Veen, H.W. (2009). Molecular basis of multidrug transport by ABC transporters. Biochim Biophys Acta *1794*, 725–737.

Smith, P.C., Karpowich, N., Millen, L., Moody, J.E., Rosen, J., Thomas, P.J., and Hunt, J.F. (2002). ATP binding to the motor domain from an ABC transporter drives formation of a nucleotide sandwich dimer. Mol. Cell. *10*, 139–149.

Springer, W. and Goebel, W. (1980). Synthesis and secretion of hemolysin by *Escherichia coli*. J. Bacteriol. *144*, 53–59.

Stanley, P., Koronakis, V., and Hughes, C. (1991). Mutational analysis supports a role for multiple structural features in the C-terminal secretion signal of *Escherichia coli* haemolysin. Mol. Microbiol. *5*, 2391–2403.

Stegmeier, J.F., Polleichtner, G., Brandes, N., Hotz, C., and Andersen, C. (2006). Importance of the adaptor (membrane fusion) protein hairpin domain for the functionality of multidrug efflux pumps. Biochem. *45*, 10303–10312.

Strathdee, C.A. and Lo, R.Y. (1989). Cloning, nucleotide sequence, and characterization of genes encoding the secretion function of the *Pasteurella haemolytica* leukotoxin determinant. J. Bacteriol. *171*, 916–928.

Su, C.C., Yang, F., Long, F., Reyon, D., Routh, M.D., Kuo, D.W., Mokhtari, A.K., Van Ornam, J.D., Rabe, K.L., Hoy, J.A., et al. (2009). Crystal structure of the membrane fusion protein CusB from *Escherichia coli*. J. Mol. Biol. *393*, 342–355.

Tamura, N., Murakami, S., Oyama, Y., Ishiguro, M., and Yamaguchi, A. (2005). Direct interaction of multidrug efflux transporter AcrB and outer membrane channel TolC detected via site-directed disulfide cross-linking. Biochem. *44*, 11115–11121.

Thanabalu, T., Koronakis, E., Hughes, C., and Koronakis, V. (1998). Substrate-induced assembly of a contiguous channel for protein export from *E. coli*: reversible bridging of an inner-membrane translocase to an outer membrane exit pore. EMBO J. *17*, 6487–6496.

Tikhonova, E.B., Dastidar, V., Rybenkov, V.V., and Zgurskaya, H.I. (2009). Kinetic control of TolC recruitment by multidrug efflux complexes. Proc. Nat. Acad. Sci. USA *106*, 16416–16421.

Uchida, K., Mori, H., and Mizushima, S. (1995). Stepwise movement of preproteins in the process of translocation across the cytoplasmic membrane of *Escherichia coli*. J. Biol. Chem. *270*, 30862–30868.

Vaccaro, L., Scott, K.A., and Sansom, M.S. (2008). Gating at both ends and breathing in the middle: conformational dynamics of TolC. Biophys. J. *95*, 5681–5691.

Vakharia, H., German, G.J., and Misra, R. (2001). Isolation and characterization of *Escherichia coli* tolC mutants defective in secreting enzymatically active alpha-hemolysin. J. Bacteriol. *183*, 6908–6916.

Wandersman, C. and Delepelaire, P. (1990). TolC, an *Escherichia coli* outer membrane protein required for hemolysin secretion. Proc. Nat. Acad. Sci. USA *87*, 4776–4780.

Welch, R.A., Dellinger, E.P., Minshew, B., and Falkow, S. (1981). Haemolysin contributes to virulence of extra-intestinal *E. coli* infections. Nature *294*, 665–667.

Welch, R.A., Hull, R., and Falkow, S. (1983). Molecular cloning and physical characterization of a chromosomal hemolysin from *Escherichia coli*. Infect. Immun. *42*, 178–186.

Wolff, N., Ghigo, J.M., Delepelaire, P., Wandersman, C., and Delepierre, M. (1994). C-terminal secretion signal of an *Erwinia chrysanthemi* protease secreted by a signal peptide-independent pathway: proton NMR and CD conformational studies in membrane-mimetic environments. Biochem. *33*, 6792–6801.

Wolff, N., Sapriel, G., Bodenreider, C., Chaffotte, A., and Delepelaire, P. (2003). Antifolding activity of the SecB chaperone is essential for secretion of HasA, a quickly folding ABC pathway substrate. J. Biol. Chem. *278*, 38247–38253.

Xu, Y., Sim, S.H., Song, S., Piao, S., Kim, H.M., Jin, X.L., Lee, K., and Ha, N.C. (2010). The tip region of the MacA alpha-hairpin is important for the binding to TolC to the *Escherichia coli* MacAB-TolC pump. Biochem. Biophys. Res. Commun. *394*, 962–965.

Xu, Y., Lee, M., Moeller, A., Song, S., Yoon, B.Y., Kim, H.M., Jun, S.Y., Lee, K., and Ha, N.C. (2011a). Funnel-like hexameric assembly of the periplasmic adapter protein in the tripartite multidrug efflux pump in gram-negative bacteria. J. Biol. Chem. *286*, 17910–17920.

Xu, Y., Song, S., Moeller, A., Kim, N., Piao, S., Sim, S.H., Kang, M., Yu, W., Cho, H.S., Chang, I., et al. (2011b). Functional implications of an intermeshing cogwheel-like interaction between TolC and MacA in the action of macrolide-specific efflux pump MacAB-TolC. J. Biol. Chem. *286*, 13541–13549.

Yum, S., Xu, Y., Piao, S., Sim, S.H., Kim, H.M., Jo, W.S., Kim, K.J., Kweon, H.S., Jeong, M.H., Jeon, H., et al. (2009). Crystal structure of the periplasmic component of a tripartite macrolide-specific efflux pump. J. Mol. Biol. *387*, 1286–1297.

Zaitseva, J., Jenewein, S., Wiedenmann, A., Benabdelhak, H., Holland, I.B., and Schmitt, L. (2005). Functional characterization and ATP-induced dimerization of the isolated ABC-domain of the haemolysin B transporter. Biochem. *44*, 9680–9690.

Zaitseva, J., Oswald, C., Jumpertz, T., Jenewein, S., Wiedenmann, A., Holland, I.B., and Schmitt, L. (2006). A structural analysis of asymmetry required for catalytic activity of an ABC-ATPase domain dimer. EMBO J. *25*, 3432–3443.

Zgurskaya, H.I. and Nikaido, H. (2000). Cross-linked complex between oligomeric periplasmic lipoprotein AcrA and the inner-membrane-associated multidrug efflux pump AcrB from *Escherichia coli*. J. Bacteriol. *182*, 4264–4267.

Zgurskaya, H.I., Yamada, Y., Tikhonova, E.B., Ge, Q., and Krishnamoorthy, G. (2009). Structural and functional diversity of bacterial membrane fusion proteins. Biochim. Biophys. Acta. *1794*, 794–807.

Zhang, F., Sheps, J.A., and Ling, V. (1993). Complementation of transport-deficient mutants of *Escherichia coli* alpha-hemolysin by second-site mutations in the transporter hemolysin B. J. Biol. Chem. *268*, 19889–19895.

Zhang, F., Yin, Y., Arrowsmith, C.H., and Ling, V. (1995). Secretion and circular dichroism analysis of the C-terminal signal peptides of HlyA and LktA. Biochem. *34*, 4193–4201.

Zhou, Z., Wang, X., Liu, H.Y., Zou, X., Li, M., and Hwang, T.C. (2006). The two ATP binding sites of cystic fibrosis transmembrane conductance regulator (CFTR) play distinct roles in gating kinetics and energetics. J. Gen. Physiol. *128*, 413–422.

Zolnerciks, J.K., Andress, E.J., Nicolaou, M., and Linton, K.J. (2011). Structure of ABC transporters. Essays Biochem. *50*, 43–61.

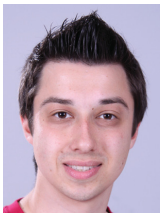

Michael Lenders studied Biochemistry at the Heinrich Heine University in Düsseldorf and graduated in 2012. His master thesis about the characterization of self-inserting membrane proteins by atomic force microscopy was prepared in cooperation with the Swiss Federal Institute of Technology Zürich. Since 2012, he is a PhD student focusing structural and functional characterization of the membrane fusion protein of the haemolysin A T1SS at the institute of Biochemistry, Heinrich Heine University Düsseldorf.

Sven Reimann studied Biochemistry at the Heinrich Heine University Düsseldorf. He did his Master's degree at the Forschungszentrum Jülich investigating a putative virulence factor of *Pseudomonas aeruginosa*. Since then he has been doing his PhD at the Institute of Biochemistry at a Heinrich Heine University Düsseldorf. His research field is the hemolysis A type 1 secretion system of *Escherichia coli* and particularly the ABC transporter HlyB.

Sander Smits obtained his PhD in Biochemistry at the Institute of Biochemistry, Heinrich Heine University Düsseldorf in 2008. Since then he has worked as a senior scientist with a special focus on membrane transporter, especially on the transporter of large unfolded proteins as well as peptides having an antimicrobial activity.

Lutz Schmitt studied Chemistry at the University of Freiburg and obtained his PhD from the Technical University Munich. After a Post Doc at Stanford University, he moved as a DFG-funded Emmy Noether Fellow to the Universities of Marburg and Frankfurt. In 2005 he was appointed as Professor of Biochemistry at the Heinrich Heine University Düsseldorf where he became full professor in 2008. His research interest are recognition processes at membranes and transport across membranes with an emphasis on ABC transporters.

3.2. Chapter II - Type I Secretion Systems in Gram-negative Bacteria - What we know and what we do not know

Title Type I Secretion Systems in Gram-negative Bacteria - What we know and what we do not know

Authors I. Barry Holland, Sandra Pehersdorfer, Kerstin Kanonenberg, Michael H. H. Lenders, Sven Reimann and Lutz Schmitt

In Preparation

Own proportion of this work 10 %;
Writing of the manuscript.

Type I Secretion Systems in Gram-negative Bacteria - What we know and what we do not know

I. Barry Holland*†, Sandra Pehersdorfer‡, Kerstin Kanonenberg‡, Michael H. H. Lenders‡, Sven Reimann‡ and Lutz Schmitt‡§

Institute of Biochemistry, Heinrich-Heine-Universität, 40225 Düsseldorf, Germany

*Institute of Genetics and Microbiology, CNRS UMR 8621, University of Paris Sud, Orsay, Cedex, France

†To whom correspondence should be addressed: barry.holland@igmors.u-psud.fr, Institute of Genetics and Microbiology, CNRS UMR 8621, University of Paris Sud, Orsay, France

‡Institute of Biochemistry, Heinrich Heine University, 40225 Düsseldorf, Germany

§To whom correspondence should be addressed: lutz.schmitt@hhu.de, Institute of Biochemistry, Heinrich Heine University, 40225 Düsseldorf, Germany

Introduction

The broad family of ABC transporters found in all kingdoms of life was first detected in E. coli as a curiously heterogenous group of membrane proteins [1] most acting as importers of a variety of small molecules but also one exporter (HlyB). HlyB became the prototype of the type I secretion system (TISS or ABC-dependent) export system for translocation of bacterial proteins. TISS can minimally be defined as having a C-terminal secretion signal and requiring an ABC transporter, with its characteristically highly conserved ATPase domain, as the energizing component of the transenvelope transport process. As we shall discuss in detail in this review, the type I secretion system (TISS), in addition to an ABC transporter, requires an MFP protein also in the inner membrane but reaching across the periplasm to contact a specific outer membrane protein to complete the translocon. A more strict definition of the TISS, but still covering the vast majority of known types, includes the requirement that the transport substrate, or allocrite as we shall interchangeably term it, contains multiple calcium binding sites. The most studied and the first group of these secreted proteins to be identified was the RTX (repeats in toxins) family [2, 3, 4]. These indeed contain a varying number of very similar nona-peptide calcium binding repeats. These are implicated in the secretion process and located 100 to 200 residues upstream of the secretion signal. The RTX motifs form a unique beta roll structure with aspartate and glycine residues involved in calcium binding [5]. As described by Linhartova *et al.* [6], over 1000 RTX proteins were easily detected by a bioinformatic screen of databases.

For other useful recent general reviews discussing different aspects of T1SS systems and allocrites, see Welch Re/a, Holland *et al.* [7], Thomas *et al.* [8], Lenders *et al.* [9] and the review by Delepelaire [10] covering a survey of a wide range of organisms having the T1SS. In addition, for two related topics not considered in this review on the regulation of expression of the *hly*-determinant and concerning the mode of action of the hemolysin HlyA see [8].

RTX proteins are major pathogenicity factors carried by many important pathogens in mammals, insects and plants. Some of the most studied proteins, secreted by different Gram negative pathogens, include haemolysins (hemolysins) produced by uropathogenic (HlyA) and the main theme of thus review, adenylate cyclase (CyaA9 [11] secreted by *Bordetella pertussis* (whooping cough), and toxins secreted by enterohemorrhagic *E. coli* strains (EHEC, [12]). In addition, the newly described TISS members with giant allocrites, the MARTX family (multifunctional - autoprocessing repeats in toxins, [13]), are found in chromosomal islands of major human pathogens. This family of

extremely large polypeptides (in the range 5000-9000 kDa) at least in one case described later having a slightly different variant of the RTX motif. These include the multitoxin MARTX Vc encoded by rtxAVc from *Vibrio cholera* [13, 14], and a giant adhesion, LapA, an RTX protein from *Pseudomonas fluorescens*, recently described by Boyd *et al.* [15]. More intriguing, however, is another giant adhesion, SiiE, containing a completely unrelated set of Ca^{2+} repeats [16] but is nevertheless secreted from *Salmonella enterica* via a TISS. Very recently, the fascinating possibility has also emerged indicating that the TISS exists in the obligate parasitic/symbiotic family of the Rickettsia. This TISS apparently secretes several members of the ankyrin protein family that appear to have no Ca^{2+} binding motifs at all.

The type I allocrites are also almost invariably characterized by having few if any cysteines, being very acidic with Pi values frequently below pH 5. In contrast, these proteins are distributed over an enormous range of sizes, extending from less than 100 to 9000 amino acids. These latter include some adhesins and others packaging a lethal string of distinct toxins that penetrates host cells before the individual toxins are released by an auto-proteolytic process [13, 17]. However, all these proteins are secreted by an ABC/MFP/OMP translocon, the secretion signal is at the C-terminus, and all have RTX repeats. Some MARTX proteins at least are also characterized by a very large number of other types of repeats (not Ca^{2+} binding), especially towards the N-terminus. These are relatively glycine rich, with an apparently conserved core consensus sequence, G7XG2XN. Recently, Kim *et al.* [18], showed that while not required for secretion from the bacteria, the N-terminal repeats are required for subsequent translocation by the pathogen *Vibrio vulnificus* into the cytosol of the host cell. The MARTX proteins and other novel groups secreting via the TISS will be discussed in a little more detail later.

A brief early history

Around 1980 no bacterial protein secretion system had been characterized and how such proteins reached the exterior was a mystery. Gram-positive bacteria were known to secrete a variety of toxins, but with only a single membrane barrier to the exterior, the general SecYEG system could be assumed to provide the pathway. Toxins such as a hemolysin released by Gram-negative bacteria were also known but the mechanism of secretion had not been investigated. In addition, specific mechanisms for translocation of some protein components of flagella and pili on to the cell surface were assumed, but nothing was known. Similarly, extracellular enzymes produced by pathogens or required for growth on particular carbon sources were secreted to the medium but by

what mechanism was a mystery.

At the same time, studies of the biogenesis of bacterial membranes were largely restricted to the model laboratory strain *E. coli* K12 that in fact appeared to secrete no proteins to the medium. Thus, interest in protein translocation was largely confined to unlocking the puzzle of the distinctive partitioning of proteins to the compartments of the cell envelope - the inner and outer membranes and the periplasm - i.e. the process dependent on the Sec-translocon, and targeted by an N-terminal "export" or "signal sequence".

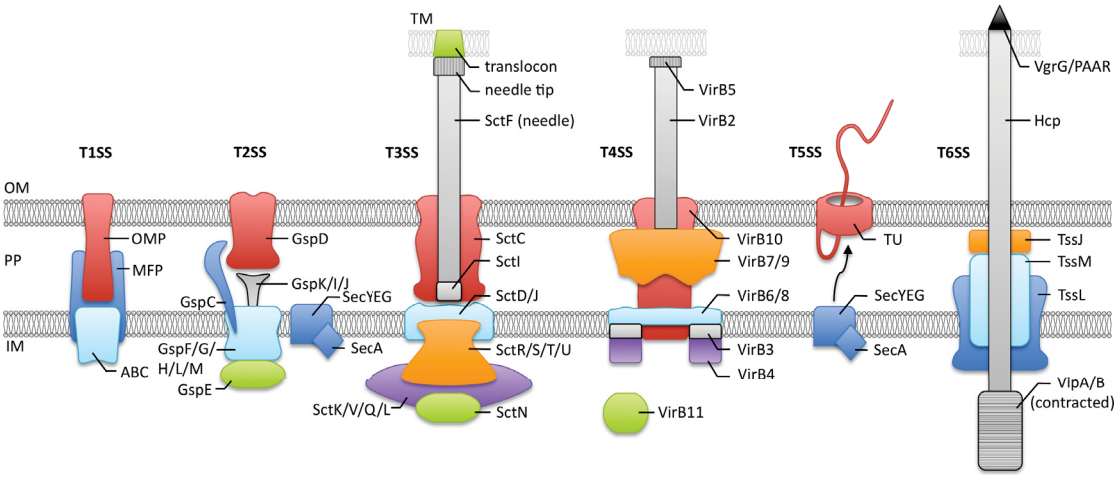

Figure 1: Schematic summary of Type 1 to Type 6 Secretion Systems in Gram-negative bacteria.

The first clear example, of a type I system (T1SS) studied in any detail, was the secretion of the hemolysin HyA discovered in the early 1980s. This is still the most studied and considered the prototype system. Remarkably, however, by the late 2000s an amazing variety of protein secretion systems, in particular in Gram-negative bacteria, had been identified - close to 20 distinct mechanisms by some counts (see Figure 1), including types III, IV and VI, form so called injectosomes, the system for translocation of components of the flagellum, two types of pili and at least 4 variations on type IV [7, 19]. Four of these, TISS, III, IV and VI, apparently involve a transenvelope 'tunnel', secreting proteins directly from the cytoplasm to the exterior. The great majority, however, involve an initial step to cross the inner membrane dependent on the Sec system, with the subsequent step to negotiate the outer membrane surprisingly involving many alternative strategies (see Figure 1 and see recent review, [20]).

The first authentic reports of a bacterial hemolysin (haemolysin)

These appeared in the early 1950s, notably by Robinson [21] working in the Seamen's Hospital, Greenwich, who identified such a toxin from *E. coli* that was cell associated (non filterable), heat labile, and calcium dependent for activity. However, an apparently truly secreted hemolysin, released from late exponential phase cells, was only identified in the 1960s [22, 23]. Pioneering the modern phase of hemolysin studies, the group of Werner Goebel in Wurzburg, in 1979 cloned a cluster of 3 genes found on a plasmid from a pathogenic *E. coli* strain, and transferred this into an *E. coli* K12 laboratory strain. Thus, Noegel *et al.* [24] identified two genes shown to be required for production of the active hemolysin molecules and at least one gene encoding a transport function. Springer and Goebel [25] studied the process of release of active hemolysin (later to be named HlyA) from *E. coli* K12. These authors used inhibitors of energy metabolism and protease processing, together with cell fractionation, to distinguish extra- and intracellular hemolysin. They concluded that HlyA was secreted in an energy dependent process via the periplasm and apparently involving processing of the protoxin to a 55 kDa form able to cross the outer membrane (see also [26]).

A novel transenvelope secretion process - HlyA is secreted directly to the medium

However, subsequent studies, benefitting from pulse chase radiolabelling experiments and more detailed cellular fractionation analysis, quickly demonstrated that HlyA (with a relative mobility equivalent to 107 kDa) was not processed and was secreted directly to the medium [2, 27, 28, 29]. Moreover, the first sequencing [3] of an *hly*-operon (see Figure 2) from a TISS genetic determinant located in the chromosome (as are the great majority) of an O4 serotype strain of *Escherichia coli*, revealed a putative toxin gene and surprisingly revealed the absence of any classical N-terminal signal sequence able to target HlyA (calculated size 110 kDa) to the Sec translocon. Then several studies, including the analysis of an other human chromosomal Hly determinant, LE 2001 [28, 30, 31], and with the plasmid determinant, pHly152, studied first by W. Goebel and then by the Cambridge group, demonstrated that HlyA secretion did not involve a periplasmic intermediate [27, 32, 33, 34] and did not require SecA [35, 36, 37]. These results indicated a novel protein translocation pathway and raised the intriguing question, how does this protein negotiate two membranes on its way to the medium?

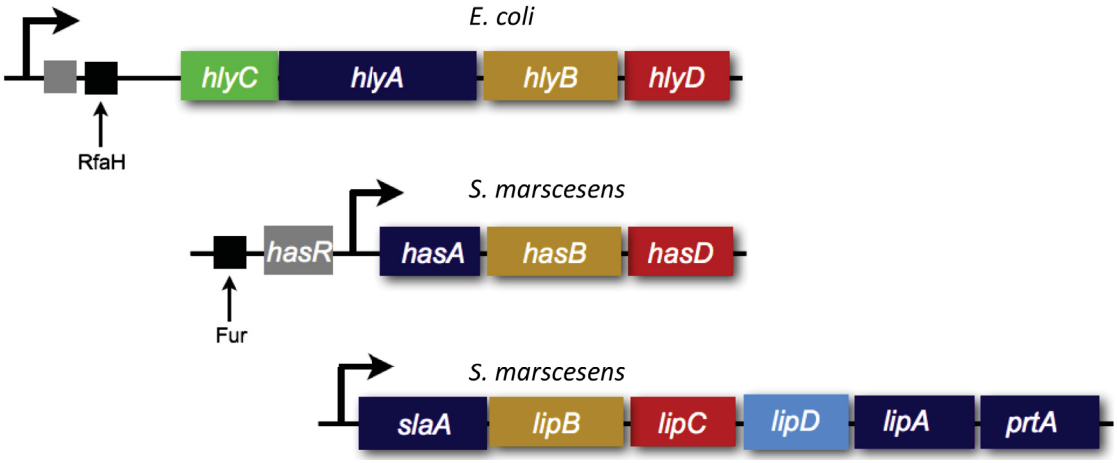

Figure 2: Organization of the *hly*, the *hasA* and the *slaA/lipA/prtA* operons. The promotor and the binding site of the transcriptional regulators RfhA [38] or Fur are indicated. In the case of the has operon, the surface receptor HasR (grey) and for the textithly operon, the acyltransferase HlyC (green) are also encoded within the operon. The textitslaA gene encodes a surface protein, textitlipA a lipase and textitprtA a metalloprotease protease. The allocrite or transport substrate genes are indicated in dark blue, the ABC transporters in brown, the MFPs in red and the OMP, if present in the operon, in light blue. Please note that the outer membrane protein (TolC in the case of HlyA) is mostly not encoded in the corresponding T1SS operon.

Identifying the genes and functions of the HlyA operon, and another *E. coli* protein essential for type I secretion

The first sequence of the *hly* operon also clearly showed that in addition to the toxin this encoded two probable membrane proteins (HlyB and HlyD) and a gene *hlyC*, subsequently shown to be required for activation of the HlyA toxin [39]. A number of laboratories using transposon mutagenesis and radiolabelling in mini and maxi cells, confirmed independently the identity of the hemolyically active product of the *hlyA* gene, as a non-processed polypeptide of 110 kDa. In addition, the products of the genes *hlyB* and *hlyD* were shown to be essential for translocation to the medium, and both proteins were located to the inner membrane [2, 3, 30, 31, 40, 41]. Then in 1990, a major advance by Wandersman and Delepelaire demonstrated that an *E. coli* outer membrane protein, TolC, was also essential for the secretion of HlyA [42]. TolC was known to be involved in excretion of a wide range of molecules as well as the import of some bacteriocins, and apparently important in some way for the overall maintenance of the integrity of the outer membrane. The *tolC* gene is not linked to the *hlyA* operon but the Wander-

sman group [43] showed that an operon in the phytopathogenic *Erwinia chrysanthemi*, encoding secretion genes for Type 1 allocrites, the metalloproteases B and PrtC, also encoded PrtF, a TolC homologue (see Figure 2). This addition of TolC to the putative Type I secretion machinery was a crucial finding, providing a potential partner for the inner membrane proteins HlyBD, and therefore the means to complete the transport pathway through the outer membrane to the medium.

Importantly, these early studies also showed that HlyC, required to activate HlyA, and later shown by Koronakis and Hughes and colleagues [44, 45] to be a specific acyl transferase, was not required for secretion [39]. This is particularly relevant since HlyC with its co-factor, the cellular enzyme ACP (acyl carrier protein-dependent fatty acylation; [46]), is an unusual enzyme, unexpectedly synthesized in equimolar amounts to HlyA, with which it forms a stoichiometric complex. This led to an appealing but ultimately incorrect hypothesis (Koronakis *et al.*) that HlyC also plays an additional chaperone-like role to maintain HlyA competent for secretion, until the secretion signal becomes available.

The acyltransferase HlyC - structure and function

The *hlyC* gene in the *hly*-operon encodes the acyltransferase HlyC. This enzyme is not required for secretion of HlyA, as indicated above but is required for modification of the unfolded HlyA [47] in the cytoplasm prior to transport, while the folded form of HlyA is not accepted as substrate. In concert with the endogenous *E. coli* acyl-ACP, HlyC transfers acyl groups on to two internal lysine residues (Lys564 and Lys690). The predominant length of the acyl chains is 14, 15 or 17 carbon atoms. Interestingly, the sequence homology with other acyltransferases such as the most studied Gcn5-like N-acstyl transferase (GNAT) family, found in all kingdoms of life and is required for acetylation or acylation of amino acids such as lysine, is very low, although a structural similarity is apparent [48]. Unlike the (GNAT) enzymes that employ coenzyme A instead of ACP, biochemical studies suggested that the transfer of fatty acids from ACP to HlyA occurs by an ordered Bi-Bi mechanism, in which a transient, ternary complex of acyl-ACP/HlyC/pro-HlyA is formed.

Recently, the Koronakis group reported the crystal structure of an HlyC homologue from Actinobacillus pleuropneumoniae, ApxC (see Figure 3) [48]. This protein shares 70 % amino acid identity with HlyC from *E. coli* and can replace *E. coli* HlyC *in vivo* to activate pro-HlyA. The structure of ApxC revealed a dimer, which was supported by analysis of the oligomeric state of ApxC in solution. The monomer is composed of a

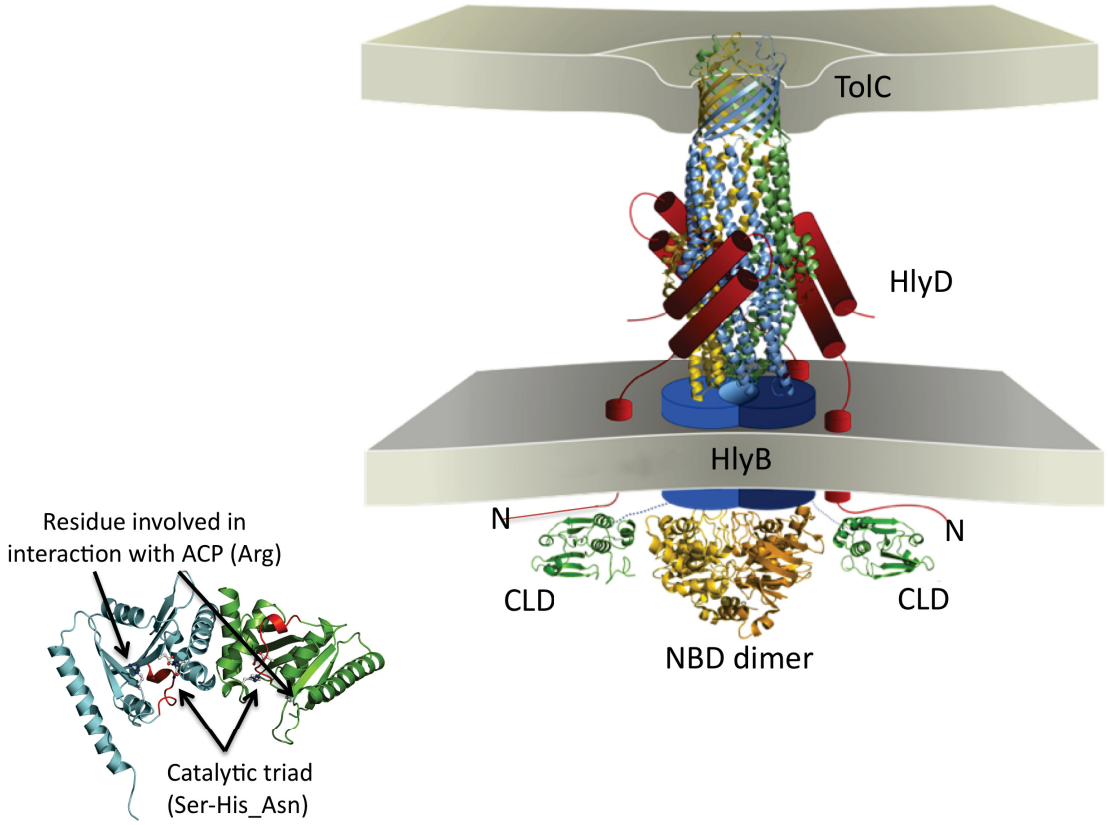

Figure 3: Summary of structural information for the hemolysin A T1SS. Left: homology model of dimeric HlyC based on the crystal structure of ApxC [48]. The TAAT specific insertion, which is unique and not present in the GNAT family, is highlighted in red. The catalytic triad composed of a Ser, His and Asn residue as well as the Arg residue that interacts with ACP is shown in ball-and-stick representation. The NMR structure of the CLD [49] and the crystal structure of the ATP-bound dimer of the NBDs [50] are shown in green and orange/green, respectively. The TMD of HlyB and for HlyD are shown schematically as blue and red cylinders, respectively. The trimeric crystal structure of TolC (green/cyan/yellow) [51] is shown in cartoon representation. No structural information for the substrate, HlyA, is available. Please note that structure and oligomeric state of HlyD (the N-terminus is labeled) are arbitrary and whether (as suggested in the cartoon) or not a direct contact between HlyB and TolC exists is also entirely speculative. It has to be stressed that no such contact exists in the recently determined single particle EM Structure of the tripartite AcrAB-TolC efflux pump [52]. Koronakis *et al.* [53] suggested a trimeric arrangement for HlyD as illustrated here, although more and more experimental evidence suggests a hexameric state (see for example Su *et al.* [54]).

five stranded β-sheet flanked by six helices. More intriguing is a deep cleft between the third and fourth strand. This cleft is also present in structures of acyl-transferases of

the GNAT family and thus appears to present a conserved structural feature of these enzymes. Combined with mutagenesis studies, active site residues important for catalysis were mapped to the deep cleft in the central β-sheet and residues important for ACP interaction were also identified. This structure therefore represents an important advance in our understanding of the mechanism of activation of HlyA-like molecules transported by T1SS and will open up new ways to suppress the activity of these toxins.

Structural organization of the HlyA molecule including the RTX motifs

Studies of hemolysin secretion have primarily involved two genetic determinants, both isolated from a human host, the plasmid derivative pHly152, [55], and the chromosomal derivative LE2001 [28, 29]. The two determinants show small deviations in primary amino acid sequence, confusingly this includes the absence of a single codon, early in the *hlyA* gene in chromosomal isolates like LE2001, encoding 1023 residues not 1024 as found with the plasmid based determinants. The large N-terminal domain of HlyA contains the hydrophobic regions involved in pore formation, together with lysine residues 564 and 690 (numbering according to the plasmid borne determinant; 563 and 689, in the chromosomal determinant), the sites of acylation by HlyC. Importantly, the sequence of the *hly*-operon (reviewed by Welch [4]), also revealed the presence of many glycine and aspartate rich nona-repeats in HlyA, designated as repeats in toxins (RTX) and located towards the C-terminus of the protein. The number of these repeats in the *E. coli* hemolysin has variously been reported, to be as few as 6 [56] or 11-17 [57] depending on the strictness of the consensus applied. The original consensus indicated by the Rod Welch group was in fact, LxGGxGND and 13 repeats were identified rather loosely linked to the consensus. In contrast, Lecher *et al.* [56], based on the strict consensus sequence, GGxGxDxUx (where U is a large or hydrophobic amino acid), containing the critical G and D residues directly involved in binding Ca^{2+}, identified 6 repeats in rather closely linked two clusters, terminating 173 residues from the C-terminus of HlyA. In contrast, for example, the proteases PrtG, PrtB, and PrtC, all from *E. chrsysanthemi*, have a single tight cluster of 3 and 4 RTX repeats, respectively, ending approximately 90 amino acids from the C-terminus [58, 59].

Structural studies have shown that two nona-peptides bind one Ca^{2+} ion (see Figure 4). The main coordination occurs via the two aspartate side chains, but backbone and side chain interaction of other amino acids within the repeat also contribute to Ca^{2+}

coordination. It is important to stress that not two consecutive repeats bind the same ion. This arrangement creates a so-called parallel β-roll or parallel β-helix. Within such a motif, a strand is present between the two repeats in the Ca^{2+} bound state so that the strand back against each other as first described in the alkaline phosphatase [5].

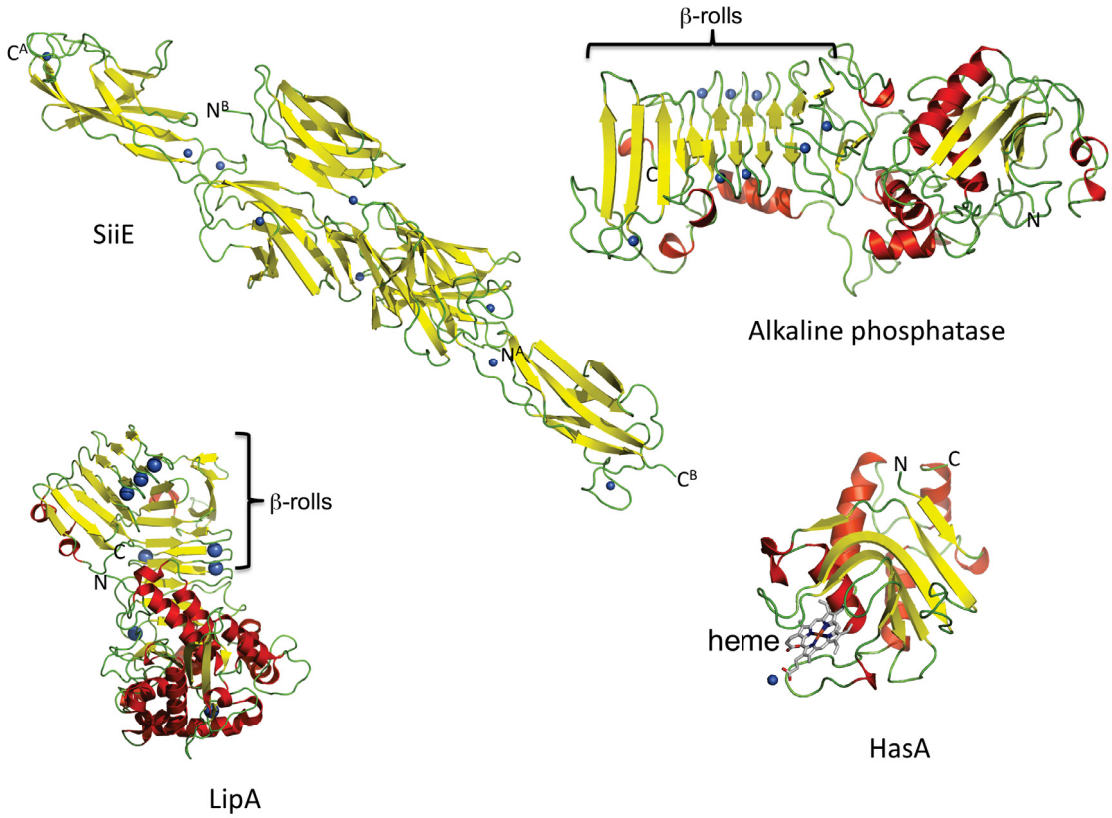

Figure 4: Known structures of substrates of T1SS. Ca^{2+} ions are highlighted by grey spheres, the proteins are displayed in cartoon representation. From top to bottom: a fragment of the giant adhesion SiiE that has non-RTX Ca^{2+} binding sites [60], alkaline phosphatase [5], the TISS RTX lipase LipA [61] and HasA [62], which does not contain an RTX domain. The β-rolls are highlighted. The N- and C-termini are indicated. Please note that SiiE forms a dimer. Here, the respective monomer is indicated by the superscripts A and B, respectively.

RTX proteins are not only toxins

Although the family is now known to be very large, extremely varied, and extending far beyond the realm of toxins, importantly, the RTX terminology, however defined, still rather tightly defines a family of prokaryotic proteins, secreted by a largely similar

mechanism (discussed below), Clearly therefore the RTX motif must normally play a crucial role in the secretion process. On the other hand, as discussed below, at least one type I allocrite produced by a common pathogen is now known to completely lack RTX repeats, but, fascinatingly, contains quite different Ca^{2+} repeats.

A unique targeting process - a C-terminal signal for bacterial secretion: determining the minimal size

In some early studies it is of note that Type 1 secretion (apparently first so designated by Salmond and Reeves, [63] was described, misleadingly as a "signal independent" secretion system, in reality meaning, lacking an N-terminal signal for targeting the SecAYEG translocon. Many subsequent studies of the now extremely large number of RTX proteins, where these have been tested, have confirmed the presence of a specific C-terminal secretion signal. Although detailed evidence is still surprisingly limited we presume that the essential role for the secretion signal is to be recognized by and to dock with the cognate ABC/MFP components of the translocon.

A potential signal required for type I secretion, was first identified when deletion of the C-terminal 27 residues of HlyA was found to completely block secretion [34]. Confirming the importance of this novel, C-terminal signal, fragments constituting the terminal 218 (23 kDa) or 113 residues (12 kDa) were shown to be autonomous for secretion, dependent on HlyBD [37, 64]. Subsequently, an HlyA autonomous fragment of only 62 residues was demonstrated [65]. Finally, using a strategy effectively of upstream internal deletions, Koronakis *et al.* [27] localized the HlyA secretion signal to the terminal 50 or so amino acids.

Another autonomous Type I secretion targeting region of 50 residues was identified for the alkaline protease from *Pseudomonas aeruginosa* by Duong *et al.* [66]. For the secretion of the protease PrtG from *E. chrysanthemi* (expressed in *E. coli*), Ghigo and Wandersman [58] showed that the C-terminal peptide of 56 residues could be secreted autonomously. Then by constructing internal deletions close to the C-terminus, these authors found that retention of only the terminal 29 amino acids was sufficient to promote secretion (albeit at 50 % of WT level).

On the other hand the secretion signal for metalloprotease B, also from *E. chrysanthemi* [67], was located within the terminal 40 residues, and more recently for a lipase, TilA secreted from *Pseudomonas fluorescens*, a secretion signal was located within the C-terminal 105 residues that includes three tightly packed RTX in this case apparently

separated from the likely secretion signal by only 20 or so residues [68]. Similarly, Angkawidjaja *et al.* [69] describe the efficient secretion of alkaline phosphatase apparently fused to the C-terminal 98 residues of the lipase PML (I.3) from Pseudomonas that includes 5 closely packed RTX motifs upstream of the secretion signal. For the adenylate cyclase toxin the secretion signal is likely located in approximately the C-terminal 75 residues [70]. Finally, the secretion signal for HasA, the small hemophore from *Serratia marcescens* was reported to be within the 56 C-terminal amino acids [71].

The C-terminal region of HlyA can be used to promote secretion of a wide variety of unrelated proteins

Clear confirmation that a specific C-terminal region signal was necessary and sufficient to promote secretion was obtained by fusing the C-terminal 218 of HlyA (now called HlyA1, and containing 3 RTX, see Figure 5) or the 102 C-terminal amino acids of HlyA (HlyA3, no RTX present) to the C-terminus of *E. coli* porin OmpF, lacking its normal N-terminal signal [37]. In addition, Gentschev *et al.*, [35] and Hess *et al.* [72] reported that alkaline phosphatase, normally an *E. coli* periplasmic protein, was secreted to the medium when its C-terminus was fused to an even smaller C-terminal fragment containing only 60 terminal residues of HlyA. However, a recurring caveat here is that in this and many other reports the efficiency of secretion, compared in this case to a fusion with a larger fragment containing RTX motifs, was not presented, rendering the significance difficult to evaluate.

Subsequently, a very large number of fusion proteins (mostly with the larger C-terminal region of HlyA, have been successfully demonstrated (see recent review by Eom *et al.* [73]). Moreover, a wide variety of heterologous passengers formed from cytoplasmic or Sec-dependent, exported proteins, were shown to have some level of functional activity, indicating normal folding (examples include [74] streptokinase, [32], β-lactamase, [75], maltose binding protein, [76], mammalian intestinal fatty acid binding protein, [77], GFP and alkaline phosphatase [69, 78]).

Post-translational secretion with no obvious mechanism to maintain the nascent polypeptides competent for secretion

The early studies of type I secretion, demonstrating the role for a C-terminal targeting signal, evidently showed that this must be a post-translational process. This was exciting

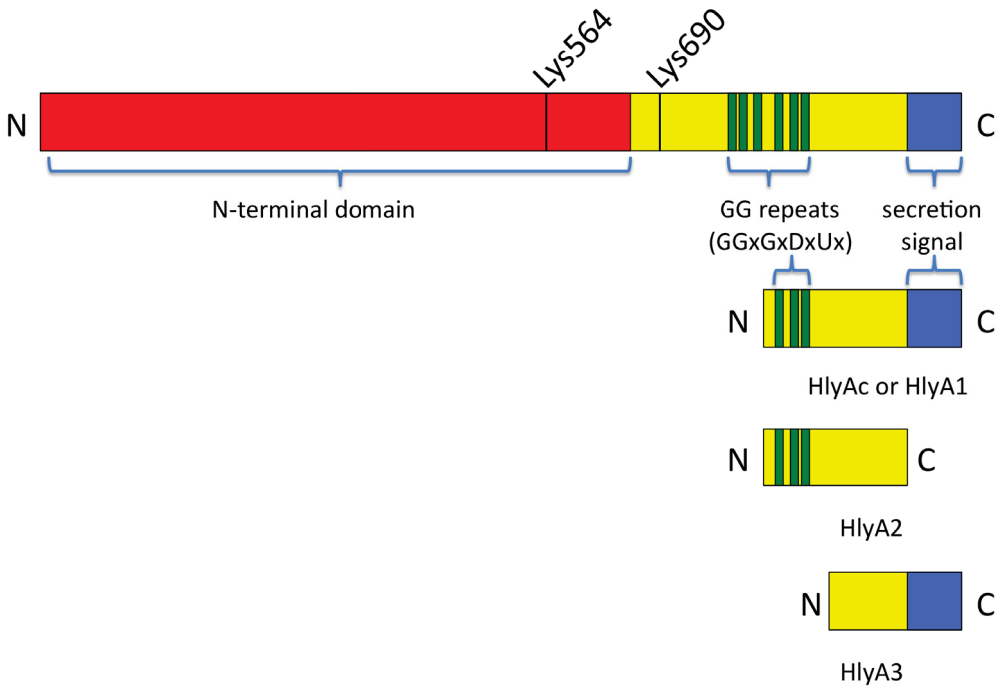

Figure 5: Schematic representation of the HlyA constructs mentioned in the text. The length of the constructs is scaled to their number of amino acids (1024 in the case of the HlyA shown here). The functional, pore-forming domain of HlyA is shown in red, the RTX domain in yellow and the secretion sequence in blue. The nona-repeats in the RTX domain are highlighted in green. N and C termini are indicated. For the fragments of HlyA, HlyA1 contains 208 amino acids, A2 has 160, and A3 has 102.

but raised further questions. For example, how was a very large polypeptide like HlyA (presumably requiring 1 to 2 min to complete its synthesis), maintained in a secretion competent form - neither aggregating nor being degraded - until the C-terminal docking signal was available. Possible explanations might include extended retention by the ribosome, early tethering to the translocator, segregated to a particular (protected) cellular compartment coupled to transcription-translation, capture by chaperone(s) or, simply the inherent stability of the unfolded or partially folded state of HlyA and other type I proteins. All these are plausible but all are predicated on the supposition that a particular *N-terminal signal region* would be required for early recognition of nascent forms of type I proteins. However, there is no evidence for such signals. This is especially puzzling regarding the many type 1 proteins that are composed of thousands of residues, while for the non-RTX HasA the Sec-system chaperone, SecB, is essential for secretion [79]. Moreover, as discussed below an apparently enormous variety of heterologous

passengers can be secreted when fused upstream of the C-terminal of type I proteins.

One study has indicated a requirement for the general chaperone GroES (J Whitehead, PhD thesis, 1994) for HlyA secretion but this has not been confirmed. Moreover, no chaperones have been implicated in the secretion of any other type 1 proteins. Therefore, it remains unclear how nascent type I polypeptides remain secretion competent long enough to make a successful docking with the translocon.

A plausible alternative scenario envisaged in a number of previous studies that avoids the need for chaperones, is that type I proteins in fact initially fold up rapidly, with the ABC protein involved in coordinating the subsequent unfolding and insertion of the protein into the transport pathway. The recent studies by Bakkes *et al.* [75] to be discussed below appear, however, to have ruled out such pre-folded state, at least for HlyA.

The RTX motifs appear to be essential for secretion of many type I allocrites but there are some important exceptions

Many studies have shown that RTX motifs, in addition to the secretion signal, also play an important role in some way in the secretion of the great majority of type I proteins. One of the best examples of this was provided by studies of the secretion of a Pseudomonas lipase. Thus, that secretion levels were clearly shown to be proportional to the number of RTX motifs that were retained in different engineered constructs, with barely detectable levels of secreted lipase when 11 or all the repeats in the WT were removed [80].

In some contrast, it is equally clear that the RTX motifs are dispensable for secretion in some contexts. Thus, type I substrates like the small HasA protein and the ColV peptide completely lack the RTX motif. However, HasA also has the special feature that secretion requires the dedicated chaperone SecB, while surprisingly the secretion signal of the 39 residues of the bacteriocin colicin V, is located at the N-terminal. Moreover, unlike HlyA and other large type I polypeptides the ColV signal sequence is cleaved and the signal removed by a cysteine protease domain found at the N- terminus of the cognate ABC transporter [81, 82]. As discussed later, such an active protease domain, found in many bacteriocins, especially secreted by Gram-positive bacteria, is not generally found in type I *polypeptides*, although it is fascinating that an inactive relic of the protease is found and plays an important role in the secretion of HlyA, for example.

In another specific exception to the rule, the minimal *autonomous* fragment of HlyA,

the C-terminal 60 residues completely lacks RTX, but is still apparently secreted quite efficiently. In addition, when certain heterologous 'passenger' polypeptides, for example, *E. coli* porin OmpF [37], alkaline phosphatase [35] were fused to the C-terminal fragment HlyA3 (that lacks RTX repeats), secretion is still obtained. However, these particular passengers have the inherent properties of being normally exported across the inner membrane, and like wild type HasA, require the SecB chaperone for normal secretion. They also share another common characteristic, relatively small size. In such cases, the role performed by the RTX - to facilitate calcium dependent folding of substrates emerging from the translocon on to the cell surface - may simply be redundant. Indeed, many of these results can reasonably be explained, as suggested by Letoffe and Wandersman [59], that beyond a maximum size, around 30 kDa, the RTX repeats are essential for secretion (and folding).

Fusion of heterologous passengers to other TISS secretion signals, have also demonstrated successful secretion, with or without RTX motifs [59, 69, 82]. In some cases at least, the passenger enzyme in the fusion was shown to be active, even in the absence of the RTX. However, in the case of a GFP fusion to the signal region of lipase TliA from *P. fluorescens*, the RTX motifs were apparently required for correct folding [68]. Finally, two notable examples of type I secretion without the requirement for RTX repeats were described recently - the naturally occurring allocrites secreted by the Rickettsia and by *Bacteroides fragilis* and the giant adhesion SiiE secreted from *Salmonella enterica*. As described below, in both cases evolution has thrown up fascinating and informative alternatives to fill the role of the RTX.

What therefore is the precise role of RTXs in the normal mechanism of secretion of type I proteins?

In vitro experiments with different T1SS substrates and fragments thereof ranging from those with the complete number of RTX repeats down to truncations to only three repeats, demonstrated that Ca^{2+} is essential for folding of these proteins [83, 84, 85]. Folding only occurs in the presence of Ca^{2+} or other divalent ions such as Sr^{2+} or Ba^{2+} but not with Mg^{2+}. Interestingly, folding studies on secreted pro-HlyA indicated that Ca^{2+} induced folding is not only restricted to the RTX domain but more importantly extends to the entire protein [85, 86].

This latter observation is supported by folding studies in vitro of fusions of MBP and MBP slow folding mutants to a C-terminal fragment of HlyA (HlyA1, [75]). The isolated MBP mutant proteins displayed a decreased folding rate, while the velocity

of unfolding was not affected. This was also observed with the MBP-HlyA1 fusions. Importantly, in the absence of Ca^{2+} (simulating the situation in the *E. coli* cytosol) the slow folding mutants displayed an even slower folding rate when fused to the C-terminal fragment of HlyA. This suggested that long-range interactions were propagated between the MBP and the HlyA moiety under these conditions. Moreover, the slower the folding of a particular mutant, the greater the influence of Ca^{2+} induced folding of the entire fusion protein. This result also raised the surprising possibility that the RTX, in the absence of Ca^{2+}, rather than accelerating folding can actually slow down the process, for example, in the *E. coli* cytoplasm, thereby facilitating maintenance of the unfolded state until translocation and surface emergence of passenger domains, their folding and release into the medium, is complete.

Importantly, a similar phenomenon was found in the analysis of long-range effects on folding involving the RTX repeats of the adenylate cyclase toxin [87, 88]. These studies of CyaA and HlyA have revealed a fascinating aspect of protein folding that was suggested to depend on an entropic stabilization effect [87] and hopefully this will be followed up.

Optimizing secretion by the Hly-TISS: The rate of folding determines substrate secretion by the Hly system

It is important to note that although many different heterologous proteins have been secreted using the C-terminal region of RTX proteins, the great majority of such studies have taken a simple empirical, trial and error approach - are particular fusions secreted or not? In addition, as noted above, in most such experiments protein levels were not measured quantitatively and no attempt was made to determine secretion efficiency, i.e. the number of molecules secreted compared the number synthesised. Moreover, when measured, yields of secreted fusions were found to be very low, restricted to the high $\mu g\, L^{-1}$ range.

Recognising these limitations, Bakkes and colleagues recently examined how at least one key factor, premature folding of a passenger domain, might compromise efficient secretion of a given fusion [75]. Debarbieux *et al.* [89] had previously shown that if HasA (albeit an atypical type I protein) was allowed to fold in the cytoplasm before inducing the synthesis of the translocator proteins, it could not be secreted. This result in fact contradicted early ideas that type I allocrites might require unwinding (by the ABC protein) prior to secretion. Bakkes *et al.*, [75], taking up this idea, conducted a

detailed study of the classical Hly-TISS by using folding variants of the maltose binding protein (MalE), fused upstream of the C-terminal secretion signal of HlyA via the HlyA1 fusion vector. The MalE mutants varied only in their folding properties, with no effect on the unfolding rate. The results showed clearly that the slower the folding rate, the higher the secretion level of the fusion protein. In other words, the folding rate dictates secretion efficiency by the Hly T1SS. Importantly, with the slow-folding mutations that best promoted secretion, the activity of MalE in the fusion was not compromised.

These results also clearly ruled out the possibility that unfolding of a secretion substrate occurs prior to the actual secretion process and demonstrated for the first time experimentally, that substrates of a T1SS fold only after secretion. Second and even more important, the study by Bakkes *et al.* [75] provided a rational platform for generating T1SS fusion proteins. If a chimeric fusion protein proves to be secreted poorly, decreasing the folding rate by introducing point mutations is recommended. This strategy was supported by secretion studies on a fusion with IFAB (intestinal fatty acid binding protein). Here mutations that slowed the folding rate of IFAB increased secretion substantially, again without apparently compromising activity [76]. However, mutations that decrease folding of a certain protein cannot be predicted *per se* but have to be determined experimentally. Thus, error prone PCR or DNA shuffling could be the best approach, combined with screening for increased secretion levels.

In addition to the importance of the folding rate of the passenger, the expression levels of the inner membrane components of the HlyA T1SS (HlyB and HlyD) are also of prime importance for high yields of secreted protein. Only under conditions in which both membrane proteins were highly expressed, was efficient secretion observed [75, 76]. In particular, however, efficient secretion of heterologous fusion proteins is likely to be a multifactorial process dependent on several factors, in addition to folding rate and expression levels. However, these studies provided an important starting point and in our hands, the Hly T1SS is a very powerful system for efficient high yield secretion (our unpublished results).

The type I C-terminal signal (plus some RTX repeats) has now been used to secrete a wide range of heterologous proteins with biotechnological implications

A large number of pro- and eukaryote proteins or fragments of proteins, have now been successfully secreted as fusions to C-terminal regions of HlyA and in several cases shown

to fold correctly [75, 90, 91, 92, 93]. We recently developed a two-vector system coding for the inner membrane components (HlyB/HlyD) on one plasmid and the fusion protein (gene of interest fused to the N-terminus of HlyA1, see Figure 5) on the other plasmid. Here, successful secretion of slow folding mutants of MBP and an internal fatty acid binding protein was demonstrated [75, 76]. Yields were approximately $15\,\mathrm{mg\,L^{-1}}$ bacteria cell culture for the slowest folding mutant of MBP and approximately $1\,\mathrm{mg\,L^{-1}}$ bacteria cell culture for IFABP.

Similar results were obtained more recently using C-terminal signals from other Type 1 proteins. In particular, a minimal C-terminal fragment of 70 residues from the Tli lipase from *P. fluorescens* was used for secretion of EGF (epidermal growth factor) or GFP (Park *et al.*, [68], while the terminal 60 residues from another Pseudomonad, the lipase PML was also able to secrete a fusion with alkaline phosphatase as passenger [69]. A new vector for use in *P. aeruginosa* was described by Ryu *et al.* [77] that harbors genes for the ABC transporter, the MFP, where genes of interest are fused to the C-terminus of the LARD domain (lipase transporter recognition domain) and successful secretion was shown for GFP and alkaline phosphatase (AP). These examples demonstrate that new approaches are also under way in other laboratories to employ T1SS as a platform for protein production and purification.

Generation of novel *hly*-fusion vectors

A vector encoding the 23 kDa C-terminal of HlyA (HlyA1) (see Figure 5) was constructed in plasmid pSU. This was designed for easy insertion of coding sequences for different passenger proteins, N-terminal to the secretion signal, plus engineered cleavage sites for subsequent enzymatic release of the passenger domain. pSU was combined with plasmid pLG575 encoding both HlyB and D, to promote secretion of different heterologous passengers [76]. This HlyA1, 208-residue fragment, contains only the distal three RTX repeats of wild-type HlyA plus the approximately 60-residue secretion signal. In addition, this C-terminal fragment of HlyA also contains, upstream of the signal sequence, the binding site for the CLD region of HlyB. This is the specialized cytoplasmic N-terminal domain that is required for secretion of HlyA, but is also required for secretion of heterologous proteins fused to HlyA1 and smaller fragments from the HlyA C-terminus.

Detailed analysis of the structure-function of the signal: the enigmatic code

1) Type I C-terminal secretion signals appear conserved only in closely related transport substrates, there may be no universal signal

The presence of specific secretion signals within the terminal 50-60 residues for *E. coli* HlyA; 75 residues for cyclotoxin (*Bordetella pertussis*) and Leukotoxin (*Pasteurella hemolytica*); perhaps only the last 29 residues for protease PrtG from *E. chrysanthemi*; around 70 for lipases from *Pseudomonas* [68]; or 50 residues for an alkaline protease from *Pseudomonas aeruginosa* [66], are now well established. However, identifying the precise N-terminal of a such a non-processed signal is difficult.

Notably, the C-terminal 60-70 residues of type I proteins reveals no obvious amino acid conservation except amongst extremely closely related transport systems. However, initial studies suggested at least two subtypes, HlyA, hemolysin-like and PrtG protease-like groups. These have respectively, at the extreme C-terminus, a short motif of hydroxylated residues, or an acidic residue followed by three hydrophobic amino acids, DVLA [58, 94, 95]. In fact, similar C-terminal 'motif' of hydrophobic amino acids preceded by an acidic residue appears to be equally conserved in type I lipases, for example LipASM [95]. Nevertheless, the hydroxylated tail is not present in all toxins described as hemolysins, for example, LktA from *Pasteurella haemolytica*. In contrast, other type I substrates, such as colicin V, adenyl cyclase toxin, HasA, or the newly studied ankyrins have C-termini lacking either of these two motifs (see Figure 6).

Although based on apparently limited studies so far, type 1 transport substrates and components of their translocon, also appear to be interchangeable only between systems with very similar allocrites (see for example, [43, 66, 67, 81, 97, 98]. This specificity in most cases appears to parallel the relative conservation of the transporter components, for example, more than 80 % within the distinct HlyA and protease-lipase type I systems, but around 25 % between families (see for example Akatsuka *et al.*, [99]). More puzzlingly, the C-terminal 70 amino acids of the leukotoxin, LktA (from *Pasteurella hemolytica*), although deemed to have no obvious similarity to the HlyA signal sequence, was functionally able to replace the C-terminal 58 amino acids of HlyA ([100] and see Figure 6).On the other hand, , the HlyA translocon appeared relatively promiscuous, able to secrete to some degree, some very unexpected proteins. These included the CyaA toxin [70, 98], protease B from *E. chrysanthemi* [67] and especially the non-RTX protein, bacteriocin ColV (see discussion [101]) that is normally dependent on a

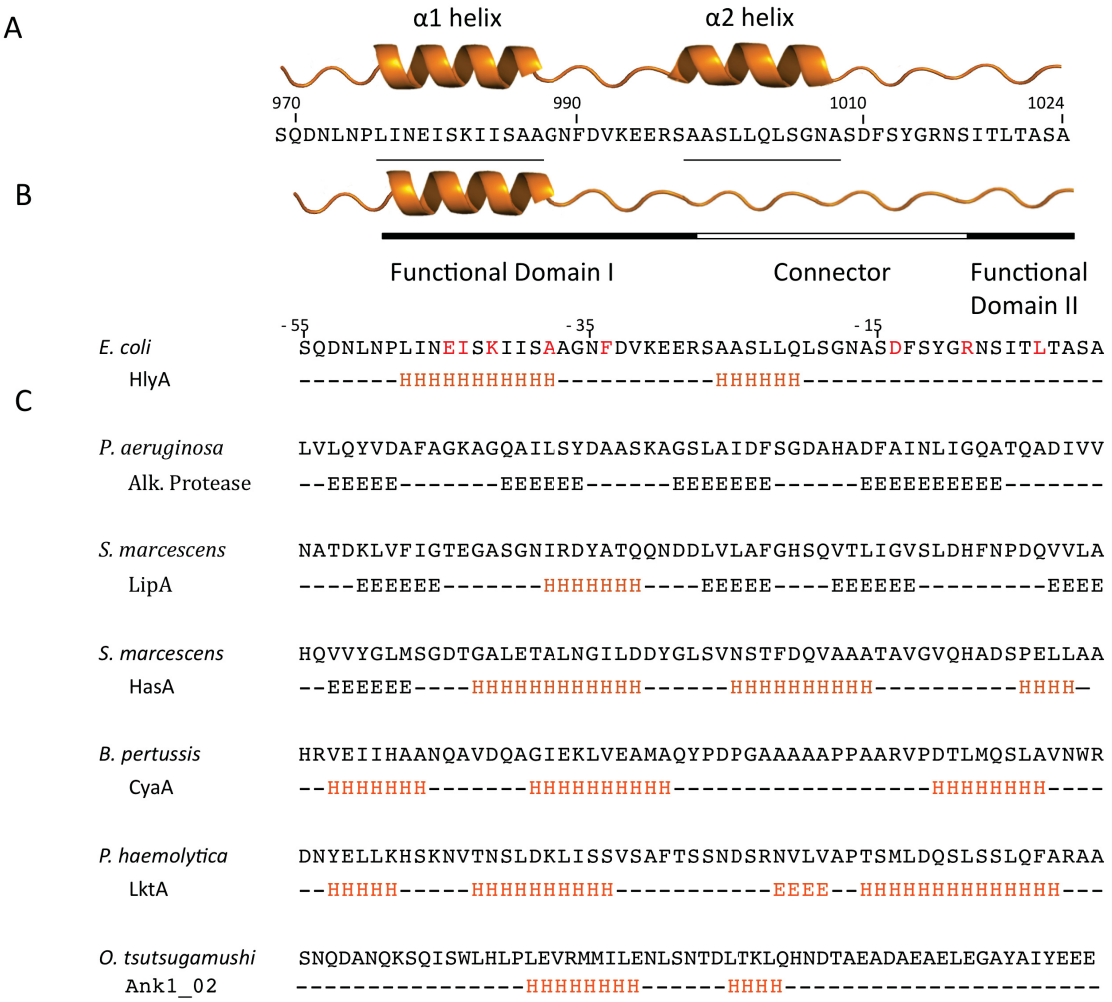

Figure 6: (A) Proposed secondary structure of the secretion sequence of HlyA. (B) Secondary structure of the secretion sequence of HlyA derived from NMR spectroscopy in solution [96]. (C) Secondary structure predictions of the secretion sequence of HlyA and other substrates of T1SS.

completely unrelated N-terminal signal. In contrast, apparently none of these heterologous systems were able to secrete HlyA. However, as stressed earlier these apparent examples of relaxed specificity may reflect the failure actually to measure what might in reality be low levels of very inefficient secretion.

2) Mutagenesis and deletion analysis of the structure-function of the HlyA C-terminal signal: linear code of individual residues or a structural code?

The great majority of attempts to elucidate the nature of code carried by the type I secretion signal have concerned the prototype HlyA. The following discussion will be focussed entirely on this system. First, as indicated above, most studies have in fact involved two *hly* determinants, one encoded on a plasmid, designated pHly152 [55], a second located in the chromosome from a pathogenic strain LE2001 [28, 29]. The two *hlyA* genes encode 1024 and 1023 residues respectively, creating some confusion when comparing the same mutated residues from different determinants used indifferent laboratories. In order to avoid this, in discussing the structure function of the signal region, residues will be identified with respect to their position from the C-terminus.

Early random mutagenesis studies from different groups, immediately suggested that the secretion signal was redundant, with many single residue substitutions having very little or only a moderate effects on HlyA protein secretion levels (summarized in [102]). However, as summarized in Figure 6, substantial, 60-70 % reductions in secretion were obtained with substitutions at positions -46 (glu), - 43 (lys), -39 (ala), -35 (phe), at -45 (ile), and reductions around 50 % at -15 (asp), -10 (arg), -5 (leu). Remarkably, one substitution at -35 (Phe to Pro) reduced HlyA secretion by more than 90 % [94], while construction of a triple mutant involving the substitutions at residues E(-45)F(-35)D(-15) gave additive effects, reducing secretion in total to less than 98 % by measuring haemolytic activity at the peak of secretion in liquid cultures.

In addition, end deletion constructs showed that removing the C-terminal 7 or 8 amino acids reduced secretion by 50-70 %, also using measurement of hemolyic activity in liquid cultures [27, 103]. However, removal of the 6 terminal residues appeared to have minimal effects on secreted protein levels but had a major effect on folding of HlyA to the fully active form [94, 104], clearly indicating an important functional role near the terminus of the signal. Overall these approaches placed the N-terminal boundary of the signal to between position -46 and -53, extending very probably to the C-terminal residue (see Figure 6).

3) Potential coding motifs in the HlyA secretion signal: alternative early coding models

As illustrated in Figure 6 simple inspection of the sequence of the HlyA signal region indicates the characteristics first considered as potential coding information. These are

charged cluster covering residues -32 to -29; a 16 residue 'aspartate' box (-30 to -15) flanked by acidic residues appeared to be conserved also in some other TISS transport substrates [105], two predicted α-helices approximately located at position -23 to -33, and at -43 to -48, in line with most subsequently published reports these will be referred to as helix 1 and helix 2, respectively. Notably however, another study predicted the presence of a much larger amphipathic helix covering amino acids from -35 to -53, including the charged cluster and overlapping Helix 1 mentioned above [27]. Nevertheless, in the absence of any strong evidence that such secondary structural features actually existed, Kenny *et al.* [102, 105] proposed the idea that a linear code depending on a few dispersed key residues act co-operatively in docking with the HlyB, by analogy with MHC ETC [106]. This model for the functional role of the C-terminal signal will be developed in more detail in later sections.

The model proposed by Koronakis and Hughes and colleagues on the other hand assumed a vital role for the predicted large amphipathic helix. These authors also noted other features that might have functional roles for the HlyA signal sequence, a block of 13 uncharged residues, distal to the charged cluster and overlapping the aspartate box, and an important role in the secretion process for the cluster of relatively hydrophobic, mostly hydroxylated residues at the extreme terminus [27, 103]. Stanley *et al.* provided mutagenesis data supporting a functional role for a large amphipathic helix (residues -29 to -53). It was also suggested that the predicted secondary structure for HlyA was conserved in other toxins and other type I proteins, such as the proteases and lipases. However, this was based on a very limited database and has not subsequently been substantiated. (see Figure 6). In fact, further mutagenesis experiments showed that the charged cluster could be deleted without loss of function [100], and when residues -60 to -39, including the proximal region of this amphiphilic helix were replaced by a proline containing peptide there was no effect on secretion [72]. Other published studies, designed to test a possible function for the proposed amphipathic helix, revealed in total 12 substitutions giving results consistent with a functional role while 10 were not consistent. However, most mutagenesis results were still consistent with a functional role for a much smaller amphiphilic helix in this region (overlapping the initially identified helix 1and centered on the 'hot spot' motif EISK (residues -45 to -43) in HlyA [94, 102].

Testing other possible motifs linked specifically to function, Kenny *et al.* [105] showed that substitution of the N-terminal Glu residue of the 'aspartate box' for lysine had in fact no effect on secretion. Finally, a targeted mutagenesis analysis [94], identified several mutations expected to disrupt the down stream helix II, but these also had little or no effect on secretion.

In summary, from the extensive random and directed mutagenesis experiments described above, most obvious possible coding motifs could seemingly be eliminated, and secondary structural motifs were not proven. Nevertheless, two competing hypotheses remained on the table. The Leicester group maintained [102, 105] that signaling information was determined through essentially a linear code of individual but dispersed residues for docking with the HlyB. In contrast, the Cambridge group [103] proposed a more complicated, but very specific model with particular importance ascribed to the presumed large amphipathic helix (helix 1), with the initial step in secretion being insertion of this proximal region of the signal C-terminal as a loop into the membrane, independently of the transporter proteins, HlyB and D. In contrast the distal region of the signal, covering 8 or so residues (including the hydroxylated 'tail') at the C-terminus of HlyA were proposed for specific docking to HlyB. This scenario also appeared to suggest, although not explicitly stated, that the C-terminal was translocated last. As discussed below this is clearly at odds with the now generally accepted hypothesis that the C-terminus should be the first to reach the surface, and thus facilitate Ca^{2+} dependent folding of HlyA. Indeed this hypothesis has now very recently been confirmed experimentally. Lenders *et al.* [107] used GFP fusions of HlyA1 and HlyA to stall the HlyA T1SS and specific antibodies to demonstrate directly that the C-terminus reaches the cell surface first. Finally, as described earlier we have shown that the extreme C-terminus is involved in post translocational folding of HlyA, rather than in initiation of secretion.

4) A combinatorial approach to evaluate functional secondary structure in the HlyA signal

Victor Ling and colleagues in a further attempt to evaluate possible structural motifs in the secretion signal, introduced random amino acid sequences, targeted to the regions called helix 1 and 2 and the intervening linker, using hemolytic colony halo size as a measure of secretion efficiency. The results [108], indicated little or no functional role for a helix 2 (see Figure 6). However, in contrast the results were consistent with an important role for the short amphiphilic helix 1, that overlaps with the putative amphiphilic helices mentioned above [27, 105].

In 2002, in a further combinatorial mutagenesis analysis, Hui and Ling [96] targeted the extreme C-terminal region of HlyA, in particular that designated as terminal region I, residues -9 to -16 and terminal region II, residues 1 to -8 (see Figure 6). The results indicated that the great majority of random sequences integrated into region I had little

or no effect on secretion (i.e. from halo size), suggesting that any a role for this region might simply be as a spacer or a "connector". In contrast, 50 % of sequences inserted into region II caused a reduced halo size. Therefore, these results support the previous findings [104] that the C- terminal 6 residues are not required for secretion *per se* but have an important function in promoting folding (and therefore activity) of the secreted HlyA. How this terminal region might contribute to folding will be discussed later.

5) Physical techniques in attempts to define possible structural codes in the secretion signal for translocon targeting

Is there indeed a linear amino acid code, particular secondary structures, a mixture of both, or something entirely different that determines recognition by the type I translocator? Since the maximum diameter of the TolC channel portion of the translocator is likely restricted to 20 Å [101], this should limit transit of any possible secondary structure to an α-helix and a similar constraint is likely to operate on any structural feature of the secretion signal in the cytoplasm presented to the translocon.

While the available evidence strongly indicates that TISS secretion signals dock *in vivo* with the translocator, probably HlyB in an unfolded form this does not exclude the presence of some secondary structure. Some NMR experiments have attempted to address this by a structural analysis of isolated type I signal peptides. However, these have not provided definitive evidence for any specific structure. The earliest studies for HasA and PrtG, [109, 110] found no secondary structures in aqueous solution while in membrane mimetic environments, including the helical promoting agent TFE (trifluoroethanol), some upstream helix was detected with the C-terminus unstructured. Essentially similar results with the analysis of the intact HasA in detergent micelles were obtained [111]. A CD spectrum analysis of the C-terminals of HlyA (61 residues) and LktA (70 residues) also indicated unstructured peptides in aqueous solution with some helical secondary structure in detergent [112]. In addition, Yin *et al.* [113] carried out an NMR analysis of the HlyA C-terminal secretion signal (61 amino acids) in SDS. This experiment was predicated on the idea that *in vivo* the signal - ABC protein interaction will take place in a membrane environment, although this has not been substantiated experimentally. The results were interpreted although with a number of caveats, to indicate the presence two short helices (approximate positions of the helices, I and II as shown in Figure 6 above). In fact, *in vitro* studies on the role of the RTX motifs and the downstream secretion signal, on folding of the type I substrates, adenylate cyclase toxin [86, 114] and the AprA protease from *P. aeruginosa* [88] indicate in the absence of

calcium a disordered structure for this C-terminal region that includes the RTX domain and the secretion signal at least up to 26 residues from the terminus [114].

On the other hand, the very few crystal structures of type I transport substrates so far available - for some proteases and lipases - show the C-terminals folded up to the extremity, as predicted (see Figure 4), as antiparallel β-strand sheets [5, 62, 61]. However, these are not informative on the possible conformation of the secretion signal *in vivo*. Thus, in addition to the contradictory genetic evidence regarding possible secondary structure, the published physical evidence, including especially the evidence indicated above for a disordered C-terminal *in vitro*, for CyaA, clearly indicates that the secretion signal *in vivo* probably lacks secondary structure.

6) HasA is an atypical type 1 protein but provides a novel insight into the nature of a C-terminal secretion signal

Previous studies indicated that the minimal HasA C-terminal fragment capable of autonomous secretion is found within the last 56 residues [71]. Subsequently, Cescau *et al.* [115] constructed a non-secreted variant of HasA with the C-terminal 14 amino acids deleted. Nevertheless, this truncate was able to fold in the cytoplasm (and therefore bind heme) but surprisingly was still able to engage the ABC and MFP proteins and to assemble a complete (but "frozen") translocator. This contained TolC, as shown by affinity purification of the complex. Indeed, with the high level of production of the ABC and MFP proteins employed in these experiments the majority of cellular TolC was titrated, rendering the cells sensitive to SDS, presumably by depletion of the AcrAB-drug and detergent transport pump. In addition, preliminary evidence indicated that this terminal fragment bound the ABC protein HasE *in vitro*. These remarkable results, unfortunately not apparently followed up, suggested that the terminal 14 residues of the secretion signal are not required for docking but play a subsequent role in translocation *per se*. This role might include reversal of signal binding to allow committed entry into the transport pathway, or at a later stage that tightly couples translocation to refolding of the protein as the C-terminal emerges on to the cell surface, as may be the case for HlyA.

7) Screening tests for some functional states of the type 1 translocator

The paper by Cescau *et al.*, [115] exploiting SDS sensitivity of cells to detect a frozen complex, also highlights the use of simple plate tests for easy monitoring of certain states of the translocon. Previous studies had also shown increased sensitivity of laboratory

strains of *E. coli* K12, associated with the presence of the *hlyA*-determinant, to the antibiotic vancomycin (normally active only against Gram positive bacteria), even in the absence of the HlyA while mutations in *hlyB* or *hlyD* reduced this sensitivity [116]. In addition, Blight *et al.*, [117], found increased vancomycin sensitivity (but not for another antibiotic, fusidic acid) in *E. coli* K12, expressing *hlyBD* and WT *hlyA*, but resistance was restored when a highly defective secretion signal mutant of HlyA was used, indicating that active translocation of the allocrite increases envelope permeability in some way. Consistent with this, the peak of secretion activity in the growth phase with the pathogenic strain LE2001 coincides with increased vancomycin sensitivity [40]. Changes in vancomycin sensitivity can therefore be used to screen mutants or the effects of suppressors to test for changes in the function of the translocon.

On the other hand competition experiments, co-expressing WT and mutant forms of T1SS allocrites in the same cells and in the presence of the transport functions, are useful in order to distinguish mutations (recessive) blocked in binding to the translocon and mutants (dominant) that engage the translocator but fail to proceed to the next stage, thus titrating available translocons and inhibiting secretion of the WT transport substrate. Combining this with testing for sensitivity to SDS or vancomycin should also provide a quick screen for classifying mutants.

8) Nature of the signal region in other TISS

Other more limited studies have been carried out to identify possible conserved motifs and essential functions in the secretion signals for lipases from different Gram-negative species. As illustrated in Figure 6 (with representative examples only), the C-terminal sequences and putative secretion signals for proteases and lipases, reveal some apparently distinctive features, although these appear quite different from those of both HlyA and HasA.

Ghigo and Wandersman [58] first suggested that the extreme C-terminal sequence DLVL was a secretion 'motif' found in both protease and lipases. Indeed for the protease PrtG, deletion of this sequence prevented secretion of the protein. However, in subsequent studies of the secretion of lipase LipA from *S. marcescens*, [95] found that a similar motif was not required for secretion. In a similar study of the I.3 (PML) lipase by Kuwarhara *et al.* [118], the hydrophobic residues in extreme C-terminal motif were shown by mutagenesis not to be required for secretion of this lipase. In addition, these authors showed that the extreme C-terminal motif in the I.3 lipase (PLM) from Pseudomonas was required for heat stability of the protein rather than for secretion

per se. However, perhaps these apparent differences can be rationalized with the overall conclusion that the extreme terminal residues in the lipase, protease, the HlyA sub group and conceivably HasA (see [115] above) are somehow involved in the folding of the polypeptides as they emerge on the surface, with, in the case of the truncated PrtG and HasA, transport itself being blocked at an early stage.

The TISS from *S. marcescens* mentioned above is particularly interesting, since as described by Omori *et al.* [95] unusually, three unrelated polypeptides are translocated by the same translocator, a metalloprotease PrtA, the lipase LipASM and a surface layer protein Sla. In fact, all these are encoded, together with the transport proteins in the same operon (see Figure 2). Moreover, this translocator is able to secrete similar proteases and a lipase from other bacteria, although again the efficiency was not reported.

S. marcescens also secretes the heme binding protein HasA and intriguingly the dedicated HasA TISS is able to secrete PrtA and LipA from this same host. However, reciprocal secretion of HasASM was not observed. Nevertheless, Omori *et al.* [95] noted that the TISSSM was able to secrete HasAPF from *P. fluorescens*. The authors did the smart thing, comparing the two HasA sequences and were able to identify a short motif around residue -17 from the C-terminus. This was present only in the Pseudomonas HasA. Site directed mutagenesis confirmed that residues - 15- to -19, VTLIG (forming a β-sheet structure in the fully folded proteins carrying this motif, [5]), were indeed critical for secretion. The authors suggested, based on the testing of hybrid translocators from the LipA and HasA translocons that this motif was specifically involved in targeting the ABC transporter. However, it is difficult to see how this short, mainly hydrophobic patch has the specificity by itself to determine specific translocon docking. Moreover, everything was not so simple since the HasASM system can still transport both of these HasA variants. Nevertheless, it is surprising that these findings, indicating a motif contributing to allocrite specificity have not apparently been followed up, although Kuwarhara *et al.*, [118], confirmed the importance for secretion of the conserved VTLIG in another lipase, (PLM) from Pseudomonas. In particular, it would be important to demonstrate directly the binding of such a motif to the cognate ABC protein.

A dual function TISS secretion signal: perhaps not so enigmatic after all

1) A linear code looks the most likely for the HlyA sub-family

Based on their combinatorial experiments described above, Hui and Ling [96] proposed a revised structure-function model for the C-terminal 55 or so amino acids as illustrated in Figure 6. As summarized in Figure 6, the model suggests that domain I (residues -38 to -49), predicted to form a short amphiphilic helix, is essential for secretion, followed by a long downstream "connector" (residues -9 to -28), presumably carrying no specific coding information, and finally a relatively hydrophobic region of 9 residues extending to the terminus, termed functional domain II. Consistent with the model, previous reports indicated that amino acid substitutions in the so-called connector region had little effect on secretion [102, 105, 103]. However, as argued above there is still no evidence that the helix exists *in vivo* and that *in vitro* on the contrary the evidence for CyaA indicates a C-terminal with a disordered structure. On the other hand, random mutagenesis studies from other laboratories support the importance for efficient secretion of the residues centred on the position of the predicted helix I that notably, contains the hotspot motif, EISK in HlyA [105]. Hui and Ling model also indicates a functional role for domain II in secretion. More recent experiments show that this region is important but at least in part this is required for post-translocational folding, rather than secretion *per se* [104].

Another limitation of the Ling and colleagues model and that of Stanley *et al.*, [103], is, highlighted by the current availability of the sequences of large numbers of type I proteins, and from structures of proteases and lipases, and it is clear that many are likely to contain β-sheets rather than α-helices. Moreover, the Cambridge model in particular ascribes a very specific role for an amphiphilic helix, apparently rather independent of precise amino acid sequence, able to partition into the membrane, en route to the translocator, leaving the docking specificity for HlyB to a few residues at the extreme C-terminal. Initial insertion of some TISS secretion signals, involving a β-sheet motif seems difficult to envisage.

On the other hand, if we discard the idea of the helical nature of domain I, the Ling model would still be compatible with the proposal [94, 102, 105] that the 8 or so individual but dispersed residues identified (so far) (see Figure 6) that reduce HlyA secretion substantially, constitute part of a linear code for docking with the translocon. Indeed Hui and Ling [96] specifically keep this possibility open. Therefore, as we shall argue in the final section of the review, looking at all the evidence available, we clearly

favor the importance of linear code in type I secretion for translocon docking, irrespective of the so far unknown secondary structure *in vivo*.

As proposed earlier this would be reminiscent of the mode of docking of antigenic peptides with the ABC TAP transporter [119]. Here, the N- and C-terminal residues in the allocrite in particular are required for efficient and high affinity binding. A similar linear coded interaction is well established for MHC class I molecules [106] and compatible with co-evolution of a ligand and its receptor in adaptive immunity.

2) Proposed role of the C-terminal regions of type 1 allocrites

Type I secretion signal regions appear to have at least two functions, a proximal recognition region (perhaps extending from -15 to -46, and a distinctive function for a few residues at the extreme terminus.

Recently discovered T1SS translocation in Salmonella, Rickettsia and other bacteria: yet more variety in secretion signals and secretion without RTX

The group of Karla Satchell has recently pioneered the study of toxins secreted by the type I system, based on the ABC, MFP, OMP translocon in many of the most important pathogenic bacteria. These "giant" MARTX (multifunctional-autoprocessing repeats in toxins) polypeptides up to 9000 residues long, frequently contain strings of several distinct toxins and many studies have concentrated on the structural organization, mode of penetration into host cells and mechanism of action [13]. In fact, these proteins have a slightly variant form of the classical RTX repeat (consensus, GGXGXDXUX) as expected close to and upstream of the C-terminal secretion signal. However, calcium binding and the 3D structure of these MARTX repeats (consensus GGX(N/D)DXHX) has not been described and as yet few details of the actual secretion mechanism have appeared. The ABC transporters, in these systems, however, like HlyB, appear to have an N-terminal CLD, and intriguingly, Boardman and Satchell [120] showed that secretion of RtxAVC, and other closely related toxins, requires a 4 rather than a 3-component translocon, with a second gene encoding an additional ABC transporter. The ATPase activity of both ABC proteins is required for secretion and the authors propose that this may take the form of a heterodimer (see also review by [18, 121]).

Several studies have now identified a novel TISS in a *Salmonella enterica* with a number of unexpected features. This involves another giant type I transport substrate,

(with over 5000 residues) constituting a non-processed, non-fimbrial adhesion SiiE that was likely missed in the screen described by Linhartova *et al.*, [6] for RTX proteins. Thus, this allocrite [122] contains 53 closely packed, but non-RTX Ca^{2+} binding blocks, constituting around 90 % of the adhesin. Each block corresponds to about 90 amino acids, with highly conserved sets of dispersed Asp residues binding Ca^{2+} ions (see also review by [16]). Secretion in this case still depends on an approximately 60-residue secretion signal at the C-terminus, plus an ABC, MFP and OMP, all encoded in the same operon [123]. Calcium is also apparently required in some way for secretion (personal communication, R Gerlach). Surprisingly, the *siiE* operon also contains two additional, proximal genes encoding membrane proteins, one with similarity to the ExbB/TolQ membrane proteins (implicated in harnessing the pmf in bacteria for import through the outer membrane) and the other similar to MotB (part of the proton driven motor controlling flagellum rotation), which the authors suggest have a novel, exciting accessory function associated with this TISS, in forming a proton conducting channel, linked in some way to secretion and or surface fixation of the transported polypeptide, an important distinguishing characteristic of this type 1 allocrite [124].

Rickettsia form a large genus of aerobic, Gram-negative bacteria, living as obligate intracellular parasites in both invertebrate and vertebrate hosts and causing many diseases in humans, including typhus. These organisms, for example, *R. typhi* have reduced genomes of less than 900 genes, relying on the host, for example, for biosynthesis of amino acids and nucleosides. The organism is frequently transmitted to humans by fleas, lice and mites through bites, allowing the bacteria to access the vascular system and to establish residence in endothelial cells of the skin and major organs. So-called scrub typhus is endemic in the Asia Pacific region with huge numbers of people dying annually from this disease.

Rickettsia and other intracellular bacteria produce several copies of ankyrin proteins as pathogenicity factors. These proteins characteristically contain a varying number of tandem repeats (mostly of 33 amino acids) of degenerate sequence but with a conserved secondary structure, allowing stacking of the repeats upon each other [125].This presents a platform maximizing opportunities for protein-protein interactions. Such broad specificity for protein interactions allows the modulation of the action of a wide variety of host proteins and therefore facilitates intracellular survival. In another recent review, Gillespie *et al.* [126], used a bioinformatics and literature search to identify likely secreted proteins and components of presumed translocation systems in Rickettsia. The results revealed at least 19 secreted proteins, including some ankyrins, together with a near classical Sec-system and genes encoding at least three secretion pathways, TSS

types I, IV and V. In parallel, a number of groups, in particular, [127], have provided intriguing evidence that many of the 47 ankyrins in the scrub typhus pathogen, *Orientia tsutsugamushi* (member of the *Ricettsiales*) are indeed type I substrates.

Even more recently, indications of 7 putative type I protein translocation systems, have been found in the Gram-negative, obligate anaerobe, *Bacteroids fragilis*, as defined by the presence of linked genes encoding, an ABC, MFP and a TolC-like homologue. *B. fragilis* is a member of the phylum Bacterioidetes, the largest group of bacteria in the human microbiota, having interesting differences in the lipid composition of membranes and the peptidoglycan, compared to the Proteobacteria. On the other hand no potential transport substrates have so far been identified. Moreover, no sequences encoding RTX motifs were detected in the *B. fragilis* genome, pointing to another interesting variation on how to fold up type I proteins following translocation that we can expect to be revealed in the future.

Structure function analysis of components of the TISS translocon

TolC: structure and function

While the MFP and ABC proteins are specifically and uniquely dedicated to transport of Type I substrates, TolC is an extraordinarily multifunctional and under some conditions apparently an essential protein [128, 129]. Thus, TolC of *E. coli* forms a tripartite pump with AcrA and AcrB (and their homologues in other bacteria), involved in the efflux of a wide range of toxic molecules. These include many cationic dyes, a wide range of antibiotics such as penicillins and macrolides, detergents such as Triton X-100, sodium dodecylsulfate, bile acids, and even simple organic solvents [130]. Remarkably, in addition, TolC, as a component of the TISS, is also essential for secretion of a variety of proteases, lipases and hemolysins. In the absence of *tolC*, *E. coli* therefore becomes more sensitive to many different molecules. Finally, other more recent studies have also indicated that the Acr-TolC pump is implicated in the export of fatty acids [131] and cyclic AMP [132].

In contrast to the very large amounts of porins present in the outer membrane of *E. coli*, the numbers of TolC molecules are relatively low at about 1500 [133]. However, interestingly, Krishnamoorthy *et al.* [134] recently demonstrated that only a small minority of these (less than 10 %), are sufficient to maintain cells free of growth inhibitory levels of an antibiotic like vancomycin. This indicates that TolC is normally present in

significant excess and well capable of participating, together with AcrA and AcrB, in the efflux of a wide range of other molecules.

For secretion via the TISS and HlyA in particular, TolC interacts with the ABC transporter, HlyB and the MFP, HlyD, both in the inner membrane. In contrast, when TolC is associated with AcrAB in extrusion of small molecules the ABC transporter is replaced by an RND (resistance-nodulation-division) membrane protein [135]. This is a secondary transporter that utilizes the proton gradient across the inner membrane to energize transport. In contrast to HlyD, the MFP component of the drug pump is anchored to the external face of the inner membrane by a specific fatty acid modification at its N-terminus and lacks the extension across the inner membrane into the cytosol. The prototype of these multidrug transporters is the AcrA (MFP), AcrB (RND), TolC complex, for which the single particle cryo-EM structure was recently determined [52]. A structure for TolC was initially obtained by two-dimensional crystallization in 1997 [136] at a resolution of 13 Å. In 2000, a seminal paper by the Koronakis laboratory described the crystal structure of TolC at a resolution of 2.1 Å [51]. This structure, combined with biochemical data, indicated that the inner membrane components, HlyB and HlyD are only transiently in contact with TolC. In other words, the IM components engage TolC only upon interaction with the unfolded substrate and remain associated during the actual secretion process. However, as in the case of assembly of TolC with AcrAB, as we shall argue later it remains a possibility that TISS transport substrates simply stabilize normally transient interactions between TolC and its different partners.

The structure of TolC also demonstrated that the functional unit is a trimer embedded in the outer membrane of *E. coli*, forming a β-barrel, typical for bacterial porins. In TolC, this is a 12-stranded antiparallel β-sheet, in which each TolC monomer contributes four β-strands to the final 12 stranded barrel. In contrast to many porins, this barrel appears to be always open to the extracellular space since the structure lacks any potential plug, such as the loop present in the ferrichrome-iron transporter FhuA, in *E. coli*. Furthermore and in contrast to classical porins, TolC extends very far (120 Å) into the periplasmic space. This part of TolC adopts an entirely α-helical fold, again composed of 12 α-helices, four from each monomer. At the periplasmic end of this α-helical extension, the helical bundle has a maximal diameter of only 3.9 Å [137]. This indicates that the structure is the closed state, since this is obviously too small to allow transit of even α-helices or small solutes (see Figure 7).

Noting a series of salt bridges and hydrogen bonds present at the periplasmic entrance of TolC, Koronakis and colleagues tested the functional implications of this by designing an elegant set of experiments to disrupt these interactions by side directed mutagenesis

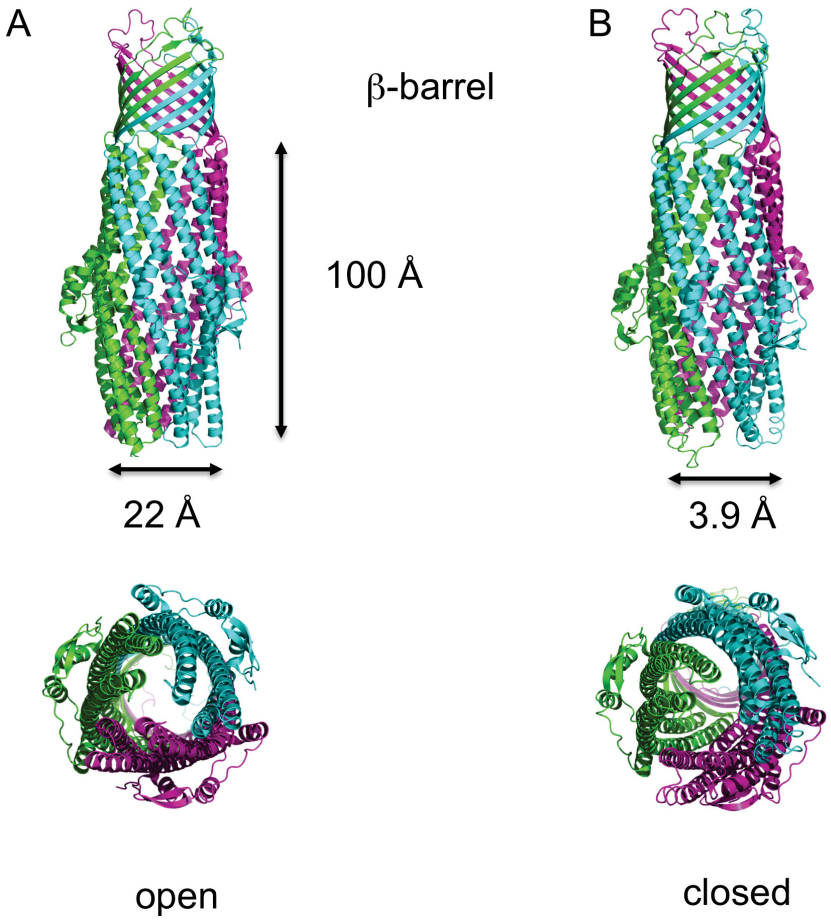

Figure 7: Crystal structures of TolC in (A) the closed (pdb entry 1EKP, [51])and (B) the open state (pdb entry 2XMN, [138]). Each monomer of the TolC trimer is colored differently. The length of the periplasmic helices is highlighted. The maximal opening of the closed and open states of TolC is also indicated below the figure.

[139, 140]. Indeed, this generated a TolC variant with a maximum diameter of 16 Å, based on conductance measurements of TolC reconstituted in black lipid membranes. This variant, as also shown in Figure 7, apparently represents the open state compatible with translocation of α-helices or small molecules via the tripartite drug efflux systems. Thus, as proposed by Koronakis *et al.* [27]) the data fit beautifully into a model whereby the molecule to be translocated induces an "iris-like" opening of the periplasmic 'tunnel' of TolC, involving outward sliding of the helices. However, one has to add that this now generally accepted mechanism was challenged by the crystal structure of the TolC homologue VceC, required for transport from *V. cholerea* of the range of xenobiotics and

small molecules as seen with TolC [141]. This structure revealed that the key residues apparently responsible for closure of the TolC entrance are not conserved in VceC, raising the interesting possibility that the "iris-like" mechanism proposed for *E. coli* TolC was not necessarily used in all other T1SS or small molecule efflux pumps.

The MFP HlyD: structure and function

1) Clues to the structural organization of HlyD from its MFP analogues

Little is known about the structure and functional roles of other Type I ABC and MFPs and the following sections will therefore consider only HlyD and HlyB. HlyD from *E. coli* is assigned to the so-called family of bacterial "membrane fusion proteins or MFPs". This is a misnomer since these proteins do not promote membrane fusion in the classical sense. Rather they provide the physical and functional coupling of proteins in transenvelope complexes that straddle the inner and outer membranes - a preferred term also used is "adapter proteins". Regrettably, just to muddy these waters more, Symmons *et al.* [142] in an otherwise excellent review now introduce a new synonym, PAPs (periplasmic adaptor proteins).

As will be discussed later the importance of HlyD in type I transport was to some extent initially underestimated, assumed simply to fulfill the role of connecting the inner membrane ABC protein with the outer membrane, TolC exit to the medium. While no HlyD structural data are available, mutational studies and in particular crystal structures of functional analogues, can bring important insights into the much more more complex role of HlyD. These homologues include the extensively studied MFPs, AcrA and MexA that form three protein component translocons with AcrB, TolC and MexB, MexX, respectively, as multidrug efflux pumps in Gram-negative bacteria.

Notably however, HlyD differs from many other MFP proteins, including AcrA, MexA (multidrug efflux), by having a single TMD anchor (close to the N-terminal) that inserts into the inner membrane. This is preceded by an approximately 60-residue extension into the cytoplasm (see Figure 8). In contrast, AcrA is anchored in the membrane from the periplasmic side by a lipid modification of the N-terminal presumably facilitating capture of drug molecules from the bilayer, while the TMD and the N-terminal extension in HlyD permits direct contact with HlyA in the cytoplasm. This arrangement of course should also permit the formation of a continuous tunnel from periplasm to the cytoplasm as discussed later.

Although HlyD, AcrA, MexA and other family members share less than 25 % identity, Johnson and Church [144] identified a number of well-conserved structural motifs in the

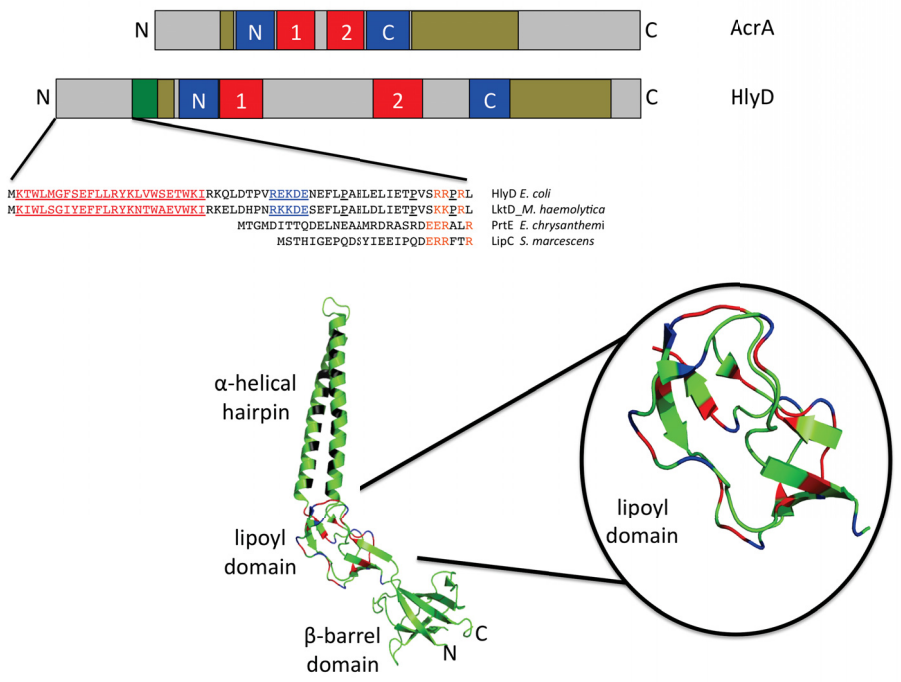

Figure 8: Top: Schematic representation of AcrA and HlyD. At the top the boxes represent the structures of AcrA and HlyD, indicating the location of the cytosolic domain, the transmembrane helix, the coiled-coil, lipoyl and β-barrel domains. Scaling is based on the number of amino acids, which build up the individual parts. The transmembrane helix of HlyD is shown in green. The two helices of the coiled-coil domain are highlighted by red boxes and labeled 1 and 2. The two parts of the lipoyl domain are indicated by blue boxes labeled N and C indicating the N- and C-terminal parts of this domain, while the β-barrel domain is indicated by brown boxes. The zoom in shows the sequences of the cytoplasmic domains of HlyD, PrtE, LipC and LktD. The putative amphipatic helix (colored in red) and charged cluster (colored in blue) in HlyD [53] is highlighted. The positions of the domains of AcrA are derived from the crystal structure shown below, while the corresponding positions in HlyD are estimated from a AcrA/MacA/ZneB/CusB/MexA-based homology domain of the periplasmic domain of HlyD. Bottom: Cartoon representation of the crystal structure of monomeric AcrA [143] and a zoom into the lipoyl domain. Black colored residues represent the predicted position of the heptad repeat of the α-helical hairpin. Blue colored residues are identical amino acids in more than 50 % of the sequences analyzed by Johnson and Church [144] of the lipoyl domain, while red colored residues are similar amino acids in more than 50 % of the sequences analyzed.

large periplasmic domains of all these proteins (see review by Symmons *et al.* [142]). As shown in Figure 8, there is an extensive helical hairpin, strongly predicted to form coiled

coils, towards the N-terminus in, for example, AcrA, although much longer and more centrally positioned than in HlyD. Importantly, the hairpin domain in all these proteins is flanked at each end by a short half "lipoyl" domain. This lipoyl module has been studied in detail as it activates particular enzymes, involving a switch in architecture from two well-separated halves to a fused globule of two domains. Johnson and Church [144] also noted the possibility in MFP adaptor proteins that the lipoyl domains provide the means to switch the hairpin from a compact structure (lipoyl domains fused) to one with extended helices stretching across the periplasm (see Figure 8). Other predicted structures conserved in these proteins are an extended β-barrel N-terminal to the helical hairpin and a disordered C-terminal domain [142, 144].

2) Structural models of complete efflux pumps: hints for HlyD assembly into the translocon

Several recent structural studies combined with model building suggest how the known crystal structures of, for example, for AcrA, AcrB and TolC are organized in the complete pump. These studies have involved much debate concerning the contribution of each subunit to the putative transenvelope transport pathway - whether the inner membrane protein (AcrB/MexB) contacts the OMP, how many subunits of the MFP in the complex, and especially contentious, does the long (approximately 140 Å) funnel shaped MFP, "wrap" around the outer membrane protein forming the periplasm to exterior "tunnel" or does it form a "tip to tip" contact. Previous analysis of mutants and cross-linking experiments have indicated that for example, AcrA interacts with both AcrB (a secondary transporter supplying the energy) and TolC [145, 146]. Now the most recent attempts to 'recreate' the complex, involved engineered fusions of AcrA with AcrB and AcrA and AcrZ (a new small protein binding to AcrB). These allowed co-purification of the complex AcrA-Z, AcrB and TolC, for cryo-EM analysis and this structure probed by overlayering with the crystal structures [52]. The results provide further confirmation for the emerging consensus (for example, see Stegmeier *et al.* [147]) for a stoichiometry 3,6,3, rather than, 3,3,3 for AcrB-A-TolC. The results show that both AcrB and AcrA form the walls of the channel also apparently confirms that AcrB and TolC do not interact. In addition, the Du *et al.*, model indicates that the termini of the long TolC helices protrude into the upper reaches of the AcrA funnel giving quite a small wrap-around of TolC by AcrA. A similar study by Kim *et al.* [18] described essentially the same overall organization with the difference that the respective tips of AcrA and TolC intermesh with no real overlapping.

It is tempting to extrapolate these results to gain important insights into the organization of HlyD within the Hly translocon. Some support for this approach was provided by Lee *et al.*, [148] who searched HlyD for the motif, R3xL6xS (RLS), that they proposed was conserved in 'adaptor proteins' including AcrA and MacA. A similar RLT motif was identified and indeed individual substitutions of each of these residues, effectively blocked secretion of HlyA. More interestingly, these mutations, particularly alanine substitutions of the R and L residues, prevented cross-linking of HlyD to TolC *in vivo*. Moreover, in an *in vitro* assay, the mutants were, unlike the WT, unable to bind TolC. Lee *et al.*, [148] in the same study on the other hand noted the obvious differences between, for example, HlyD and AcrA, in overall primary and secondary sequence. As illustrated in Figure 8, HlyD is significantly larger, in particular in the putative hairpin region (between the lipoyl motifs). In HlyD these apparently contain less (predicted) α-helical structure. As Lee *et al.*, [148], also point out, however, in another *E. coli* MFP or adaptor protein, CusB, the equivalent hairpin region forms an even more distinctive three-helix bundle for docking with TolC. Although these analogous structures are useful in gaining insights into the structure function, and particularly the nature of the assembly of HlyD into the translocon, its distinctive primary sequence and the contrasting size of the transport substrate, HlyA, necessitate that the structure of HlyD itself will be essential in order to obtain a detailed molecular understanding of its role.

3) Spring-like structural flexibility of MFP proteins: importance for function

As first proposed by Johnson and Church [144], the two conserved lipoyl domains of the MFP family, building on knowledge of the regulatory switch function of such domains in a number of enzymes, could provide important structural flexibility required for the role in secretion. Lipoyl domains are capable of switching between a compact state where they interact to form a globular structure or whether they remain separated. In the MFP family it is suggested that in the compact state, for example, in HlyD or AcrA, the intervening coiled coil region will remain paired and HlyD will be unable to contact TolC (see Figure 8). Consequently, when in the case of HlyD the Lip domains separate - spontaneously, when bound to HlyB or when triggered by contact with HlyA, the now extended helical domains would spring apart and allow contact of the C-terminal with TolC.

Genetic analysis of HlyD suggests possible functional domains

1) Topological organization of HlyD

Wang *et al.* [41] using fusions of β-lactamase to different sites in HlyD, identified regions rendering cells sensitive or resistant to the antibiotic, indicating exposure to the cytoplasm or periplasm respectively. This and cellular fractionation analysis demonstrated that HlyD has a single transmembrane domain (approximately residues 60-80 for insertion into the inner membrane with its N-terminal extension of 55 to 60 residues in the cytoplasm, predicted to form mostly α-helices (see Figure 8). More detailed analysis using alkaline phosphatase fusions confirmed this topology [149]. Surprisingly in both studies, viable fusions could not be obtained in the central region of HlyD approximately residues, 150 to 325, largely covering the coiled coil domain.

2) Mutations revealing possible HlyD functional domains

A genetic approach to the function of HlyD has been surprisingly limited nevertheless deletion and mutagenesis analysis has revealed four possible functional roles for HlyD, docking with HlyA, final folding of HlyA, oligomerization of HlyD, and possibly interactions with TolC. As described below the largely helical N-terminal extension of HlyD plays a key role in the recruitment of HlyA and then TolC into a fully competent translocon, and deletion of the first 40 amino acids blocks secretion completely. The truncated HlyD, however, remains stably localized to the membrane. In contrast, this same region is required for oligomerization of HlyD *in vivo* but this does not require the ATPase activity of HlyB. Surprisingly, in competition experiments the deleted HlyD mutant co-produced with WT HlyD, does not affect secretion of HlyA but greatly reduces its hemolytic activity. This suggests perturbed packing in a mixed oligomer of WT and mutant molecules, resulting in misfolded hemolysin as found with other mutants described below (unpublished results, J Young, A Pimenta and IB Holland). In a further analysis Schulein *et al.*, [150] noted some conservation of the C-terminal amino acids of HlyD (especially the last 35 residues) when compared to the short list of a range of TISS allocrites available at that time. When they deleted the 10 C-terminal residues of HlyD secretion of HlyA was completely blocked. Similarly, site directed mutagenesis of any one of the terminal, Leu, Glu or Arg residues of HlyD demonstrated that these were essential for secretion. Importantly, in competition experiments expressing both WT HlyD and (HlyB) and mutant HlyD, secretion of HlyA was greatly reduced indicating that the different forms of HlyD were unable to oligomerize or the mixed oligomer was defective in translocating the toxin. Curiously, these authors also identified a region

of 44 amino acids in HlyD (residues 127-170) showing a surprising 47 % identity with residues, 233-274 in the β-barrel region of TolC. Deletion of this region unsurprisingly completely blocked HlyA secretion but regrettably analysis of the role of these residues in HlyD function was not followed up.

In a different approach Pimenta *et al.* [151] used random mutagenesis of *hlyD* in LE2001, to obtain several mutants located in the periplasmic domain, whose expression, stability and membrane association were unaffected. The mutants had novel properties suggesting an interesting range of important functional differences. For example, three mutants, T85I, K402E and D411N secreted very little if any HlyA but HlyA was not detectable in cell envelopes, suggesting a block early in initiation of secretion. Moreover, D411N appears defective in oligomerization and in competition experiments, co-produced with WT HlyB and D, although secretion levels of HlyA are normal oligomerization of HlyD is reduced and markedly, hemolyic activity is also significantly reduced, suggesting that a mixed HlyD oligomer is formed but its structure is perturbed. A similar phenotype for the mutant K404E, co-produced with WT HlyD, was also obtained (unpublished results, J Young, A Pimenta and IB Holland).

Two other mutants V334I and L165Q (in the TolC-like region indicated above), although still secreting low levels of HlyA, showed an apparently distinct phenotype appearing to be blocked in translocation, since cytoplasmic levels of HlyA did not increase, while HlyA accumulated in the cell envelope in a state insensitive (apparently inaccessible) to extracellular trypsin digestion. Moreover, the proteins recovered from culture supernatants of L165Q, together with another mutant V349I, secreting around 25 % the level of WT HlyD, also displayed greatly reduced levels of haemolytic activity. However, in denaturation-renaturation experiments the specific activity of these molecules could be restored close to that of the WT HlyA, a clear indication that the initially secreted proteins were misfolded. In the case of V349I the secreted protein was also hypersensitive to trypsin.

As noted above a particular motif 'RLS' involved in binding AcrA to TolC is apparently also found in HlyD and in at least some homologues in the form RLT. This motif was shown by Lee *et al.* [148] to be required for secretion of HlyA by substitution of these residues, including alanine replacement of R and L, while these HlyD mutants were unable to bind to TolC *in vivo* and *in vitro*. This motif, in reality RxxxLxxxxxxT, is located about 125 residues downstream of the TMD and within the predicted hairpin region of HlyD and Lee *et al.*, suggested that HlyD, like AcrA contacts TolC "tip to tip", involving the 12 residues of the RLT 'motif'.

Genetic analysis of HlyB

1) Topological organization of HlyB

The topology of HlyB was deduced experimentally in 1991 [41] from the construction of β-lactamase fusions throughout the length of the protein. The results, where an externally exposed β-lactamase should confer penicillin resistance on strains carrying a fusion, indicated six TMDs (transmembrane domains). The fusion data also appeared to indicate two additional domains near the N-terminus but these were poorly predicted. In fact, sequence data indicated strong homology with a cysteine protease although the sequence suggested that the catalytic site was likely non-functional. Interestingly, Gentschev and Goebel [152] reported a topology analysis using β-galactosidase and alkaline phosphatase fusions, although showing differences in the precise position of the TMDS they also identified eight possible TMDs, including two in the N-terminal region. However, as described above the N-terminal domain up to at least residue 130, now designated CLD (C39-like domain), was recently shown by Lecher *et al.* [56] to constitute an ancient but inactive C39 cysteine protease, required for secretion of HlyA. The topology of HlyB now shown in Figure 9, is a composite taking account of all the fusion data from Wang *et al.* [41] and Gentschev and Goebel [152] but now showing the N-terminal as the cytoplasmic domain CLD. The model in particular indicates a single large periplasmic loop P1, exposed to the periplasm, and two very small loops P2 and P3, with two relatively large cytoplasmic loops, C1 and C2, and two regions of approximately 25 and 36 amino acids, with presumably important functional roles, flanking respectively, the TMDs from the CLD and NBD domains.

2) Mutagenesis analysis of HlyB

Very few mutagenesis studies for HlyB have been reported, in particular concerning the membrane domain. This unfortunately is a very important approach that has been seriously neglected. Of course several mutants (including in HlyB) have enlightened the analysis of the catalytic action of the NBDs of the ABC family by confirming the important role of many of the classical conserved residues. These have been studied in detail in many different ABC proteins and will not be considered further here.

As summarized in Figure 9 some mutations linked to the membrane domain give intriguing phenotypes but so far have been much less instructive in linking structure to function than comparable HlyD studies. Several mutants were isolated by random mutagenesis by Blight *et al.* [117] two of these (G10R and P624L) showed novel temperature sensitive secretion defects. Residue G10 was located close to the N-terminus

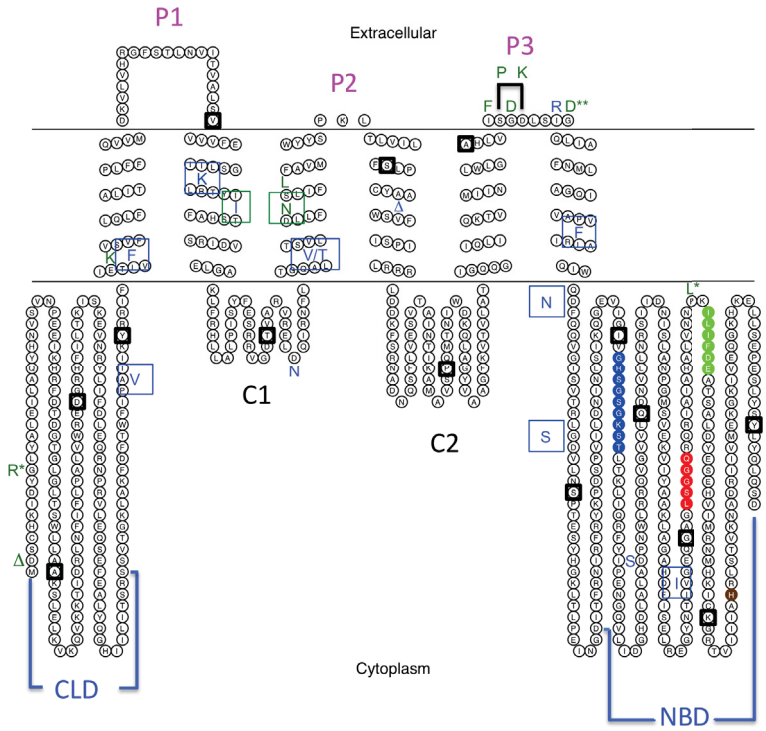

Figure 9: Topology model of HlyB based on β-lactamase, β-galactosidase and alkaline phosphatase insertions. The conserved motifs Walker A, C-loop, Walker B and H-loop are highlighted in blue, red, green and brown, respectively. Letters indicate mutations identified in different genetic screens. Letters in squares indicate supressor mutations. Here, green letters highlight those mutations that affected the level of secretion including ts mutations, marked *, while letters in blue are mutations in HlyB suppressing mutations in the HlyA secretion signal, reducing the hemolytic activity of HlyA (but not necessarily affecting secretion *per se*, see text). Residues marked by an asterix affected the oligomerization of HlyD. Note the 'hotspot' for mutations in the predicted periplasmic domain P3 that is discussed in the text. In case of ambiguities, the residue below or to the right was affected by the mutation. Black circle indicate every 50^{th} residue.

indicating that this region that we now call the CLD might have a specific role in the secretion process. Similarly insertion of an epitope (C494) into the N-terminus of HlyB also blocked secretion. On the other hand, proline 624 is highly conserved in both pro- and eukaryote ABC transporters, forming part of the Pro-loop linking the two domains of the NBD [153], and just downstream of the "signature" motif of these proteins, LSGG. Moreover, in HisP, mutation of the corresponding Leu residue results in uncoupling of ATPase activity, from transport of histidine.

Another ts secretion mutant G408D, was located in the deduced periplasmic loop,

P3, while the corresponding region extending to 12 to 15 amino acids we found was quite well conserved in a wide range of bacterial ABC transporters, as well as in eukaryotic Pgp, Pfmdr and CFTR. Saturation mutagenesis of the region, residues 399 to 412 (see Figure 9), yielded mutations, I401T and D404G giving no hemolyic colonies and around 20 % of WT levels measured in liquid cultures. In addition, a double mutant S402P, D404K completely lacking secretion of HlyA was obtained by site directed mutagenesis. Therefore in this region of 8 residues, predicted to locate close to the membrane between TMDs 5 and 6, 4 possibly 5 amino acids are essential for HlyB function.

Figure 9 also illustrates the position of the suppressor mutations and isolated by Zhang *et al.* [154] that restored to varying extents the secretion of HlyA deleted for the proximal or the distal halves of the secretion signal. These mutations are widely dispersed in virtually all regions of HlyB and consequently for this and for the reasons already discussed above, it seems much more likely that they represent a variety of structural changes bypassing the need for the full signal rather than a specific docking area for the normal signal sequence.

As shown in Figure 9 two mutants E256K and S279L were found to be defective in oligomer formation of HlyD *in vivo* in cross linking experiments (unpublished results, A. Pimenta, J. Young and B. Holland). This suggests possible regions involved in the HlyB, HlyD complex. Finally, Figure 9 also indicates that an epitope C494, recognized by a specific monoclonal antibody, was successfully inserted at the C-terminus of HlyB without preventing secretion of HlyA. This is a useful marker for HlyB.

Structure function of the T1SS ABC protein: the prototype HlyB

The structure of ABC NBDs

The first crystal structure of a purified ABC NBD domain was reported in 1998 by Hung *et al.* [155]. This structure of HisP, the ATPase component of the histidine importer complex from *S. typhymurium*, revealed a monomer with bound ATP sandwiched between the conserved Walker A and B motifs. In addition to the conserved RecA or F1 ATPase fold, two ABC protein specific subdomains were identified (see Figure 10). These are respectively, a β-strand that harbors an aromatic residue interacting with the adenine moiety of bound nucleotides, and an entirely helical subdomain that contains the conserved C-loop motif, the hallmark of ABC transporters. No other interactions between the adenine ring and the NBD were detected in the HisP structure and all subsequently determined structures. This explains why ABC transporters do not possess a true nucleotide specificity and ATPase activity can also be energized by different

nucleotides such as GTP, CTP or UTP.

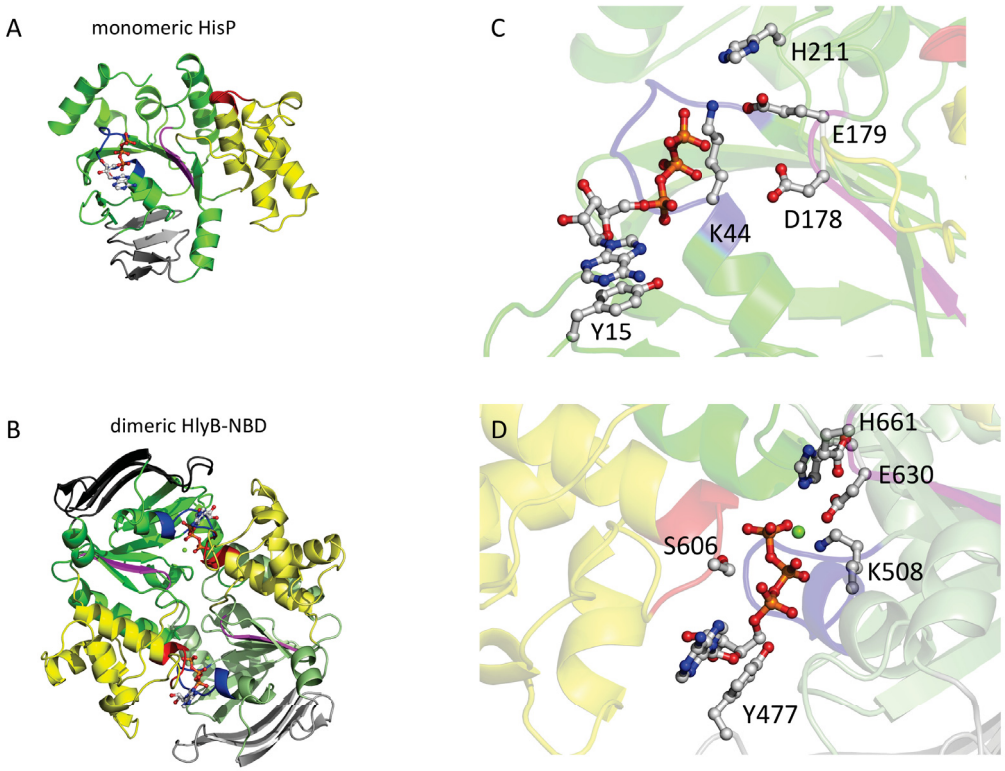

Figure 10: (A) Crystal structure of monomeric HisP [155] with bound ATP shown in ball-and-stick representation. The RecA core oft he NBD is shown in green, the α-helical subdomain in yellow and the β-subdomain in grey. The conserved motifs Walker A, Walker B and C-loop are highlighted in blue, magenta and red, respectively. (B) Zoom-in into the ATP binding site. Conserved residues interacting with the nucleotide are highlighted in ball-and-stick representation and labelled. (C) Model of the ATP/Mg^{2+} bound wild type structure of the head-to-tail dimer of the HlyB-NBD [156]. Color coding is identical to (A), with the second monomer colored in pale colors. The bound cofactor Mg^{2+} is shown as green sphere. (D) Zoom-in into one of the two ATP-binding sites. Conserved residues interacting with the nucleotide are highlighted in ball-and-stick representation and labelled. Please note that S606 resides in the opposite monomer.

Several biochemical analyses of HisP, other isolated NBDs, or full-length transporter systems have revealed co-operativity in ATP hydrolysis. This by definition indicates the presence of more than one ATP binding site during a single catalytic cycle. Therefore, since the initial HisP monomeric structure was unable to explain the ATPase activity and to solve the puzzle, subsequently various dimeric arrangements of the NBDs were

suggested. In fact, the correct architecture of the NBD dimer was proposed by Jones and George [157], based on simulations. The elegantly simplistic solution they arrived at was then subsequently verified by the crystal structure of MJ0796, an isolated NBD from *M. janaschii* [158]. As shown in Figure 10, in the dimer one ATP molecule is sandwiched between the Walker A of one monomer and the C-loop of the opposing monomer - the so-called 'head-to-tail' arrangement of NBDs. Thus, ATP acts as molecular glue and the dimer is only stable in the presence of ATP, but not ADP, since the C-loop of the opposing NBD interacts only with the γ-phosphate moiety of ATP. This fundamental arrangement has now been observed in all structures of isolated NBDs in the presence of ATP, with more than 40 structures deposited in the protein data bank. These include the NBD of HlyB, published in [156, 50] but more recently also the structures of several full-length ABC transporters determined at resolutions ranging from 2.5 to 4.5 Å (see review [159]).

Structure of the extinct peptidase domain CLD in HlyB: a newly identified interaction of HlyB with the HlyA C-terminal

In addition to TolC, atomic level structural information for TISS components is available for the isolated NBD and the N-terminal domain of HlyB. Early studies noted that HlyB, compared to other bacterial ABC transporters has an extended N-terminal domain but its role has been a mystery. Curiously, this N-terminal domain, covering approximately 130 amino acid residues, was identified from the sequence as a member of the cysteine dependent C39 peptidase family. These particular peptidases are only found so far in active form in bacterial ABC transporters involved in the secretion of small peptides. These include a number of bacteriocins - primarily in Gram-positive bacteria. In these molecules the corresponding protease cleavage sites are found in the *N-terminal secretion signal*, C-terminal to a double glycine motif. Obviously, HlyA does not contain an N-terminal targeting signal and does not undergo any proteolytic processing. Moreover, the catalytically essential cysteine of the C39 peptidase domain in HlyB is replaced by a tyrosine. Thus, the N-terminal domain of HlyB was termed a 'C39-like peptidase domain' (CLD).

In a major advance in 2012, Lecher *et al.* [56] revealed an important function for the CLD, since its deletion completely abolished secretion of HlyA. In further detailed studies to explore the precise function, the purified CLD was shown to interact with the unfolded but not with folded HlyA or the truncate HlyA1. However, the 160-residue HlyA2, C-terminal fragment that lacks the C-terminal 58 residues, encompassing the secretion

signal (see Figure 5), still binds to the CLD. This clearly showed that the binding site was located upstream of the secretion signal close to 3 RTX repeats (characterized, coincidently or otherwise by double GG motifs), somewhere between residues 805 and 965.

To explore the structural details of the CLD and possible residues that are involved in binding to HlyA, the solution structure was determined by NMR. First, this revealed no significant structural differences between the CLD and an authentic C39 peptidase domain (ComA-PEP, [160]). However, subtle differences in the respective active sites were detected. While the aspartate residue of the catalytic triad of C39 peptidase domains were found in an identical conformation in the CLD, the histidine residue in the CLD was flipped by nearly 180° out of its canonical conformation. This novel position was stabilized by π-π interactions with a tryptophan residue. Interestingly, pairwise sequence comparison of many CLD and C39 peptidase domains revealed that in CLDs associated with TISS, the combination of the absence of cysteine and the flipped histidine positioning was always present, while in the authentic peptidase domains the expected histidine and cysteine residues were also found and located to the same position. This analysis might allow in the future a robust and easy identification of new RTX transporting systems based on the sequence of the CLD.

Finally, some exciting results were obtained when an NMR analysis was used to determine the localization of residues in the CLD specifically engaged in binding to the HlyA C-terminal. First, it is important to note that the published binding site for the normal C39 substrate - the GG cleavage motif - does not coincide with the site of binding of HlyA to the CLD. Nevertheless and intriguingly, the residues binding to HlyA were found to be on the on opposite side of the molecule to that shown to bind the classical GG motif. Here, one has to keep in mind that the C39 recognition sequence is located in the N-terminal secretion signal of bacteriocins. However, it is likely that not only residues of the secretion signal, but also residues of the core sequence of the bacteriocin, C-terminal to the GG motif, participate in binding. If this assumption is correct, the observation that the HlyA binding site within the CLD does not coincide with that found for the active protease suggests that a functional interaction occurs only with residues C-terminal to the GG residues. However, the functional significance of this important finding may have to await determination of the molecular details of the CLD binding site within the RTX. The functional significance of this important finding may have to await determination of the molecular details of the CLD binding site within the RTX domain of HlyA. Notwithstanding this, the current data strongly suggest that the CLD participates in a very early step of the secretion process. Thus, Lecher *et al.* [56] propose

that the role of the CLD may be to act as a receptor to position the unfolded HlyA in the close vicinity of the T1SS.

Currently favoured model for the mechanism of translocation of small molecules by ABC transporters

The first crystal structure of a full-length ABC transporter in 2002 [161] was for the vitamin B12 importer from *E. coli* (BtuCD) and there are now more than 15 structures of ABC import and export systems deposited in the protein data bank at various stages of their transport and catalytic cycles. However, the most complete system, in terms of structural information for the entire transport cycle concern, is that for maltose import in *E. coli* [162, 163, 164]. Moreover, this is also supplemented by a wealth of functional data. From all these studies (recently reviewed by Jones and George [159]) an atomic resolution picture is emerging of how, at least for small molecules, the chemical energy stored in ATP is coupled to the movement across a biological membrane. Without going into great detail, the "two-side-access" model proposed in 1966 by Oleg Jardetszky [165] to explain the mode of action of membrane pumps appears to be valid for many ABC transporters. In the resting state of the transporter, the allocrite binding site is accessible from the exterior (importers) or from the cytosol (exporters). Binding of ATP induces dimerization of the NBDs, and the effect of resulting conformational changes, is transmitted to the TMDs, via the so-called coupling helices. These are present at the terminus of particular long helices extending directly from the TMDs into the cytoplasm. In the case of ABC import systems only one coupling helix per TMD is present, while ABC export systems possess two per TMD. Thus, each TMD in exporters is in constant contact with both NBDs. The coupling helices were first defined based on the crystal structure of the putative bacterial drug transporter, Sav1866 [166]. This has now been confirmed by structures of other ABC transporters [167, 168, 169, 170, 171, 172, 173]. The coupling helices are roughly oriented parallel to the membrane plane and form crucial contact points between TMDs and NBDs, communicating the status of the membrane domain and the energy source to drive transport.

In current models, largely constructed to explain the translocation of molecules such as anti-cancer drugs or nutrients, the consequence of NBD dimerization switches the accessibility of the transport substrate (allocrite), binding site, from the exterior to the cytosol (importers) or from the cytosol to the exterior (exporters), resulting in allocrite release. Subsequent ATP hydrolysis resets the system and the resting state is restored. One has to keep in mind that in addition to the two important alternating conforma-

tional states (inward-facing and outward-facing), an intervening occluded state must be adopted during the transport cycle, in which both sides of the transporter must be sealed. Otherwise, the transporter would adopt a conformation during its transport cycle, where both sides are accessible, a scenario producing an immediate, lethal dissipation of any existing gradient across the membrane.

Structure and catalytic mechanism of the HlyB NBD

The isolated NBD of HlyB has been investigated in great detail in terms of biochemistry and structure [153, 156, 50, 174, 175, 176]. Crystal structures of all states of the catalytic cycle have been determined for the wild type or mutant NBDs. Combined with biochemical data determination of these structures was essential in order to investigate the mechanism of ATP hydrolysis (see below). In addition, structural analysis was essential to identify residues of the NBD responsible for co-operativity in ATP hydrolysis and, for example, to define a role for the D-loop, a highly conserved motif of ABC transporters but without apparent function hitherto [50].

As in many other ABC-ATPases the isolated NBDs of HlyB display co-operativity with a Hill coefficient of approximately 1.4 [176]. In other words, the two ATP binding sites are not equal, that is, one of the many events leading to hydrolysis of bound ATP (binding, dimerization of the NBDs, ADP and or phosphate release and dimer dissociation) is differently timed in one of the two sites. Otherwise classic Michaelis-Menten kinetics would be observed. However, co-operativity requires asymmetry between the two ATP binding sites and the structures of the ATP-bound states of ABC dimers did not reveal any asymmetry, rather any structural differences between the two NBD monomers forming the ATP sandwich dimer were marginal. However, after analysis of this crystal structure and a subsequent sequence analysis of more than 10000 NBD structures, two residues apparently of particular significance were identified for site directed mutagenesis [50]. These residues (R611 and D551 in the HlyB-NBD) are located one residue downstream of the C-loop and Q-loop, respectively. In the ATP/Mg^{2+}-bound form captured in the crystal structure of the HlyB dimer, these two residues are able to form a salt bridge but only within one monomer. This is because, in the other monomer, the distance between the two residues is too great. Importantly, in the absence of the bridge a tunnel opens reaching from the position of the γ-phosphate to the exterior, while the tunnel is closed by the salt bridge in the other monomer. These findings represent a first glimpse of asymmetry in an ABC-NBD dimer.

Zaitseva *et al.*, excitingly also showed that the exchange of only one of these bridge

residues to alanine (R/D to R/A or A/D), drastically reduced ATPase activity, but more importantly abolished cooperativity. Changing the R-D interaction to K-E resulted in reduced ATPase activity, but restored co-operativity [50]. These results indicate that the R-D interaction is at the heart of co-operativity as it could regulate phosphate release from one of the two ATP binding sites. In the case of the alanine mutations, the tunnel would be open at both sites and the two phosphates released simultaneously, rather than sequentially.

The importance of the above-described interaction was subsequently confirmed for the antigen (peptide) transporter (TAP) [177].

The role of the D-loop, a highly conserved motif very useful for the identification of ABC proteins, has been elusive. In the crystal structure of the NBD of HlyB, the aspartate of the D-loop interacts with a serine residue of the Walker A motif of the opposing NBD. This is another example of an inter-domain interaction between the two NBDs involving highly conserved motifs, in this case indicating an important role for the D-loop in sensing the presence of ATP in the opposing ATP-binding site. Recent elegant studies by the Tampé laboratory have also emphasized the importance of the D-loop in the transport of immuno-peptides by the TAP transporter [178]. Similar conclusions were and from the analysis of other ABC transporters like the vitamin B12 importer [179].

Analysis of the catalytic mechanism of HlyB and its regulation

Results of experiments designed to uncover the mechanism of ATP hydrolysis, including those for HlyB, interestingly point to subtle differences in the mode of action of individual ABC transporters. Mutational studies have identified two amino residues crucial for ATP hydrolysis, one is the glutamate adjacent to the classic Walker B motif present in all P-loop NTPases [180], the other is the histidine of the H-loop, another universally conserved sequence motif of ABC transporters [181]. Replacement of this glutamate by glutamine abolished ATPase activity *in vitro*, in for example, MalK, the NBD of the maltose importer [164], BmrA, a bacterial drug transporter [182], or MJ0796 , the NBD of an ABC transporter with an unknown allocrite [183]. This mutation was actually employed to crystallize the ATP-bound, dimer state of the MJ0796 NBD [158]. However, in the isolated NBD of HlyB, the same substitution E to Q, resulted in a residual ATPase activity of approximately 10 % [176], while the isolated, similarly mutated NBD of the yeast mitochondrial ABC transporter Mdl1, displayed a very low ATPase activity [184]. On the other hand, an approximately 20 % residual activity was also

identified for the mutant form of GlcV, an NBD from a thermophilic ABC transporter [185]. In contrast, mutation of the conserved histidine of HlyB resulted in a complete loss of ATPase activity. Similar results were obtained for the maltose and histidine importers [186, 187], while in the case of the yeast ABC transporter Pdr5 ATPase activity was completely unaffected when the histidine was substituted. Intriguingly, however, this mutated transporter displayed a changed spectrum of transported substrates [188] emphasizing the importance of the histidine residue in determining allocrite specificity. Together these results might suggest different mechanisms of ATP hydrolysis in certain ABC transporters and extrapolations from one system to the other should be done with caution.

As discussed above, two amino acids have been identified in different NBDs, the glutamate of the Walker B motif, involved in binding magnesium, and the histidine of the conserved H-loop that play crucial roles in hydrolytic activity of the NBD. In MJ0796, mutation of the glutamate to glutamine abolished ATPase activity completely and the term "catalytic base" was coined [183]. The role of the histidine was investigated in the isolated NBD of HlyB, and as indicated above its substitution by alanine in HlyB abolished ATPase activity completely, while residual activity was observed in the case of the E/Q mutant [156, 176]. Moreover, in a detailed biochemical analysis of ATP hydrolysis *in vitro*, several lines of evidence were obtained more consistent with a mechanism of substrate assisted catalysis, emphasizing the role of the histidine, rather than general base catalysis as suggested previously [156, 183], giving the key role to glutamate. Therefore, the term 'linchpin' was also coined and a critical role for a catalytic dyad composed of the histidine and the glutamate was postulated, in which the side chain of the glutamate interacts with the imidazole side chain of the histidine that in turn stabilizes the attacking water.

Subsequently, in 2011, Oldham *et al.* described structures of the maltose importer in the ground and transition states [163]. For the latter, transition state analogous, i.e. vanadate and metallofluorides, were used. In these structures, the attacking water molecule, which has to be in line with bond to break, was unambiguously identified as the glutamate, while the histidine was not in direct contact with the attacking water. However, the conclusion of Senior [189] that ABC transporters therefore operate by using 'general base catalysis' is in our opinion flawed. The term "general base catalysis" refers to the kinetics of a reaction and operates if and only if proton abstraction is the rate-limiting step of the reaction. This can by no means be deduced from a static crystal structure. Rather, for example, isotope experiments should be used to demonstrate general base catalysis, where the reaction is performed in D_2O instead of H_2O or in

a mixture of both. Since the mass of D_2O is larger than that of H_2O more energy is required to abstract a deuterium compared to a proton. If proton abstraction is the rate-limiting step, the overall reaction velocity will be slower in D_2O. Such experiments have been performed so far only for the isolated NBD of HlyB [156] and the isolated NBD of Mdl1 [190]. In both cases no evidence for 'general base catalysis' was observed. Thus, the precise catalytic mechanism for ATP hydrolysis is still not finally resolved and will require further investigation. Consequently, the possibility that different ABC-ATPases employ different mechanisms to fuel allocrite translocation through the hydrolysis of ATP, is not excluded.

Translocation of large polypeptides is incompatible with a classical alternating access model

Choudhury *et al.* reported the crystal structure of a microcin-specific ABC transporter, McjD from *E. coli* in the presence of its peptide allocrite (MccJ25), in an outward-occluded state [168]. Here the microcin, a 21 amino acid antimicrobial peptide, is accommodated is a large cavity, approximately 5900 $Å^3$ ($40 \cdot 21 \cdot 10$ Å), sufficient to bind MccJ25. The outward-occluded conformation strongly suggests that McjD will also use the alternating access mechanism to couple ATP hydrolysis to microcin transport across the inner membrane of *E. coli*. Furthermore, very recently, highly important and exciting new structural information was obtained from the crystals of an ABC transporter (PCAT) from *Clostridium thermocellum* also apparently secreting a peptide. The structure was obtained both for the nucleotide-free and the ATP-bound conformation at 3.6 Å and 5.5 Å resolution, respectively [191]. The PCAT transporter contains a C39 domain at its N-terminus that cleaves N-terminal secretion signals of some bacteriocins prior to translocation across the cell membrane. Although the natural transport substrate has not been characterized, one gene of the operon encodes a 90 amino acid protein that likely represents the bacteriocin. Interestingly, the C39 peptidase domain was only visible in the electron density of the nucleotide-free state, while it was invisible in the ATP-bound state. This indicated a large degree of flexibility for the C39 domain in the latter conformation. Based on the two conformations, open to the cytosol in the nucleotide-free state and closed on both sides of the membrane in the ATP-bound state, a translocation pathway could be envisaged. Thus, a cavity was identified in the ATP-bound state large enough to accommodate a small folded protein such as a bacteriocin [191].

However, in contrast to bacteriocins the great majority of substrates of T1SS range

from 20 kDa to SI900kDa and experimental evidence suggests that all of them are transported in the unfolded state [75]. Thus, as also concluded by the authors of the PCAT structure, one has to question whether the 'simple' alternative access mechanism also applies to most T1SS ABC transporter, since the size of the unfolded substrate is evidently too large to be transported in one step. On the other hand, if type I secretion requires multiple cycles of ATP hydrolysis, accompanying ratchet-like translocation as seen with the classical Sec-system, it is difficult, if not impossible to envision an occluded state and therefore an alternative access process for such large allocrites. Alternatively, if HlyB in reality is not integral to the transport tunnel but rather is required to control the opening of the HlyD, TolC channel for continuous extrusion of HlyA, then conformational changes mimicking the alternating access transition might still play a role. Clearly, structural data are required to solve this puzzling question.

Genetic analysis of HlyB - and functional domains

The accumulating evidence discussed above, including the recent structural analysis of McjD and PCAT1, the bacterial ABC transporters required for translocation of two different peptides indicates that the ABC component of these TISS-like translocons, although lacking both the OMP and OMP components, specifically interacts with the HlyA signal sequence (via the NBD domain), with the RTX region of HlyA (via the CLD), and with HlyD, while the CLD and NBD may form intramolecular interactions as in the case of the PCAT1 molecule. Mutagenesis studies as summarized in Figure 9.

Interaction of the secretion signal with the ABC component of the translocator

1) Genetic analysis

Attempts to show that recognition of the translocator by the secretion signal involves direct interaction with the ABC protein have included different genetic approaches. For the Hly system, an analysis of the ability of hybrid translocators (mixing components from different translocons) to secrete HlyA, indicated that HlyB was an important specificity determinant [192]. In addition, several mutations in the C-terminal signal and defective in secretion were shown to be recessive [102, 105], indicating inhibition of initiation of secretion, likely therefore to involve interaction with HlyB and/or HlyD.

Interesting attempts to demonstrate specific interactions between the secretion signal and HlyB, were described by the Ling group and are summarised in Zhang et al. [154]. The approach involved the isolation of HlyB mutations suppressing the effect of either

of two secretion signal mutants - one mutation (residual secretion reduced to less than 1 %) deleted essentially the distal half of the signal in HlyA (including helix II) and the other (residual secretion about 5 %) taking out the proximal half (includes helix I). It is important to note that the putative suppressors induced after mutagenesis of *hlyB* were screened and apparently quantified by measuring hemolytic colony halo sizes. Unfortunately, this complicates the interpretation of the results, since this method is not considered to be quantitative. Moreover, loss of haemolytic activity in the case of the mutant signal lacking the C-terminal region, could be misleadingly construed as affecting the secretion process, while in reality being due to misfolding of HlyA (see [104]).

Despite the above reservations (combined with some assays of hemolyic activity in liquid cultures of the mutants) (reported by Zhang *et al.* [154]) several suppressors were obtained by random mutagenesis of *hlyB* that restored levels of secretion significantly (increased halo size), even with both deleted signals deletion. In total, 21 suppressors were obtained, 9 mapped by sequencing, to the same three codons, one (identical) suppressor was selected independently by both deletions. Eleven of the suppressors mapped to or close to the cytosolic part of the transmembrane domain of HlyB, as predicted by previous topology analysis (see Figure 9) [193]. However, the interpretation of the underlying mechanism revealed by the suppressors is further complicated, notably, because deletions cannot be suppressed allele specifically (as argued by the Authors). Therefore, these mutations in HlyB cannot directly define individual residues forming cytoplasmic docking sites for the secretion signal. The data in our view may reflect much more indirect mechanisms of suppression.

2) Biochemical studies

Using a biochemical approach, surface plasmon resonance studies of the isolated NBD of HlyB in the presence of a C-terminal fragment of HlyA demonstrated directly an interaction with an affinity of 4 µM [174]. This interaction was strictly dependent on the presence of the secretion sequence, as its deletion completely abolished the interaction. Interestingly, the dissociation rate of the interaction was accelerated in the presence of nucleotides, ATP or ADP, suggesting that the interaction is fine-tuned in the biological context. Moreover, if we assume that ATP binding and dimerization of HlyB initiates secretion and, as described above, since the C-terminal of HlyA is translocated first, binding of the signal region to HlyB must be readily reversible.

With a different TISS, Delepelaire [194] also demonstrated that the ABC-ATPase activity of a partially purified PrtD from *Erwinia chrysanthemi*, was regulated *in vitro*

by the cognate protease. In this case the presence of the natural C-terminal secretion sequence was required to inhibit ATPase activity almost completely, although with perhaps a surprisingly low K_i of 0.2. These results for both HlyB and PrtD point to a common interaction between the secretion sequence of the substrate and the ABC transporter and in combination with the data on the CLD, contribute to a molecular picture of the sequence of events leading to initiation of HlyA secretion is emerging.

Evidence for other interactions between components of the HlyA TISS

A number of studies of chaemeric translocons have indicated that interactions between MFP and ABC and MFP and OMPs are required for secretion of a particular polypeptide. However, there was no evidence of interactions between the OMP and the ABC protein, as proposed by most laboratories for the inner and outer membrane components of bacterial multidrug transporters.

HlyB and HlyD appear to form a stable constitutive complex; stability of HlyD also affected by TolC

A number of genetic studies have indicated that the ABC and MFP proteins of the Hly, Prt (protease) and Cva (colicin V) translocons, interact, and more directly, interactions have been demonstrated using co-purification with an affinity tag or in cross-linking experiments [195, 196, 197]. Other support for an interaction between the ABC and MFP proteins comes from measuring their stabilities in cells. For the Hly T1SS, both HlyD [40] and HlyB (J Young, A Pimenta and B Holland, unpublished) are synthesized constitutively throughout the growth phase with both the laboratory strain and the pathogenic strain LE 2001. Notably, this expression, is not coupled to the synthesis of HlyA, whose synthesis is usually restricted to a relatively brief window during late exponential phase [29, 40, 85]. Moreover, in the presence of TolC but in the absence of HlyB, HlyD becomes less stable with a half-life at 37 °C of around 100 min, compared to 5 h when both HlyB and TolC are present. However, in the absence of TolC, the presence of HlyB renders HlyD highly unstable with a half-life of 36 min [40].

Somewhat similarly, the ABC and the MFP proteins of the Colicin V translocator were found to depend on each other for stability, but are both very unstable in the absence of TolC [195]. Notably in these studies the transport substrate was absent, thus suggesting that the three T1SS translocator proteins can form a complex independently of the allocrite. In addition, interaction with HlyB appears to induce structural changes in HlyD enhancing its sensitivity to intracellular proteases when TolC is absent. However,

some of these conclusions appear to be contradicted by other important studies indicating in particular that the allocrites, HlyA, PrtG and HasA are required for the recruitment of the OMP into the T1SS machinery.

Ordered assembly of T1SS translocons

Letoffe *et al.*, [196] first showed that a type 1 transporter complex - required for secretion of a protease by *E. chrysanthemi* - could be isolated as a single complex containing an allocrite and the ABC, MFP and OMP proteins from detergent solubilised membrane proteins. This was obtained by co-purification through specific affinity binding to the tagged allocrite, however, no cross-linking to stabilize protein interactions was used. The system chosen for analysis however, was also unduly complex, since the - Prt transport proteins were expressed in the heterologous host, *E. coli* and the transport substrate was the non cognate HasA (with affinity for heme). This is not secreted but apparently 'engages' the translocon to form a "frozen" complex, although the actual nature and physiological relevance of the abortive complex was not established. This is unfortunate since in another study by this group the analysis of a frozen complex with HasA was very revealing [115].

When only a single transport protein (ABC, MPF or OMP) was expressed in cells together with the allocrite, Letoffe *et al.* [196] also showed that the PrtD ABC protein, but not the other transport proteins (including the MFP) could be detected in association with HasA, while the co-expressed ABC and MFP proteins, but not ABC with OMP, co-purified with HasA. In other experiments, the authors also studied the Prt TISS (still expressed in *E. coli*), with the cognate allocrite, protease C, but as a C-terminal fusion to glutathione in order to provide an affinity tag (for glutathione agarose) that also formed an abortive complex. Again the three transport proteins were co-purified with the allocrite, and the authors concluded that secretion in this T1SS involves an initial ABC-allocrite association, followed by interaction of the ABC and MFP proteins that then finally triggers incorporation of the OMF, to complete the assembly.

Other experiments, using an HlyB mutant defective in ATPase activity showed while assembly of the whole complex was unaffected, including oligomerization of HlyD (detected as trimers using the cross-linker DSG), although of course secretion was blocked. Similarly, blocking secretion by masking the C-terminal of HlyD by addition of a 10 residue c-Myc epitope had no detectable effect on HlyA dependent assembly of the complex, or on HlyD oligomerization. The Authors thus concluded that a continuous transport pathway to the exterior In a subsequent and more easily interpretable analysis,

Thananbalu *et al.* [197], analyzed the interactions of HlyB or HlyD affinity tagged by an N-terminal fusion of 6-residues of histidine and the complexes "frozen" in this case by cross-linking *in vivo* with the reversible linker DSP. A complex of HlyB and HlyD was detected even in the absence of HlyA, but TolC did not co-purify with the complex, nor was TolC required for its formation. However, all three transporter proteins could be co-purified in a complex with HlyA clearly showing that the allocrite was required to recruit the outer membrane component, TolC, presumably to complete the assembly of the transenvelope translocon. Importantly, tagged HlyD and in particular HlyB, when either was produced alone, could still be co-purified together with HlyA. Moreover, since the level of co-purified TolC appeared substantially greater when His tagged HlyD, rather than His tagged was assembled, "on demand", by the transport substrate, with both inner membrane proteins involved in early docking to HlyA (region unspecified), while the periplasmic region of HlyD formed the bridge across the periplasm to link up with TolC. Notably, in contrast to the analysis of protease C secretion discussed above, the Cambridge group identified an important early role for the MFP. This was surprising given the many, apparently highly conserved, global features of the T1SS. Consequently, it is important to consider whether the allocrite interaction with PrtE (MFP) was missed due to insufficient stability, in the absence of cross-linking, to be detected by the methods employed by Letoffe *et al.* [196].

On the other hand, the Thananbalu *et al.* experiments [197] gave no indication whether the observed apparent HlyD interaction with HlyA had a significant role in the secretion process. As described in the following section, further analysis by Balakrishnan *et al.*, [53] indeed revealed most elegantly that the HlyD protein plays the key role in the secretion mechanism by coupling binding of the allocrite to assembly of the continuous translocator from cytoplasm to exterior.

The cytoplasmic domain of HlyD is specifically required for the HlyA dependent recruitment of TolC

MFPs that participate in ABC dependent (T1SS) protein translocation invariably so far, have a single TMD anchor and a short N-terminal extension into the cytoplasm, although there are differences in length in the different sub groups. In the case of HlyD, the TMD is preceded by an approximate 59 residue extension [41, 149], and importantly, Pimenta *et al.*, [40] showed that when the first 40 amino acids of HlyD were deleted, the protein was still stably integrated into the inner membrane but secretion was completely blocked.

Balakrishnan *et al.* [53] then provided the precise role of this critical region. Using a similar N-terminal deletion of HlyD to block secretion, they demonstrated that the mutant HlyD was unable to recruit TolC into the transenvelope complex, although other properties of HlyD, such as oligomerization and its interaction with HlyB, as determined by cross-linking, were retained. The first 40 residues of HlyD incorporate an N-terminal 25 residue, completely conserved (at least in close relatives) amphipathic helix, and a conserved five amino acid cluster of charged residues in the distal half. Again using cross-linking with intact cells and other HlyD N-terminal deletions, Balakrishnan *et al.* importantly also showed that the 45 terminal residues of HlyD were required, with the essential participation of HlyB, for binding to HlyA [53]. Moreover, while the helical region was not required for recruiting TolC, the charged cluster was especially important for this function. The results emphasized the importance of cooperative action of the three proteins of the translocator. Excitingly, the results also suggest that the cytoplasmic N-terminal of HlyD senses the presence of HlyA and mediates transduction of a conformational signal, presumably to its periplasmic domain, to allow recruitment of TolC. However, in our view the results do not the exclude the possibility that pre-existing transient contacts between D and TolC could rather be simply stabilized. Similarly the results do not exclude the possibility that the HlyD binding to HlyA also lead to required structural changes in HlyB. Finally, the probability that the HlyA secretion signal was involved in the observed interactions with HlyD in this study was regrettably not examined, and it is even more unfortunate that this key question has not been followed up.

Mechanism of secretion of type I proteins: conclusions and a model for HlyA translocation

General conclusions focussing primarily on the Hly system

The TISS constitutes an important pathogenicity factor in both mammals and plants and uniquely an ABC transporter provides the chemical energy to fuel the process. This system clearly also possesses other distinctive features not shared by any other known protein translocation systems. Moreover, at the heart of the translocon the ABC transporter itself has novel characteristics distinguishing it from other members of this super family.

Structural studies combined with biochemical analyses of the HlyB-NBD, have in fact provided some of the most detailed information concerning the catalytic mechanism

of ATP hydrolysis of any ABC transporter. In addition, the structural analysis of the N-terminal region of HlyB, the CLD, shared as far as we know only with TISS translocating large polypeptides (at least when greater than 50 kDa). Intriguingly, the CLD was clearly shown to interact with HlyA upstream of the C-terminal signal sequence in the vicinity of the RTX repeats. The CLD retains the overall 3D structure of the ancestral C39 protease family including that of its closer modern relatives in TISS that secrete peptide bacteriocins that also specifically cleave at G-G sequences. Given this evolutionary history we propose that the CLD although having no enzymatic activity still binds to one or more GG motifs of the RTX region and that this is essential for secretion. Nevertheless, how this interaction facilitates secretion and why smaller proteins like the proteases and lipases do not require this accessory domain is a mystery. However, identification of the precise stage that is blocked in HlyA secretion when the CLD is absent should be a fruitful approach. In addition, an interesting test of whether the need for the CLD is only a question of size is to ask if large passenger polypeptides fused to the C-terminal of a type I protease can be secreted by the cognate translocon.

Regarding the nature of the signal code required for type I secretion and discussed in detail above, the simplest hypothesis based on the available evidence, clearly indicates that this is composed of a pattern of specific individual residues. This pattern may involve residues rather dispersed throughout much of the C-terminal of HlyA, based on the clearly additive effect of combining mutations E (-46) (R -15) and (D -10). This signal codec would provide a 'lock and key' mechanism for docking with either or both HlyD and HlyB. As proposed earlier an important hotspot in this signal centers around the HlyA motif, EISK and recent studies provide strong support for this (unpublished). Whether these residues also need to be presented to the translocon as part of a helical structure seems now unlikely but is not definitively excluded. The composition of a linear HlyA code seems likely to be conserved among closely related toxins and degenerate versions of a common theme may exist in a broader range of type I proteins but this requires further examination.

Thus far, there is no high-resolution structural information for HlyA itself or for HlyD. However, with respect to the latter, residue conservation and in particular the predicted secondary structure suggest that the atomic level structures obtained for the equivalent adaptor or MFPs involved in multidrug transport are very good models.

At least in laboratory strains HlyB and HlyD (trimers or hexamers) form independently of HlyA a constitutively produced stable complex, possibly in transient but non productive association with TolC (trimers). In the HlyBD complex it is unclear in particular whether HlyB is able to bind ATP and whether the NBDs are tightly closed or

not. When HlyA is synthesized potentially there is the possibility for the secretion signal and some GG residues to bind not only to HlyD, but to both the CLD and NBDs of HlyB. One known consequence at least is that TolC is now locked into a functionally active tranlocon. We also know that since HlyA is translocated C-terminal first all these critical interactions must be rapidly reversed.

References

[1] C F Higgins, I D Hiles, G P Salmond, D R Gill, J A Downie, I J Evans, I B Holland, L Gray, S D Buckel, and A W Bell. A family of related atp-binding subunits coupled to many distinct biological processes in bacteria. *Nature*, 323(6087):448–50, 1986.

[2] T Felmlee, S Pellett, E Y Lee, and R A Welch. Escherichia coli hemolysin is released extracellularly without cleavage of a signal peptide. *J Bacteriol*, 163(1):88–93, Jul 1985.

[3] T Felmlee, S Pellett, and R A Welch. Nucleotide sequence of an escherichia coli chromosomal hemolysin. *J Bacteriol*, 163(1):94–105, Jul 1985.

[4] R A Welch. Pore-forming cytolysins of gram-negative bacteria. *Mol Microbiol*, 5(3):521–8, Mar 1991.

[5] U Baumann, S Wu, K M Flaherty, and D B McKay. Three-dimensional structure of the alkaline protease of pseudomonas aeruginosa: a two-domain protein with a calcium binding parallel beta roll motif. *EMBO J*, 12(9):3357–64, Sep 1993.

[6] Irena Linhartová, Ladislav Bumba, Jiří Mašín, Marek Basler, Radim Osička, Jana Kamanová, Kateřina Procházková, Irena Adkins, Jana Hejnová-Holubová, Lenka Sadílková, Jana Morová, and Peter Sebo. Rtx proteins: a highly diverse family secreted by a common mechanism. *FEMS Microbiol Rev*, 34(6):1076–112, Nov 2010.

[7] I Barry Holland, Lutz Schmitt, and Joanne Young. Type 1 protein secretion in bacteria, the abc-transporter dependent pathway (review). *Mol Membr Biol*, 22(1-2):29–39, 2005.

[8] Sabrina Thomas, I Barry Holland, and Lutz Schmitt. The type 1 secretion pathway - the hemolysin system and beyond. *Biochim Biophys Acta*, 1843(8):1629–41, Aug 2014.

[9] Michael H H Lenders, Sven Reimann, Sander H J Smits, and Lutz Schmitt. Molecular insights into type i secretion systems. *Biol Chem*, 394(11):1371–84, Nov 2013.

[10] P Delepelaire. Type i secretion in gram-negative bacteria. *Biochim Biophys Acta*, 1694(1-3):149–61, Nov 2004.

[11] D Ladant and A Ullmann. Bordatella pertussis adenylate cyclase: a toxin with multiple talents. *Trends Microbiol*, 7(4):172–6, Apr 1999.

[12] Martina Bielaszewska, Thomas Aldick, Andreas Bauwens, and Helge Karch. Hemolysin of enterohemorrhagic escherichia coli: structure, transport, biological activity and putative role in virulence. *Int J Med Microbiol*, 304(5-6):521–9, Jul 2014.

[13] Karla J F Satchell. Structure and function of martx toxins and other large repetitive rtx proteins. *Annu Rev Microbiol*, 65:71–90, 2011.

[14] Jazel Dolores and Karla J F Satchell. Analysis of vibrio cholerae genome sequences reveals unique rtxa variants in environmental strains and an rtxa-null mutation in recent altered el tor isolates. *MBio*, 4(2):e00624, 2013.

[15] Chelsea D Boyd, T Jarrod Smith, Sofiane El-Kirat-Chatel, Peter D Newell, Yves F Dufrêne, and George A O'Toole. Structural features of the pseudomonas fluorescens biofilm adhesin lapa required for lapg-dependent cleavage, biofilm formation, and cell surface localization. *J Bacteriol*, 196(15):2775–88, Aug 2014.

[16] Britta Barlag and Michael Hensel. The giant adhesin siie of salmonella enterica. *Molecules*, 20(1):1134–50, 2015.

[17] Katerina Prochazkova, Ludmilla A Shuvalova, George Minasov, Zdenek Voburka, Wayne F Anderson, and Karla J F Satchell. Structural and molecular mechanism for autoprocessing of martx toxin of vibrio cholerae at multiple sites. *J Biol Chem*, 284(39):26557–68, Sep 2009.

[18] Byoung Sik Kim, Hannah E Gavin, and Karla J F Satchell. Distinct roles of the repeat-containing regions and effector domains of the vibrio vulnificus multifunctional-autoprocessing repeats-in-toxin (martx) toxin. *MBio*, 6(2), 2015.

[19] Andreas Kuhn. Introduction to special issue on protein trafficking and secretion. *Biochim Biophys Acta*, 1843(8):1429–32, Aug 2014.

[20] Tiago R D Costa, Catarina Felisberto-Rodrigues, Amit Meir, Marie S Prevost, Adam Redzej, Martina Trokter, and Gabriel Waksman. Secretion systems in gram-negative bacteria: structural and mechanistic insights. *Nat Rev Microbiol*, 13(6):343–59, Jun 2015.

[21] G L Robinson. The haemolysin of bacterium coli. *J Gen Microbiol*, 5(4):788–92, Oct 1951.

[22] R Lovell and T A Rees. A filterable haemolysin from escherichia coli. *Nature*, 188:755–6, Nov 1960.

[23] I S Snyder and N A Koch. Production and characteristics of hemolysins of escherichia coli. *J Bacteriol*, 91(2):763–7, Feb 1966.

[24] A Noegel, U Rdest, W Springer, and W Goebel. Plasmid cistrons controlling synthesis and excretion of the exotoxin alpha-haemolysin of escherichia coli. *Mol Gen Genet*, 175(3):343–50, Oct 1979.

[25] W Springer and W Goebel. Synthesis and secretion of hemolysin by escherichia coli. *J Bacteriol*, 144(1):53–9, Oct 1980.

[26] M Härtlein, S Schiessl, W Wagner, U Rdest, J Kreft, and W Goebel. Transport of hemolysin by escherichia coli. *J Cell Biochem*, 22(2):87–97, 1983.

[27] V Koronakis, E Koronakis, and C Hughes. Isolation and analysis of the c-terminal signal directing export of escherichia coli hemolysin protein across both bacterial membranes. *EMBO J*, 8(2):595–605, Feb 1989.

[28] N Mackman and I B Holland. Functional characterization of a cloned haemolysin determinant from e. coli of human origin, encoding information for the secretion of a 107k polypeptide. *Mol Gen Genet*, 196(1):129–34, 1984.

[29] N Mackman and I B Holland. Secretion of a 107 k dalton polypeptide into the medium from a haemolytic e. coli k12 strain. *Mol Gen Genet*, 193(2):312–5, 1984.

[30] N Mackman, J M Nicaud, L Gray, and I B Holland. Genetical and functional organisation of the escherichia coli haemolysin determinant 2001. *Mol Gen Genet*, 201(2):282–8, 1985.

[31] N Mackman, J M Nicaud, L Gray, and I B Holland. Identification of polypeptides required for the export of haemolysin 2001 from e. coli. *Mol Gen Genet*, 201(3):529–36, 1985.

[32] C Chervaux, N Sauvonnet, A Le Clainche, B Kenny, A L Hung, J K Broome-Smith, and I B Holland. Secretion of active beta-lactamase to the medium mediated by the escherichia coli haemolysin transport pathway. *Mol Gen Genet*, 249(2):237–45, Nov 1995.

[33] T Felmlee and R A Welch. Alterations of amino acid repeats in the escherichia coli hemolysin affect cytolytic activity and secretion. *Proc Natl Acad Sci U S A*, 85(14):5269–73, Jul 1988.

[34] L Gray, N Mackman, J M Nicaud, and I B Holland. The carboxy-terminal region of haemolysin 2001 is required for secretion of the toxin from escherichia coli. *Mol Gen Genet*, 205(1):127–33, Oct 1986.

[35] I Gentschev, J Hess, and W Goebel. Change in the cellular localization of alkaline phosphatase by alteration of its carboxy-terminal sequence. *Mol Gen Genet*, 222(2-3):211–6, Jul 1990.

[36] L Gray, K Baker, B Kenny, N Mackman, R Haigh, and I B Holland. A novel c-terminal signal sequence targets escherichia coli haemolysin directly to the medium. *J Cell Sci Suppl*, 11:45–57, 1989.

[37] N Mackman, K Baker, L Gray, R Haigh, J M Nicaud, and I B Holland. Release of a chimeric protein into the medium from escherichia coli using the c-terminal secretion signal of haemolysin. *EMBO J*, 6(9):2835–41, Sep 1987.

[38] Irina Artsimovitch and Robert Landick. The transcriptional regulator rfah stimulates rna chain synthesis after recruitment to elongation complexes by the exposed nontemplate dna strand. *Cell*, 109(2):193–203, Apr 2002.

[39] J M Nicaud, N Mackman, L Gray, and I B Holland. Characterisation of hlyc and mechanism of activation and secretion of haemolysin from e. coli 2001. *FEBS Lett*, 187(2):339–44, Aug 1985.

[40] A L Pimenta, J Young, I B Holland, and M A Blight. Antibody analysis of the localisation, expression and stability of hlyd, the mfp component of the e. coli haemolysin translocator. *Mol Gen Genet*, 261(1):122–32, Feb 1999.

[41] R C Wang, S J Seror, M Blight, J M Pratt, J K Broome-Smith, and I B Holland. Analysis of the membrane organization of an escherichia coli protein translocator, hlyb, a member of a large family of prokaryote and eukaryote surface transport proteins. *J Mol Biol*, 217(3):441–54, Feb 1991.

[42] C Wandersman and P Delepelaire. Tolc, an escherichia coli outer membrane protein required for hemolysin secretion. *Proc Natl Acad Sci U S A*, 87(12):4776–80, Jun 1990.

[43] S Létoffé, P Delepelaire, and C Wandersman. Protease secretion by erwinia chrysanthemi: the specific secretion functions are analogous to those of escherichia coli alpha-haemolysin. *EMBO J*, 9(5):1375–82, May 1990.

[44] P Stanley, C Hyland, V Koronakis, and C Hughes. An ordered reaction mechanism for bacterial toxin acylation by the specialized acyltransferase hlyc: formation of a ternary complex with acylacp and protoxin substrates. *Mol Microbiol*, 34(5):887–901, Dec 1999.

[45] P Stanley, L C Packman, V Koronakis, and C Hughes. Fatty acylation of two internal lysine residues required for the toxic activity of escherichia coli hemolysin. *Science*, 266(5193):1992–6, Dec 1994.

[46] J P Issartel, V Koronakis, and C Hughes. Activation of escherichia coli prohaemolysin to the mature toxin by acyl carrier protein-dependent fatty acylation. *Nature*, 351(6329):759–61, Jun 1991.

[47] Sabrina Thomas, Sander H J Smits, and Lutz Schmitt. A simple in vitro acylation assay based on optimized hlya and hlyc purification. *Anal Biochem*, 464:17–23, Nov 2014.

[48] Nicholas P Greene, Allister Crow, Colin Hughes, and Vassilis Koronakis. Structure of a bacterial toxin-activating acyltransferase. *Proc Natl Acad Sci U S A*, 112(23):E3058–66, Jun 2015.

[49] Justin Lecher, Matthias Stoldt, Christian K W Schwarz, Sander H J Smits, Lutz Schmitt, and Dieter Willbold. 1h, 15n and 13c resonance assignment of the n-terminal c39 peptidase-like domain of the abc transporter haemolysin b (hlyb). *Biomol NMR Assign*, 5(2):199–201, Oct 2011.

[50] Jelena Zaitseva, Christine Oswald, Thorsten Jumpertz, Stefan Jenewein, Alexander Wiedenmann, I Barry Holland, and Lutz Schmitt. A structural analysis of asymmetry required for catalytic activity of an abc-atpase domain dimer. *EMBO J*, 25(14):3432–43, Jul 2006.

[51] V Koronakis, A Sharff, E Koronakis, B Luisi, and C Hughes. Crystal structure of the bacterial membrane protein tolc central to multidrug efflux and protein export. *Nature*, 405(6789):914–9, Jun 2000.

[52] Dijun Du, Zhao Wang, Nathan R James, Jarrod E Voss, Ewa Klimont, Thelma Ohene-Agyei, Henrietta Venter, Wah Chiu, and Ben F Luisi. Structure of the acrab-tolc multidrug efflux pump. *Nature*, 509(7501):512–5, May 2014.

[53] L Balakrishnan, C Hughes, and V Koronakis. Substrate-triggered recruitment of the tolc channel-tunnel during type i export of hemolysin by escherichia coli. *J Mol Biol*, 313(3):501–10, Oct 2001.

[54] Chih-Chia Su, Feng Yang, Feng Long, Deepak Reyon, Mathew D Routh, Dennis W Kuo, Adam K Mokhtari, Jonathan D Van Ornam, Katherine L Rabe, Julie A Hoy, Young Jin Lee, Kanagalaghatta R Rajashankar, and Edward W Yu. Crystal structure of the membrane fusion protein cusb from escherichia coli. *J Mol Biol*, 393(2):342–55, Oct 2009.

[55] J L Hess, J M Pyper, and J E Clements. Nucleotide sequence and transcriptional activity of the caprine arthritis-encephalitis virus long terminal repeat. *J Virol*, 60(2):385–93, Nov 1986.

[56] Justin Lecher, Christian K W Schwarz, Matthias Stoldt, Sander H J Smits, Dieter Willbold, and Lutz Schmitt. An rtx transporter tethers its unfolded substrate during secretion via a unique n-terminal domain. *Structure*, 20(10):1778–87, Oct 2012.

[57] Lissete Sánchez-Magraner, Ana R Viguera, Marcos García-Pacios, M Pilar Garcillán, José-Luis R Arrondo, Fernando de la Cruz, Félix M Goñi, and Helena Ostolaza. The calcium-binding c-terminal domain of escherichia coli alpha-hemolysin is a major determinant in the surface-active properties of the protein. *J Biol Chem*, 282(16):11827–35, Apr 2007.

[58] J M Ghigo and C Wandersman. A carboxyl-terminal four-amino acid motif is required for secretion of the metalloprotease prtg through the erwinia chrysanthemi protease secretion pathway. *J Biol Chem*, 269(12):8979–85, Mar 1994.

[59] S Létoffé and C Wandersman. Secretion of cyaa-prtb and hlya-prtb fusion proteins in escherichia coli: involvement of the glycine-rich repeat domain of erwinia chrysanthemi protease b. *J Bacteriol*, 174(15):4920–7, Aug 1992.

[60] Martin H Griessl, Benedikt Schmid, Kristin Kassler, Christoph Braunsmann, Regina Ritter, Britta Barlag, York-Dieter Stierhof, Karina U Sturm, Claudia Danzer, Carolin Wagner, Tilman E Schäffer, Heinrich Sticht, Michael Hensel, and Yves A Muller. Structural insight into the giant ca2+-binding adhesin siie: implications for the adhesion of salmonella enterica to polarized epithelial cells. *Structure*, 21(5):741–52, May 2013.

[61] Reto Meier, Thomas Drepper, Vera Svensson, Karl-Erich Jaeger, and Ulrich Baumann. A calcium-gated lid and a large beta-roll sandwich are revealed by the crystal structure of extracellular lipase from serratia marcescens. *J Biol Chem*, 282(43):31477–83, Oct 2007.

[62] P Arnoux, R Haser, N Izadi, A Lecroisey, M Delepierre, C Wandersman, and M Czjzek. The crystal structure of hasa, a hemophore secreted by serratia marcescens. *Nat Struct Biol*, 6(6):516–20, Jun 1999.

[63] G P Salmond and P J Reeves. Membrane traffic wardens and protein secretion in gram-negative bacteria. *Trends Biochem Sci*, 18(1):7–12, Jan 1993.

[64] J M Nicaud, N Mackman, L Gray, and I B Holland. The c-terminal, 23 kda peptide of e. coli haemolysin 2001 contains all the information necessary for its secretion by the haemolysin (hly) export machinery. *FEBS Lett*, 204(2):331–5, Aug 1986.

[65] T Jarchau, T Chakraborty, F Garcia, and W Goebel. Selection for transport competence of c-terminal polypeptides derived from escherichia coli hemolysin: the shortest peptide capable of autonomous hlyb/hlyd-dependent secretion comprises the c-terminal 62 amino acids of hlya. *Mol Gen Genet*, 245(1):53–60, Oct 1994.

[66] F Duong, A Lazdunski, and M Murgier. Protein secretion by heterologous bacterial abc-transporters: the c-terminus secretion signal of the secreted protein confers high recognition specificity. *Mol Microbiol*, 21(3):459–70, Aug 1996.

[67] P Delepelaire and C Wandersman. Protein secretion in gram-negative bacteria. the extracellular metalloprotease b from erwinia chrysanthemi contains a c-terminal secretion signal analogous to that of escherichia coli alpha-hemolysin. *J Biol Chem*, 265(28):17118–25, Oct 1990.

[68] Yeonwoo Park, Yuseok Moon, Jungmin Ryoo, Nayeon Kim, Hyounghoon Cho, and Jung Hoon Ahn. Identification of the minimal region in lipase abc transporter

recognition domain of pseudomonas fluorescens for secretion and fluorescence of green fluorescent protein. *Microb Cell Fact*, 11:60, 2012.

[69] C Angkawidjaja, K Kuwahara, K Omori, Y Koga, K Takano, and S Kanaya. Extracellular secretion of escherichia coli alkaline phosphatase with a c-terminal tag by type i secretion system: purification and biochemical characterization. *Protein Eng Des Sel*, 19(7):337–43, Jul 2006.

[70] P Sebo and D Ladant. Repeat sequences in the bordetella pertussis adenylate cyclase toxin can be recognized as alternative carboxy-proximal secretion signals by the escherichia coli alpha-haemolysin translocator. *Mol Microbiol*, 9(5):999–1009, Sep 1993.

[71] S Létoffé, J M Ghigo, and C Wandersman. Secretion of the serratia marcescens hasa protein by an abc transporter. *J Bacteriol*, 176(17):5372–7, Sep 1994.

[72] J Hess, I Gentschev, W Goebel, and T Jarchau. Analysis of the haemolysin secretion system by phoa-hlya fusion proteins. *Mol Gen Genet*, 224(2):201–8, Nov 1990.

[73] Gyeong Tae Eom, Seung Hwan Lee, Young Hoon Oh, Ji Eun Choi, Si Jae Park, and Jae Kwang Song. Efficient extracellular production of type i secretion pathway-dependent pseudomonas fluorescens lipase in recombinant escherichia coli by heterologous abc protein exporters. *Biotechnol Lett*, 36(10):2037–42, Oct 2014.

[74] I Kern and P Cegłowski. Secretion of streptokinase fusion proteins from escherichia coli cells through the hemolysin transporter. *Gene*, 163(1):53–7, Sep 1995.

[75] Patrick J Bakkes, Stefan Jenewein, Sander H J Smits, I Barry Holland, and Lutz Schmitt. The rate of folding dictates substrate secretion by the escherichia coli hemolysin type 1 secretion system. *J Biol Chem*, 285(52):40573–80, Dec 2010.

[76] Christian K W Schwarz, Christine D Landsberg, Michael H H Lenders, Sander H J Smits, and Lutz Schmitt. Using an e. coli type 1 secretion system to secrete the mammalian, intracellular protein ifabp in its active form. *J Biotechnol*, 159(3):155–61, Jun 2012.

[77] Jaewook Ryu, Ukjin Lee, Jiye Park, Do-Hyun Yoo, and Jung Hoon Ahn. A vector system for abc transporter-mediated secretion and purification of recombinant proteins in pseudomonas species. *Appl Environ Microbiol*, 81(5):1744–53, Mar 2015.

[78] K Erb, M Vogel, W Wagner, and W Goebel. Alkaline phosphatase which lacks its own signal sequence becomes enzymatically active when fused to n-terminal sequences of escherichia coli haemolysin (hlya). *Mol Gen Genet*, 208(1-2):88–93, Jun 1987.

[79] Guillaume Sapriel, Cécile Wandersman, and Philippe Delepelaire. The n terminus of the hasa protein and the secb chaperone cooperate in the efficient targeting and secretion of hasa via the atp-binding cassette transporter. *J Biol Chem*, 277(8):6726–32, Feb 2002.

[80] Hyun-Ju Kwon, Mitsuru Haruki, Masaaki Morikawa, Kenji Omori, and Shigenori Kanaya. Role of repetitive nine-residue sequence motifs in secretion, enzymatic activity, and protein conformation of a family i.3 lipase. *J Biosci Bioeng*, 93(2):157–64, 2002.

[81] M J Fath, R C Skvirsky, and R Kolter. Functional complementation between bacterial mdr-like export systems: colicin v, alpha-hemolysin, and erwinia protease. *J Bacteriol*, 173(23):7549–56, Dec 1991.

[82] L Gilson, H K Mahanty, and R Kolter. Genetic analysis of an mdr-like export system: the secretion of colicin v. *EMBO J*, 9(12):3875–84, Dec 1990.

[83] H Ostolaza, A Soloaga, and F M Goñi. The binding of divalent cations to escherichia coli alpha-haemolysin. *Eur J Biochem*, 228(1):39–44, Feb 1995.

[84] A Soloaga, J M Ramírez, and F M Goñi. Reversible denaturation, self-aggregation, and membrane activity of escherichia coli alpha-hemolysin, a protein stable in 6 m urea. *Biochemistry*, 37(18):6387–93, May 1998.

[85] Sabrina Thomas, Patrick J Bakkes, Sander H J Smits, and Lutz Schmitt. Equilibrium folding of pro-hlya from escherichia coli reveals a stable calcium ion dependent folding intermediate. *Biochim Biophys Acta*, 1844(9):1500–10, Sep 2014.

[86] Alexandre Chenal, J Iñaki Guijarro, Bertrand Raynal, Muriel Delepierre, and Daniel Ladant. Rtx calcium binding motifs are intrinsically disordered in the absence of calcium: implication for protein secretion. *J Biol Chem*, 284(3):1781–9, Jan 2009.

[87] Mark A Blenner, Oren Shur, Géza R Szilvay, Donald M Cropek, and Scott Banta. Calcium-induced folding of a beta roll motif requires c-terminal entropic stabilization. *J Mol Biol*, 400(2):244–56, Jul 2010.

[88] Liang Zhang, James F Conway, and Patrick H Thibodeau. Calcium-induced folding and stabilization of the pseudomonas aeruginosa alkaline protease. *J Biol Chem*, 287(6):4311–22, Feb 2012.

[89] L Debarbieux and C Wandersman. Folded hasa inhibits its own secretion through its abc exporter. *EMBO J*, 20(17):4657–63, Sep 2001.

[90] M A Blight, C Chervaux, and I B Holland. Protein secretion pathway in escherichia coli. *Curr Opin Biotechnol*, 5(5):468–74, Oct 1994.

[91] I Gentschev, H Mollenkopf, Z Sokolovic, J Hess, S H Kaufmann, and W Goebel. Development of antigen-delivery systems, based on the escherichia coli hemolysin secretion pathway. *Gene*, 179(1):133–40, Nov 1996.

[92] S Spreng, G Dietrich, W Goebel, and I Gentschev. The escherichia coli haemolysin secretion apparatus: a potential universal antigen delivery system in gram-negative bacterial vaccine carriers. *Mol Microbiol*, 31(5):1596–8, Mar 1999.

[93] B D Tzschaschel, C A Guzmán, K N Timmis, and V de Lorenzo. An escherichia coli hemolysin transport system-based vector for the export of polypeptides: export of shiga-like toxin iieb subunit by salmonella typhimurium aroa. *Nat Biotechnol*, 14(6):765–9, Jun 1996.

[94] C Chervaux and I B Holland. Random and directed mutagenesis to elucidate the functional importance of helix ii and f-989 in the c-terminal secretion signal of escherichia coli hemolysin. *J Bacteriol*, 178(4):1232–6, Feb 1996.

[95] K Omori, A Idei, and H Akatsuka. Serratia atp-binding cassette protein exporter, lip, recognizes a protein region upstream of the c terminus for specific secretion. *J Biol Chem*, 276(29):27111–9, Jul 2001.

[96] David Hui and Victor Ling. A combinatorial approach toward analyzing functional elements of the escherichia coli hemolysin signal sequence. *Biochemistry*, 41(17):5333–9, Apr 2002.

[97] J Guzzo, F Duong, C Wandersman, M Murgier, and A Lazdunski. The secretion genes of pseudomonas aeruginosa alkaline protease are functionally related to those of erwinia chrysanthemi proteases and escherichia coli alpha-haemolysin. *Mol Microbiol*, 5(2):447–53, Feb 1991.

[98] H R Masure, D C Au, M K Gross, M G Donovan, and D R Storm. Secretion of the bordetella pertussis adenylate cyclase from escherichia coli containing the hemolysin operon. *Biochemistry*, 29(1):140–5, Jan 1990.

[99] H Akatsuka, E Kawai, K Omori, and T Shibatani. The three genes lipb, lipc, and lipd involved in the extracellular secretion of the serratia marcescens lipase which lacks an n-terminal signal peptide. *J Bacteriol*, 177(22):6381–9, Nov 1995.

[100] F Zhang, D I Greig, and V Ling. Functional replacement of the hemolysin a transport signal by a different primary sequence. *Proc Natl Acad Sci U S A*, 90(9):4211–5, May 1993.

[101] M J van Belkum, R W Worobo, and M E Stiles. Double-glycine-type leader peptides direct secretion of bacteriocins by abc transporters: colicin v secretion in lactococcus lactis. *Mol Microbiol*, 23(6):1293–301, Mar 1997.

[102] B Kenny, C Chervaux, and I B Holland. Evidence that residues -15 to -46 of the haemolysin secretion signal are involved in early steps in secretion, leading to recognition of the translocator. *Mol Microbiol*, 11(1):99–109, Jan 1994.

[103] P Stanley, V Koronakis, and C Hughes. Mutational analysis supports a role for multiple structural features in the c-terminal secretion signal of escherichia coli haemolysin. *Mol Microbiol*, 5(10):2391–403, Oct 1991.

[104] Thorsten Jumpertz, Christian Chervaux, Kathleen Racher, Maria Zouhair, Mark A Blight, I Barry Holland, and Lutz Schmitt. Mutations affecting the extreme c terminus of escherichia coli haemolysin a reduce haemolytic activity by altering the folding of the toxin. *Microbiology*, 156(Pt 8):2495–505, Aug 2010.

[105] B Kenny, S Taylor, and I B Holland. Identification of individual amino acids required for secretion within the haemolysin (hlya) c-terminal targeting region. *Mol Microbiol*, 6(11):1477–89, Jun 1992.

[106] D R Madden. The three-dimensional structure of peptide-mhc complexes. *Annu Rev Immunol*, 13:587–622, 1995.

[107] Michael H H Lenders, Stefanie Weidtkamp-Peters, Diana Kleinschrodt, Karl-Erich Jaeger, Sander H J Smits, and Lutz Schmitt. Directionality of substrate translocation of the hemolysin a type i secretion system. *Sci Rep*, 5:12470, 2015.

[108] D Hui, C Morden, F Zhang, and V Ling. Combinatorial analysis of the structural requirements of the escherichia coli hemolysin signal sequence. *J Biol Chem*, 275(4):2713–20, Jan 2000.

[109] N Wolff, P Delepelaire, J M Ghigo, and M Delepierre. Spectroscopic studies of the c-terminal secretion signal of the serratia marcescens haem acquisition protein (hasa) in various membrane-mimetic environments. *Eur J Biochem*, 243(1-2):400–7, Jan 1997.

[110] N Wolff, J M Ghigo, P Delepelaire, C Wandersman, and M Delepierre. C-terminal secretion signal of an erwinia chrysanthemi protease secreted by a signal peptide-independent pathway: proton nmr and cd conformational studies in membrane-mimetic environments. *Biochemistry*, 33(22):6792–801, Jun 1994.

[111] N Izadi-Pruneyre, N Wolff, V Redeker, C Wandersman, M Delepierre, and A Lecroisey. Nmr studies of the c-terminal secretion signal of the haem-binding protein, hasa. *Eur J Biochem*, 261(2):562–8, Apr 1999.

[112] F Zhang, Y Yin, C H Arrowsmith, and V Ling. Secretion and circular dichroism analysis of the c-terminal signal peptides of hlya and lkta. *Biochemistry*, 34(13):4193–201, Apr 1995.

[113] Y Yin, F Zhang, V Ling, and C H Arrowsmith. Structural analysis and comparison of the c-terminal transport signal domains of hemolysin a and leukotoxin a. *FEBS Lett*, 366(1):1–5, Jun 1995.

[114] Ana-Cristina Sotomayor Pérez, Johanna C Karst, Marilyne Davi, J Iñaki Guijarro, Daniel Ladant, and Alexandre Chenal. Characterization of the regions involved in the calcium-induced folding of the intrinsically disordered rtx motifs from the bordetella pertussis adenylate cyclase toxin. *J Mol Biol*, 397(2):534–49, Mar 2010.

[115] Sandra Cescau, Laurent Debarbieux, and Cécile Wandersman. Probing the in vivo dynamics of type i protein secretion complex association through sensitivity to detergents. *J Bacteriol*, 189(5):1496–504, Mar 2007.

[116] C Wandersman and S Létoffé. Involvement of lipopolysaccharide in the secretion of escherichia coli alpha-haemolysin and erwinia chrysanthemi proteases. *Mol Microbiol*, 7(1):141–50, Jan 1993.

[117] M A Blight, A L Pimenta, J C Lazzaroni, C Dando, L Kotelevets, S J Séror, and I B Holland. Identification and preliminary characterization of temperature-sensitive mutations affecting hlyb, the translocator required for the secretion of haemolysin (hlya) from escherichia coli. *Mol Gen Genet*, 245(4):431–40, Nov 1994.

[118] K Kuwahara, C Angkawidjaja, Y Koga, K Takano, and S Kanaya. Importance of an extreme c-terminal motif of a family i.3 lipase for stability. *Protein Eng Des Sel*, 24(5):411–8, May 2011.

[119] S Uebel, W Kraas, S Kienle, K H Wiesmüller, G Jung, and R Tampé. Recognition principle of the tap transporter disclosed by combinatorial peptide libraries. *Proc Natl Acad Sci U S A*, 94(17):8976–81, Aug 1997.

[120] Bethany Kay Boardman and Karla J Fullner Satchell. Vibrio cholerae strains with mutations in an atypical type i secretion system accumulate rtx toxin intracellularly. *J Bacteriol*, 186(23):8137–43, Dec 2004.

[121] Karla J Fullner Satchell. Martx, multifunctional autoprocessing repeats-in-toxin toxins. *Infect Immun*, 75(11):5079–84, Nov 2007.

[122] Martin H Griessl, Benedikt Schmid, Kristin Kassler, Christoph Braunsmann, Regina Ritter, Britta Barlag, York-Dieter Stierhof, Karina U Sturm, Claudia Danzer, Carolin Wagner, Tilman E Schäffer, Heinrich Sticht, Michael Hensel, and Yves A Muller. Structural insight into the giant ca2+-binding adhesin siie: implications for the adhesion of salmonella enterica to polarized epithelial cells. *Structure*, 21(5):741–52, May 2013.

[123] Roman G Gerlach, Daniela Jäckel, Bärbel Stecher, Carolin Wagner, Andrei Lupas, Wolf-Dietrich Hardt, and Michael Hensel. Salmonella pathogenicity island 4 encodes a giant non-fimbrial adhesin and the cognate type 1 secretion system. *Cell Microbiol*, 9(7):1834–50, Jul 2007.

[124] Thorsten Wille, Carolin Wagner, Wilrun Mittelstädt, Kathrin Blank, Erik Sommer, Gabriele Malengo, Daniela Döhler, Anna Lange, Viktor Sourjik, Michael Hensel, and Roman G Gerlach. Siia and siib are novel type i secretion system subunits controlling spi4-mediated adhesion of salmonella enterica. *Cell Microbiol*, 16(2):161–78, Feb 2014.

[125] Kristin K Jernigan and Seth R Bordenstein. Ankyrin domains across the tree of life. *PeerJ*, 2:e264, 2014.

[126] Joseph J Gillespie, Timothy P Driscoll, Victoria I Verhoeve, Tadanobu Utsuki, Claudia Husseneder, Vladimir N Chouljenko, Abdu F Azad, and Kevin R Macaluso. Genomic diversification in strains of rickettsia felis isolated from different arthropods. *Genome Biol Evol*, 7(1):35–56, Jan 2015.

[127] Lauren VieBrock, Sean M Evans, Andrea R Beyer, Charles L Larson, Paul A Beare, Hong Ge, Smita Singh, Kyle G Rodino, Robert A Heinzen, Allen L Richards, and Jason A Carlyon. Orientia tsutsugamushi ankyrin repeat-containing protein family members are type 1 secretion system substrates that traffic to the host cell endoplasmic reticulum. *Front Cell Infect Microbiol*, 4:186, 2014.

[128] Girija Dhamdhere and Helen I Zgurskaya. Metabolic shutdown in escherichia coli cells lacking the outer membrane channel tolc. *Mol Microbiol*, 77(3):743–54, Aug 2010.

[129] Cristian Ruiz and Stuart B Levy. Regulation of acrab expression by cellular metabolites in escherichia coli. *J Antimicrob Chemother*, 69(2):390–9, Feb 2014.

[130] H Nikaido. Multidrug efflux pumps of gram-negative bacteria. *J Bacteriol*, 178(20):5853–9, Oct 1996.

[131] Rebecca M Lennen, Mark G Politz, Max A Kruziki, and Brian F Pfleger. Identification of transport proteins involved in free fatty acid efflux in escherichia coli. *J Bacteriol*, 195(1):135–44, Jan 2013.

[132] Klaus Hantke, Karin Winkler, and Joachim E Schultz. Escherichia coli exports cyclic amp via tolc. *J Bacteriol*, 193(5):1086–9, Mar 2011.

[133] Elena B Tikhonova and Helen I Zgurskaya. Acra, acrb, and tolc of escherichia coli form a stable intermembrane multidrug efflux complex. *J Biol Chem*, 279(31):32116–24, Jul 2004.

[134] Ganesh Krishnamoorthy, Elena B Tikhonova, Girija Dhamdhere, and Helen I Zgurskaya. On the role of tolc in multidrug efflux: the function and assembly of acrab-tolc tolerate significant depletion of intracellular tolc protein. *Mol Microbiol*, 87(5):982–97, Mar 2013.

[135] Klaas M Pos. Drug transport mechanism of the acrb efflux pump. *Biochim Biophys Acta*, 1794(5):782–93, May 2009.

[136] V Koronakis, J Li, E Koronakis, and K Stauffer. Structure of tolc, the outer membrane component of the bacterial type i efflux system, derived from two-dimensional crystals. *Mol Microbiol*, 23(3):617–26, Feb 1997.

[137] Vassilis Koronakis, Jeyanthy Eswaran, and Colin Hughes. Structure and function of tolc: the bacterial exit duct for proteins and drugs. *Annu Rev Biochem*, 73:467–89, 2004.

[138] Xue-Yuan Pei, Philip Hinchliffe, Martyn F Symmons, Eva Koronakis, Roland Benz, Colin Hughes, and Vassilis Koronakis. Structures of sequential open states in a symmetrical opening transition of the tolc exit duct. *Proc Natl Acad Sci U S A*, 108(5):2112–7, Feb 2011.

[139] Christian Andersen, Eva Koronakis, Evert Bokma, Jeyanthy Eswaran, Daniel Humphreys, Colin Hughes, and Vassilis Koronakis. Transition to the open state of the tolc periplasmic tunnel entrance. *Proc Natl Acad Sci U S A*, 99(17):11103–8, Aug 2002.

[140] Christian Andersen, Eva Koronakis, Colin Hughes, and Vassilis Koronakis. An aspartate ring at the tolc tunnel entrance determines ion selectivity and presents a target for blocking by large cations. *Mol Microbiol*, 44(5):1131–9, Jun 2002.

[141] Luca Federici, Dijun Du, Fabien Walas, Hiroyoshi Matsumura, Juan Fernandez-Recio, Kenneth S McKeegan, M Ines Borges-Walmsley, Ben F Luisi, and Adrian R Walmsley. The crystal structure of the outer membrane protein vcec from the bacterial pathogen vibrio cholerae at 1.8 a resolution. *J Biol Chem*, 280(15):15307–14, Apr 2005.

[142] Martyn F Symmons, Robert L Marshall, and Vassiliy N Bavro. Architecture and roles of periplasmic adaptor proteins in tripartite efflux assemblies. *Front Microbiol*, 6:513, 2015.

[143] Jonathan Mikolosko, Kostyantyn Bobyk, Helen I Zgurskaya, and Partho Ghosh. Conformational flexibility in the multidrug efflux system protein acra. *Structure*, 14(3):577–87, Mar 2006.

[144] J M Johnson and G M Church. Alignment and structure prediction of divergent protein families: periplasmic and outer membrane proteins of bacterial efflux pumps. *J Mol Biol*, 287(3):695–715, Apr 1999.

[145] H I Zgurskaya and H Nikaido. Cross-linked complex between oligomeric periplasmic lipoprotein acra and the inner-membrane-associated multidrug efflux pump acrb from escherichia coli. *J Bacteriol*, 182(15):4264–7, Aug 2000.

[146] Fasahath Husain, Matthew Humbard, and Rajeev Misra. Interaction between the tolc and acra proteins of a multidrug efflux system of escherichia coli. *J Bacteriol*, 186(24):8533–6, Dec 2004.

[147] Johannes F Stegmeier, Georg Polleichtner, Nicolas Brandes, Christian Hotz, and Christian Andersen. Importance of the adaptor (membrane fusion) protein hairpin domain for the functionality of multidrug efflux pumps. *Biochemistry*, 45(34):10303–12, Aug 2006.

[148] Minho Lee, So-Young Jun, Bo-Young Yoon, Saemee Song, Kangseok Lee, and Nam-Chul Ha. Membrane fusion proteins of type i secretion system and tripartite efflux pumps share a binding motif for tolc in gram-negative bacteria. *PLoS One*, 7(7):e40460, 2012.

[149] R Schülein, I Gentschev, H J Mollenkopf, and W Goebel. A topological model for the haemolysin translocator protein hlyd. *Mol Gen Genet*, 234(1):155–63, Jul 1992.

[150] R Schülein, I Gentschev, S Schlör, R Gross, and W Goebel. Identification and characterization of two functional domains of the hemolysin translocator protein hlyd. *Mol Gen Genet*, 245(2):203–11, Oct 1994.

[151] A L Pimenta, K Racher, L Jamieson, M A Blight, and I B Holland. Mutations in hlyd, part of the type 1 translocator for hemolysin secretion, affect the folding of the secreted toxin. *J Bacteriol*, 187(21):7471–80, Nov 2005.

[152] I Gentschev and W Goebel. Topological and functional studies on hlyb of escherichia coli. *Mol Gen Genet*, 232(1):40–8, Mar 1992.

[153] Lutz Schmitt, Houssain Benabdelhak, Mark A Blight, I Barry Holland, and Milton T Stubbs. Crystal structure of the nucleotide-binding domain of the abc-transporter haemolysin b: identification of a variable region within abc helical domains. *J Mol Biol*, 330(2):333–42, Jul 2003.

[154] F Zhang, J A Sheps, and V Ling. Structure-function analysis of hemolysin b. *Methods Enzymol*, 292:51–66, 1998.

[155] L W Hung, I X Wang, K Nikaido, P Q Liu, G F Ames, and S H Kim. Crystal structure of the atp-binding subunit of an abc transporter. *Nature*, 396(6712):703–7, Dec 1998.

[156] Jelena Zaitseva, Stefan Jenewein, Thorsten Jumpertz, I Barry Holland, and Lutz Schmitt. H662 is the linchpin of atp hydrolysis in the nucleotide-binding domain of the abc transporter hlyb. *EMBO J*, 24(11):1901–10, Jun 2005.

[157] Peter M Jones and Anthony M George. Mechanism of abc transporters: a molecular dynamics simulation of a well characterized nucleotide-binding subunit. *Proc Natl Acad Sci U S A*, 99(20):12639–44, Oct 2002.

[158] Paul C Smith, Nathan Karpowich, Linda Millen, Jonathan E Moody, Jane Rosen, Philip J Thomas, and John F Hunt. Atp binding to the motor domain from an abc transporter drives formation of a nucleotide sandwich dimer. *Mol Cell*, 10(1):139–49, Jul 2002.

[159] Peter M Jones and Anthony M George. A reciprocating twin-channel model for abc transporters. *Q Rev Biophys*, 47(3):189–220, Aug 2014.

[160] Seiji Ishii, Takato Yano, Akio Ebihara, Akihiro Okamoto, Miho Manzoku, and Hideyuki Hayashi. Crystal structure of the peptidase domain of streptococcus coma, a bifunctional atp-binding cassette transporter involved in the quorum-sensing pathway. *J Biol Chem*, 285(14):10777–85, Apr 2010.

[161] Kaspar P Locher, Allen T Lee, and Douglas C Rees. The e. coli btucd structure: a framework for abc transporter architecture and mechanism. *Science*, 296(5570):1091–8, May 2002.

[162] Dheeraj Khare, Michael L Oldham, Cedric Orelle, Amy L Davidson, and Jue Chen. Alternating access in maltose transporter mediated by rigid-body rotations. *Mol Cell*, 33(4):528–36, Feb 2009.

[163] Michael L Oldham and Jue Chen. Snapshots of the maltose transporter during atp hydrolysis. *Proc Natl Acad Sci U S A*, 108(37):15152–6, Sep 2011.

[164] Michael L Oldham, Dheeraj Khare, Florante A Quiocho, Amy L Davidson, and Jue Chen. Crystal structure of a catalytic intermediate of the maltose transporter. *Nature*, 450(7169):515–21, Nov 2007.

[165] O Jardetzky. Simple allosteric model for membrane pumps. *Nature*, 211(5052):969–70, Aug 1966.

[166] Roger J P Dawson and Kaspar P Locher. Structure of a bacterial multidrug abc transporter. *Nature*, 443(7108):180–5, Sep 2006.

[167] Stephen G Aller, Jodie Yu, Andrew Ward, Yue Weng, Srinivas Chittaboina, Rupeng Zhuo, Patina M Harrell, Yenphuong T Trinh, Qinghai Zhang, Ina L Urbatsch, and Geoffrey Chang. Structure of p-glycoprotein reveals a molecular basis for poly-specific drug binding. *Science*, 323(5922):1718–22, Mar 2009.

[168] Hassanul G Choudhury, Zhen Tong, Indran Mathavan, Yanyan Li, So Iwata, Séverine Zirah, Sylvie Rebuffat, Hendrik W van Veen, and Konstantinos Beis. Structure of an antibacterial peptide atp-binding cassette transporter in a novel outward occluded state. *Proc Natl Acad Sci U S A*, 111(25):9145–50, Jun 2014.

[169] Mi Sun Jin, Michael L Oldham, Qiuju Zhang, and Jue Chen. Crystal structure of the multidrug transporter p-glycoprotein from caenorhabditis elegans. *Nature*, 490(7421):566–9, Oct 2012.

[170] Atsushi Kodan, Tomohiro Yamaguchi, Toru Nakatsu, Keita Sakiyama, Christopher J Hipolito, Akane Fujioka, Ryo Hirokane, Keiji Ikeguchi, Bunta Watanabe, Jun Hiratake, Yasuhisa Kimura, Hiroaki Suga, Kazumitsu Ueda, and Hiroaki Kato. Structural basis for gating mechanisms of a eukaryotic p-glycoprotein homolog. *Proc Natl Acad Sci U S A*, 111(11):4049–54, Mar 2014.

[171] Jonas Y Lee, Janet G Yang, Daniel Zhitnitsky, Oded Lewinson, and Douglas C Rees. Structural basis for heavy metal detoxification by an atm1-type abc exporter. *Science*, 343(6175):1133–6, Mar 2014.

[172] Chitra A Shintre, Ashley C W Pike, Qiuhong Li, Jung-In Kim, Alastair J Barr, Solenne Goubin, Leela Shrestha, Jing Yang, Georgina Berridge, Jonathan Ross, Phillip J Stansfeld, Mark S P Sansom, Aled M Edwards, Chas Bountra, Brian D Marsden, Frank von Delft, Alex N Bullock, Opher Gileadi, Nicola A Burgess-Brown, and Elisabeth P Carpenter. Structures of abcb10, a human atp-binding cassette transporter in apo- and nucleotide-bound states. *Proc Natl Acad Sci U S A*, 110(24):9710–5, Jun 2013.

[173] Vasundara Srinivasan, Antonio J Pierik, and Roland Lill. Crystal structures of nucleotide-free and glutathione-bound mitochondrial abc transporter atm1. *Science*, 343(6175):1137–40, Mar 2014.

[174] Houssain Benabdelhak, Stephan Kiontke, Carsten Horn, Robert Ernst, Mark A Blight, I Barry Holland, and Lutz Schmitt. A specific interaction between the nbd of the abc-transporter hlyb and a c-terminal fragment of its transport substrate haemolysin a. *J Mol Biol*, 327(5):1169–79, Apr 2003.

[175] Houssain Benabdelhak, Lutz Schmitt, Carsten Horn, Kornelia Jumel, Mark A Blight, and I Barry Holland. Positive co-operative activity and dimerization of the isolated abc atpase domain of hlyb from escherichia coli. *Biochem J*, 386(Pt 3):489–95, Mar 2005.

[176] Jelena Zaitseva, Stefan Jenewein, Alexander Wiedenmann, Houssain Benabdelhak, I Barry Holland, and Lutz Schmitt. Functional characterization and atp-induced dimerization of the isolated abc-domain of the haemolysin b transporter. *Biochemistry*, 44(28):9680–90, Jul 2005.

[177] Erik Procko and Rachelle Gaudet. Functionally important interactions between the nucleotide-binding domains of an antigenic peptide transporter. *Biochemistry*, 47(21):5699–708, May 2008.

[178] Nina Grossmann, Ahmet S Vakkasoglu, Sabine Hulpke, Rupert Abele, Rachelle Gaudet, and Robert Tampé. Mechanistic determinants of the directionality and energetics of active export by a heterodimeric abc transporter. *Nat Commun*, 5:5419, 2014.

[179] Vladimir M Korkhov, Samantha A Mireku, and Kaspar P Locher. Structure of amp-pnp-bound vitamin b12 transporter btucd-f. *Nature*, 490(7420):367–72, Oct 2012.

[180] I R Vetter and A Wittinghofer. Nucleoside triphosphate-binding proteins: different scaffolds to achieve phosphoryl transfer. *Q Rev Biophys*, 32(1):1–56, Feb 1999.

[181] Lutz Schmitt and Robert Tampé. Structure and mechanism of abc transporters. *Curr Opin Struct Biol*, 12(6):754–60, Dec 2002.

[182] Cédric Orelle, Olivier Dalmas, Philippe Gros, Attilio Di Pietro, and Jean-Michel Jault. The conserved glutamate residue adjacent to the walker-b motif is the

catalytic base for atp hydrolysis in the atp-binding cassette transporter bmra. *J Biol Chem*, 278(47):47002–8, Nov 2003.

[183] Jonathan E Moody, Linda Millen, Derk Binns, John F Hunt, and Philip J Thomas. Cooperative, atp-dependent association of the nucleotide binding cassettes during the catalytic cycle of atp-binding cassette transporters. *J Biol Chem*, 277(24):21111–4, Jun 2002.

[184] Eva Janas, Matthias Hofacker, Min Chen, Simone Gompf, Chris van der Does, and Robert Tampé. The atp hydrolysis cycle of the nucleotide-binding domain of the mitochondrial atp-binding cassette transporter mdl1p. *J Biol Chem*, 278(29):26862–9, Jul 2003.

[185] Grégory Verdon, Sonja-Verena Albers, Niels van Oosterwijk, Bauke W Dijkstra, Arnold J M Driessen, and Andy-Mark W H Thunnissen. Formation of the productive atp-mg2+-bound dimer of glcv, an abc-atpase from sulfolobus solfataricus. *J Mol Biol*, 334(2):255–67, Nov 2003.

[186] A L Davidson and S Sharma. Mutation of a single malk subunit severely impairs maltose transport activity in escherichia coli. *J Bacteriol*, 179(17):5458–64, Sep 1997.

[187] V Shyamala, V Baichwal, E Beall, and G F Ames. Structure-function analysis of the histidine permease and comparison with cystic fibrosis mutations. *J Biol Chem*, 266(28):18714–9, Oct 1991.

[188] Robert Ernst, Petra Kueppers, Cornelia M Klein, Tobias Schwarzmueller, Karl Kuchler, and Lutz Schmitt. A mutation of the h-loop selectively affects rhodamine transport by the yeast multidrug abc transporter pdr5. *Proc Natl Acad Sci U S A*, 105(13):5069–74, Apr 2008.

[189] Alan E Senior. Reaction chemistry abc-style. *Proc Natl Acad Sci U S A*, 108(37):15015–6, Sep 2011.

[190] Chris van der Does, Chiara Presenti, Katrin Schulze, Stephanie Dinkelaker, and Robert Tampé. Kinetics of the atp hydrolysis cycle of the nucleotide-binding domain of mdl1 studied by a novel site-specific labeling technique. *J Biol Chem*, 281(9):5694–701, Mar 2006.

[191] David Yin-wei Lin, Shuo Huang, and Jue Chen. Crystal structures of a polypeptide processing and secretion transporter. *Nature*, 523(7561):425–30, Jul 2015.

[192] R Binet and C Wandersman. Protein secretion by hybrid bacterial abc-transporters: specific functions of the membrane atpase and the membrane fusion protein. *EMBO J*, 14(10):2298–306, May 1995.

[193] I Barry Holland, Houssain Benabdelhak, Joanne Young, de Lima, A Pimenta, Lutz Schmitt, and Mark A Blight. Bacterial abc-transporters involved in protein translocation. *ABC proteins: From bacteria to man*, 2003.

[194] P Delepelaire. Prtd, the integral membrane atp-binding cassette component of the erwinia chrysanthemi metalloprotease secretion system, exhibits a secretion signal-regulated atpase activity. *J Biol Chem*, 269(45):27952–7, Nov 1994.

[195] J Hwang, X Zhong, and P C Tai. Interactions of dedicated export membrane proteins of the colicin v secretion system: Cvaa, a member of the membrane fusion protein family, interacts with cvab and tolc. *J Bacteriol*, 179(20):6264–70, Oct 1997.

[196] S Létoffé, P Delepelaire, and C Wandersman. Protein secretion in gram-negative bacteria: assembly of the three components of abc protein-mediated exporters is ordered and promoted by substrate binding. *EMBO J*, 15(21):5804–11, Nov 1996.

[197] T Thanabalu, E Koronakis, C Hughes, and V Koronakis. Substrate-induced assembly of a contiguous channel for protein export from e.coli: reversible bridging of an inner-membrane translocase to an outer membrane exit pore. *EMBO J*, 17(22):6487–96, Nov 1998.

3.3. Chapter III - Using an *E. coli* Type 1 secretion system to secrete the mammalian, intracellular protein IFABP in its active form

Title Using an *E. coli* Type 1 secretion system to secrete the mammalian, intracellular protein IFABP in its active form

Authors Christian K. W. Schwarz, Christine D Landsberg, Michael H.H. Lenders, Sander H. J. Smits and Lutz Schmitt

Published in *Journal of biotechnology* (2012)

Impact factor 3.045

Own proportion of this work 15 %;
Construction of the plasmids, secretion analysis.

Journal of Biotechnology 159 (2012) 155–161

Contents lists available at SciVerse ScienceDirect

Journal of Biotechnology

journal homepage: www.elsevier.com/locate/jbiotec

Using an *E. coli* Type 1 secretion system to secrete the mammalian, intracellular protein IFABP in its active form

Christian K.W. Schwarz, Christine D. Landsberg, Michael H.H. Lenders, Sander H.J. Smits, Lutz Schmitt*

Institute of Biochemistry, Heinrich-Heine-Universität Düsseldorf, Universitätsstrasse 1, 40225 Düsseldorf, Germany

ARTICLE INFO

Article history:
Received 4 October 2011
Received in revised form 7 February 2012
Accepted 9 February 2012
Available online 17 February 2012

Keywords:
Type 1 secretion
Haemolysin A
IFABP
Inclusion bodies
FKBP
Purification protocol

ABSTRACT

A biotechnological production of proteins through protein secretion systems might be superior to the conventional cytoplasmic production, because of the absence of large amounts of proteases present in the extracellular space and the ease of purification or downstream processing. However, secretion of proteins is still a trial-and-error approach and many proteins fail to be secreted. Recently, a study of a Type 1 secretion system revealed that the folding rate of the passenger protein dictates secretion efficiency. Here, the well-known MalE failed to be secreted when fused to a C-terminal fragment of the natural substrate haemolysin A. In contrast, slow-folding mutants of MalE were secreted in high yields. However, MalE is a bacterial protein that is targeted to the periplasmic space of *E. coli* and possesses the intrinsic capability to cross a membrane. Therefore, we applied the same approach for another eukaryotic protein that resides in the cytoplasm. As an example, we chose the intestinal fatty acid binding protein (IFABP) and highlight the universal potential of this Type 1 secretion system to secrete proteins with slow-folding kinetics (here the G121V mutant). Finally, a one-step purification protocol was established yielding 1 mg of pure IFABP G121V per liter culture supernatant. Moreover, secreted IFABP G121V was shown to reach a folded state, which is biologically active.

1. Introduction

Substrates of Type 1 secretion systems (T1SS) are translocated in one step from the cytoplasm to the exterior via dedicated transport systems in Gram-negative bacteria. The substrate spectrum of these T1SS contains structurally and functionally unrelated proteins and, more importantly, proteins of different molecular weights ranging from, for example, the hemophore HasA (19 kDa) (Letoffe et al., 1994) or the lipase LipA (65 kDa) of *Serratia marcescens* (Meier et al., 2007) to the 800 kDa protein LapA that is involved in the biofilm formation by *Pseudomonas fluorescence* (Hinsa et al., 2003).

In general, T1SS mediate the passage across the inner and outer membrane of Gram-negative bacteria in one step, through the concerted interaction of two inner membrane proteins, a membrane fusion protein (MFP) and an ATP binding cassette (ABC) transporter, and an outer membrane factor (OMF). These proteins form a complex that catalyzes the secretion without the appearance of a periplasmic intermediate (Holland et al., 2005; Thanabalu et al., 1998).

The paradigm of such a T1SS is the haemolysin A (HlyA) secretion system of *Escherichia coli* (*E. coli*), which is composed of the ABC transporter haemolysin B (HlyB), the MFP haemolysin D (HlyD), and the multi-functional TolC (Jarchau et al., 1994). Upon interaction of the substrate, HlyA, with HlyB and/or HlyD, TolC is recruited and a continuous export channel is formed from the cytosol directly to the exterior (Benabdelhak et al., 2003; Thanabalu et al., 1998). HlyA is a 110 kDa toxin, which lyses, for example, erythrocytes (Linggood and Ingram, 1982). The non-cleavable secretion signal of HlyA is located at the C-terminal 50–60 amino acids and is essential and, by itself, sufficient for secretion (Gray et al., 1986; Hess et al., 1990; Jarchau et al., 1994; Kenny et al., 1994; Stanley et al., 1991).

The common denominator of HlyA and the vast majority of T1SS substrates are glycine-rich nonapeptide repeats (GG repeats) that contain the consensus sequence GGxGxDxUx (x: any amino acid and U: large or hydrophobic amino acid), which are located upstream of the secretion signal. These GG repeats increase the secretion levels as demonstrated by the higher yields of secreted proteins, when compared to the secretion signal alone (Kenny et al., 1991; Sanchez-Magraner et al., 2007). Therefore, a 23 kDa C-terminal fragment of HlyA consisting of 218 amino acids and three GG repeats was used for the secretion of a couple of fusion proteins, such as β-lactamase or scFv. Here, the gene of interest was fused 5′ to the gene encoding the 23 kDa C-terminal fragment of

Abbreviations: DAUDA, 11-(dansylamino)undecanoic acid; ddFKBP, destabilizing domain FKBP12; FKBP12, human FK506- or rapamycin-binding protein; GG repeats, glycine-rich, nonapeptide repeats; HlyA, haemolysin A; HlyAc, C-terminal fragment of HlyA; IFABP, rat intestinal fatty acid binding protein; IMAC, immobilized metal-ion affinity chromatography; MalE, maltose binding protein; T1SS, Type 1 secretion system.

* Corresponding author. Tel.: +49 211 81 10773; fax: +49 211 81 15310.
E-mail address: Lutz.Schmitt@hhu.de (L. Schmitt).

0168-1656/$ – see front matter © 2012 Elsevier B.V. All rights reserved.
doi:10.1016/j.jbiotec.2012.02.005

HlyA (Blight and Holland, 1994; Chervaux et al., 1995; Fernandez et al., 2000; Mackman et al., 1987). Despite promising initial results, many of the chimeras employed could not be secreted, which limited the biotechnological exploitation of this T1SS (Blight and Holland, 1994). Recently, Bakkes et al. (2010) showed that a fusion protein composed of the maltose binding protein (MalE) and the above-mentioned 23 kDa fragment of HlyA (HlyAc), which was initially not secreted, could be secreted by the introduction of slow-folding mutations in MalE (Bakkes et al., 2010). However, MalE endows intrinsic properties to pass membranes as it is normally translocated via the Sec pathway into the periplasm of *E. coli* (Cover et al., 1987). Although the slow-folding strategy was successfully applied for MalE, several questions remained such as if the described T1SS is capable of secreting: (1) proteins of heterologous origin, for example, from eukaryotic origin, (2) proteins, which are normally not transported across membranes, (3) proteins that are normally expressed as inclusion bodies or (4) biologically active proteins?

To answer these questions, the eukaryotic, cytoplasmic intestinal fatty acid binding protein (IFABP) from rats was fused to HlyAc. The protein consists of 132 amino acids (15.1 kDa), binds a single molecule of a long-chain fatty acid and is important in the fatty acid metabolism of humans as well as other mammals (Rowland et al., 2009; Sweetser et al., 1987). In vitro, it is also used for binding analysis of lipophilic drugs and the prediction of drug pharmacokinetic parameters (Chuang et al., 2008; Rowland et al., 2009).

The slow-folding mutant G121 V of IFABP binds fatty acids with high affinity (K_D = 120 nM ± 25 nM) but forms, in contrast to the wild-type, inclusion bodies during its expression in *E. coli* (Kim and Frieden, 1998). Therefore, we chose IFABP G121V to investigate the general applicability of the HlyA T1SS for the secretion of heterologous, slow-folding substrates, the impact of inclusion body formation onto the secretion system and to compare the biological activity of secreted IFABP with the biological activity of IFABP G121V purified from inclusion bodies.

If slow-folding mutations of a desired protein are not available, directed evolution experiments might be used (Crameri et al., 1996, 1998). However, these methods are based on trial-and-error approaches and high-throughput screening methods are necessary to identify high-secreting clones (Farinas et al., 2001). Therefore, this approach is time-consuming and cost-intensive. A solution might be the incorporation of a "destabilizing domain" in front of the passanger protein. Such domains confer instability to the fused proteins and induce a subsequent degradation of the fusion proteins. The destabilizing domain FKBP (ddFKBP), an engineered version of the human FK506- or the rapamycin-binding protein (FKBP12), is the best-characterized destabilization domain in eukaryotes (Armstrong and Goldberg, 2007; Banaszynski et al., 2006; Herm-Gotz et al., 2007; Park et al., 1992). However, no studies in bacteria are available. Thus, the fusion of the protein of interest to a destablizing domain might provide a general tool to decrease its folding kinetics. This, in principle, should facilitate the secretion of these chimeras through the T1SS.

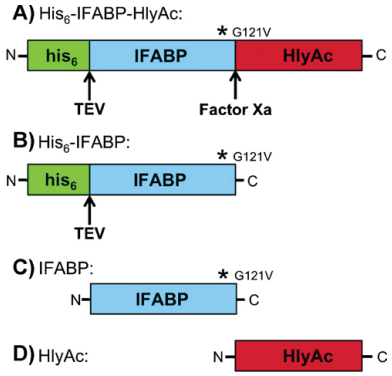

Fig. 1. Schematic view of the constructs used in this study. (A) Rat IFABP(wt) or IFABP(G121V) (blue) with an N-terminal his_6-tag (green) were cloned in front of the secretion module HlyAc (red); 42.1 kDa. (B) After the factor Xa digest, his_6-IFABP was separated from HlyAc; 18.3 kDa. (C) The his_6-tag was removed with the TEV protease; 15.3 kDa. (D) HlyAc, used as secretion module, is shown; 27.2 kDa.

Accordingly, we compared the potential of the destabilizing domain with the introduction of slow-folding mutants on the secretability of IFABP. Our results demonstrated that the ddFKBP is not applicable to increase the secretion levels, but that the introduction of a slow-folding mutation into IFABP converts a non-secreted protein into a well-accepted substrate of the HlyA T1SS. Furthermore, we show that secreted IFABP is correctly folded and biologicl active, suggesting that this secretion system is an attractive candidate for a biotechnological protein production system in appropiate yields.

2. Materials and methods

2.1. Construction of the vectors

The genes of rat IFABP WT and rat IFABP G121V were encoded on plasmids pQE IFABP WT and pQE IFABP G121V, respectively (kind gift of Dr. Carl Frieden, Department of Biochemistry and Molecular Biophysics, Washington University School of Medicine, St. Louis, USA) (Kim and Frieden, 1998). The plasmids pSOI-IFABP(wt), pSOI-ddFKBP IFABP(wt), pSOI-IFABP(G121V) and pSOI-ddFKBP IFABP(G121V) were prepared using the *In-Fusion® Advantage PCR Cloning Kit* (Clontech). Employing this strategy, IFABP–HlyAc and ddFKBP–IFABP–HlyAc fusion proteins were generated according to Bakkes et al. (2010) including a factor Xa cleavage site located between IFABP and HlyAc and an N-terminal his_6-tag followed by a TEV protease cleavage site (see Fig. 1). The sequences of all used constructs (see Table 1) were verified by DNA sequencing.

Table 1
Plasmids used in this study.

Plasmids		
Name	Description	Reference
pK184-HlyBD	Plasmid encoding for the genes *hlyB* and *hlyD*	Bakkes et al. (2010)
pSOI-HlyAc	Plasmid encoding for the 23 kDa C-terminal fragment of HlyA (HlyAc)	Bakkes et al. (2010)
pSOI-IFABP(wt)	IFABP(wt) inserted in pSOI-HlyAc (his_6–IFABP(wt)–HlyAc)	This study
pSOI-IFABP(G121V)	IFABP(G121V) inserted in pSOI-HlyAc (his_6–IFABP(G121V)–HlyAc)	This study
pSOI-ddFKBP IFABP(wt)	ddFKBP inserted in pSOI-IFABP(wt) N-terminally of IFABP(wt) (ddFKBP–IFABP(wt)–HlyAc)	This study
pSOI-ddFKBP IFABP(G121V)	ddFKBP inserted in pSOI-IFABP(G121V) N-terminally of IFABP(G121V) (ddFKBP–IFABP(G121V)–HlyAc)	This study

2.2. Protein expression, secretion and purification

2.2.1. Secretion experiments

All secretion experiments were performed with small variations as described (Bakkes et al., 2010). In brief, *E. coli* WM2429 carrying both, pK184-HlyBD and a pSOI construct, was grown in 2xYT medium supplemented with kanamycin (30 μg mL^{-1}) and ampicillin (100 μg mL^{-1}) at 37 °C with agitation. At an OD_{600} of 0.5, expression of *hlyB* and *hlyD* and the fusion genes, encoded by the pSOI plasmids, were induced with 1.5 mM IPTG and 10 mM arabinose. The pSOI plasmids carry an arabinose promoter, while a *lac* promotor controls the expression of HlyB/D. After 4 h growth, cell cultures were centrifuged for 20 min at 14,000 × *g*, 4 °C and cells (OD_{eq} = 0.1) and supernatant samples (16 μL) were analyzed by SDS-PAGE using Coomassie Brilliant Blue (CBB) staining and/or Western blotting using a HlyA specific, polyclonal antibody or an anti-his-tag antibody (Qiagen, Hilden). An HRP-conjugated, secondary antibody in combination with the ECL advance kit (GE Healthcare) was used for the visualization of the fusion bands. If indicated, 160 μL culture supernatant was precipitated for 30 min on ice with 20% trichloroacedic acid (TCA). After centrifugation for 20 min at 4 °C, the pellet was resolved and used for SDS-PAGE analysis.

2.2.2. Purification of the secreted proteins HlyAc or his_6–IFABP(G121V)–HlyAc

Cells secreting either HlyAc or his_6–IFABP(G121V)–HlyAc were grown for 4 h at 37 °C with agitation. After centrifugation for 20 min and 14,000 × *g*, 4 °C, the supernatant was supplemented with 10 mM imidazole and 20 mM $MgCl_2$. For the subsequent immobilized metal-ion affinity chromatography (IMAC), the supernatant was loaded on a HiTrap IMAC HP column (5 mL, GE Healthcare) preloaded with Ni^{2+} and pre-equilibrated in buffer (10 mM Tris–HCl, 150 mM NaCl, 10 mM imidazole, pH 8.0) using a FPLC system (ÄktaSystem, GE Healthcare). After washing the column with this buffer, HlyAc or his_6–IFABP(G121V)–HlyAc was eluted with the buffer supplemented with 250 mM imidazole and a linear gradient of 10 column volumes ranging from 10 to 250 mM imidazole. Protein fractions were pooled and concentrated by ultrafiltration (Amicon Filter devices, 10 kDa MWCO). The protein concentration was determined with a NanoDrop device (PeqLab) using the calculated extinction coefficients and molecular masses (HlyAc: 23,380 M^{-1} cm^{-1}, 27.2 kDa; his_6–IFABP(G121V)–HlyAc: 40,340 M^{-1} cm^{-1}, 42.1 kDa; his_6–IFABP(G121V): 18,450 M^{-1} cm^{-1}, 18.3 kDa) (http://expasy.org/tools/protparam.html).

2.2.3. Factor Xa digestion and anion-exchange chromatography

50 μg his_6–IFABP(G121V)–HlyAc was cleaved with 1 μg factor Xa (NEB) overnight at 25 °C. An anion-exchange chromatography was performed to separate cleaved his_6–IFABP(G121V) and uncleaved his_6–IFABP(G121V)–HlyAc, HlyAc and factor Xa. The digestion mixture was diluted tenfold in 10 mM NaH_2PO_4, 20 mM NaCl, pH 7.3 and loaded on a Q HP column (GE Healthcare) with a FPLC system (GE Healthcare). The his_6–IFABP(G121V) eluted in the flow through.

2.2.4. Removal of the his_6-tag with the TEV protease

4 μg his_6–IFABP(G121V) was digested with 1 U of TEV protease (ProSpec) overnight at 25 °C in buffer supplemented with 10 mM dithiothreitol (DTT). After cleavage, the his_6-tag and the TEV protease (containing a his-tag) were removed by incubation of the mixture with magnetic Ni^{2+} beads (Qiagen) and the supernatant was stored until further analysis.

2.2.5. Expression and purification of rat IFABP G121V from E. coli

Chemically competent *E. coli* BL21 (DE3) was transformed with pQE IFABP G121V and grown on LB agar plates supplemented with 100 μg mL^{-1} ampicillin. Overnight cultures of single colonies were used to inoculate 2 L 2xYT medium containing 100 μg mL^{-1} ampicillin with a start OD_{600} of 0.1 at 37 °C and gene expression was induced with 1 mM IPTG at OD_{600} of 0.5. Cells were grown for 4 h at 160 rpm and agitation, harvested by centrifugation and directly used or stored at −20 °C. Rat IFABP G121V was purified from inclusion bodies with minor changes as described (Kim and Frieden, 1998). Briefly, cells were broken with a cell disruptor (Constant Systems) and the lysate was centrifuged (20 min, 13,500 × *g*). The pellet was washed twice with 20 mM Tris–HCl, 0.25 mM EDTA, 0.5% Triton X-100, pH 8.0 and twice with 20 mM Tris–HCl, 0.25 mM EDTA, pH 8.0. Crude inclusion bodies were dissolved in 20 mM Tris–HCl, 0.25 mM EDTA, 6 M guanidinium-hydrochloride, pH 8.0 and the protein concentration was determined with a NanoDrop device (PeqLab) as above. For refolding, IFABP G121V was diluted to 0.2 mg mL^{-1} in 20 mM Tris–HCl, 0.25 mM EDTA, pH 8.0 and residual guanidinium-hydrochloride was removed by extensive dialysis overnight at 4 °C. Dialyzed, refolded IFABP G121V was centrifuged (20 min, 50,000 × *g*, 4 °C) and the supernatant was purified by anion-exchange chromatography (5 mL HP Q column, GE Healthcare). IFABP G121V eluted in the flow through. IFABP G121V was concentrated via ultrafiltration (Amicon filter device, MWCO: 10 kDa) and applied to a size-exclusion chromatography (Superdex 75 16/60, GE Healthcare) pre-equilibrated in 20 mM K_2HPO_4, 0.25 mM EDTA, pH 7.3. Protein containing fractions were concentrated by ultrafiltration (Amicon filter device, MWCO: 10 kDa) and stored at −80 °C.

2.3. Folding state of secreted IFABP (G121V)

Intrinsic tryptophane fluorescence measurements were performed using 0.5 μM protein at 20 °C and a Fluorolog®-3 (Horiba) in buffer (20 mM K_2HPO_4, 0.25 mM EDTA, pH 7.3) with or without 6 M urea. 290 nm was used as excitation wavelength and the emission spectrum was recorded between 300 nm and 440 nm (slit width 5 nm for both, excitation and emission).

2.4. Binding affinity determination of DAUDA to IFABP G121V

11-(Dansylamino)undecanoic acid (DAUDA, Cayman Chemical) was prepared as a 1 mM stock solution in 50% isopropanol and 50% buffer (20 mM KH_2PO_4, 0.25 mM EDTA, pH 7.3) and further diluted to the appropriate concentrations with buffer. 100 nM IFABP was used in buffer and a 1 mL silica glass cuvette. The fluorescence signal was recorded at a wavelength of 500 nm after excitation of DAUDA at 350 nm using a Fluorolog®-3 (Horiba) (Kim and Frieden, 1998). The slit width was adjusted to 3.5 nm for both, the excitation and emission, and the signal was integrated for 0.5 s. Fluorescence signals of DAUDA in buffer in the absence of protein was subtracted as background. The corrected and normalized fluorescence signals were plotted against the DAUDA concentration. Assuming one binding site per monomer in IFABP, the K_D for substrate binding was determined by non-linear, least-squares fitting of the data to the following equation: $F = F_0 + (\Delta F/2P_0)[(K_D + P_0 + L_0) - ((K_D + P_0 + L_0)^2 - 4L_0P_0)^{1/2}]$, which corrected the data for the concentration of the receptor. F is the measured fluorescence; F_0 the fluorescence of IFABP in the absence of DAUDA; ΔF is the change of fluorescence; P_0 and L_0 are the total concentrations of protein and substrate. Data were fitted using the program Prism 5.

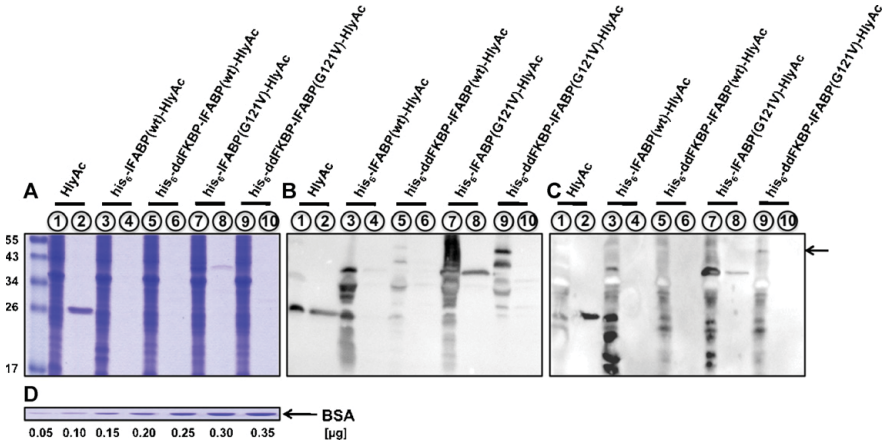

Fig. 2. Secretion experiments and analysis of whole cell extracts and supernatant samples. The arrow indicates the position of his_6–ddFKBP–IFABP(wt)–HlyAc and his_6–ddFKBP–IFABP(G121V)–HlyAc (54.0 kDa). (A) CBB staining, (B) and (C) western blott using a polyclonal antibody raised against HlyA or an antibody against a his-tag (Qiagen, Hilden). (D) SDS-PAGE gel of BSA with indicated amounts. Molecular weight markers with corresponding sizes are shown in (A). For pictures A–C, lanes are numbered from 1 to 10. Odd numbers: whole cell extracts (OD_{eq} = 0.1), even numbers: 16 µL cell-free supernatant.

3. Results

3.1. Slow-folding IFABP is secreted via the HlyA system

In a previous study, a fusion protein of wild-type MBP and HlyAc was not secreted, while slow-folding mutants of MalE were secretable with different efficiencies, indicating an inverse correlation between the folding rate and the secretion efficiency (Bakkes et al., 2010). However, MalE originates from *E. coli* and is a protein that is endowed with intrinsic properties for the translocation across membranes (Cover et al., 1987). Therefore, we challenged the HlyA secretion system with the eukaryotic rat intestinal fatty acid binding protein (IFABP), which is naturally localized in the cytoplasm (Hardy and Randall, 1991; Sweetser et al., 1987; Weiss et al., 1988). The pSOI-IFABP plasmids, encoding fusions of IFABP(wt) or IFABP(G121V) with HlyAc, were designed as described in Bakkes et al. (2010). His_6-IFABP(wt)-HlyAc and his_6–IFABP(G121V)–HlyAc (42.1 kDa) were produced intracellularly as shown by SDS-PAGE analysis and CBB staining. This was confirmed by western blotting using a polyclonal antibody against HlyA or the N-terminal his-tag of the proteins (see Fig. 2B and C, lanes 3 and 7). However, the wild-type IFABP fusion protein was not detected in the culture supernatant by CBB staining or western blots with the anti-his antibody, and the anti-HlyA antibody (Fig. 2A–C, lane 4 and Fig. 3). In striking contrast, the fusion protein of slow-folding IFABP(G121V) with HlyAc was secreted with good yields (Fig. 2A, lane 8 and Fig. 3). Remarkably, the secreted fusion protein could already be visualized by CBB staining without previous concentration of the sample. Nevertheless, TCA precipitated supernatants were analyzed by SDS-PAGE and CBB staining to highlight the purity of secreted IFABP(G121V) (see Fig. 3). Based on a comparison with known amounts of BSA (Fig. 2A, lane 8 with D), the amount of secreted his_6–IFABP(G121V)–HlyAc was quantified to be ~6 mg L^{-1} of culture corresponding to 2 mg/OD_{600}. Importantly, IFABP(G121V) was secreted as a soluble protein and no aggregation could be observed, which is in contrast to the cytoplasmic expression, which leads to insoluble inclusion bodies (Kim and Frieden, 1998).

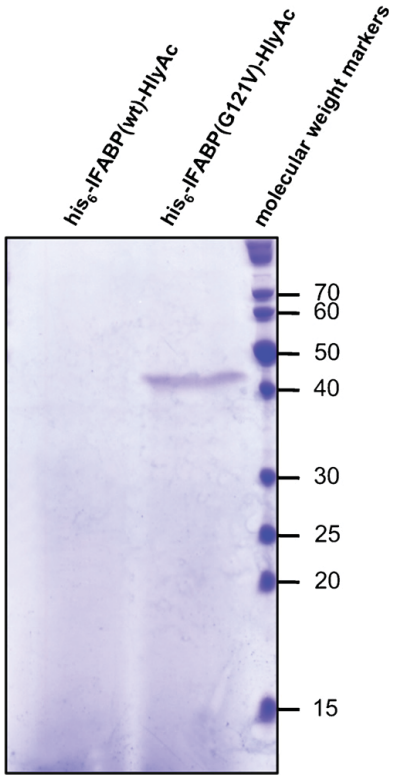

Fig. 3. TCA precipitation of supernatant samples. Cells carrying pK184-HlyBD and either pSOI-IFABP(wt) or pSOI-IFABP(G121V) were grown as described in Section 2 160 µL cell-free supernatant was TCA precipitated, the pellets were resolved, loaded on a SDS-PAGE gel and visualized with CBB. Molecular weight standards with corresponding masses are shown in the right panel.

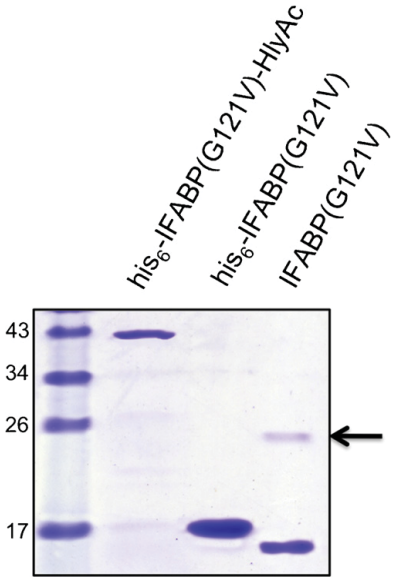

Fig. 4. SDS-PAGE analysis of the purification and the proteolytic digestion of secreted his_6–IFABP(G121V)–HlyAc fusion protein. His_6–IFABP(G121V)–HlyAc was eluted from an IMAC column (left lane), digested with Factor Xa to remove HlyAc and produce his_6–IFABP(G121V) (middle lane), and subsequently with the TEV protease (ProSpec) to remove the his_6-tag from secreted IFABP(G121V) (right lane). The arrow indicates the TEV protease (27 kDa), which was not entirely removed. Molecular weight markers with corresponding sizes are shown on the left.

3.2. ddFKBP does not promote secretion

The above results indicated that the folding rate of a protein dictates the secretion efficiency. Therefore, we were intrigued whether a "folding-destabilizer", such as ddFKBP, would result in secretion of wild-type IFABP-HlyAc in *E. coli*. Thus, ddFKBP was inserted behind the TEV protease cleavage site, at the N-terminus of IFABP(wt)–HlyAc and IFABP(G121V)–HlyAc, respectively. Full-length proteins (54.0 kDa) were expressed inside the cells since the N-terminal his_6-tag and HlyAc were both detectable by Western blot analysis of whole cell extracts (see Fig. 2B and C, lanes 5 and 9). However, the overall protein levels were reduced in the ddFKBP contexts when compared to the levels of proteins without ddFKBP. This suggests either a reduced expression rate or a ddFKBP-induced proteolysis. Also, IFABP WT was still not secreted (see Fig. 2, lane 6) and the secretion levels of IFABP(G121V)–HlyAc with the ddFKBP decreased (compare Fig. 2, lanes 8–10).

3.3. Purification and concentration of his_6–IFABP(G121V)–HlyAc in one step

For the separation of the his-tagged IFABP from the few impurities present in the culture medium (Mergulhao et al., 2005; Sandkvist and Bagdasarian, 1996), a one-step purification protocol was established. SDS-PAGE analysis (see Fig. 4) indicated the high purity of the eluted protein. In addition, the 260/280 ratio between 0.57 and 0.60 (data not shown) is in good agreement with the theoretical ratio of 0.57 for pure proteins (Glasel, 1995) and suggests the absence of RNA or DNA impurities in the protein sample. In summary, 1 mg of pure and homogenous his_6–IFABP(G121V)–HlyAc could be obtained from a 1 L bacterial cell culture.

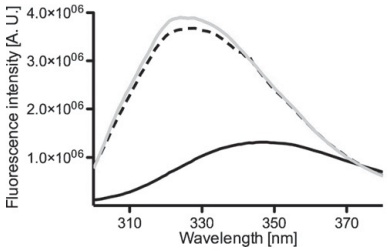

Fig. 5. Intrinsic tryptophan fluorescence measurements of IFABP G121V. The proteins (0.5 μM) were excitated with a wavelength of 290 nm and the fluorescence was recorded between 300 and 380 nm. The fluorescence maximum of IFABP G121V in 6 M urea is at 346 nm, whereas the maximum shifts towards 326 nm in buffer without urea. The emission spectrum of secreted his_6–IFABP(G121V) superimposes with IFABP G121V in buffer without urea, indicating a folded state. Dashed line: IFABP G121V purified from inclusion bodies in buffer without urea; black line: IFABP G121 V purified from inclusion bodies in buffer with 6 M urea; grey line: his_6–IFABP(G121V) in buffer without urea.

3.4. Removal of HlyAc and the his_6-tag to generate IFABP(G121V)

In addition to the proteins of interest (wild-type IFABP or IFABP (G121V)), the constructed plasmids encode the C-terminal fragment HlyAc (23 kDa), an N-terminal his_6-tag and two specific protease cleavage sites for the TEV protease and factor Xa (see Fig. 1). Therefore, passenger proteins can be separated from HlyAc by a proteolytic digestion with factor Xa. His_6–IFABP(G121V)–HlyAc was incubated with factor Xa (NEB) and the flow-through of an anion-exchange chromatography contained pure, cleaved his_6–IFABP(G121V) (see Fig. 4). The his_6-tag was removed with the TEV protease. However, the TEV protease could not be removed quantitatively (see Fig. 4).

3.5. Folding and substrate binding activity of his_6–IFABP(G121V)–HlyAc, his_6–IFABP(G121V) and IFABP(G121V)

In this study, we investigated the folding state of secreted IFABP(G121V) by intrinsic tryptophan fluorescence spectroscopy and compared it with the IFABP G121V purified from inclusion bodies. The emission spectrum of IFABP G121V in 6 M urea showed a maximum at 346 nm. In buffer without urea, the emission intensity significantly increased and the maximum shifted to 326 nm, which is in line with previous studies (see Fig. 5) (Li and Frieden, 2007). Secreted his_6–IFABP(G121V) exhibited the same emission spectrum as IFABP G121V from inclusion bodies without urea. Similar results were obtained for his_6–IFABP(G121V)–HlyAc. However, the emission spectrum was slightly influenced by the presence of HlyAc (data not shown). These data indicate that secreted IFABP(G121V) is folded comparable to the protein purified from inclusion bodies.

Next, we investigated the binding activity of secreted IFABP(G121V) in titration experiments with the fatty acid analog 11-(dansylamino)undecanoic acid (DAUDA). The fluorescence increase at 500 nm upon binding was monitored as described before (see Fig. 6) (Kim and Frieden, 1998; Wilkinson and Wilton, 1986). Fluorescence was corrected for the IFABP concentrations (100 nM) with the "receptor correction equation" (see Section 2). For a validation of the experimental setup, IFABP G121V was purified directly from inclusion bodies and the binding of DAUDA was measured. The determined dissociation constant (K_D) of 126 nM ± 7 nM is, within experimental errors, identical to the published data for IFABP G121V (120 nM ± 25 nM; see Table 2) (Kim and Frieden, 1998). The K_D value of secreted his_6–IFABP(G121V)–HlyAc (see Fig. 6 and Table 2) was determined to be 195 nM ± 13 nM, which is in the same range. As a control, HlyAc without fused

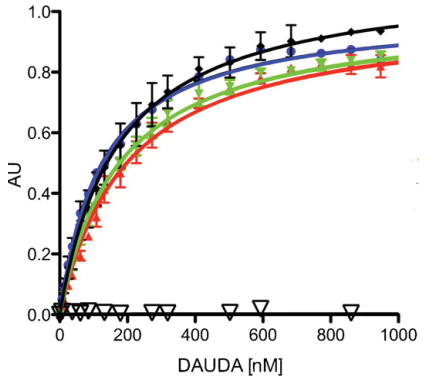

Fig. 6. Fluorescence titration plots using DAUDA, a fluorescence fatty acid analog. All of the IFABP variants share a similar binding curve and similar K_D values for the DAUDA binding, whereas HlyAc does not bind (see also Table 2). Corrected and normalized signals were plotted against the DAUDA concentration, and the solid line represents the fit employing a 1:1 binding-site model corecting for the protein concentration (see Section 2) with the program Prism 5. All plots represent two independent measurements with the error representing the standard deviation. Blue: IFABP G121V purified, refolded from inclusion bodies, red: his_6–IFABP(G121V)–HlyAc, green: his_6–IFABP(G121V), black: IFABP(G121V), open-triangles: HlyAc.

Table 2
Summary of the dissociation constants of the DAUDA/IFAB complexes used in this study. Data were analyzed as described in Section 2.

Protein	Dissociation constant (K_D)
IFABP G121V (Kim and Frieden, 1998)	120 ± 25 nM
IFABP G121V (out of IB)	126 ± 7 nM
His_6–IFABP(G121V)–HlyAc	195 ± 13 nM
His_6–IFABP(G121V)	174 ± 9 nM
IFABP(G121V)	138 ± 11 nM
HlyAc	No binding

IFABP was used under identical experimental conditions, and no binding of DAUDA was detected (see Fig. 6, open triangles). Nevertheless, a possible influence of HlyAc and the his_6-tag onto the binding behavior of IFABP was investigated. After proteolysis and subsequent purification of his_6–IFABP(G121V) and IFABP(G121V), respectively (see Fig. 4), the titration experiments were repeated. The K_D values of his_6–IFABP(G121V) without HlyAc and the K_D value of IFABP(G121V) were measured to be 174 nM ± 9 nM and 138 nM ± 11 nM, respectively. Therefore, secreted IFABP(G121V) exhibits the same binding affinity for DAUDA as the mutant protein purified directly from inclusion bodies.

4. Discussion

Secretion of proteins to the culture medium exhibits many advantages compared to a conventional, cytoplasmic protein location. For example, proteolytic degradation by intracellular proteases is prevented, the formation of disulfide bonds is enhanced in the oxidative environment of the medium and the subsequent purification protocols are simplified due to less proteinogenic impurities in the medium. These features allow faster downstream processing in combination with lower production costs. Many improvements in the protein production via secretion have been made in the recent decades and numerous systems are already commercially exploited. However, the secretion efficiency of these systems depends on the combination of the host strain, the signal peptide and the target protein and needs to be optimized by trial-and-error approaches for each specific task (Yoon et al., 2010).

With the HlyA T1SS of Gram-negative bacteria, high yields of secreted proteins can be produced in principle, and only three proteins are required to catalyze the secretion. The efficiency in combination with the simplicity of the secretion apparatus make this system an attractive candidate for the biotechnological production or proteins (Blight and Holland, 1994). However, the most important application so far has been the presentation of heterologous antigens in live-attenuated bacterial vaccines (Gentschev et al., 2002). The biotechnological usage is still hampered by the fact that many fusion proteins are not or only poorly secreted (Blight and Holland, 1994; Holland et al., 1990). Bakkes et al. (2010) demonstrated that the rate of folding of the passenger MalE dictates the efficiency of the secretion with the HlyA T1SS. While wild-type MalE was virtually not secreted, slow-folding mutants of MalE were secreted in yields that directly correlated with the folding rate of the corresponding mutant. Although, such mutations are an interesting approach to convert a protein into a secretion-competent substrate, the identification of mutations, which affect the folding rate without interfering with the function, is likely to be a very time-consuming process. As an alternative to this approach, the destabilizing domain ddFKBP was investigated (Armstrong and Goldberg, 2007; Banaszynski et al., 2006; Herm-Gotz et al., 2007). Despite the intriguing rational behind this approach, the secretion of wild-type IFABP failed completely, and the secretion levels of slow-folding IFABP(G121V) decreased, ruling out the applicability of the destabilizing domain.

MalE is an intrinsic *E. coli* protein designed for crossing a membrane. In this study, we wanted to expand the applicability of the system to a broader range of proteins. Indeed, we demonstrated that cytoplasmic, eukaryotic IFABP was not secreted when fused to HlyAc, whereas the fusion protein of the slow-folding IFABP G121V was secreted in yields of up to 6 mg L^{-1} cell culture. Nevertheless, the maximal secretion capacity of fusion proteins is not reached yet, as HlyAc alone without a passenger protein is secreted in much higher yields (see Fig. 2, lane 2).

Importantly, his_6–IFABP(G121V)–HlyAc was secreted as a soluble protein and no aggregation was observed, which is in clear contrast to IFABP G121V that forms inclusion bodies in *E. coli* (Kim and Frieden, 1998).

Moreover, we demonstrate that secreted IFABP(G121V) is capable of binding DAUDA with a binding affinity identical, within experimental error, to the protein produced from inclusion bodies (Kim and Frieden, 1998). This emphasizes the advantage of the T1SS, since a functional re-folding of proteins from inclusion bodies is often problematic and accounts for the major costs in the production of recombinant proteins in *E. coli* (Blight and Holland, 1994; Singh and Panda, 2005). Beneficially, the covalently linked HlyAc of the fusion protein has only a minor effect on the activity of IFABP(G121V), as indicated by a K_D value in the same range (see Table 2). In this study, wild-type IFABP could not be secreted as a fusion protein with HlyAc, indicating that the folding is too fast. In contrast, a single point mutation (G121V), which displays an approximately 100-fold reduced refolding rate (Chattopadhyay et al., 2002; Kim and Frieden, 1998), was secreted efficiently.

5. Conclusions

The results of this study further support our initial conclusion that the folding rate of a fusion protein dictates its secretion efficiency in T1SS. Not only bacterial proteins, targeted to the periplasmic space, can be designed to become a substrate of a T1SS, but also cytosolic, eukaryotic proteins. Furthermore, our data show that the described method results in the production of correctly folded, active protein in sufficient yields for biochemical studies. IFABP G121V is produced in inclusion bodies when expressed in

E. coli. The re-folding of denatured inclusion bodies, which accounts for the major costs in the production of recombinant proteins (Singh and Panda, 2005), can therefore be circumvented with this T1SS. In summary, our T1SS is a very attractive candidate for the biotechnological production of proteins via secretion into the extracellular space.

Acknowledgements

We acknowledge the assistance of Antonia Konczwald during the initial stages of the project. We thank Dr. Carl Frieden (Department of Biochemistry and Molecular Biophysics, Washington University School of Medicine, St. Louis, USA) for providing us with the genes IFABP WT and IFABP G121V. We thank the Ministry of Innovation, Science and Research of the German Federal State North Rhine-Westphalia (NRW) and the Heinrich Heine University Düsseldorf (scholarship from the CLIB Graduate Cluster Industrial Biotechnology to CKWS).

References

Armstrong, C.M., Goldberg, D.E., 2007. An FKBP destabilization domain modulates protein levels in *Plasmodium falciparum*. Nat. Methods 4, 1007–1009.
Bakkes, P.J., Jenewein, S., Smits, S.H., Holland, I.B., Schmitt, L., 2010. The rate of folding dictates substrate secretion by the *Escherichia coli* haemolysin type 1 secretion system. J. Biol. Chem. 285, 40573–40580.
Banaszynski, L.A., Chen, L.C., Maynard-Smith, L.A., Ooi, A.G., Wandless, T.J., 2006. A rapid, reversible, and tunable method to regulate protein function in living cells using synthetic small molecules. Cell 126, 995–1004.
Benabdelhak, H., Kiontke, S., Horn, C., Ernst, R., Blight, M.A., Holland, I.B., Schmitt, L., 2003. A specific interaction between the NBD of the ABC-transporter HlyB and a C-terminal fragment of its transport substrate haemolysin A. J. Mol. Biol. 327, 1169–1179.
Blight, M.A., Holland, I.B., 1994. Heterologous protein secretion and the versatile *Escherichia coli* haemolysin translocator. Trends Biotechnol. 12, 450–455.
Chattopadhyay, K., Zhong, S., Yeh, S.R., Rousseau, D.L., Frieden, C., 2002. The intestinal fatty acid binding protein: the role of turns in fast and slow folding processes. Biochemistry 41, 4040–4047.
Chervaux, C., Sauvonnet, N., Le Clainche, A., Kenny, B., Hung, A.L., Broome-Smith, J.K., Holland, I.B., 1995. Secretion of active beta-lactamase to the medium mediated by the *Escherichia coli* haemolysin transport pathway. Mol. Gen. Genet. 249, 237–245.
Chuang, S., Velkov, T., Horne, J., Porter, C.J., Scanlon, M.J., 2008. Characterization of the drug binding specificity of rat liver fatty acid binding protein. J. Med. Chem. 51, 3755–3764.
Cover, W.H., Ryan, J.P., Bassford Jr., P.J., Walsh, K.A., Bollinger, J., Randall, L.L., 1987. Suppression of a signal sequence mutation by an amino acid substitution in the mature portion of the maltose-binding protein. J. Bacteriol. 169, 1794–1800.
Crameri, A., Raillard, S.A., Bermudez, E., Stemmer, W.P., 1998. DNA shuffling of a family of genes from diverse species accelerates directed evolution. Nature 391, 288–291.
Crameri, A., Whitehorn, E.A., Tate, E., Stemmer, W.P., 1996. Improved green fluorescent protein by molecular evolution using DNA shuffling. Nat. Biotechnol. 14, 315–319.
Farinas, E.T., Bulter, T., Arnold, F.H., 2001. Directed enzyme evolution. Curr. Opin. Biotechnol. 12, 545–551.
Fernandez, L.A., Sola, I., Enjuanes, L., de Lorenzo, V., 2000. Specific secretion of active single-chain Fv antibodies into the supernatants of *Escherichia coli* cultures by use of the hemolysin system. Appl. Environ. Microbiol. 66, 5024–5029.
Gentschev, I., Dietrich, G., Goebel, W., 2002. The *E. coli* alpha-hemolysin secretion system and its use in vaccine development. Trends Microbiol. 10, 39–45.
Glasel, J.A., 1995. Validity of nucleic acid purities monitored by 260 nm/280 nm absorbance ratios. Biotechniques 18, 62–63.
Gray, L., Mackman, N., Nicaud, J.M., Holland, I.B., 1986. The carboxy-terminal region of haemolysin 2001 is required for secretion of the toxin from *Escherichia coli*. Mol. Gen. Genet. 205, 127–133.
Hardy, S.J., Randall, L.L., 1991. A kinetic partitioning model of selective binding of nonnative proteins by the bacterial chaperone SecB. Science 251, 439–443.
Herm-Gotz, A., Agop-Nersesian, C., Munter, S., Grimley, J.S., Wandless, T.J., Frischknecht, F., Meissner, M., 2007. Rapid control of protein level in the apicomplexan *Toxoplasma gondii*. Nat. Methods 4, 1003–1005.
Hess, J., Gentschev, I., Goebel, W., Jarchau, T., 1990. Analysis of the haemolysin secretion system by PhoA-HlyA fusion proteins. Mol. Gen. Genet. 224, 201–208.
Hinsa, S.M., Espinosa-Urgel, M., Ramos, J.L., O'Toole, G.A., 2003. Transition from reversible to irreversible attachment during biofilm formation by *Pseudomonas fluorescens* WCS365 requires an ABC transporter and a large secreted protein. Mol. Microbiol. 49, 905–918.
Holland, I.B., Kenny, B., Steipe, B., Pluckthun, A., 1990. Secretion of heterologous proteins in *Escherichia coli*. Methods Enzymol. 182, 132–143.
Holland, I.B., Schmitt, L., Young, J., 2005. Type 1 protein secretion in bacteria, the ABC-transporter dependent pathway. Mol. Membr. Biol. 22, 29–39.
Jarchau, T., Chakraborty, T., Garcia, F., Goebel, W., 1994. Selection for transport competence of C-terminal polypeptides derived from *Escherichia coli* hemolysin: the shortest peptide capable of autonomous HlyB/HlyD-dependent secretion comprises the C-terminal 62 amino acids of HlyA. Mol. Gen. Genet. 245, 53–60.
Kenny, B., Chervaux, C., Holland, I.B., 1994. Evidence that residues −15 to −46 of the haemolysin secretion signal are involved in early steps in secretion, leading to recognition of the translocator. Mol. Microbiol. 11, 99–109.
Kenny, B., Haigh, R., Holland, I.B., 1991. Analysis of the haemolysin transport process through the secretion from *Escherichia coli* of PCM, CAT or beta-galactosidase fused to the Hly C-terminal signal domain. Mol. Microbiol. 5, 2557–2568.
Kim, K., Frieden, C., 1998. Turn scanning by site-directed mutagenesis: application to the protein folding problem using the intestinal fatty acid binding protein. Protein Sci. 7, 1821–1828.
Letoffe, S., Ghigo, J.M., Wandersman, C., 1994. Secretion of the *Serratia marcescens* HasA protein by an ABC transporter. J. Bacteriol. 176, 5372–5377.
Li, H., Frieden, C., 2007. Observation of sequential steps in the folding of intestinal fatty acid binding protein using a slow folding mutant and ^{19}F NMR. Proc. Natl. Acad. Sci. U.S.A. 104, 11993–11998.
Linggood, M.A., Ingram, P.L., 1982. The role of alpha haemolysin in the virulence of *Escherichia coli* for mice. J. Med. Microbiol. 15, 23–30.
Mackman, N., Baker, K., Gray, L., Haigh, R., Nicaud, J.M., Holland, I.B., 1987. Release of a chimeric protein into the medium from *Escherichia coli* using the C-terminal secretion signal of haemolysin. EMBO J. 6, 2835–2841.
Meier, R., Drepper, T., Svensson, V., Jaeger, K.E., Baumann, U., 2007. A calcium-gated lid and a large beta-roll sandwich are revealed by the crystal structure of extracellular lipase from *Serratia marcescens*. J. Biol. Chem. 282, 31477–31483.
Mergulhao, F.J., Summers, D.K., Monteiro, G.A., 2005. Recombinant protein secretion in *Escherichia coli*. Biotechnol. Adv. 23, 177–202.
Park, E.C., Finley, D., Szostak, J.W., 1992. A strategy for the generation of conditional mutations by protein destabilization. Proc. Natl. Acad. Sci. U.S.A. 89, 1249–1252.
Rowland, A., Knights, K.M., Mackenzie, P.I., Miners, J.O., 2009. Characterization of the binding of drugs to human intestinal fatty acid binding protein (IFABP): potential role of IFABP as an alternative to albumin for in vitro–in vivo extrapolation of drug kinetic parameters. Drug Metab. Dispos. 37, 1395–1403.
Sanchez-Magraner, L., Viguera, A.R., Garcia-Pacios, M., Garcillan, M.P., Arrondo, J.L., de la Cruz, F., Goni, F.M., Ostolaza, H., 2007. The calcium-binding C-terminal domain of *Escherichia coli* alpha-hemolysin is a major determinant in the surface-active properties of the protein. J. Biol. Chem. 282, 11827–11835.
Sandkvist, M., Bagdasarian, M., 1996. Secretion of recombinant proteins by Gram-negative bacteria. Curr. Opin. Biotechnol. 7, 505–511.
Singh, S.M., Panda, A.K., 2005. Solubilization and refolding of bacterial inclusion body proteins. J. Biosci. Bioeng. 99, 303–310.
Stanley, P., Koronakis, V., Hughes, C., 1991. Mutational analysis supports a role for multiple structural features in the C-terminal secretion signal of *Escherichia coli* haemolysin. Mol. Microbiol. 5, 2391–2403.
Sweetser, D.A., Heuckeroth, R.O., Gordon, J.I., 1987. The metabolic significance of mammalian fatty-acid-binding proteins: abundant proteins in search of a function. Annu. Rev. Nutr. 7, 337–359.
Thanabalu, T., Koronakis, E., Hughes, C., Koronakis, V., 1998. Substrate-induced assembly of a contiguous channel for protein export from *E. coli*: reversible bridging of an inner-membrane translocase to an outer membrane exit pore. EMBO J. 17, 6487–6496.
Weiss, J.B., Ray, P.H., Bassford Jr., P.J., 1988. Purified secB protein of *Escherichia coli* retards folding and promotes membrane translocation of the maltose-binding protein in vitro. Proc. Natl. Acad. Sci. U.S.A. 85, 8978–8982.
Wilkinson, T.C., Wilton, D.C., 1986. Studies on fatty acid-binding proteins. The detection and quantification of the protein from rat liver by using a fluorescent fatty acid analogue. Biochem. J. 238, 419–424.
Yoon, S.H., Kim, S.K., Kim, J.F., 2010. Secretory production of recombinant proteins in *Escherichia coli*. Recent Pat. Biotechnol. 4, 23–29.

3.4. Chapter IV - Secretion of slow-folding proteins by a Type 1 secretion system

Title Secretion of slow-folding proteins by a Type 1 secretion system

Authors Christian K. W. Schwarz, Michael H.H. Lenders, Sander H. J. Smits and Lutz Schmitt

Published in *Bioengineered* (2012)

Impact factor not available

Own proportion of this work 20 %;
Writing of the manuscript.

ARTICLE ADDENDUM

Bioengineered 3:5, 289–292; September/October 2012; © 2012 Landes Bioscience

Secretion of slow-folding proteins by a Type 1 secretion system

Christian K.W. Schwarz, Michael H.H. Lenders, Sander H.J. Smits and Lutz Schmitt*

Institute of Biochemistry; Heinrich-Heine-Universität Düsseldorf; Düsseldorf, Germany

Protein production through dedicated secretion systems might offer an potential alternative to the conventional cytoplasmical expression. The application of Type 1 secretion systems of Gram-negative bacteria, however, where often not successful in the past for a wide range of proteins. Recently, two studies using the *E. coli* maltose binding protein (MalE) and the rat intestinal fatty acid binding protein (IFABP) revealed a rational to circumvent these limitations. Here, wild-type passenger proteins were not secreted, while folding mutants with decreased folding kinetics were efficiently exported to the extracellular space. Subsequently, an one-step purification protocol yielded homogeneous and active protein. Taken together, theses two studies suggest that the introduction of slow-folding mutations into a protein sequence might be the key to use Type 1 secretion systems for the biotechnological production of proteins.

Keywords: type 1 secretion, HlyB, protein folding, mutation, relaxation, IFABP, maltose, western blot

Submitted: 03/27/12

Revised: 05/09/12

Accepted: 05/10/12

http://dx.doi.org/10.4161/bioe.20712

*Correspondence to: Lutz Schmitt; Email: lutz.schmitt@hhu.de

Addendum to: Schwarz CK, Landsberg CD, Lenders MH, Smits SH, Schmitt L. Using an *E. coli* Type 1 secretion system to secrete the mammalian, intracellular protein IFABP in its active form. J Biotechnol 2012; 159:155–61; PMID:22366493; http://dx.doi.org/10.1016/j.jbiotec.2012.02.005.

Introduction

Type 1 secretion systems (T1SS) of Gram-negative bacteria transport substrates directly form the cytoplasm to the exterior without the formation of any periplasmic intermediate. The substrate spectrum contains functional unrelated and different-sized proteins, i.e., the hemophore HasA (19 kDa) and the lipase LipA (65 kDa) of *Serratia marcescens*[1,2] or the 900 kDa protein LapA that is involved in biofilm formation of *Pseudomonas fluorescence*.[3] A transport machinery composed of two inner membrane proteins, a membrane fusion protein (MFP) and an ATP-binding-cassette (ABC) transporter, as well as an outer membrane factor (OMF) catalyzes the secretion process.[4,5] The paradigm of T1SS is the hemolysin A (HlyA) secretion system of *Escherichia coli* (*E. coli*), which consists of the ABC transporter hemolysin B (HlyB), the MFP hemolysin D (HlyD) and the multi-functional TolC (OMF).[6] TolC is recruited, upon interaction of the substrate (HlyA) with HlyB and HlyD, and a continuous export channel is formed bridging the cytoplasm directly to the exterior.[4,7]

HlyA and other T1SS substrates are suggested to be transported in an unfolded state[8] and folding is triggered by binding of Ca^{2+} ions to so-called GG repeats in the extracellular space, directly after transport. Previously, several proteins were successfully secreted as fusion proteins with a 23 kDa C-terminal fragment of HlyA (HlyAc), for example β-lactamase or antibody fragments.[9-12] However, many proteins could not be secreted limiting the exploitation of the T1SS pathway for biotechnological purposes.[9] Recently, two publications investigated these limitations.[8,13] Here, the maltose binding protein (MalE) and the intestinal fatty acid binding protein (IFABP) could initially not be secreted when fused to HlyAc. However, the use of slow-folding proteins with decreased folding kinetics allowed the secretion into the culture medium.[8,13] Interestingly, the mutant IFABP(G121V), accumulates in *E. coli* as inclusion bodies, whereas secreted IFABP(G121V) was soluble and active. Taken together, both studies suggest a rational to secrete proteins of interest in good yields and in a soluble, functional state with an *E. coli* T1SS. However, the successful application requires proteins with slow-folding kinetics and the identification of such mutants might hamper the general applicability

of the approach. In other words, the general application of this approach requires screening of protein libraries that contain random mutations generated by, for example, error-prone PCR. This should be performed with suitable activity assays that allow a simple read-out to identifiy secreted and moreover, active proteins.

Secretion of a Functional Cytoplasmic Protein

The HlyA T1SS was investigated for its applicability to secrete an eukaryotic cytoplasmic protein, the rat intestinal fatty acid binding protein (IFABP).[15] IFABP is a 131 residue (15 kDa) cytoplasmical protein, which belongs to the family of fatty acid binding proteins in mammals and binds a single molecule of fatty acids.[16] The binding to lipophilic drugs, for example, is used for the prediction of drug pharmacokinetic parameters in vitro.[17,18] The slow-folding mutant IFBAP G121V still binds fatty acids with high affinity (K_D = 120 nM ± 25 nM) and is currently produced in *E. coli* out of inclusion bodies.[19]

Both, wild-type IFABP and the slow-folding variant IFABP(G121V), were cloned inside a secretion vector in front of HlyAc. In the background of the T1SS, wild-type IFABP(wt)-HlyAc was not secreted into the medium of the *E. coli* culture, whereas IFABP(G121V)-HlyAc was secreted in good yields of up to 6 mg per liter cell culture (corresponding to 2 mg/OD). The secreted fusion protein could even be visualized by Coommassie brilliant blue (CBB) staining in the supernatant without concentrating the sample. Interestingly, the secreted fusion protein was soluble and stable in the culture medium and during the subsequent purification steps, which displays an advantage compared with its currently expressed form being insoluble inclusion bodies.[19]

Bakkes et al. demonstrated the secretion of a slow-folding mutant of MalE. The passenger MalE with two introduced slow-folding mutations was secreted and shown to be active in binding to amylose, although the major fraction did not bind to the ligand.[14] The reason for this behavior, however, was not investigated. Therefore, Schwarz et al. investigated the folding state and the activity of secreted IFABP in more detail and compared it with published results. The folding state of secreted IFABP(G121V) was studied by intrinsic tryptophane fluorescence spectroscopy and compared with IFABP(G121V), which was purified out of cytosolic inclusion bodies and refolded.[20] These studies indicated that secreted IFABP(G121V) was folded comparable to the reference protein. Since the folding state of a protein does not directly imply that the protein is active, the activity of secreted IFABP(G121V) was analyzed. The fatty acid analog 11-(dansylamino) undecanoic acid (DAUDA) was used for titration experiments to determine the binding activity of IFABP(G121V). For the validation of the experimental setup, the binding affinity of the reference protein IFABP(G121V) (non-secreted control) was examined by fluorescence spectroscopy. The determined dissociation constant (K_D) of 126 nM ± 7 nM is in line with the published data (120 nM ± 25 nM).[19] The K_D value of secreted IFABP(G121V)-HlyAc was determined to be 195 nM ± 13 nM. This is in the same range as the K_D for the non-secreted control demonstrating that secreted IFABP G121V exhibits similar binding parameters.

Unfolding Domains—Useful Tools for Secretion?

The major bottleneck of this secretion technology is its dependency on slow-folding proteins. As an alternative route to directed evolution appoaches (see below), a destabilizing domain was analyzed to transfer instability to the fusion proteins. The destabilizing domain ddFKBP, an engineered version of the human FKBP12, was used, which was already applied successfully in eukaryotes to destabilize fused proteins,[21-24] however, no studies were performed in bacteria so far. Schwarz et al. investigated, whether the ddFKBP destabilizes fusion proteins in *E. coli* and if this domain allows the secretion of proteins via the T1SS without the introduction of slow-folding mutations. The ddFKBP was fused N-terminally to HlyAc, IFABP(wt)-HlyAc and IFABP(G121V)-HlyAc, respectively. All protein constructs were expressed as indicated by CBB staining and western blot analysis of whole cell extracts. Obviously, ddFKBP did not increase secretion levels of the fusion constructs. These results indicate that the intrinsic folding state of HlyAc, IFABP(wt) and IFABP(G121V) is not changed drastically and that the ddFKBP does not facilitate the secretion of a protein of interest with the T1SS. This raises the question whether the ddFKBP transmits instability to fused proteins or induces their degradation in bacteria?

Engineering of Proteins with Slow Folding Characteristics

The successful secretion of proteins via the HlyA T1SS depends on the availability of slow-folding mutants. Besides wild-type proteins with slow-folding kinetics, many proteins fold too quickly inside cells, which hampers the general applicability of T1SS. Up to now, the a priori prediction and alteration of folding properties is impossible with biochemical, computational or bioinformatical approaches. Nevertheless, directed evolution methods are available to generate proteins with desired characteristics, i.e., altered folding characteristics.[25,26] Basically, this can be performed within three relatively easy experimental steps (see **Fig. 1**).

Step 1 represents the random mutagenesis of the wild-type protein of interest (POI_*wt*). Various methods are available to mutate the gene, which are summarized in, for example Wong et al.[27] The mutagenesis products are inserted inside the secretion plasmid in front of the secretion signal (HlyAc) DNA sequence. This results in a library of mutated POI (POI_*mut*) fusion proteins. *E. coli* cells are transformed with the plasmid library together with the plasmid encoding the T1SS complex (Step 2) and obtained colonies are analyzed in secretion experiments (Step 3). Since the secretion signal is localized at the C-terminal end of the fusion protein, only full-length fusion proteins will be secreted; fusion proteins with artificial stop codons introduced via the error prone PCR reaction are not secreted and thereby automatically eliminated from the screen. Mutations that do not alter the folding kinetics will not be secreted either.

However, proteins with slow-folding kinetics can be detected, by SDS-PAGE analysis of the culture supernatants. Staining of the gels or immunochemical detection visualizes the secreted proteins and allows the densometrical quantification of secreted proteins. A great advantage is that the amount of secreted protein is inversely correlated with the folding rate of the protein. In other words, the protein secreted most efficiently will have the slowest folding kinetics. Furthermore, supernatant samples can be used immediately for enzyme-linked activity or immunosorbent assays (ELISA). If such an activity of the POI can be visualized, the secretion system enables high-throughput screening of a vast pool of mutants. For example, the lipolytic activity of secreted lipases can be visualized on agar plates, which contain the appropiate substrate of the lipase.[28] In summary, the technology described in Schwarz et al. represents a valuable and novel tool, usable for various experimental setups, for example, the generation of folding mutants allowing secretion and subsequently the screening of secreted proteins with improved characteristics which are interesting within the biotechnological area.

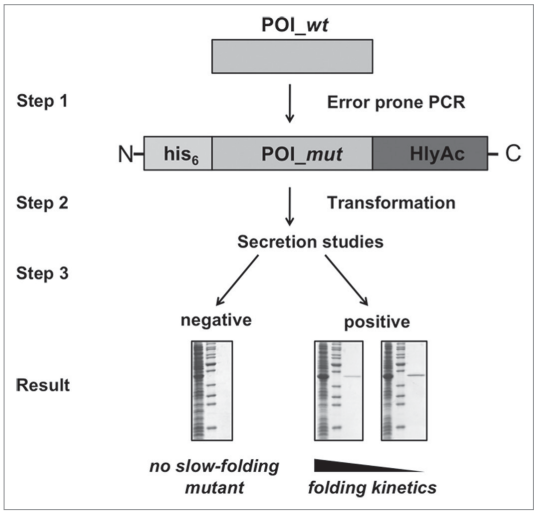

Figure 1. Identification of slow-folding mutants employing an *E. coli* T1SS. Scheme of the three-step protocol for the generation of slow-folding mutants of a protein of interest. Step 1: random mutation of a POI_wt sequence and insertion of the resulting POI_mut in front of HlyAc. Step 2: transformation of *E. coli* cells with the generated plasmid library in combination with the plasmid encoding the T1SS components. Step 3: small-scale secretion studies to identify clones that secrete fusion proteins. The plasmids of secretion-positive clones are subsequently sequenced to identify the corresponding slow-folding mutations. If available, agar plate assays might be used to test the activity of these secreted proteins (see text).

Acknowledgments

We are indebted to Diana Clausnitzer, Protein Production Facility, of the Heinrich Heine University, for valuable discussion during the cloning of the constructs. We thank the Ministry of Innovation, Science and Research of the German Federal State North Rhine-Westphalia (NRW) and the Heinrich Heine University Düsseldorf (scholarship from the CLIB Graduate Cluster Industrial Biotechnology to C.K.W.S. and scholarship from the Biostruct NRW Graduate School to M.H.H.L.).

References

1. Meier R, Drepper T, Svensson V, Jaeger KE, Baumann U. A calcium-gated lid and a large beta-roll sandwich are revealed by the crystal structure of extracellular lipase from *Serratia marcescens*. J Biol Chem 2007; 282:31477-83; PMID:17728256; http://dx.doi.org/10.1074/jbc.M704942200.
2. Létoffé S, Ghigo JM, Wandersman C. Secretion of the *Serratia marcescens* HasA protein by an ABC transporter. J Bacteriol 1994; 176:5372-7; PMID:8071214.
3. Hinsa SM, Espinosa-Urgel M, Ramos JL, O'Toole GA. Transition from reversible to irreversible attachment during biofilm formation by *Pseudomonas fluorescens* WCS365 requires an ABC transporter and a large secreted protein. Mol Microbiol 2003; 49:905-18; PMID:12890017; http://dx.doi.org/10.1046/j.1365-2958.2003.03615.x.
4. Thanabalu T, Koronakis E, Hughes C, Koronakis V. Substrate-induced assembly of a contiguous channel for protein export from *E. coli*: reversible bridging of an inner-membrane translocase to an outer membrane exit pore. EMBO J 1998; 17:6487-96; PMID:9822594; http://dx.doi.org/10.1093/emboj/17.22.6487.
5. Holland IB, Schmitt L, Young J. Type 1 protein secretion in bacteria, the ABC-transporter dependent pathway (review). Mol Membr Biol 2005; 22:29-39; PMID:16092522; http://dx.doi.org/10.1080/09687860500042013.
6. Jarchau T, Chakraborty T, Garcia F, Goebel W. Selection for transport competence of C-terminal polypeptides derived from *Escherichia coli* hemolysin: the shortest peptide capable of autonomous HlyB/HlyD-dependent secretion comprises the C-terminal 62 amino acids of HlyA. Mol Gen Genet 1994; 245:53-60; PMID:7531275; http://dx.doi.org/10.1007/BF00279750.
7. Benabdelhak H, Kiontke S, Horn C, Ernst R, Blight MA, Holland IB, et al. A specific interaction between the NBD of the ABC-transporter HlyB and a C-terminal fragment of its transport substrate haemolysin A. J Mol Biol 2003; 327:1169-79; PMID:12662939; http://dx.doi.org/10.1016/S0022-2836(03)00204-3.
8. Bakkes PJ, Jenewein S, Smits SH, Holland IB, Schmitt L. The rate of folding dictates substrate secretion by the *Escherichia coli* hemolysin type 1 secretion system. J Biol Chem 2010; 285:40573-80; PMID:20971850; http://dx.doi.org/10.1074/jbc.M110.173658.
9. Blight MA, Holland IB. Heterologous protein secretion and the versatile *Escherichia coli* haemolysin translocator. Trends Biotechnol 1994; 12:450-5; PMID:7765544; http://dx.doi.org/10.1016/0167-7799(94)90020-5.
10. Fernández LA, Sola I, Enjuanes L, de Lorenzo V. Specific secretion of active single-chain Fv antibodies into the supernatants of *Escherichia coli* cultures by use of the hemolysin system. Appl Environ Microbiol 2000; 66:5024-9; PMID:11055959; http://dx.doi.org/10.1128/AEM.66.11.5024-9.2000.
11. Chervaux C, Sauvonnet N, Le Clainche A, Kenny B, Hung AL, Broome-Smith JK, et al. Secretion of active beta-lactamase to the medium mediated by the *Escherichia coli* haemolysin transport pathway. Mol Gen Genet 1995; 249:237-45; PMID:7500946; http://dx.doi.org/10.1007/BF00290371.
12. Mackman N, Baker K, Gray L, Haigh R, Nicaud JM, Holland IB. Release of a chimeric protein into the medium from *Escherichia coli* using the C-terminal secretion signal of haemolysin. EMBO J 1987; 6:2835-41; PMID:3119330.
13. Schwarz CK, Landsberg CD, Lenders MH, Smits SH, Schmitt L. Using an *E. coli* Type 1 secretion system to secrete the mammalian, intracellular protein IFABP in its active form. J Biotechnol 2012; 159:155-61; PMID:22366493; http://dx.doi.org/10.1016/j.jbiotec.2012.02.005.

14. Bakkes PJ, Jenewein S, Smits SH, Holland IB, Schmitt L. The rate of folding dictates substrate secretion by the *Escherichia coli* hemolysin type 1 secretion system. J Biol Chem 2010; 285:40573-80; PMID:20971850; http://dx.doi.org/10.1074/jbc.M110.173658.
15. Sweetser DA, Heuckeroth RO, Gordon JI. The metabolic significance of mammalian fatty-acid-binding proteins: abundant proteins in search of a function. Annu Rev Nutr 1987; 7:337-59; PMID:3300738; http://dx.doi.org/10.1146/annurev.nu.07.070187.002005.
16. Veerkamp JH, Peeters RA, Maatman RG. Structural and functional features of different types of cytoplasmic fatty acid-binding proteins. Biochim Biophys Acta 1991; 1081:1-24; PMID:1991151.
17. Chuang S, Velkov T, Horne J, Porter CJ, Scanlon MJ. Characterization of the drug binding specificity of rat liver fatty acid binding protein. J Med Chem 2008; 51:3755-64; PMID:18533710; http://dx.doi.org/10.1021/jm701192w.
18. Rowland A, Knights KM, Mackenzie PI, Miners JO. Characterization of the binding of drugs to human intestinal fatty acid binding protein (IFABP): potential role of IFABP as an alternative to albumin for in vitro-in vivo extrapolation of drug kinetic parameters. Drug Metab Dispos 2009; 37:1395-403; PMID:19398502; http://dx.doi.org/10.1124/dmd.109.027656.
19. Kim K, Frieden C. Turn scanning by site-directed mutagenesis: application to the protein folding problem using the intestinal fatty acid binding protein. Protein Sci 1998; 7:1821-8; PMID:10082380; http://dx.doi.org/10.1002/pro.5560070818.
20. Li H, Frieden C. Observation of sequential steps in the folding of intestinal fatty acid binding protein using a slow folding mutant and 19F NMR. Proc Natl Acad Sci USA 2007; 104:11993-8; PMID:17615232; http://dx.doi.org/10.1073/pnas.0705253104.
21. Banaszynski LA, Chen LC, Maynard-Smith LA, Ooi AG, Wandless TJ. A rapid, reversible and tunable method to regulate protein function in living cells using synthetic small molecules. Cell 2006; 126:995-1004; PMID:16959577; http://dx.doi.org/10.1016/j.cell.2006.07.025.
22. Armstrong CM, Goldberg DE. An FKBP destabilization domain modulates protein levels in *Plasmodium falciparum*. Nat Methods 2007; 4:1007-9; PMID:17994030; http://dx.doi.org/10.1038/nmeth1132.
23. Herm-Götz A, Agop-Nersesian C, Münter S, Grimley JS, Wandless TJ, Frischknecht F, et al. Rapid control of protein level in the apicomplexan *Toxoplasma gondii*. Nat Methods 2007; 4:1003-5; PMID:17994029; http://dx.doi.org/10.1038/nmeth1134.
24. Park EC, Finley D, Szostak JW. A strategy for the generation of conditional mutations by protein destabilization. Proc Natl Acad Sci USA 1992; 89:1249-52; PMID:1311090; http://dx.doi.org/10.1073/pnas.89.4.1249.
25. Crameri A, Whitehorn EA, Tate E, Stemmer WP. Improved green fluorescent protein by molecular evolution using DNA shuffling. Nat Biotechnol 1996; 14:315-9; PMID:9630892; http://dx.doi.org/10.1038/nbt0396-315.
26. Crameri A, Raillard SA, Bermudez E, Stemmer WP. DNA shuffling of a family of genes from diverse species accelerates directed evolution. Nature 1998; 391:288-91; PMID:9440693; http://dx.doi.org/10.1038/34663.
27. Wong TS, Roccatano D, Zacharias M, Schwaneberg U. A statistical analysis of random mutagenesis methods used for directed protein evolution. J Mol Biol 2006; 355:858-71; PMID:16325201; http://dx.doi.org/10.1016/j.jmb.2005.10.082.
28. Eom GT, Song JK, Ahn JH, Seo YS, Rhee JS. Enhancement of the efficiency of secretion of heterologous lipase in *Escherichia coli* by directed evolution of the ABC transporter system. Appl Environ Microbiol 2005; 71:3468-74; PMID:16000750; http://dx.doi.org/10.1128/AEM.71.7.3468-74.2005.
29. Farinas ET, Bulter T, Arnold FH. Directed enzyme evolution. Curr Opin Biotechnol 2001; 12:545-51; PMID:11849936; http://dx.doi.org/10.1016/S0958-1669(01)00261-0.

3.5. Chapter V - Directionality of substrate translocation of the hemolysin A Type I secretion system

Title Directionality of substrate translocation of the hemolysin A Type I secretion system

Authors Michael H. H. Lenders, Stefanie Weidtkamp-Peters, Diana Kleinschrodt, Karl-Erich Jaeger, Sander H. J. Smits and Lutz Schmitt

Published in *Scientific Reports* (2015)

Impact factor 5.578

Own proportion of this work 60 %;
Construction of the plasmids, competition secretion assay, immunofluorescence labeling of formaldehyde treated cells, confocal laser scanning microscopy and image processing, writing of the manuscript.

www.nature.com/scientificreports

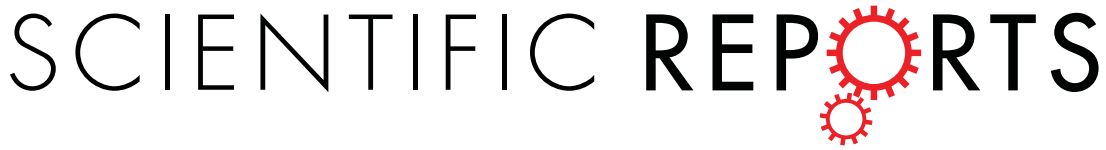

OPEN

Directionality of substrate translocation of the hemolysin A Type I secretion system

Received: 25 March 2015
Accepted: 25 June 2015
Published: 27 July 2015

Michael H. H. Lenders[1], Stefanie Weidtkamp-Peters[2], Diana Kleinschrodt[3], Karl-Erich Jaeger[4,5], Sander H. J. Smits[1] & Lutz Schmitt[1,5]

Type 1 secretion systems (T1SS) of Gram-negative bacteria are responsible for the secretion of various proteases, lipases, S-layer proteins or toxins into the extracellular space. The paradigm of these systems is the hemolysin A (HlyA) T1SS of *Escherichia coli*. This multiple membrane protein complex is able to secrete the toxin HlyA in one step across both *E. coli* membranes. Common to all secreted T1SS substrates is a C-terminal secretion sequence being necessary as well as sufficient for secretion. However, it is not known whether transport occurs directionally, i.e. the N- or the C-terminus of T1SS substrates is secreted first. We have addressed this question by constructing HlyA fusions with the rapidly folding eGFP resulting in a stalled T1SS. Differential labeling and subsequent fluorescence microscopic detection of C- and N-terminal parts of the fusions allowed us to demonstrate vectorial transport of HlyA through the T1SS with the C-terminus appearing first outside the bacterial cells.

Gram-negative bacteria transport a broad range of compounds ranging from small molecules to intact proteins into the extracellular space. Transport occurs *via* dedicated cellular nanomachineries either directly from the cytoplasm to the extracellular space or *via* periplasmic intermediates. Among these nanomachineries, type 1 secretion systems (T1SS) adopt the most simple architecture consisting of an ATP-binding cassette (ABC) transporter and a membrane fusion protein (MFP) located in the inner membrane and an outer membrane protein (OMP). In the presence of the substrate, they form a continuous tripartite channel reaching directly from the cytoplasm into the extracellular space[1,2]. The secretion of substrates occurs in one step across both, the inner and outer membrane of Gram-negative bacteria, without a periplasmic intermediate.

T1SS substrates include adenylate cyclases, lipases, proteases, surface layer proteins and toxins. They vary in size from relatively small proteins such as the hemophore HasA (19 kDa, 188 amino acids) from *S. marescens* to large proteins of approximately 900 kDa (8682 amino acids) such as the adhesion factor LapA from *P. fluorescence*[3–5]. These secreted proteins have in common that the information for secretion is encoded within the 50–60 C-terminal amino acids that were shown to be essential and sufficient for the secretion process[6–10]. This is in contrast to other protein translocation systems localized in the inner membrane such as the Sec system where the secretion signal is localized at the N-terminus[11] and cleaved during translocation by a dedicated peptidase.

The most prominent substrates of T1SS are the repeats in toxin (RTX) proteins (Supplementary Fig. 1). They are characterized by glycine-rich repeats (GG repeats) located in the C-terminal part of the

[1]Institute of Biochemistry, Heinrich-Heine-Universitaet, D-40225 Duesseldorf, Germany. [2]Center for Advanced Imaging (CAi), Heinrich-Heine-Universitaet, D-40225 Duesseldorf, Germany. [3]Protein Production Facility, Heinrich-Heine-Universitaet, 40225 Duesseldorf, Germany. [4]Institute of Molecular Enzyme Technology, Heinrich-Heine-Universitaet and Institute of Bio- and Geosciences IBG-1: Biotechnology, Forschungszentrum Juelich GmbH, D-52426 Juelich, Germany. [5]Center of Excellence on Plant Sciences (CEPLAS), Heinrich-Heine-Universitaet, D-40225 Duesseldorf, Germany. Correspondence and requests for materials should be addressed to L.S. (email: Lutz.Schmitt@hhu.de)

respective protein upstream of the secretion signal. The consensus sequence of the GG repeats forming the RTX domain[12] of these proteins is GGxGxDxUx, where x can be any amino acid and U is a large or hydrophobic amino acid[13]. The number of these repeats depends on the size of the secreted protein and they are in general separated by number of amino acids, totaling on average 6–12 kDa within the RTX domain[13,14]. The GG repeats bind calcium thereby promoting folding of the secreted substrate[15]. Since the level of calcium is low (approximately 300 nM) in the cytosol of *E. coli*, but high (up to 10 mM) in the extracellular space[16], it is generally assumed that T1SS substrates adopt their final, folded conformation only after secretion into the extracellular space[16].

One of the best-characterized T1SS substrates is the pore forming RTX toxin hemolysin A (HlyA). HlyA is an alpha toxin, consisting of 1024 amino acids with a molecular weight of 110 kDa. Six consensus GG repeats are present within the RTX domain of HlyA[14]. The HlyA specific T1SS consists of the ABC transporter hemolysin B (HlyB), the MFP hemolysin D (HlyD) and the endogenously expressed OMP, TolC. HlyA is transported in one step from the cytoplasm to the extracellular space[2]. It has been demonstrated that the secretion signal of HlyA initiates secretion and is responsible for the assembly of the T1SS complex. HlyA is secreted in an unfolded state[17] and its secretion signal contains all information necessary for secretion since it can be secreted alone[7]. High levels of secretion were also obtained with a fragment consisting of the 218 C-terminal amino acids of HlyA (HlyAc) containing three GG repeats and the secretion signal[17].

Importantly, the orientation of the substrate during secretion is currently not known. The question arises whether directionality of secretion exists and if so, whether the N- or C-terminus of HlyA is translocated first through the T1SS. In general, at least two possibilities exist for the passage of the substrate through a T1SS. Since HlyB interacts with the secretion signal of HlyA with its nucleotide-binding domain[18], one could envision that such binding to the nucleotide-binding domains of HlyB or to the cytoplasmic part of HlyD[19] would stabilize the C-terminal part of the HlyA in the vicinity of the translocon. Furthermore, the so-called C39 peptidase -like domain (CLD) at the N-terminus of HlyB interacts with the substrate *via* binding of the RTX region of HlyA to facilitate secretion in some way[20]. This interaction might stabilize the interaction of the inner membrane components of the T1SS with the RTX domain and the secretion sequence providing further support for the idea that the N-terminal part enters the translocation channel first, with the final release of the C-terminal of HlyA into the translocon to complete translocation.

On the other hand C-terminal directed secretion might also be envisaged since many heterologous passenger proteins fused at their C-terminus to a C-terminal fragment of HlyA (containing the secretion signal) are secreted[17,21–24]. Intuitively, one would expect that the secretion process can only start after translation of the secretion signal. Since all fusion proteins have only the C-terminal secretion signal in common, one could envisage that the C-terminal part of these fusion proteins is secreted first. However, these two alternatives have not been addressed experimentally so far.

Here, we describe that a fusion of the enhanced Green Fluorescence Protein (eGFP) to the N-terminus of HlyAc stalled in the HlyA T1SS, presumably due to the fast folding properties of eGFP with a refolding half-time of 90.6 s[25]. Apparently, the eGFP-HlyAc fusion protein is fixed and stably oriented within the translocator *in vivo*. We only observed the N-terminal fragment within the cytoplasm whereas the C-terminal fragment was exclusively detected at the cell surface. Our results clearly demonstrate the presence of directionality during secretion with the C-terminal secretion sequence transported first. Our data further suggest that the secretion sequence is responsible for inserting the substrate into the T1SS.

Results

Stalling the T1SS with fast folding proteins. The secretion signal of HlyA is essential and sufficient for secretion of HlyA by its cognate T1SS[22,26,27]. HlyAc, a truncated version of HlyA containing the 218 C-terminal amino acids including the secretion signal, is secreted in high amounts comparable to full-length HlyA when expressed simultaneously with the inner membrane components HlyB and HlyD[17,23,24,28]. Interestingly, if HlyAc is fused to the C-terminus of, for example, the maltose binding protein (MBP), secretion is completely abolished. However, secretion can be restored with MBP fusion proteins that contain mutations reducing the folding rates[17]. Similar behavior has been observed for the Has secretion system where only unfolded HasA could be exported by its cognate ABC transporter, whereas the presence of folded cytosolic HasA resulted in an inhibition of secretion of its unfolded isoform[29]. This led to the conclusion that T1SS substrates, including HlyA, are transported in an unfolded state. This assumption is in line with the fact that calcium ions are required for folding of HlyA, which is prevented in the cytoplasm due to the low concentration of calcium ions[16,30,31]. These data suggest that HlyAc fusion to a fast folding passenger could block the translocator resulting in a stalled T1SS. If so this should allow us to address the question whether, with such a stalled intermediate, the secretion signal localized inside the cytosol, inside the translocation machinery or on the extracellular side.

In order to confirm that such a stalled intermediate does indeed form, we performed a competition experiment, in which HlyAc as well as an eGFP-HlyAc fusion were expressed in combination with the inner membrane components of the T1SS. Genes encoding both proteins, HlyAc and eGFP-HlyAc, were present on the same plasmid, but their expression could be induced independently of each other (further details are provided in material and methods).

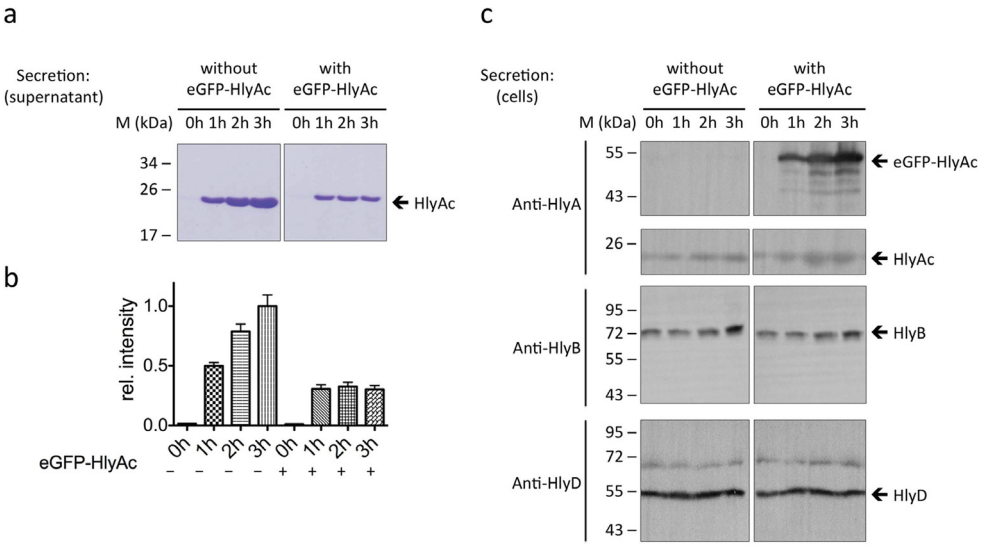

Figure 1. The eGFP-HlyAc fusion protein stalls the translocator and prevents HlyAc secretion. (**a**) SDS-PAGE analysis of the HlyAc secretion level (with Coomassie blue staining) in the culture supernatant over time without and with induction of eGFP-HlyAc expression. (**b**) Relative intensity of the SDS-PAGE bands illustrates HlyAc secretion levels without and with induction of eGFP-HlyAc. (**c**) Western blot analysis of the cells (comparison with the supernatants in (**a**)) show that eGFP-HlyAc is only present in the induced cells and that the levels of HlyB and HlyD remain constant over time.

Upon expression of the T1SS and both proteins, HlyAc and eGFP-HlyAc, a drastic reduction of the secretion levels of HlyAc was observed already after one hour of expression (Fig. 1a), clearly indicating competitive inhibition of HlyAc by the fusion protein. Quantification of the Coomassie stained protein bands normalized to the signal with the highest intensity, suggested that the amount of HlyAc in the supernatant was reduced to 30% when eGFP-HlyAc was co-expressed (Fig. 1b). The amount of secreted HlyAc in the presence of eGFP-HlyAc remained constant over time (Fig. 1b). This strongly suggests competition between the expressed HlyAc and eGFP-HlyAc consistent with stalling of the translocon by the latter already within the first hour, leading to substantially reduced amounts of secreted HlyAc.

The presence of intracellular eGFP-HlyAc was confirmed by Western blot analysis with a polyclonal HlyA antibody (Fig. 1c). The data show that the amount of cytosolic eGFP-HlyAc increased throughout incubation following induction of expression and furthermore, HlyAc was also detected within the cells. Thus, a direct comparison of the amounts of HlyAc and eGFP-HlyAc is possible. In cells expressing only the T1SS and HlyAc, the amount of cytosolic HlyAc remained constant over time whereas HlyAc accumulated in cells co-expressing eGFP-HlyAc and HlyAc (Fig. 1c). This observation indicates that eGFP-HlyAc has stalled the T1SS and secretion of HlyAc is blocked.

Western blot analysis confirmed as found in all subsequent experiments that the expression levels of HlyB and HlyD remained similar throughout incubation (Fig. 1c) and were not affected by expression of proteins to be secreted.

T1SS is stalled only in the presence of the secretion signal. Previous studies showed that the C-terminal located secretion signal of HlyA is crucial and necessary for secretion[23,32]. To analyze its role for stalling the secretion machinery, we engineered an eGFP-HlyAc fusion protein lacking the secretion signal (i.e. with the C-terminal 60 residues deleted) designated eGFP-HlyAc-Δss (Supplementary Fig. 4). A competition experiment (Fig. 2a) with independently induced expression of HlyAc and eGFP-HlyAc-Δss revealed that in the presence of HlyB and HlyD, now an inhibition of secretion of HlyA, did not occur. In contrast to the results shown in Fig. 1, the co-expression of HlyAc and eGFP-HlyAc-Δss in the presence of HlyB and HlyD did not result in a detectable reduction of the secretion levels of HlyAc with equal amounts of secreted HlyAc after three hours in the two experimental set-ups (Fig. 2b). Western blot analysis confirmed that the T1SS target protein eGFP-HlyAc-Δss as well as the corresponding transporter proteins HlyB and HlyD were expressed at a similar level under both experimental conditions (Fig. 2c).

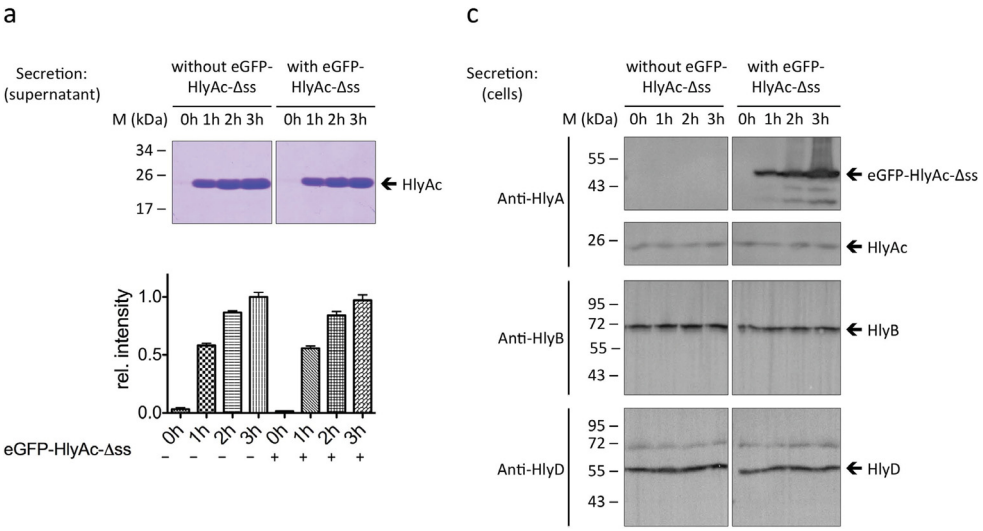

Figure 2. The eGFP-HlyAc-Δss fusion protein is unable to block the translocator. (**a**) SDS-PAGE analysis of the HlyAc secretion level in the culture supernatant over time without and with induction of eGFP-HlyAc-Δss expression. (**b**) Relative intensity of the SDS-PAGE bands illustrates the HlyAc secretion levels without and with induction of eGFP-HlyAc-Δss. (**c**) Western blot analysis of the cells (correlating to the supernatants in (**a**)) show that eGFP-HlyAc-Δss is only present in the induced cells and that the level of HlyB and HlyD remain constant over time.

The HlyAc fragment of the fusion protein is exposed on the cell surface accessible to HlyA antibody. The secretion signals of HlyA as well as of other T1SS substrates are localized at the extreme C-terminus. The competition experiments described above demonstrated that the HlyA secretion signal is also required for stalling the secretion machinery. To address the question, whether the C- or the N-terminal of the fusion appears first on the surface, we took advantage of the eGFP fluorescence (Supplementary Fig. 5). This fluorescence allowed the detection of the eGFP part of the fusion protein, while the HlyAc part can be visualized *via* an HlyA specific antibody in combination with a secondary antibody that harbors the fluorophore Cy3 resulting in a red fluorescence.

If the N-terminus is transported first, intrinsic eGFP fluorescence but no red fluorescence should be detectable extracellularly because the Cy3-labeled second antibody can only bind to the HlyA specific first antibody if part of HlyAc has exited the TolC component of the translocon to the exterior. In contrast, if the C-terminal part of the fusion protein is transported first, one would detect red fluorescence in combination with the green fluorescence derived from intracellular eGFP.

E. coli cells containing a stalled T1SS were analyzed with confocal laser scanning microscopy (CLSM). Cells expressing only HlyB and HlyD, but lacking the eGFP-HlyAc encoding plasmid were used to determine the cellular autofluorescence (Fig. 3, top row). The expression of HlyB and HlyD was confirmed by Western blots analysis (Supplementary Fig. 6).

Next, we analyzed cells producing HlyB, HlyD and eGFP-HlyAc. CLSM images confirmed that both eGFP as well as Cy3 fluorescence was detected (Fig. 3, second row). The eGFP fluorescence signal was found homogenously distributed within the cells, although sometimes accumulating at the cell poles and the Cy3 fluorescence signal also appeared evenly distributed over the cells. Due to the limited optical resolution of CLSM, the localization of both proteins could not be analyzed more precisely.

The eGFP fluorescence in cells expressing the different constructs was quantified by normalization of eGFP intensity values to the fluorescence intensities measured with cells expressing HlyB, HlyD and eGFP-HlyAc (Fig. 4a, left bar).

The Cy3 fluorescence of cells expressing HlyB, HlyD and eGFP-HlyAc reflected the presence of HlyA antibodies bound to the cell surface and Cy3 fluorescence intensity values were normalized to this value (Fig. 4b, left bar).

As a control, cells expressing eGFP-HlyAc, but not HlyB and HlyD, were also analyzed. The CLSM images confirmed that eGFP fluorescence could be detected in the cytosol of cells (Fig. 3, third row). Quantification of the eGFP and Cy3 fluorescence demonstrated that eGFP fluorescence was approximately

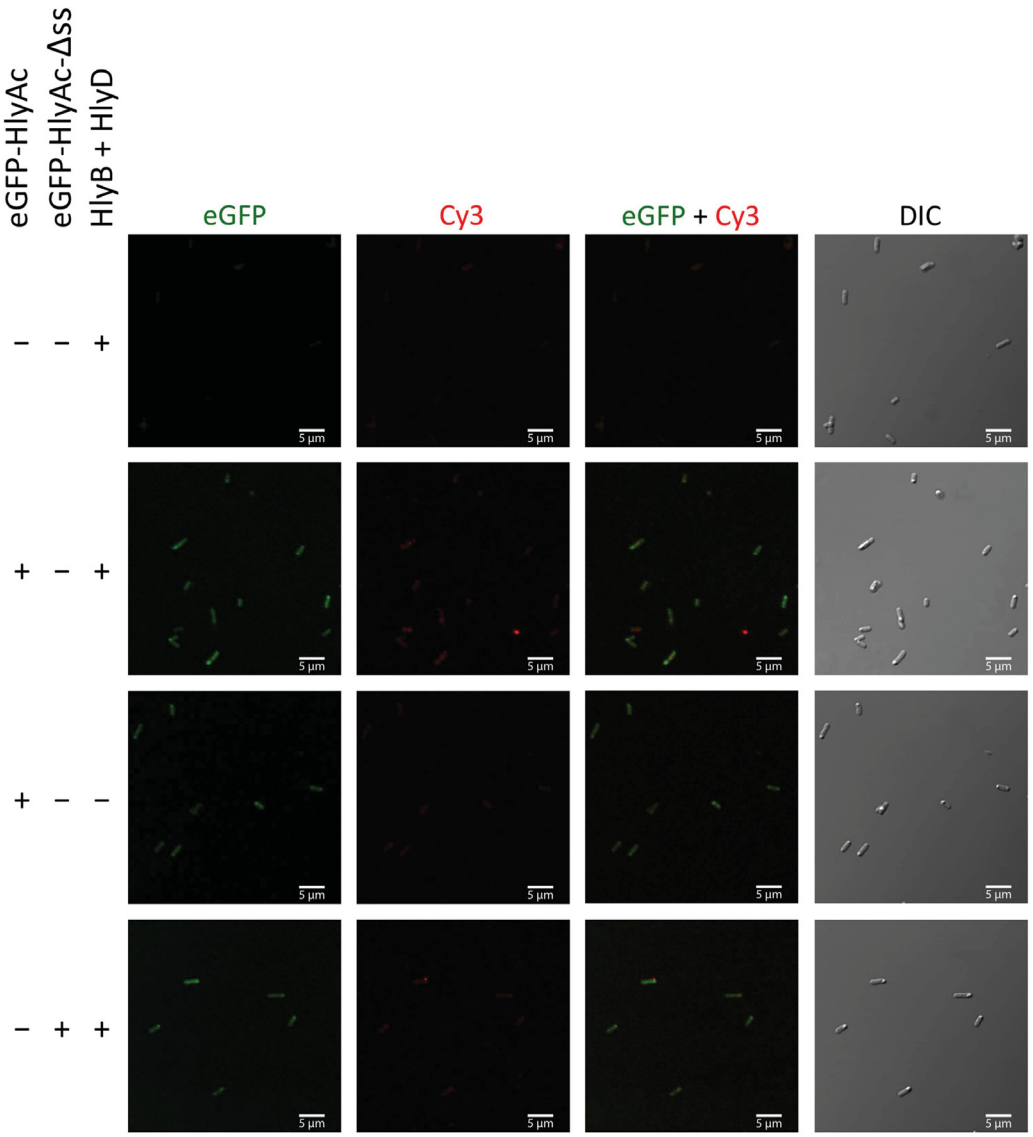

Figure 3. Detection of the surface exposed HlyAc fragment of eGFP-HlyAc by confocal laser scanning microscopy. *E. coli* cells expressed HlyB and HlyD, as well as additional eGFP-HlyAc and eGFP-HlyAc-Δss. Shown is the eGFP fluorescence (left panel) of the fusion proteins, the HlyA mediated Cy3 fluorescence at the cell surface (second left panel), merged images of eGFP and Cy3 fluorescence (second right panel) and differential interference contrast (DIC) images of the cells (right panel). The different combinations of proteins employed are indicated to the left.

88 ± 5.5% as compared to cells expressing the eGFP-HlyAc fusion protein (Fig. 4a, middle bar) whereas almost no Cy3 fluorescence could be detected (8 ± 2.8%, Fig. 4b, middle bar).

The competitive secretion assay with eGFP-HlyAc-Δss revealed that the secretion signal was needed for stalling of the translocator. Accordingly, cells expressing eGFP-HlyAc-Δss, HlyB and HlyD were analyzed by CLSM confirming that eGFP fluorescence was detected in the cytosol (Fig. 3, fourth row). eGFP

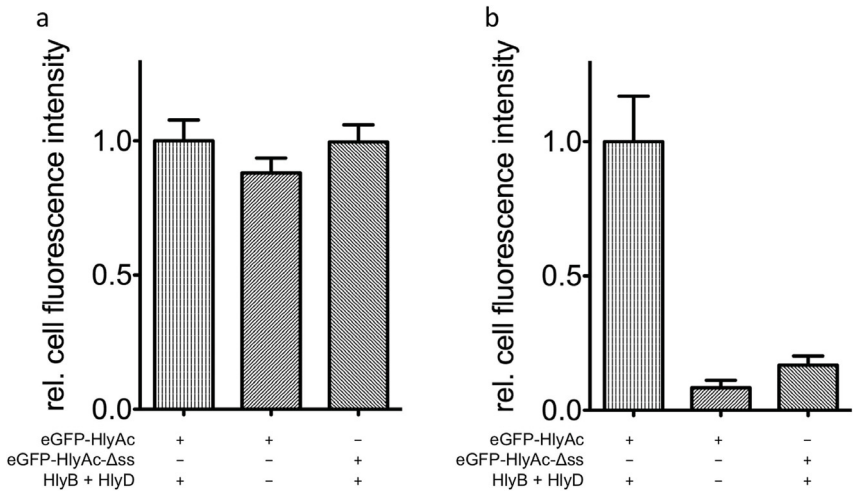

Figure 4. (**a**) Relative cell fluorescence of eGFP. All values were normalized to the eGFP fluorescence of the eGFP-HlyAc fusion protein (error bars represent the standard error of the mean) after subtraction of autofluorescence. (**b**) Relative fluorescence of Cy3. All values are normalized to Cy3 fluorescence of the eGFP-HlyAc fusion protein (error bars represent the standard error of the mean) after subtraction of autofluorescence. The different combinations of proteins employed are indicated below the bars.

fluorescence is approximately $100 \pm 6.3\%$ compared to cells expressing the eGFP-HlyAc fusion protein (Fig. 4a, right bar) and only $17 \pm 3.4\%$ of Cy3 fluorescence in comparison to cells expressing HlyB, HlyD and eGFP-HlyAc was detected (Fig. 4b, right bar).

In summary, these results demonstrate that the eGFP-HlyAc fusion protein is specifically orientated during secretion. The constructs used here allow the assignment of the N-terminal eGFP fluorescence to the cytosol, whereas the C-terminal part of the fusion protein harboring the HlyAc fragment is exposed at the cell surface and accessible to antibody.

Analysis of the secretion of full-length eGFP-HlyA. Next, cells expressing HlyB, HlyD and a fusion protein of eGFP and full-length HlyA (eGFP-HlyA) were analyzed. Due to the fast folding of eGFP, the eGFP-HlyA fusion should not be secreted and should also stall the T1SS.

CLSM images confirmed that eGFP and Cy3 fluorescence were observed (Fig. 5, first row). Quantification of the eGFP and Cy3 fluorescence intensities of the cells demonstrated that the eGFP fluorescence was approximately $103 \pm 6.8\%$ (Fig. 6a, second bar on the left) compared to cells that expressed the eGFP-HlyAc fusion protein (Fig. 6a, first bar from the left). Localization of eGFP fluorescence appeared identical to cells expressing the eGFP-HlyAc fusion together with HlyB and HlyD (Fig. 3, second row) confirming that the eGFP part of the fusion protein is localized in the cytoplasm. Cy3 fluorescence reflecting the binding of anti-HlyA antibody at the cell surface was ten times higher (Fig. 6b, second bar from the left) than Cy3 fluorescence of cells expressing eGFP-HlyAc (Fig. 6b, first bar from the left). Obviously, the full-length Hly A provides many more epitopes for binding of the polyclonal HlyA antibody than the HlyAc. Furthermore, staining revealed a heterogeneous distribution of HlyA protein showing accumulations on the cell surface. This result confirmed that the C-terminal portion of eGFP-HlyA is exposed on the cell surface.

These results clearly indicate that a fusion protein consisting of eGFP and full-length HlyA was recognized and transported by the T1SS. However, secretion was stalled with a high probability with eGFP detected in the cytoplasm as shown by the corresponding eGFP fluorescence signal. In control experiments either with cells not expressing the translocator components of the inner membrane (Fig. 5, second row) or eGFP-HlyA-Δss, HlyB and HlyD (Fig. 5, third row) greatly reduces levels of the C-terminal HlyA fragment were detected on the cell surface as indicated by specific Cy3 fluorescence resulting from binding of the HlyA antibody.

To gain more detailed insights into the cellular localization of the HlyA constructs we applied Structured illumination microscopy (SIM) to eGFP-HlyAc and eGFP-HlyA samples. To improve the optical resolution in SIM a grid pattern is repeatedly projected into the image plane in different orientations to produce interference patterns with sample structures. In a post-processing step a high-resolution image of the underlying structures can be generated using a computer algorithm. Under optimal conditions the lateral resolution in the resulting image is two times better than in a conventional confocal

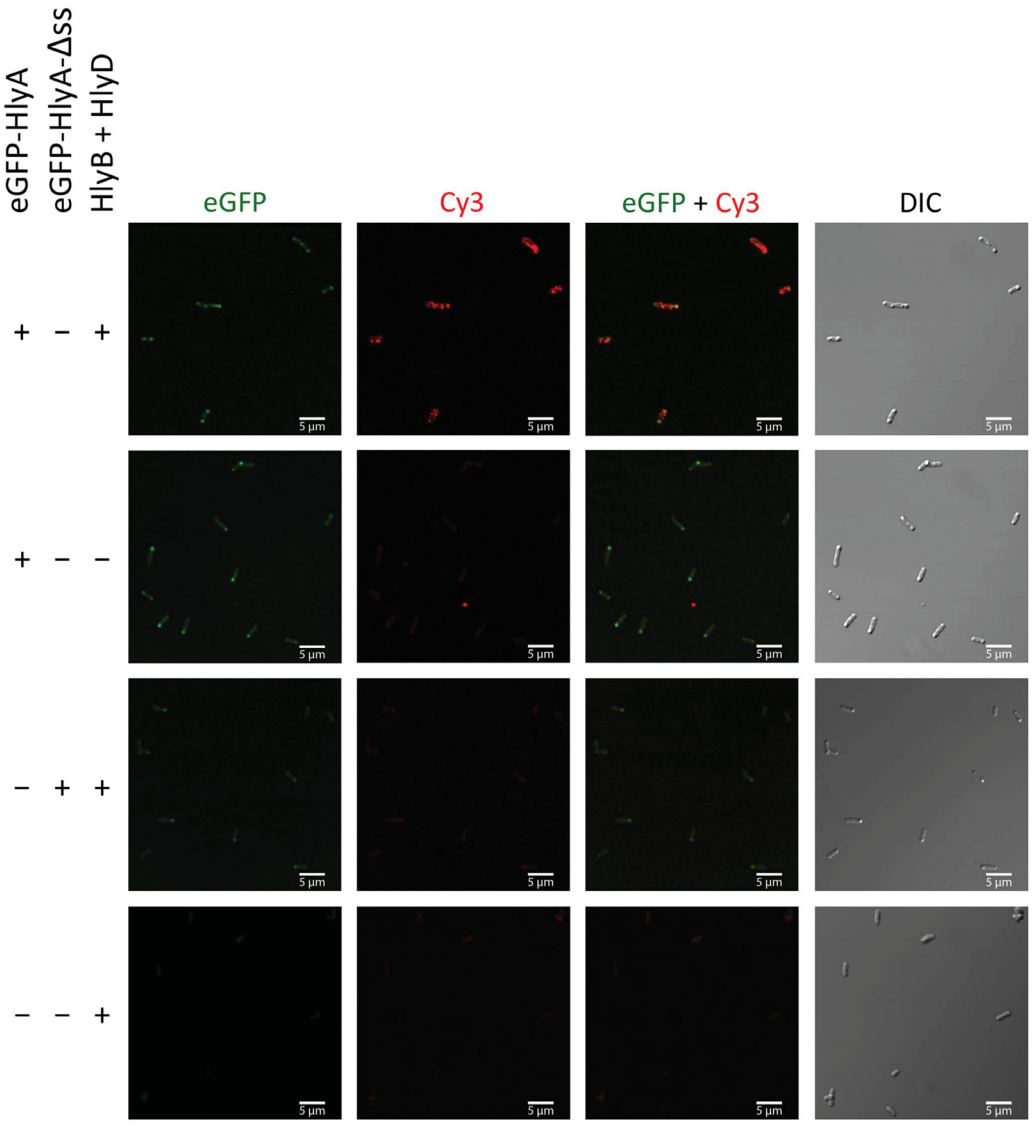

Figure 5. Detection of the surface exposed HlyA fragment of eGFP-HlyA by confocal laser scanning microscopy. *E. coli* cells expressed HlyB and HlyD, as well as additional eGFP-HlyAc and eGFP-HlyAc-Δss, respectively. Shown is the eGFP fluorescence (left panel) of the fusion proteins, the HlyA mediated Cy3 fluorescence at the cell surface (second left panel), merged images of eGFP and Cy3 fluorescence (second right panel) and differential interference contrast (DIC) images of the cells (right panel). The different combinations of proteins tested are indicated to the left.

image[33]. As expected, Cy3 fluorescence was detected at the cell surface of cells expressing HlyB, HlyD and eGFP-HlyAc (Fig. 7, first row) and of cells expressing HlyB, HlyD and eGFP-HlyA (Fig. 7, second row) oriented in a distinct helical pattern. Also, wide field microscopy of eGFP fluorescence confirmed its cytosolic localization. Merged eGFP and Cy3 fluorescence signals further emphasized the extracellular localization of the Cy3 fluorescence, while the eGFP fluorescence was clearly localized in the cytoplasm (Fig. 7).

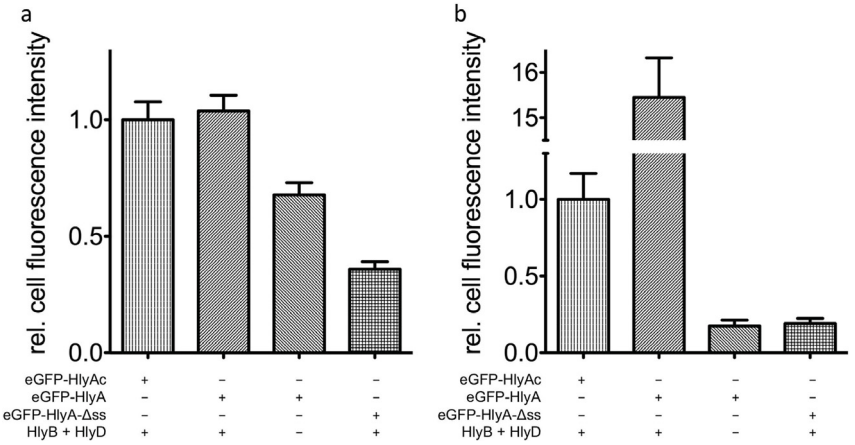

Figure 6. (**a**) Relative cell fluorescence of eGFP. All values were normalized to the eGFP fluorescence of the eGFP-HlyAc fusion protein (error bars represent the standard error of the mean) after subtraction of autofluorescence. (**b**) Relative fluorescence of Cy3. All values are normalized to Cy3 fluorescence of the eGFP-HlyAc fusion protein (error bars represent the standard error of the mean) after subtraction of autofluorescence. The different combinations of proteins employed are indicated below the bars.

Discussion

Recent experiments demonstrated that substrates of T1SS are secreted in an unfolded manner[17]. This observation is in line with geometrical restraints, since the interior diameter of TolC is maximally 20 Å[34]. Thus, assuming an average helical diameter of 12 Å, TolC could accommodate only a single α-helix. Consequently, substrates must enter the translocation machinery with their N- or C-terminus first, but a hairpin insertion is highly unlikely. Our experiments indeed demonstrated that fusion proteins of eGFP with HlyAc or HlyA stalled the T1SS, and furthermore, indicated that their C-terminal parts were exposed on the cell surface, while the N-terminal eGFP was always located in the cytosol in a folded state as deduced from its intrinsic fluorescence.

As show in the competition secretion assay the amount of HlyAc in the supernatant was reduced to 30% when eGFP-HlyAc was co-expressed (Fig. 2b). This suggests a competition between the expressed HlyAc and eGFP-HlyAc for free T1SS. In the first hour HlyAc is able to pass the cell membranes by the free T1SS and remain stable in the supernatant. After an hour the eGFP-HlyAc fusion protein blocks all T1SS and HlyAc is not able to secrete anymore. The level of HlyAc in the supernatant remains constant over the complete secretion time and contains only the stable HlyAc that was secreted in the beginning.

These results obviously raise the question whether the observed directionality of secretion represents a universal feature of T1SS. The inner membrane components of the ABC transporter can be divided in three different protein families defined by the presence or absence of additional domains. These families are ABC transporters with (I) C39 peptidase domains, (II) CLD domains, corresponding to an inactive peptidase which lack protease activity[20] and (III) transporters without any additional domains[20,35]. Transporters with an authentic C39 peptidase domain transport rather small substrates ($<$10 kDa) that belong mainly to the bacteriocin family containing a cleavable N-terminal leader peptide for secretion (Supplementary Fig. 1). Due to the cleavable, N-terminal leader sequence and the fact that these systems are also present in Gram-positive bacteria, we shall exclude family (I) from our discussion.

Transporters with a CLD transport larger substrates ($>$55 kDa) that are all members of the RTX toxin family[20,35]. The RTX toxins have their secretion signals located at the C terminus (50–60 C-terminal amino acids) together with GG repeats located close to the secretion signal (Supplementary Fig. 1) that promote active folding of the secreted protein by binding of calcium ions in the extracellular medium[15].

An example for transporters without any additional domains is the hemophore transporter HasD of *Serratia marcescens*[4,36]. Here, the C-terminal secretion signal is not cleaved during transport, but HasA, like other substrates of this family, does not contain conserved GG repeats (Supplementary Fig. 1). Instead, HasA appears to contain so-called primary recognition sites scattered throughout the protein and the secretion of HasA is dependent on SecB[36,37]; a feature that was not observed for substrates belonging to the RTX protein family[17].

From an energetic point of view, the initial appearance of GG repeats at the cell surface following translocation would allow binding of calcium ions thereby inducing folding of the secreted part of the protein. This process we propose would pull the protein through the T1SS[13] and, in parallel, prevent back sliding into the secretion machinery because a tertiary structure would be formed which is larger in size

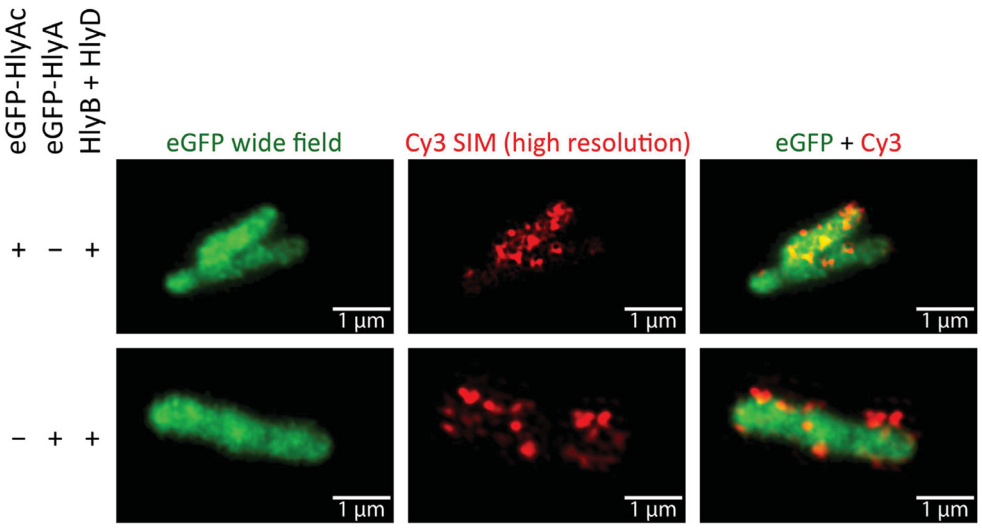

Figure 7. Detection of the surface exposed HlyA fragment of eGFP-HlyAc and eGFP-HlyA by structured illumination microscopy. Shown are maximum intensity projections of z-stacks of representative *E. coli* cells expressing eGFP-HlyAc or eGFP-HlyA together with HlyB and HlyD. The eGFP fluorescence (left panel in green) is displayed in wide field mode, the HlyA signal (medium panel in red) is displayed in high resolution mode after SIM processing. The right panel shows merged images derived from eGFP and Cy3 fluorescence recordings.

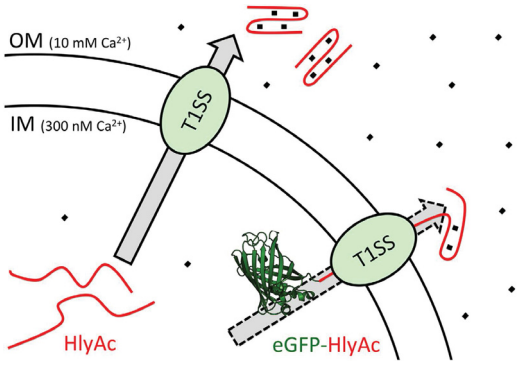

Figure 8. Model for secretion by the T1SS. The T1SS is indicated by an oval box and the substrate, here HlyA, is depicted as a red line, while eGFP is shown in green (pdb file 2Y0G). HlyAc is secreted (indicated by the grey arrow) and folds in the extracellular space due to the higher calcium concentration. eGFP-HlyAc can only enter the T1SS but is not able to complete the secretion process (indicated by the dotted grey arrow) due to the fast folding of eGFP and stalling inside the translocator. The model also assumes that cell surface exposed HlyAc fragment of the fusion protein folds due to the higher extracellular calcium concentration. Calcium ions are indicted by small black boxes. For further details see text.

than the maximal diameter of TolC (20 Å). This leads to the assumption that the C-terminus of RTX proteins may lead the way through the translocator and GG repeats appear at the cell surface thus providing the driving force for secretion (depicted schematically in Fig. 8). In line with these arguments is the observation that the amount of GG repeats correlates with the size of the secreted substrate[13,14]. Our results also suggest that the directionality of secretion determined for the HlyAc/HlyA fusion proteins is

a universal feature of the RTX protein family, which may also apply for other T1SS substrates containing a C-terminal secretion sequence.

Methods

Bacterial strains and plasmids. The *E. coli* strain DH5α was used for all cloning procedures. The pK184 plasmid (Supplementary Fig. 2) was used for HlyB and HlyD production under the control of a P_{lac} promoter, inducible with IPTG (isopropyl β-D-1-thiogalactopyranoside)[17]. All plasmids and oligonucleotides used in this study are summarized in Supplementary Table 1 and 2.

Plasmid pSOI-eGFP-HlyAc was used for eGFP-HlyAc expression under the control of a P_{BAD} promoter. Plasmid pSOI-eGFP-HlyAc was cloned through the restriction free cloning (RF-cloning) method[38]. The *eGFP* gene was amplified by PCR using the vector pcDNA3-eGFP and primers RF_pSOI_eGFP_for and RF_pSOI_eGFP_rev to generate the mega-primer. Amplified eGFP gene and pSOI-HlyAc[17] were used with a vector-to-insert-ratio of 1 to 2.5. After successful cloning, the eGFP-HlyAc-Δss variant was created by using PCR where the base pairs encoding for amino acid position 425 to 485 were deleted. Primer pair Deletion-HlyAc-for and Deletion-HlyAc-rev was used.

The HlyAc gene was exchanged for full-length *hlyA* to generate plasmid pSOI-eGFP-HlyA by RF-cloning. The *hlyA* gene was amplified by PCR using plasmid pSU-*hlyA*[39] and primers RF_pSOI_HlyA_for and RF_pSOI_HlyA_rev. The amplified genes were used with a vector-to-insert-ratio of 1 to 10. To generate plasmid pSOI-eGFP-HlyA-Δss, which expresses the eGFP-HlyA-Δss variant lacking the secretion signal, a stop-codon was introduced by site directed mutagenesis applying the primers HlyAΔss_for and HlyAΔSS_rev.

For the simultaneous expression of eGFP-HlyAc and HlyAc, we constructed a plasmid (pSOI-eGFP-$HlyAc^{BAD}$/$HlyAc^{lac}$) designed for a co-expression of both target genes under the control of two different promoters (Supplementary Fig. 3). In the case of eGFP-HlyAc we chose a P_{BAD} promoter, while a P_{lac} promoter was selected for the expression of HlyAc. Cloning was achieved with the In-Fusion® Advantage PCR Cloning Kit (ClonTech). Therefore, plasmid pSOI-eGFP-HlyAc was linearized by PCR using primers pSOI_ColE1_for and pSOI-AMP_rev. The insert, the *hlyAc* gene with a P_{lac} promoter and terminator, was amplified by PCR applying pSU-*hlyA* as template with the primers Inf_pSOI_HlyA_F and Inf_pSOI_HlyA_R. The In-Fusion reaction with the linearized plasmid and the insert was performed according to the manufactures protocol. After successful cloning of pSOI-eGFP-$HlyAc^{BAD}$/$HlyAc^{lac}$, the eGFP-HlyAc-Δss variant was created by deleting amino acids 425 to 485 as described above. The resulting plasmid pSOI-eGFP-HlyAc-Δss^{BAD}/$HlyAc^{lac}$ confers expression of HlyAc and the eGFP-HlyAc-Δss fusion protein that lacks the secretion signal (Supplementary Fig. 4).

Competition secretion assay. Chemically competent *E. coli* BL21 (DE3) cells were transformed with pK184-HlyBD and pSOI-eGFP-$HlyAc^{BAD}$/$HlyAc^{lac}$ or pSOI-eGFP-HlyAc-Δss^{BAD}/$HlyAc^{lac}$ and grown on LB agar plates supplemented with 100 μg mL^{-1} ampicillin and 30 μg mL^{-1} kanamycin. Overnight cultures of single colonies were used to inoculate 25 mL 2 YT medium supplemented with 100 μg mL^{-1} ampicillin and 30 μg mL^{-1} kanamycin at an OD_{600} of 0.1. Cultures were grown at 37 °C and 180 rpm. The expression of HlyAc, HlyB and HlyD was induced with 1 mM IPTG at an OD_{600} of 0.6–0.8. The secretion levels were significantly enhanced by addition of 5 mM $CaCl_2$ (final concentration) to the culture media. Cells were grown for 3 h at 180 rpm and 37 °C to obtain sufficient amounts of the translocator components of the inner membrane and a constant expression and secretion level of HlyAc. Subsequently, cells were spun down for 15 min at 8000 g and re-suspended in fresh 2 YT media supplemented with 100 μg mL^{-1} ampicillin, 30 μg mL^{-1} kanamycin, 1 mM IPTG and 5 mM $CaCl_2$. This procedure ensured removal of secreted HlyAc from the supernatant. To monitor newly secreted HlyAc in cells expressing the translocation machinery, HlyAc in combination with eGFP-HlyAc or eGFP-HlyAc-Δss, respectively, the culture was split into two halves. 10 mM arabinose was added to one culture for inducing expression of the fusion protein eGFP-HlyAc or eGFP-HlyAc-Δss. The culture without added arabinose was used as a control. Cells were grown for 3 h at 180 rpm and 37 °C. A 1 mL aliquot was taken and centrifuged for 5 min at 14000 g, 4 °C each hour during growth. Cells were adjusted with water to an $OD_{equivalent}$ of 0.1 and supernatant samples were analyzed by SDS-PAGE and/or Western blot analysis.

The expression levels of HlyB and HlyD as well as the expression of eGFP-HlyAc or eGFP-HlyAc-Δss and the intracellular amount of HlyAc were determined via Western blots using polyclonal antibodies against HlyA, HlyB or HlyD in combination with an horseradish peroxidase (HRP)-conjugated, secondary antibody using the ECL advance kit (GE Healthcare).

Cell cultivation and protein expression for confocal laser scanning microscopy. *E. coli* BL21 (DE3) were prepared and induced identically to cells used in the competition assay. Cells were grown for 2 h at 180 rpm and 37 °C and harvested by centrifugation and directly used for cell fixation and immunofluorescence labeling.

Cell fixation by formaldehyde treatment. 50 μL of cells grown until an OD_{600} of 2.0 were mixed with 3% (v/v) formaldehyde in 2 YT medium for fixation and incubated at 37 °C and 180 rpm for one hour.

Immunofluorescence labeling of formaldehyde treated cells. Formaldehyde treated cells expressing eGFP-HlyAc, eGFP-HlyAc-Δss, eGFP-HlyA or pSOI-eGFP-HlyA-Δss in the presence or absence of HlyB and HlyD as well as cells that only expressed HlyB and HlyD were centrifuged at 11000 g for 5 min and re-suspended in the 50 μl PBS buffer containing 3% (w/v) BSA. Cells were transferred in a 1:50 diluted rabbit anti-HlyA antibody solution and incubated for one hour. Subsequently, cells were washed three times with PBS buffer containing 3% (w/v) BSA and suspended in a solution containing a secondary antibody conjugated with the fluorophore Cy3. Cells were incubated for one hour at 37 °C and washed two times in 50 μl PBS buffer.

Confocal laser scanning microscopy and image processing. 10 μL of labeled cells were mixed with 2 μL of ProLong®Gold antifade reagent on a poly-lysine coated slide, covered with a cover slip and sealed with clear varnish.

Imaging was performed with an Olympus FV1000 confocal laser scanning microscope (Olympus GmbH, Hamburg, Germany) equipped with a 60x oil immersion objective, numerical aperture 1.35. The eGFP fluorescence was excited at 488 nm using an argon laser at an output power of 5% and the Cy3 fluorescence was excited at 559 nm using a DPSS laser at 5%. The emission of eGFP was detected between 500 nm and 540 nm and the emission of Cy3 was detected between 565 nm and 600 nm using a spectral detector. Images of 1024 × 1024 pixels were taken with a pixel size of 0.05 μm.

The program ImageJ was used for processing and determination of cell fluorescence. The integrated intensity from all focused cells of all images of each type were determined and subtracted from the product of the mean background fluorescence multiplied by the area of the determined integrated intensity.

The program Prism 5.0 (GrapPad Inc) was used for a statistical analysis of the data. Mean cell fluorescence of each type of cell was determined together with the corresponding errors of the mean. Auto fluorescence represented by cells expressing only HlyB and HlyD were subtracted. Normalization was performed for eGFP and Cy3 fluorescence on the mean value of cells expressing eGFP-HlyAc, HlyB and HlyD (Figs 4 and 6).

Structured illumination microscopy and image processing. Structured illumination microscopy (SIM) was performed on a Zeiss ELYRA PS.1 system (Carl Zeiss Microscopy GmbH, Goettingen, Germany) equipped with an Andor EM-CCD iXON DU-885 with 1004 × 1002 pixels. Z-stacks were taken using a 63x oil immersion objective with a numerical aperture of 1.46. To generate structured illumination a grid pattern was projected onto the image plane in five different positions and at five different modulation angles to obtain high frequency information within the low frequency information captured by the optical system. For the Cy3-channel back-computation of the lower frequencies using Fourier transformation was performed using the Zeiss ZEN Structured Illumination Processing tool to increase the resolution in the final image. Due to the almost homogeneous distribution of the eGFP signal there was no gain in resolution by image processing in the eGFP channel.

References

1. Letoffe, S., Delepelaire, P. & Wandersman C. Protein secretion in gram-negative bacteria: assembly of the three components of ABC protein-mediated exporters is ordered and promoted by substrate binding. *EMBO J* **15,** 5804–5811 (1996).
2. Thanabalu, T., Koronakis, E., Hughes, C. & Koronakis, V. Substrate-induced assembly of a contiguous channel for protein export from *E. coli*: reversible bridging of an inner-membrane translocase to an outer membrane exit pore. *EMBO J* **17,** 6487–6496 (1998).
3. Hinsa, S. M., Espinosa-Urgel, M., Ramos, J. L. & O'Toole, G. A. Transition from reversible to irreversible attachment during biofilm formation by *Pseudomonas fluorescens* WCS365 requires an ABC transporter and a large secreted protein. *Mol Microbiol* **49,** 905–918 (2003).
4. Letoffe, S., Ghigo, J. M. & Wandersman, C. Secretion of the *Serratia marcescens* HasA protein by an ABC transporter. *J Bacteriol* **176,** 5372–5377 (1994).
5. Satchell, K. J. Structure and function of MARTX toxins and other large repetitive RTX proteins. *Annu Rev Microbiol* **65,** 71–90 (2011).
6. Ghigo, J. M. & Wandersman, C. A carboxyl-terminal four-amino acid motif is required for secretion of the metalloprotease PrtG through the *Erwinia chrysanthemi* protease secretion pathway. *J Biol Chem* **269,** 8979–8985 (1994).
7. Jarchau, T., Chakraborty, T., Garcia, F. & Goebel, W. Selection for transport competence of C-terminal polypeptides derived from *Escherichia coli* hemolysin: the shortest peptide capable of autonomous HlyB/HlyD-dependent secretion comprises the C-terminal 62 amino acids of HlyA. *Mol Gen Genet* **245,** 53–60 (1994).
8. Koronakis, V., Koronakis, E. & Hughes, C. Isolation and analysis of the C-terminal signal directing export of *Escherichia coli* hemolysin protein across both bacterial membranes. *EMBO J* **8,** 595–605 (1989).
9. Omori, K., Idei, A. & Akatsuka, H. Serratia ATP-binding cassette protein exporter, Lip, recognizes a protein region upstream of the C terminus for specific secretion. *J Biol Chem* **276,** 27111–27119 (2001).
10. Sebo, P. & Ladant, D. Repeat sequences in the *Bordetella pertussis* adenylate cyclase toxin can be recognized as alternative carboxy-proximal secretion signals by the Escherichia coli alpha-haemolysin translocator. *Mol Microbiol* **9,** 999–1009 (1993).
11. Mori, H. & Ito, K. The Sec protein-translocation pathway. *Trends Microbiol* **9,** 494–500 (2001).
12. Strathdee, C. A. & Lo, R. Y. Cloning, nucleotide sequence, and characterization of genes encoding the secretion function of the *Pasteurella haemolytica* leukotoxin determinant. *J Bacteriol* **171,** 916–928 (1989).
13. Linhartova, I. *et al.* RTX proteins: a highly diverse family secreted by a common mechanism. *FEMS Microbiol Rev* **34,** 1076–1112 (2010).
14. Delepelaire, P. Type I secretion in gram-negative bacteria. *Biochim Biophys Acta* **1694,** 149–161 (2004).
15. Rhodes, C. R. *et al.* Structural consequences of divalent metal binding by the adenylyl cyclase toxin of *Bordetella pertussis*. *Arch Biochem Biophys* **395,** 169–176 (2001).

16. Jones, H. E., Holland, I. B., Baker, H. L. & Campbell, A. K. Slow changes in cytosolic free Ca^{2+} in *Escherichia coli* highlight two putative influx mechanisms in response to changes in extracellular calcium. *Cell Calcium* **25,** 265–274 (1999).
17. Bakkes, P. J., Jenewein, S., Smits, S. H., Holland, I. B. & Schmitt, L. The rate of folding dictates substrate secretion by the *Escherichia coli* hemolysin type 1 secretion system. *J Biol Chem* **285,** 40573–40580 (2010).
18. Benabdelhak, H. *et al.* A specific interaction between the NBD of the ABC-transporter HlyB and a C-terminal fragment of its transport substrate haemolysin A. *J Mol Biol* **327,** 1169–1179 (2003).
19. Balakrishnan, L., Hughes, C. & Koronakis, V. Substrate-triggered recruitment of the TolC channel-tunnel during type I export of hemolysin by *Escherichia coli*. *J Mol Biol* **313,** 501–510 (2001).
20. Lecher, J., Schwarz, C. K., Stoldt, M., Smits, S. H., Willbold, D. & Schmitt, L. An RTX transporter tethers its unfolded substrate during secretion via a unique N-terminal domain. *Structure* **20,** 1778–1787 (2012).
21. Blight, M. A. & Holland, I. B. Heterologous protein secretion and the versatile Escherichia coli haemolysin translocator. *Trends Biotechnol* **12,** 450–455 (1994).
22. Kenny, B., Chervaux, C. & Holland, I. B. Evidence that residues –15 to –46 of the haemolysin secretion signal are involved in early steps in secretion, leading to recognition of the translocator. *Mol Microbiol* **11,** 99–109 (1994).
23. Mackman, N., Baker, K., Gray, L., Haigh, R., Nicaud, J. M. & Holland, I. B. Release of a chimeric protein into the medium from *Escherichia coli* using the C-terminal secretion signal of haemolysin. *EMBO J* **6,** 2835–2841 (1987).
24. Schwarz, C. K., Landsberg, C. D., Lenders, M. H., Smits, S. H. & Schmitt, L. Using an *E. coli* Type 1 secretion system to secrete the mammalian, intracellular protein IFABP in its active form. *J Biotechnol* **159,** 155–161 (2012).
25. Evdokimov, A. G. *et al.* Structural basis for the fast maturation of Arthropoda green fluorescent protein. *EMBO Rep* **7,** 1006–1012 (2006).
26. Gray, L., Mackman, N., Nicaud, J. M. & Holland, I. B. The carboxy-terminal region of haemolysin 2001 is required for secretion of the toxin from *Escherichia coli*. *Mol Gen Genet* **205,** 127–133 (1986).
27. Stanley, P., Koronakis, V. & Hughes, C. Mutational analysis supports a role for multiple structural features in the C-terminal secretion signal of *Escherichia coli* haemolysin. *Mol Microbiol* **5,** 2391–2403 (1991).
28. Nicaud, J. M., Mackman, N., Gray, L. & Holland, I. B. The C-terminal, 23 kDa peptide of *E. coli* haemolysin 2001 contains all the information necessary for its secretion by the haemolysin (Hly) export machinery. *FEBS Lett* **204,** 331–335 (1986).
29. Debarbieux, L. & Wandersman, C. Folded HasA inhibits its own secretion through its ABC exporter. *EMBO J* **20,** 4657–4663 (2001).
30. Gangola, P. & Rosen, B. P. Maintenance of intracellular calcium in *Escherichia coli*. *J Biol Chem* **262,** 12570–12574 (1987).
31. Ludwig, A., Jarchau, T., Benz, R. & Goebel, W. The repeat domain of *Escherichia coli* haemolysin (HlyA) is responsible for its Ca^{2+}-dependent binding to erythrocytes. *Mol Gen Genet* **214,** 553–561 (1988).
32. Kenny, B., Taylor, S. & Holland, I. B. Identification of individual amino acids required for secretion within the haemolysin (HlyA) C-terminal targeting region. *Mol Microbiol* **6,** 1477–1489 (1992).
33. Schermelleh, L., Heintzmann, R. & Leonhardt, H. A guide to super-resolution fluorescence microscopy. *J Cell Biol* **190,** 165–175 (2010).
34. Koronakis, V., Eswaran, J. & Hughes, C. Structure and function of TolC: the bacterial exit duct for proteins and drugs. *Annu Rev Biochem* **73,** 467–489 (2004).
35. Kanonenberg, K., Schwarz, C. K. & Schmitt, L. Type I secretion systems—a story of appendices. *Res Microbiol* **164,** 596–604 (2013).
36. Masi, M. & Wandersman, C. Multiple signals direct the assembly and function of a type 1 secretion system. *J Bacteriol* **192,** 3861–3869 (2010).
37. Delepelaire, P. & Wandersman, C. The SecB chaperone is involved in the secretion of the *Serratia marcescens* HasA protein through an ABC transporter. *EMBO J* **17,** 936–944 (1998).
38. Bond, S. R. & Naus, C. C. RF-Cloning.org: an online tool for the design of restriction-free cloning projects. *Nucleic Acids Res* **40,** W209–213 (2012).
39. Thomas, S., Smits, S. H. & Schmitt, L. A simple *in vitro* acylation assay based on optimized HlyA and HlyC purification. *Anal Biochem* **464,** 17–23(2014).

Acknowledgements
We would like to thank Iris Fey, Protein Production Facility, Heinrich-Heine-Universitaet, for technical support. We thank all members of the Institute of Biochemistry, Heinrich-Heine-Universitaet Duesseldorf, for helpful and very fruitful discussions. We gratefully acknowledge support (and training) from the International NRW Research School BioStruct, granted by the Ministry of Innovation, Science and Research of the State North Rhine-Westphalia, the Heinrich-Heine-Universitaet Duesseldorf, and the Entrepreneur Foundation at the Heinrich-Heine-Universitaet of Duesseldorf.

Author Contributions
M.L., S.W.P. and D.K. performed the experiments, M.L., S.W.P., D.K., K.E.J., S.H.J.S. and L.S. designed the experiments, M.L., S.W.P., S.H.J.S. and L.S. evaluated the data and all authors wrote the manuscript.

Additional Information
Supplementary information accompanies this paper at http://www.nature.com/srep

Competing financial interests: The authors declare no competing financial interests.

How to cite this article: Lenders, M. H. H. *et al.* Directionality of substrate translocation of the hemolysin A Type I secretion system. *Sci. Rep.* **5**, 12470; doi: 10.1038/srep12470 (2015).

Supplementary

Directionality of substrate translocation of the hemolysin Type I secretion system

Michael H. H. Lenders[1], Stefanie Weidtkamp-Peters[2], Diana Kleinschrodt[3], Karl-Erich Jaeger[4,5], Sander H. J. Smits[1] and Lutz Schmitt[1,5]*

[1]Institute of Biochemistry, Heinrich-Heine-Universitaet, 40225 Duesseldorf, Germany

[2]Center for Advanced Imaging (CAi), Heinrich-Heine-Universitaet, 40225 Duesseldorf, Germany

[3]Protein Production Facility, Heinrich-Heine-Universitaet, 40225 Duesseldorf, Germany

[4]Institute for Molecular Enzyme Technology (IMET), Forschungszentrum Jülich, 52426 Jülich, Germany

[5]Center of Excellence on Plant Sciences (CEPLAS), Heinrich-Heine-Universitaet, 40225 Duesseldorf, Germany

*To whom correspondence should be addressed:

Lutz.Schmitt@hhu.de

Tel. +49 211 81-10773

Fax +49 211 81-15310

Universitaetsstraße 1

40225 Duesseldorf

Germany

Figures legends

Supplementary Fig. 1

Domain organization of different T1SS substrates. Boxes on the left highlight the ABC transporter families involved in the T1SS. “CLD” describes a T1SS with an ABC transporter with an N-terminal CLD extension, contributing defective peptidase, “C39” describes a T1SS with an ABC transporter having an active N-terminal C39 peptidase domain and “no” describes an ABC transporter without additional domains. Proteins are abbreviated as follows and listed with their corresponding UniProtKB entries: HlyA, hemolysin A; LktA, leukotoxin; RtxA, RtxA; CyaA, bifunctional hemolysin/adenylate cyclase; PaxA, exotoxin PaxA; CvaC, colicin V protein; ComC, competence-stimulating peptide type 1; HasA, hemophore HasA; EprA, metalloprotease EprA. Domains of the substrates are labeled as follows: AC, adenylate cyclase domain; RTX, RTX domain; GG, GG repeats; SEC, secretion signal; L, N-terminal leader peptide; MP, metalloprotease domain.

Supplementary Fig. 2

Plasmid map pK184-HlyBD. The map was created using the PlasMapper web server [1].

Supplementary Fig. 3

Plasmid map pSOI-eGFP-HlyAc^{BAD} / HlyAc^{lac}. The map was created using the PlasMapper web server [1].

Supplementary Fig. 4

Plasmid map pSOI-eGFP-HlyAc-Δss^{BAD} / HlyAc^{lac}. The map was created using the PlasMapper web server [1].

Supplementary Fig. 5

Plasmid map pSOI-eGFP-HlyAc. The map was created using the PlasMapper web server [1].

Supplementary Fig. 6

Western blot analysis of supernatants and total cells content of CLSM analyzed cells. eGFP-HlyAc respectively eGFP-HlyAc-Δss, HlyB and HlyD are only present if the corresponding promotors were induced.

Supplementary Fig. 7

Western blot analysis of supernatants and total cells content of CLSM analyzed cells. eGFP-HlyA respectively eGFP-HlyA-Δss, HlyB and HlyD are only present if the corresponding promotors were induced.

Figures

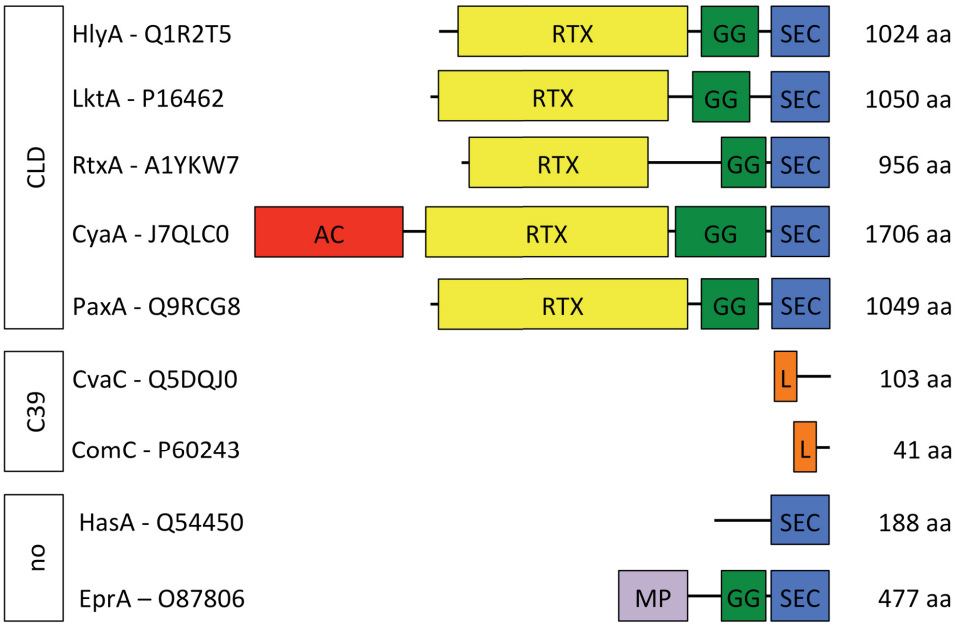

Supplementary Figure 1

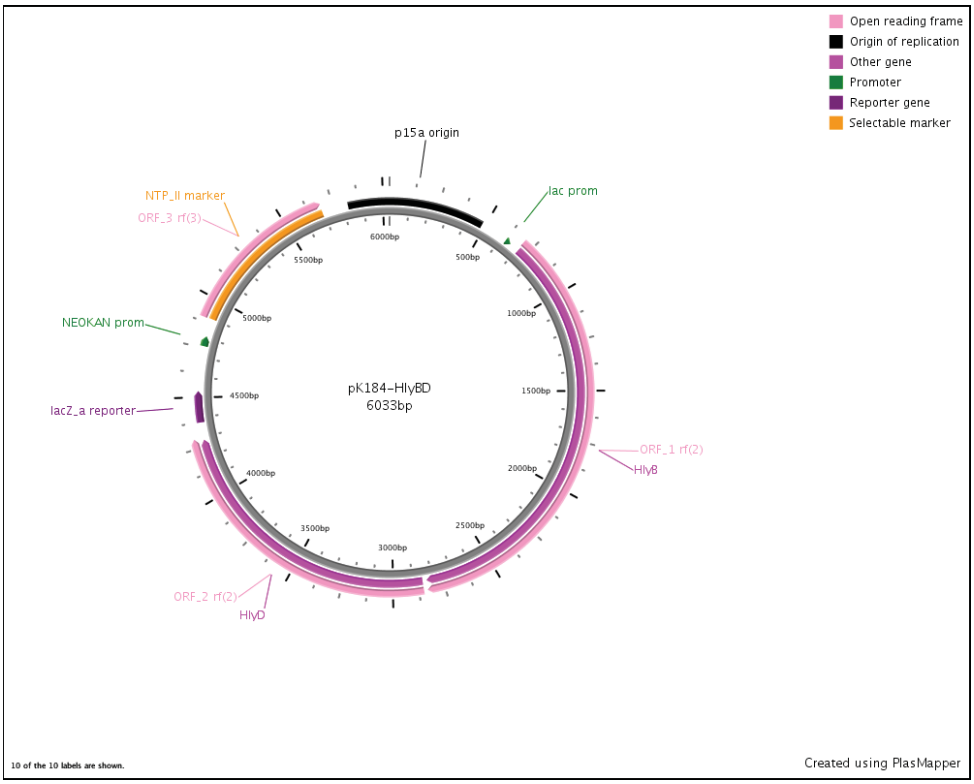

Supplementary Figure 2

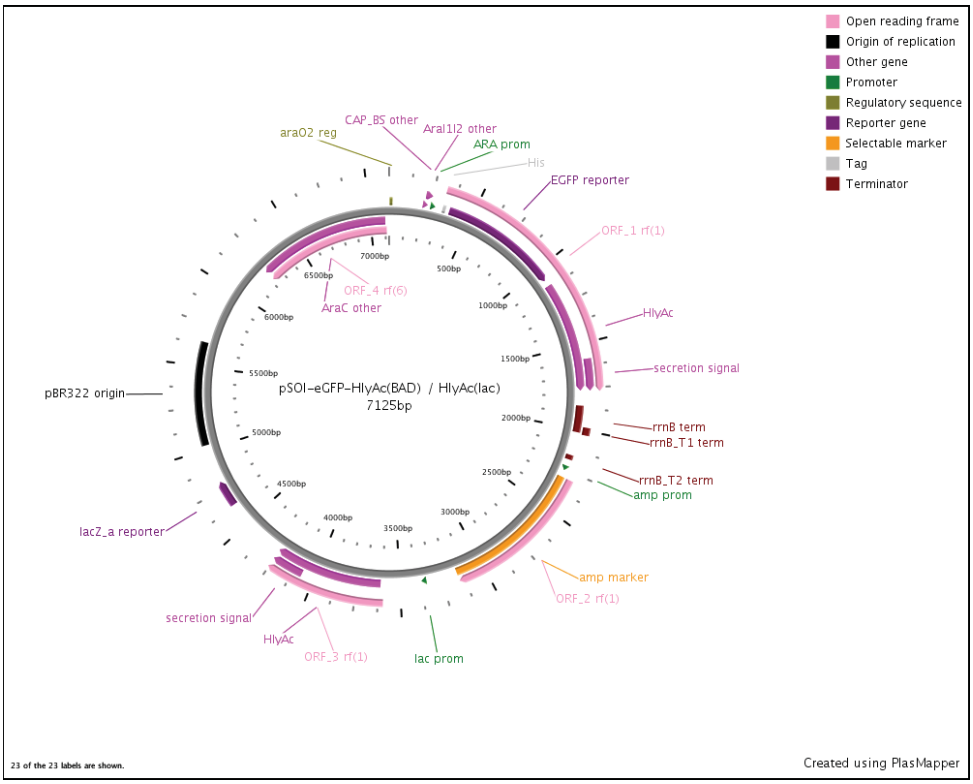

Supplementary Figure 3

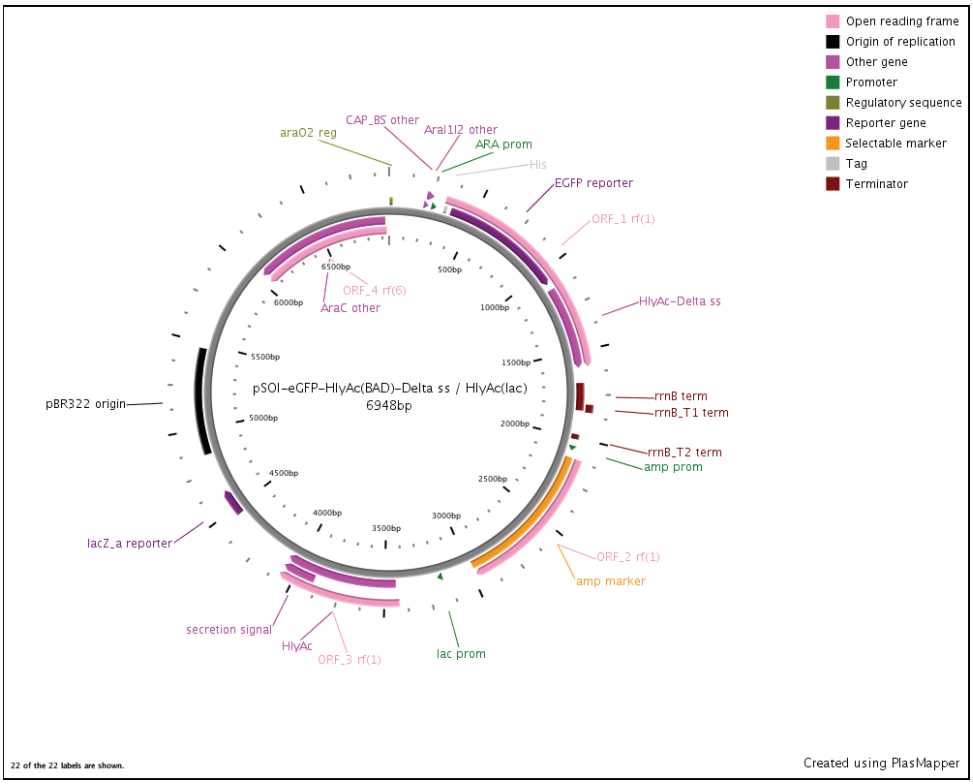

Supplementary Figure 4

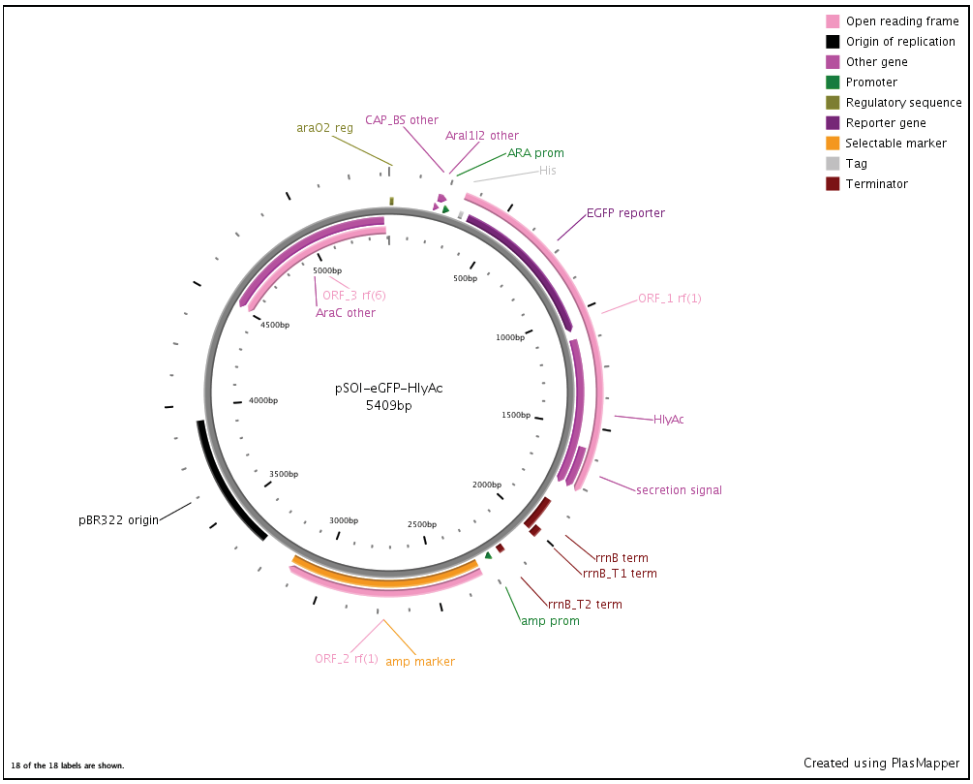

Supplementary Figure 5

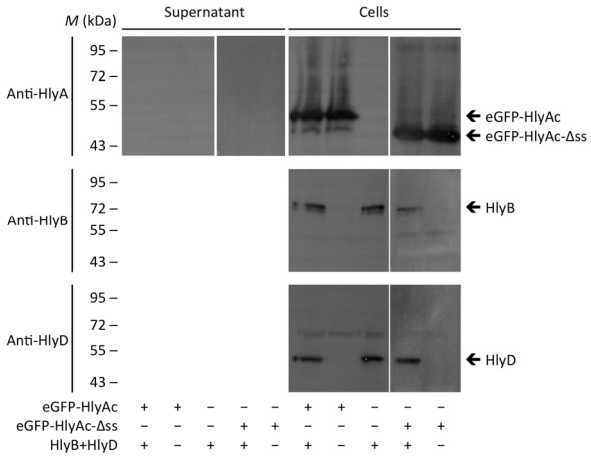

Supplementary Figure 6

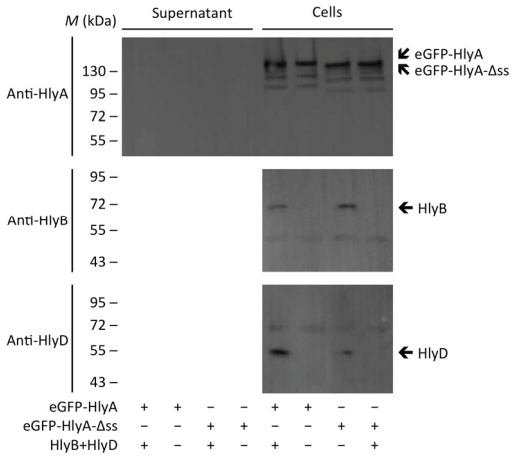

Supplementary Figure 7

Tables

Supplementary Table 1

Primers used in this study

Name	Sequence
HlyAcΔ-ss-for	5’-GGACATGATGCATGAACTTATGGGAG-3’
HlyAcΔ-ss-rev	5’-CTCCCATAAGTTCATGCATCATGTCC-3’
pSOI-ColE1-for	5’-CATTTTTAATTTAAAAGGATCTAGGTGAAG-3’
pSOI-AMP-rev	5’-AGTTTTAAATCAATCTAAAGTATATATGAGTAAAC-3’
Inf-pSOI-HlyA-F	5’-GATTGATTTAAAACTGCCAATACGCAAACCGCCTCTC-3’
Inf-pSOI-HlyA-R	5’-TTTAAATTAAAAATGTAGGGGTTCCGCGCACATTTCC-3’
RF_pSOI_eGFP_for	5’-CCATCATGGTGAGAATTTATATTTTCAAGGTGTGAGCAAGGGCGAGG-3’
RF_pSOI_eGFP_rev	5’-TGGAAGGGTGGGATTTACCGGACTTGTACAGCTCGTCCATGC-3’
RF_pSOI_HlyA_for	5’-CCCTTCCAGCATCGAAGGCCGCATGACAACAATAACCACTGCAC-3’
RF_pSOI_HlyA_rev	5’-TCCGCCAAAACAGCCAAGCTTATGCTGATGTGGTCAGGGT-3’
HlyAΔss_for	5’-GGGAATGATGCATAAGCCTATGGAAG-3’
HlyAΔss_rev	5’-CTTCCATAGGCTTATGCATCATTCCC-3’
Deletion-HlyAc-for	5’-TAAGCTTGGCTGTTTTGGCGGATG-3’
Deletion-HlyAc-rev	5’-TCATGCATCATGTCCATACACATAACTTACCTT-3’

Supplementary Table 2

Plasmids used in this study

Name	Description	Reference
pK184-HlyB	Plasmid encoding *hlyB* and *hlyD*	[2]
pSU-*hlyA*	Plasmid *hlyA*	[3]
pSOI-eGFP-HlyAc	eGFP inserted in pSOI-HlyAc [2] *via* restriction free cloning	This study
pSOI-eGFP-HlyAc-Δss	Plasmid pSOI-eGFP-HlyAc with a stop codon in front of the HlyAc secretion signal *via* site-directed mutagenesis	This study
pSOI-eGFP-HlyAc^{BAD} / HlyAc^{lac}	HlyAc with *lac* promoter inserted in pSOI-eGFP-HlyAc *via* In-Fusion® Advantage PCR Cloning Kit (Clontech)	This study
pSOI-eGFP-HlyAc-Δss ^{BAD} / HlyAc^{lac}	Plasmid pSOI-eGFP-HlyAc^{BAD} / HlyAc^{lac} without the base pairs coding for the last 60 C-terminal amino acids (HlyAc secretion signal)	This study
pSOI-eGFP-HlyA	HlyAc is exchanged for HlyA from pSU-*hlyA* in plasmid pSOI-eGFP-HlyAc	This study
pSOI-eGFP-HlyA-Δss	Plasmid pSOI-eGFP-HlyA with a stop codon in front of the HlyA secretion signal *via* site-directed mutagenesis	This study

1 Dong, X., Stothard, P., Forsythe, I. J. & Wishart, D. S. PlasMapper: a web server for drawing and auto-annotating plasmid maps. *Nucleic acids research* **32**, W660-664, doi:10.1093/nar/gkh410 (2004).

2 Bakkes, P. J., Jenewein, S., Smits, S. H., Holland, I. B. & Schmitt, L. The rate of folding dictates substrate secretion by the Escherichia coli hemolysin type 1 secretion system. *The Journal of biological chemistry* **285**, 40573-40580, doi:10.1074/jbc.M110.173658 (2010).

3 Thomas, S., Smits, S. H. & Schmitt, L. A simple in vitro acylation assay based on optimized HlyA and HlyC purification. *Analytical biochemistry*, doi:10.1016/j.ab.2014.07.001 (2014).

3.6. Chapter VI - Secretion rates of substrate translocation of a Type I secretion system

Title Secretion rates of substrate translocation of a Type I secretion system

Authors Michael H. H. Lenders, Tobias Beer, Sander H. J. Smits and Lutz Schmitt

In Preparation

Own proportion of this work 60 %;
Construction of the plasmids, secretion system quantification, secretion rate determination, immunofluorescence labeling of formaldehyde treated cells, confocal laser scanning microscopy and image processing, writing of the manuscript.

Secretion rates of substrate translocation of a Type I secretion system

Michael H.H. Lenders, Tobias Beer, Sander H.J. Smits and Lutz Schmitt*

Institute of Biochemistry, Heinrich-Heine-Universität,
40225 Düsseldorf, Germany

Abstract

Type 1 secretion systems (T1SS) allow Gram-negative bacteria to secrete a broad range of substrates into the extracellular space. Substrates varies in size from small molecules up to large proteins. Proteases, lipases, adhesion factors and toxins function as substrates. An important member of this family is the hemolysin A (HlyA) T1SS of *Escherichia coli*. The membrane protein complex consists of HlyB, HlyD and TolC and allows the translocation of unfolded HlyA in one step across the inner and outer membrane. We have addressed the question of the secretion rate of the HlyA T1SS by secretion studies using immunofluorescence to quantify the T1SS amount as well as the amount of secreted HlyA. We observed that the secretion rate is constant even for different protein length or the amount of glycine-rich repeats (GG repeats). Furthermore, the secretion rate is independent of the extracellular Ca^{2+} concentration.

*To whom correspondence should be addressed: Lutz.Schmitt@hhu.de,
Tel. +49 211 81-10773, Fax +49 211 81-15310, Universitätsstraße 1, 40225 Düsseldorf, Germany

Introduction

Type 1 secretion systems (T1SS) are essential cellular nanomachineries found in the membranes of many Gram-negative bacteria. They consist of an ATP-binding cassette (ABC) transporter and a membrane fusion protein (MFP) both located in the inner membrane and an outer membrane protein (OMP). T1SS are able to transport a broad range of substrates ranging from small molecules up to large proteins [Delepelaire, 2004]. Substrate binding leads to the formation of the T1SS complex. It has been shown that the translocation of the substrate occurs in an unfolded state and without any periplasmic intermediate from the cytosol across both membranes directly into the extracellular space [Létoffé et al., 1996, Thanabalu et al., 1998, Bakkes et al., 2010, Schwarz et al., 2012].

Substrates of T1SS can perform many different functions. For example, they are hemophores such as HasA (188 amino acids) from *S. marcescens*, lipases such as LipA (613 amino acids) from *S. marcescens* or large adhesion factors such as LapA (8682 amino acids) from *P. fluorescens* [Létoffé et al., 1994, Hinsa et al., 2003, Delepelaire, 2004]. All substrates of type 1 secretion contain a secretion signal that is encoded within the last C-terminal 50-60 amino acids. In contrast to other secretion systems the secretion signal is not cleaved during or after secretion and has been shown to be essential and sufficient for the secretion process [Koronakis et al., 1989, Sebo and Ladant, 1993, Ghigo and Wandersman, 1994, Jarchau et al., 1994, Omori et al., 2001].

One of the most prominent families of T1SS substrates are the repeats in toxin (RTX) proteins. Characteristic for these proteins are glycine-rich repeats (GG repeats) located mainly in the C-terminal part of the protein upstream of the secretion signal. GG repeats have the consensus sequence GGxGxDxUx (x can be any amino acid and U is a large or hydrophobic amino acid) [Linhartová et al., 2010]. The number of these repeats depends on the size of the protein with roughly one repeat for every 6 - 12 kDa [Delepelaire, 2004, Linhartová et al., 2010]. After secretion, Ca^{2+} binding to the repeats with a K_D of 100 µM induces the folding of the secreted protein [Thomas et al., 2014]. The folding is induced only extracellular because only here the Ca^{2+} concentration exceeds the K_D [Jones et al., 1999, Thomas et al., 2014].

Hemolysin A (HlyA) is a prominent example of a RTX protein. The pore building toxin consists of 1024 amino acids (110 kDa) and harbors six conserved GG repeats [Delepelaire, 2004]. The HlyA T1SS secretion system is composed of the ABC transporter hemolysin B (HlyB), the MFP hemolysin D (HlyD) and TolC, the endogenously expressed OMP. Unfolded HlyA is secreted [Bakkes et al., 2010] in one step across both

membranes without any periplasmic intermediate. The secretion signal of HlyA is essential [Gray et al., 1986, Stanley et al., 1991, Kenny et al., 1994, Lenders et al., 2015] and sufficient for secretion since it can be secreted alone [Jarchau et al., 1994]. Furthermore, a C-terminal fragment of HlyA (HlyAc) consisting of the last 218 amino acids and containing the secretion signal and three conserved GG repeats could also been shown to secrete in high yields [Bakkes et al., 2010].

The secretion rate of the hemolysin T1SS is unknown. For other secretion systems the rate has been determined. The injection speed of the SipA type 3 secretion system (T3SS) is within the scope of 4795-41100 amino acids per sec [Schlumberger et al., 2005] whereas the speed for Sec dependent transport by SecYEG is 152 - 228 amino acids per sec and transporter [Robson et al., 2009].

Furthermore, the exact role of ATP hydrolysis within the translocation cycle is unknown. It could be shown by an ATP hydrolyzing defiant mutant that hydrolyzes is necessary for completing the secretion process [Thanabalu et al., 1998]. Nevertheless, it is unclear whether ATP hydrolysis is necessary for threading the substrate into the translocator.

To address these questions, we used a fusion protein consisting of the enhance Green Fluorescence Protein (eGFP), N-terminally fused to HlyAc that is able to stall the hemolysin T1SS by the fast folding properties of eGFP [Evdokimov et al., 2006]. This has been used to stall the HlyA T1SS in action [Lenders et al., 2015]. This allowed us to quantify the number of active T1SS per cell *in vivo* and as a consequence the secretion rate of HlyA, respectively HlyAc. Our data suggest that the initial binding of the secretion signal is not limiting secretion and that the length of the protein is not important for the speed of secretion. Furthermore, our results demonstrate that ATP hydrolysis is necessary for threading the substrate into the translocator and that the postulated 'pulling' mechanism by Ca^{2+} induced extracellular protein folding could not be supported in our experiments. Furthermore, different extracellular Ca^{2+} concentration did not influence the secretion rate of HlyA or HlyAc.

Results

Determining the amount of T1SS

HlyAc C-terminally fused to rapidly folding eGFP can stall the HlyA T1SS [Lenders et al., 2015]. The fusion protein is treading into the T1SS with the C-terminus ahead and the N-terminal eGFP remains inside the cytosol whereas the C-terminal HlyAc

is exposed at the cell surface [Lenders et al., 2015]. The extracellular exposed HlyA fragment could visualized via an HlyA specific antibody in combination with a secondary antibody that harbored the fluorophore Cy3 resulting in red fluorescence (see Figure 1).

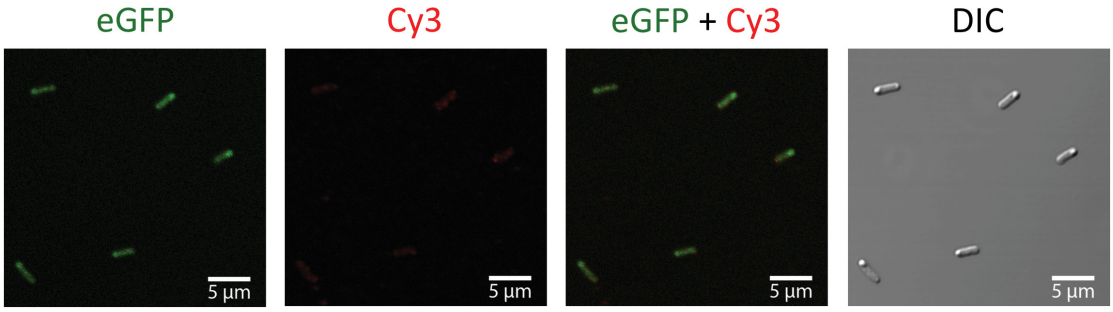

Figure 1: **Detection of the surface exposed HlyAc fragment of eGFP-HlyAc by confocal laser scanning microscopy.** *E. coli* cells expressed HlyB, HlyD and eGFP-HlyAc. Shown is the eGFP fluorescence (left panel) of the fusion proteins, the HlyA mediated Cy3 fluorescence at the cell surface (second left panel), merged images of eGFP and Cy3 fluorescence (second right panel) and differential interference contrast (DIC) images of the cells (right panel).

We used the Cy3 fluorescence of the stalled T1SS to determine the number of active T1SS within the *E. coli* membrane. Only if the T1SS was active and fully functional the fusion protein will be threaded into the translocon. Here, we assume that on average only one HlyA specific antibody and one monoclonal Cy3 linked secondary antibody binds to a single surface exposed fragment of HlyAc. Cy3 fluorescence was fluorometric determined (see Figure 2, left bar). Thereby, an amount of 290 fmol monoclonal Cy3 coupled antibody (1.75×10^{11} particles) represented, for example, a fluorescence intensity of 283 000 CPS µA^{-1}. The determined fluorescence intensity's were plotted against the corresponding amount of antibodies. The resulting regression curve (slope: 1.53×10^{-18} mol µA CPS^{-1}; see Supplementary Figure 1) was used to determine the amount of active T1SS. Unspecific binding of Cy3 linked secondary antibody to cell surface was monitored by detecting the fluorescence intensity of cells lacking the T1SS. These cells did not expose an HlyA fragment at the cell surface and displayed the Cy3 background fluorescence (see Figure 2, right bar).

For that purpose, cells expressing the stalled HlyA T1SS showed a fluorescence intensity of 319 000 CPS µA^{-1} whereas cells without T1SS showed showed a fluorescence intensity of 65 000 CPS µA^{-1}. In total, 254 000 CPS µA^{-1} represent the specific fluorescence intensity of the stalled translocator. The intensity was multiplied with the slope of the regression curve to get the exact amount of translocator. We ended up with

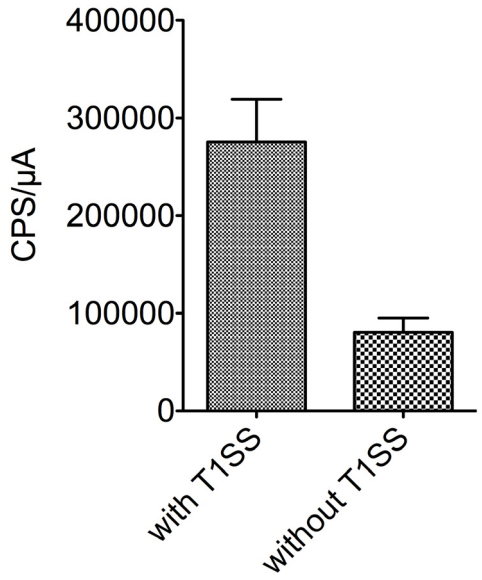

Figure 2: **Total cell fluorescence of Cy3.** Immunofluorescence labeled *E. coli* cells expressed eGFP-HlyAc in the presence (left bar) and absence (right bar) of HlyB and HlyD. Shown is the fluorescence of Cy3 in CPS μA^{-1}. Error bars represent the standard deviation of the Cy3 fluorescence.

389 fmol (2.39×10^{11} particles). Divided by the number of cells (4×10^7 cells in 50 µL solution with an OD_{600} of 1), resulted in 5840 active HlyA T1SS $cell^{-1}$.

We used Western blot as a second method to gain information about the amount of HlyB expression per cell. For that purpose, immunofluorescence of purified HlyB and for a distinct number of cells expressing the HlyA T1SS was determined on the same Western blot. The band intensity of different concentrations of HlyB was used to calculate the fluorescence intensity dependency on the HlyB concentration (slope: 1.26×10^{-16} mol; see Supplementary Figure 2). For example, an integrated density of 10702 represent 1.35 pmol (8.13×10^{11} particles) HlyB. Divided by the number of cells (8×10^7 cells per band), resulted in 10150 HlyB molecules per cell. Biochemical studies of the crystalized HlyB NBDs indicated that the active form of HlyB is a dimer [Zaitseva et al., 2005]. According to this, we end up with 5075 T1SS $cell^{-1}$.

In summary, the stalled T1SS allowed us to determine the number of active T1SS for each cell whereas the Western blot as a second method allowed us to gain information about the total amount of HlyB expression per cell. Both methods gave similar results and averaging all values (see Supplementary Table 1), resulted in 5024 ± 1301 T1SS $cell^{-1}$. This determined value was used further in the analysis.

Quantifying the secretion rate of HlyA and HlyAc

The HlyA T1SS can secrete HlyA and HlyAc [Nicaud et al., 1986, Delepelaire, 2004]. The exact rate for secretion is unknown. The determined amount of T1SS cell^{-1} gave us the opportunity to quantify the secretion rate for HlyA. For that purpose, HlyA was secreted into the culture supernatant by cells expressing the HlyA T1SS. Western blots confirm that the amount of transporters are identical to cells that were used for T1SS quantification (see Figure 3).

Cells secreted HlyA over a four-hour period and the secretion rate was determined by taking supernatant samples every hour. Furthermore, cell growth was determined after each hour of secretion and the total number of cells was calculated. Supernatant samples and different concentrated purified HlyA were analyzed by SDS-PAGE. The band intensity of different HlyA concentration was used to calculate the integrated density dependency on the HlyA concentration. The resulting regression curve allowed the quantification of secreted HlyA. For example, an integrated density of 10940 represent 9.6 pmol (5.781×10^{12} particles) HlyA. The different amounts of HlyA for each time point allowed the definition of the HlyA secretion level. In this case, the HlyA secretion was 0.13 pmol min^{-1} (7.83×10^{10} HlyA min^{-1}). Divided by the cell growth (2.01×10^{7} cells min^{-1}), this resulted in 3895 HlyA cell^{-1} min^{-1}. Together with the HlyA length (1024 aa) and the amount of 5024 T1SS cell^{-1}, we determined a secretion rate of 13 aa T1SS^{-1} s^{-1} in this example.

Only number of cells and amount of secreted HlyA was used for secretion rate calculation that fit in the exponential phase of *E. coli* cell growth. This phase is normally within the first two hours of induction. The resulting concentration of HlyA represents the amount of translocated substrate [mol cell^{-1} min^{-1}]. Supplementary Table 2 and 3 highlight all values for secreted HlyA/HlyAc for 2 and 4 h secretion, the corresponding HlyA secretion level [mol min^{-1}], the cell growth [cells min^{-1}] and the final secretion rate of HlyA/HlyAc [aa T1SS^{-1} s^{-1}].

Our experiments allowed the determination of the total amount of active T1SS cell^{-1}. Accordingly, the amount of HlyA T1SS^{-1} s^{-1} could be determined. Finally, the secretion rate of could be calculated in aa T1SS^{-1} s^{-1}. Full length HlyA showed a secretion rate of approximated 15.2 ± 1.7 aa T1SS^{-1} s^{-1}. Furthermore, the secretion rate of HlyAc was determined similarly. HlyAc showed a secretion rate of 14.1 ± 1.0 aa T1SS^{-1} s^{-1}.

As a control, Western blots of HlyB and HlyD confirm that the expression levels of cell expressing the T1SS in the presence of HlyA, HlyAc or eGFP-HlyAc were identical and not effected by the co-expression of the substrates (see Figure 3). The control

indicated that our determined amount of T1SS is similar in all cases.

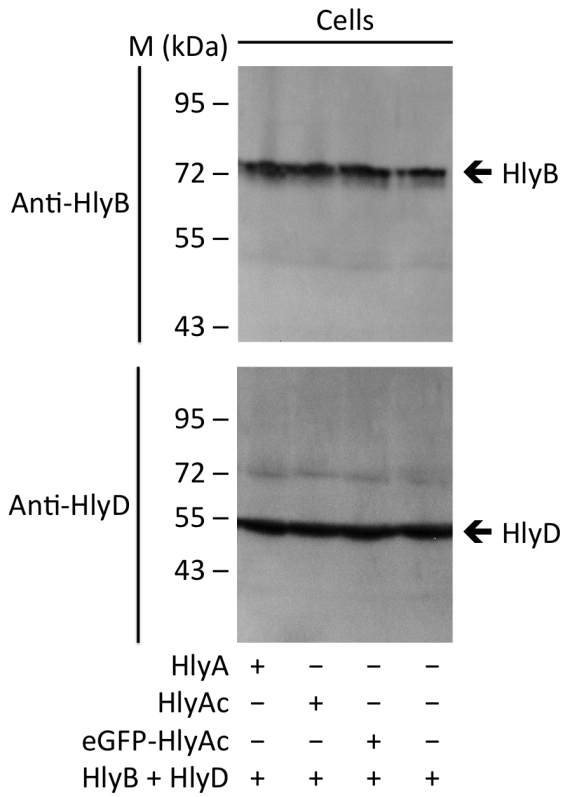

Figure 3: **HlyB and HlyD expression in HlyA, HlyAc and eGFP-HlyAc expressing *E. coli*.** Expression levels of HlyB and HlyD are identical. Western blot analysis of *E. coli* cells show that the level of HlyB and HlyD are equal for eGFP-HlyAc expressing and HlyA respectively HlyAc secreting cells.

The results showed that the HlyA secretion rate was similar to that of HlyAc. The netto amount of secreted HlyA is 4 to 5 fold lower compared to HlyAc. Due to the fact that HlyA has a length of 1024 aa, HlyAc is with a length of 218 aa 4 to 5 fold smaller. According to this, the HlyA T1SS secreted in the same time a similar total amount of amino acids in case of HlyA and HlyAc. Due to the different sizes of the substrates, the total amount of HlyAc is higher compared to HlyA.

Moreover, the amount of GG repeats differs between the different substrates. HlyA has six highly conserved GG repeats whereas HlyAc harbors only three repeats. The protein length/GG repeat ratio is for HlyA 170 aa repeat^{-1} whereas the ratio for HlyAc is 73 aa repeat^{-1}. It is know that the GG repeats are involved in protein stability and folding by binding extracellular Ca^{2+} [Rose et al., 1995, Jones et al., 1999, Rhodes et al.,

2001, Thomas et al., 2014]. So far, it is unknown if the are influencing the secretion rate of the substrates. In this case, HlyAc secretion should be faster compared to HlyA secretion. In case of HlyAc, more GG repeats are present on a smaller protein compared to HlyA. Our experimental data indicated that the secretion rates of HlyA and HlyAc were identical and not affected by the length of the protein or by the total amount of GG repeats.

Ca^{2+} concentration is not affecting the secretion rate

T1SS secrete a broad number of substrates. For example, HlyA has a size of 1024 aa. The amount of consumed ATP per translocation cycle is however still unknown. For substrates like HlyA or the 900 kDa LapA from *Pseudomonas fluorescens* [Hinsa et al., 2003], it seems to be unlikely that only two ATP are required for one transport cycle. A common theory is that the GG repeats provide the inherent driving force for the transportation process [Linhartová et al., 2010]. According to this, it could be shown that the GG repeats bind Ca^{2+} with a high affinity. Ca^{2+} binding induces protein folding whereas folding only take place at the extracellular surface due to the high Ca^{2+} concentration [Rose et al., 1995, Jones et al., 1999, Rhodes et al., 2001]. It is assumed that protein folding is induced once the GG repeats reaches the extracellular surface and that this creates an inherent driving force that "pulls" the rest of the protein out of the translocator [Linhartová et al., 2010, Lenders et al., 2013].

We addressed this question of a "pulling" mechanism by providing secretion experiments in presence of different Ca^{2+} concentration in the extracellular media. If the assumption of a 'pulling' mechanism is correct, the secretion rate will be dependent on the extracellular Ca^{2+} level. Nevertheless, if such a 'pulling' mechanism provides the inherent driving force for substrate transport, the secretion rate will decrease by deceeding the K_D for Ca^{2+} binding of the GG repeats because without extracellular Ca^{2+} an inherent driving force can not provided. Whereas the secretion rate will increase or will stay constant, after the Ca^{2+} level exceeds the K_D.

Similar to the secretion rate determination for HlyA and HlyAc above, only number of cells and amount of secreted HlyA/HlyAc was used that fit in the exponential phase of cell growth. This could normally observed within the first two hours. The amount of both substrates remained on the same level even if the extracellular Ca^{2+} concentration exceeded or deceeded the GG repeat specific K_D of 100 µM (see Figure 4 dark grey bars). Only after four hours, differences in the amount of secreted HlyA/HlyAc in presence of different Ca^{2+} concentration could be observed. In absence of Ca^{2+}, secretion level of

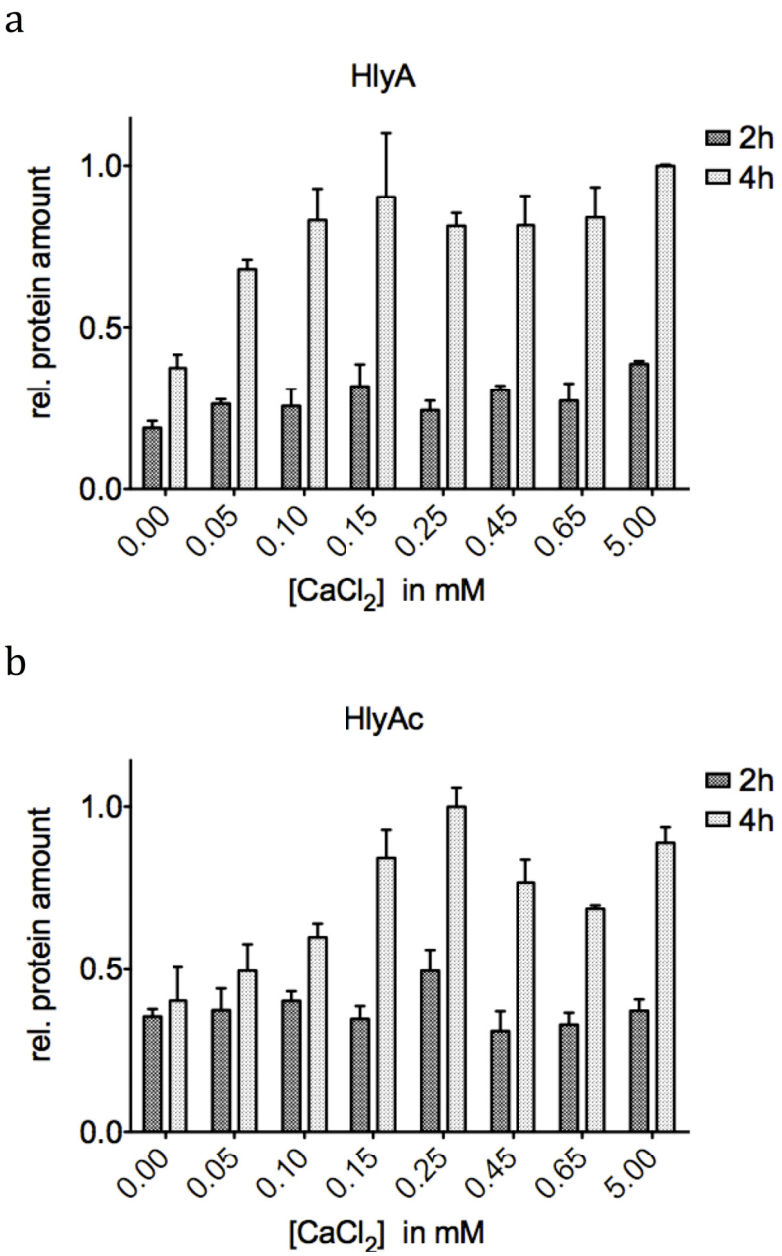

Figure 4: **Relativ amount of secreted protein in presence of different extracellular Ca^{2+} concentration.** Shown are the relativ protein amount of (a) HlyA and (b) HlyAc in presence of different extracellular Ca^{2+} concentration after 2 h (dark grey bars) and 4 h (light grey bars). Values are normalized on the highest mean value of secreted (a) HlyA respectively (b) HlyAc after 4 h secretion time. Error bars represent the standard deviation.

HlyA and HlyAc was reduced by half and was only reaching normal secretion levels by exceeding the K_D of the GG repeats in presents of higher Ca^{2+} concentration (see Figure 4 light grey bars). Due to the fact that HlyA and HlyAc are instable in the absence of Ca^{2+}, aggregation of secreted substrates could be observed for secretion experiments with extracellular Ca^{2+} concentration that deceeded the GG repeat specific K_D. This aggregation appeared if HlyA and HlyAc reached a critical concentration, typically after three hours and resulted in aggregation that settles down at the rim of the incubation flasks.

The secretion rates for HlyA and HlyAc are shown in Table 2 and 3. The results highlight that the secretion rate of HlyA stays constantly between 12.9 ± 0.2 to 15.7 ± 1.7 aa $T1SS^{-1}$ s^{-1} respectively between 11.5 ± 0.7 to 17.6 ± 1.0 aa $T1SS^{-1}$ s^{-1} for HlyAc. The secretion rate was not influenced by the calcium ion concentration (see Figure 5) even if the GG repeats K_D for Ca^{2+} binding exceeded respectively deceeded its specific value of 100 µM [Thomas et al., 2014].

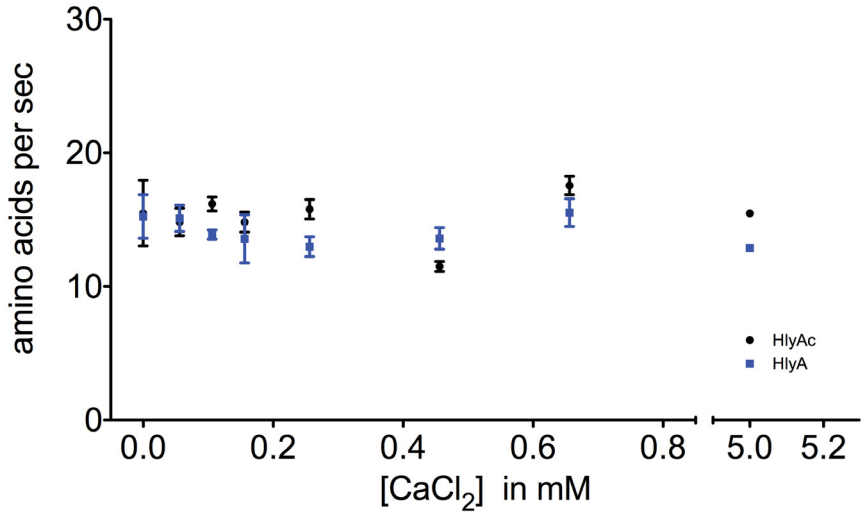

Figure 5: **Secretion rate of HlyA and HlyAc is not influenced by Ca^{2+} concentration.** Determined secretion rate of *E. coli* cells secreting HlyA (blue cubes) and HlyAc (black dots) in the presence of different Ca^{2+} concentration (abscissa). Shown are the mean secretion rate of triplicate secretions in aa $T1SS^{-1}$ s^{-1}. Error bars represent the standard deviation.

In summary, a "pulling" mechanism that provide an inherent driving force for HlyA secretion could not observed. The Ca^{2+} concentration was not influencing the secretion behavior of HlyA and HlyAc. Nevertheless, Ca^{2+} were absolutely essential for the sta-

bility of the protein and its correct folding. The question remains open what provides the driving force for the translocation process.

ATP hydrolysis is necessary for threading the substrate into the T1SS

ATP hydrolysis is an essential factor for the type I secretion process. Previous studies could show that secretion is abolished without ATP hydrolysis but did not effect the complex assembly [Thanabalu et al., 1998]. Nevertheless, the question arises if the substrate is still threaded into the translocator even in absence of ATP hydrolysis. This question leads to two fundamental different ways of how ATP hydrolysis is influencing the secretion process. According to this, ATP hydrolysis can initiate or terminate transport. In case of an initializing process, ATP hydrolysis energizes the transport process and/or leads to translocator opening. In case of a terminating process, ATP hydrolysis will appear at the end of secretion after the substrate pass nearly completely the translocator. Than, hydrolysis will result in a reset of the ABC transporter by dissolving the HlyB NBD dimerization.

To address this question, the ATP hydrolysis deficient mutant H662A of HlyB was used. This mutant is able to bind ATP, leads to dimerization of the NBDs but not to ATP hydrolysis [Zaitseva et al., 2005]. As mentioned above, we could show that the HlyA T1SS can be stalled by an HlyAc respectively HlyA fusion with the rapidly folding eGFP. These fusion proteins stuck inside the translocator and led to a stalled T1SS with a C-terminal exposed HlyA fragment at the cell surface. Furthermore, the surface exposed HlyA fragment could be visualized via an HlyA specific antibody in combination with a Cy3 fluorophore linked secondary antibody resulting in red fluorescence. eGFP fluorescence is detectable inside the cells. If ATP hydrolysis is essential for initiating the transport process, no specific Cy3 fluorescence will be detectable at the cellular surface. In case of a terminating function on the transport process by ATP hydrolysis, the HlyA fragment will be exposed at the extracellular surface and detectable via an HlyA specific antibody in combination with a Cy3 fluorophore linked secondary antibody.

E. coli cells with T1SS having the HlyB-H662A variant (Figure 6, first row) were analyzed with confocal laser scanning microscopy (CLSM). The eGFP fluorescence signal was found homogeneously distributed within the cells and although sometimes accumulated at the cell poles. Specific Cy3 fluorescence could not been detected. When comparing the cells with cells expressing the native HlyA T1SS (see Figure 6, second row) we observed in similar eGFP fluorescence but with a twenty times higher Cy3 fluorescence signal.

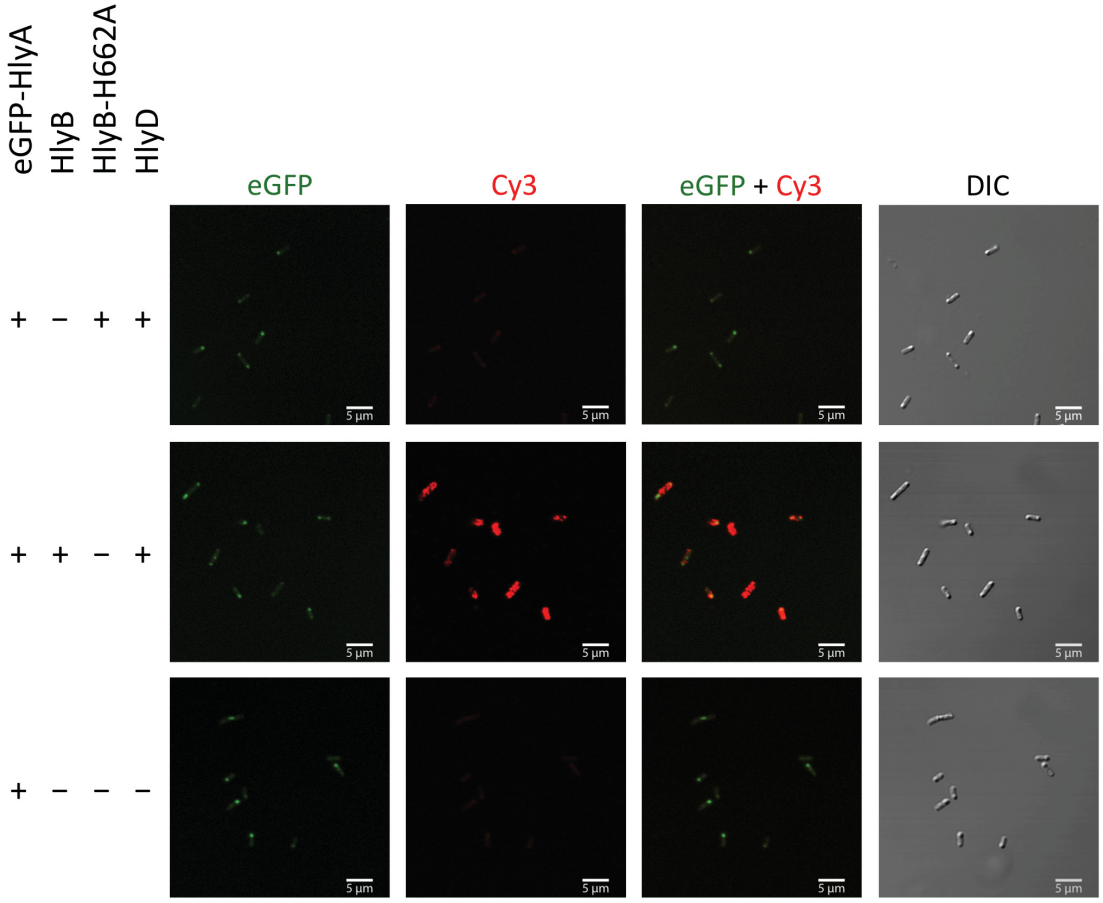

Figure 6: **Detection of the surface exposed HlyA fragment of eGFP-HlyA by confocal laser scanning microscopy.** *E. coli* cells expressed eGFP-HlyA and HlyD, as well as additional HlyB or HlyB-H662A. Shown is the eGFP fluorescence (left panel) of the fusion proteins, the HlyA mediated Cy3 fluorescence at the cell surface (second left panel), merged images of eGFP and Cy3 fluorescence (second right panel) and differential interference contrast (DIC) images of the cells (right panel). The different combinations of proteins employed are indicated to the left.

As a control, *E. coli* cells expressing eGFP-HlyA but not HlyB and HlyD were also analyzed (see Figure 6, third row). They show similar eGFP fluorescence comparable to HlyB-H662A expressing cells basically no Cy3 fluorescence.

Western blot analysis confirmed that HlyB, HlyB-H662A and HlyD as well as eGFP-HlyA are in the corresponding cells expressed and that the expression levels were equal and not influenced by the different T1SS composition.

Quantification of eGFP and Cy3 fluorescence demonstrates that the eGFP fluores-

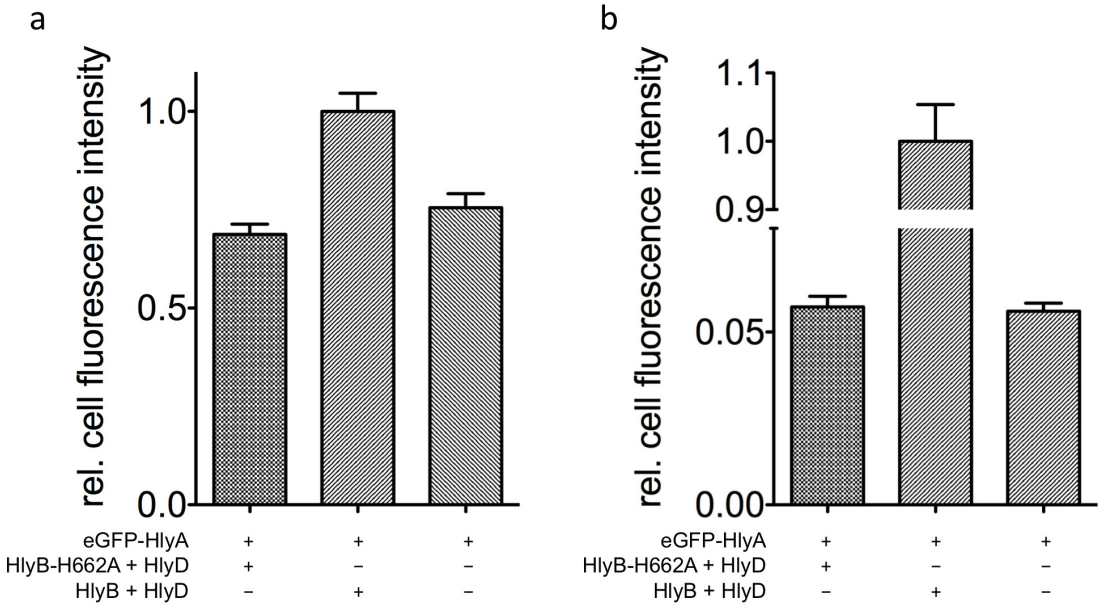

Figure 7: (a) Relative cell fluorescence of eGFP. All values were normalized to the eGFP fluorescence of the eGFP-HlyA fusion protein (error bars represent the standard error of the mean). (b) Relative fluorescence of Cy3. All values are normalized to Cy3 fluorescence of the eGFP-HlyA fusion protein (error bars represent the standard error of the mean). The different combinations of proteins employed are indicated below the bars.

cence of cells expressing eGFP-HlyA, HlyB-H662A and HlyD was approximately 68.8 ± 2.6 % (see Figure 7a, left bar) normalized to cells expressing eGFP-HlyA and native HlyB and HlyD (see Figure 7a, middle bar). eGFP fluorescence of cells only expressing eGFP-HlyA was with 75.5 ± 3.6 % in the same range (see Figure 7a, right bar). Cy3 fluorescence remains for cells expressing eGFP-HlyA, HlyB and HlyD with 5.7 ± 0.3 % (see Figure 7b, left bar) and for cells expressing eGFP-HlyA alone with 5.6 ± 0.2 % (see Figure 7b, right bar) on background level. Cy3 fluorescence was normalized to cells expressing eGFP-HlyA and native HlyB and HlyD (see Figure 7b, middle bar).

In summary, these results demonstrate that the eGFP-HlyA fusion protein only reached the cell surface if the ATP hydrolysis works properly and confirms that it is essential for initializing the translocation and threading the substrate into the translocator.

Discussion

Stalling the HlyA T1SS by an HlyAc fusion with the rapidly folding eGFP allowed analyzes of the translocator *in vivo*. It also allowed to analyze the orientation of the substrate during secretion [Radics et al., 2014, Lenders et al., 2015] and to quantify the number of active T1SS per cell (this study).

Recent experiments showed that substrates of T1SS are secreted in an unfolded state [Bakkes et al., 2010] and that substrates fused to a rapidly folding domain blocking all translocation pores of a cell [Lenders et al., 2015]. It can be assumed that for eGFP-HlyAc the eGFP could not enter the translocon and that HlyAc threads into the T1SS in an unfolded way. We assume that on average only one HlyA specific antibody and one monoclonal Cy3 linked secondary antibody binds to a single surface exposed fragment of HlyAc. Furthermore, even if more than one antibody bind per exposed HlyA fragment, the overall score of T1SS is a constant value in our secretion rate calculations. An increased value for T1SS will only decrease the secretion rate whereas lower T1SS value will increase it. Furthermore, a second method to determine the total amount of HlyB by Western blot was employed. Together with the assumption that HlyB is a dimer [Zaitseva et al., 2005], the method reproduced our fluoremetric determined value of around 5000 T1SS (see Supplementary Table 1).

In common, most substrates of T1SS have GG repeats. They correspond to the length of the protein and may have an influence on the secretion process itself [Delepelaire, 2004]. To analyze the GG repeat influence on the secretion process we used the native substrate HlyA (1024 aa amino acids and 6 GG repeats) and HlyAc (218 aa and 3 GG repeats). HlyA is 4 to 5 fold larger than HlyAc but has only the double amount of GG repeats. As described above the secretion rates for HlyA are $15.2 \pm 1.7\,\mathrm{aa\,T1SS^{-1}\,s^{-1}}$ and $14.1 \pm 1.0\,\mathrm{aa\,T1SS^{-1}\,s^{-1}}$ for HlyAc respectively are nearly identical. These clearly demonstrated that the protein length and GG repeat ratio has no influence on the secretion process itself and that the initial binding of the secretion signal to the T1SS is not rate limiting for the secretion process. There must be an alternative evolutionary reason for the protein length/GG repeat ratio. It could be possible that the GG repeats are important for the folding velocity of the protein and for its stability [Thomas et al., 2014].

GG repeats bind Ca^{2+} with an affinity of 100 µM and induces folding of the protein at the extracellular surface due to the high Ca^{2+} concentration [Rose et al., 1995, Jones et al., 1999, Rhodes et al., 2001]. Extracellular protein folding could involve an inherent driving force, which 'pulls' the protein out of the transporter. Our results did not

confirm this proposed mechanism [Linhartová et al., 2010]. After two hours of secretion, the secretion rate is not decreasing by deceeding the K_D and it is not increasing after exceeding it. After four hours of secretion, differences in the secreted amount of HlyA and HlyAc in the supernatant are detectable. This appeared due to the fact that the substrates reached a critical concentration inside the supernatant, resulting in aggregation of the protein. Here, HlyA is more stable as HlyAc in presence of low Ca^{2+} concentration that deceeds the K_D of the GG repeats. According to this, it could be shown that HlyA is more stable due to the folding stability of the N-terminal part of the protein [Thomas et al., 2014]. The N-terminal part is missing in HlyAc, which results in less stabile protein in the presence of lower Ca^{2+} concentration. These results indicate that the proposed "pulling" mechanism is not working and that the Ca^{2+} binding of the GG repeats mediates only protein stability. Another argument against this proposed mechanism is the fact that the GG repeats in most substrates are located in a cluster in the last third of the protein in front of the secretion signal. To get a continuous pulling effect a more homogeneous distribution of the GG repeats would be more likely.

Previous studies highlight the importance of ATP hydrolysis for protein translocation in the HlyA T1SS. HlyA secretion is completely abolished by using an HlyB ATP hydrolysis deficient mutants. Nevertheless, cross-linking experiments in the same study confirm that the translocator still assembles even in absence of ATP consumption [Thanabalu et al., 1998]. Our results show that ATP hydrolysis is essential for threading the substrate into the translocator. HlyA is not reaching the cell surface without ATP hydrolysis. This leads to two fundamental different working mechanisms of how HlyA T1SS is operating. First, continuous ATP consumption could be necessary for energizing the transport process. In that case, a defined number of ATP is consumed per transported amino acid. Such an iterative mechanism was observed for the protein SecA of the Sec pathway. Here, 152 - 228 amino acids per sec and transporter are transporter [Robson et al., 2009]. This process is faster than our observed secretion rate with at least $15.2 \pm 1.7\,\mathrm{aa\,T1SS^{-1}\,s^{-1}}$. However, the Sec pathway is one of the most essential nanomachineries in Gram-negative bacteria and responsible for the integration of most transmembrane proteins and the transport for many secretory proteins. Another possibility could be that ATP hydrolysis acts as a effector in some kind of ATP hydrolysis gated channel. Therefore, ATP hydrolysis initiates channel opening and allow transport of the substrate through the HlyA T1SS pore. In this proposed system, energizes of the secretion by ATP consumption is highly unlikely. T1SS substrates can have a size of more than 8000 aa and hydrolysis of only one or two ATP molecules can hardly energize the transport process. Other possibilities that can energize the transport process

are the proton motive force (which could be excluded in late stages of HlyA secretion [Koronakis et al., 1991]) or diffusion along a concentration or an electrostatic gradient. The proposed "pulling" mechanism as the inherent driving force is unlikely due to the result of our experiments.

In summary, our results allow for the first time the determination of the secretion rate of a T1SS. Furthermore, the proposed "pulling" mechanism for GG repeat containing substrates could not confirmed. Nevertheless, the driving force for type I secretion is still unknown. ATP hydrolysis could found to be essential for threading the protein into the translocator. If ATP hydrolysis is responsible for energizing the translocation is unproved and need further investigation.

Methods

Bacterial strains and plasmids

The *E. coli* strain DH5α was used for all cloning procedures. The pK184 plasmid (see Supplementary Figure 4) was used for HlyB and HlyD production under the control of a P_{lac} promotor, inducible with IPTG (isopropyl-β-D-1-thiogalactopyranoside) [Bakkes et al., 2010]. All plasmids and oligonucleotides used in this study are summarized in Supplementary Table 4 and 5.

Plasmids pSOI-eGFP-HlyAc and pSOI-eGFP-HlyA were used for eGFP-HlyAc respectively eGFP-HlyA expression under the control of a P_BAD promoter [Lenders et al., 2015].

Plasmids pSU-*hlyA* and pSU-*hlyA1* were used for HlyA respectively HlyAc expression under the control of a P_{lac} promotor, inducible with IPTG (isopropyl-β-D-1-thiogalactopyranoside) [Lecher et al., 2012, Thomas et al., 2014].

The HlyB-H662A mutant was expressed by using a variant of the pK184 plasmid (called pK184-HlyB-H662A-HlyD). To generate this variant a base pair substitution was induced by site-directed mutagenesis applying the primers H662A-5for-B-NBD and H662A-5rev-B-NBD.

Cell cultivation and protein expression for confocal laser scanning microscopy

Chemically competent *E. coli* BL21 (DE3) cells were transformed with or without pK184-HlyBD or pK184-HlyB-H662A-HlyD and pSOI-eGFP-HlyAc or pSOI-eGFP-HlyA and grown on LB agar plates supplemented with 100 µg mL^{-1} ampicillin and/or 30 µg mL^{-1}

kanamycin. *E. coli* BL21 (DE3) cells were prepared and induced identical as previously described [Lenders et al., 2015].

Cell fixation by formaldehyde treatment and immunofluorescence labeling of formaldehyde treated cells

Cell fixation and immunofluorescence labeling were carried out as previously described [Lenders et al., 2015].

Confocal laser scanning microscopy and image processing

Microscopy and image processing were carried out as previously described [Lenders et al., 2015].

Fluorescence spectrophotometer of immunofluorescence labeled formaldehyde treated cells

Immunofluorescence labeled formaldehyde treated *E. coli* BL21 (DE3) cells expressing eGFP-HlyAc with and without HlyB and HlyD and adjusted to an OD_600 of 1.0 were analyzed via a Jobin-Ivon Horiba Fluorolog-3 fluorescence spectrophotometer to quantify the amount of T1SS. All measurements were performed at 25 °C in a 50 µL cuvette. Excitation was performed at 547 nm, and fluorescence emission was monitored at 563 nm with slit widths set to 5 and 5 nm. Fluorescence were recorded for 0.5 s. An identical experiment was carried out with PBS buffer and different concentration of free Cy3 fluorophore linked secondary antibody starting from 1.5 µM and going down by halving to 0.5 pM.

Secretion experiments with HlyA and HlyAc in presence of different $CaCl_2$ concentration

Chemically competent *E. coli* BL21 (DE3) cells were transformed with pK184-HlyBD and pSU-*hlyA* and pSU-*hlyA1* and grown on LB agar plates supplemented with 100 µg mL^{-1} ampicillin and 30 µg mL^{-1} kanamycin.

Calcium concentration of 2YT medium was determined using atomic absorption spectroscopy.

Overnight cultures of single colonies were used to inoculate 25 mL 2YT medium supplemented with 100 µg mL^{-1} ampicillin and 30 µg mL^{-1} at an OD_{600} of 0.1.

Cultures were grown at 37 °C and 180 rpm. The expression of HlyA, HlyAc, HlyB and HlyD was induced with 1 mM IPTG at an OD_{600} of 0.6 - 0.8. EGTA respectively $CaCl_2$ were added at this point to adjust the final calcium concentration in the culture media. Cells were grown for 4 h at 180 rpm and 37 °C. A 1 mL aliquot was taken and centrifuged for 5 min at 14 000 g, 4 °C each hour during growth. Cells were adjusted with water to $OD_{equivalents}$ of 0.1 and supernatant were analyzed eightfold diluted on SDS-PAGE.

A concentration line of purified HlyA reaching from 40 µg mL^{-1} and going down by halving to 625 ng mL^{-1} or HlyAc reaching from 50 µg mL^{-1} and going down by halving to 758 ng mL^{-1} were loaded on each SDS-PAGE.

Gels were stained using Coomassie Brilliant Blue (CBB) staining. The expression levels of HlyB and HlyD as well as the expression of intracellular amount of HlyA and HlyAc were determined via Western blots using polyclonal antibodies against HlyA, HlyB or HlyD in combination with an horseradish peroxidase (HRP)-conjugated, secondary antibody using the ECL advance kit (GE Healthcare).

Secretion experiments data processing

The program ImageJ was used for processing and determining the SDS-PAGE band intensity. HlyA and HlyAc bands were marked and plotted. The intensity of the band of purified HlyA and HlyAc bands for the concentration line was used to determine the concentration of the secreted HlyA respectively HlyAc. The slop of the plotted HlyA and HlyAc amount represents the amount of secreted HlyA or HlyAc per time. This amount can be divided by the growth factor of the cells in their exponential growing phase. The quotient represents the amount of secreted HlyA or HlyAc per time and cell and can transformed by the amount of T1SS per cell and the length of HlyA or HlyAc to amino acids per sec and T1SS.

Determining the amount of T1SS by HlyB western blot

Cells from the secretion experiments with HlyA or HlyAc were used. Cell from the 1 mL aliquot adjusted with water to $OD_{equivalents}$ of 0.1 and 2 h after induction of HlyB and HlyD were analyzed via Western blots as described above. A concentration line of purified HlyB reaching from 9 µg mL^{-1} and going down by halving to 144 ng mL^{-1} was loaded on the western blot.

Western blots were analyzed using the program ImageJ. The HlyB bands were marked and plotted. The intensity of purified HlyB bands for the concentration line

were used to determine the concentration of expressed HlyB by the cells. The amount was divided by the cell count. We end up with the amount of HlyB per cell. Dividing by half gives the total number of T1SS per cell.

Purification of HlyA, HlyAc and HlyB for regression curves

Purification of HlyA and HlyAc were carried out as previously described [Lecher et al., 2012, Thomas et al., 2014].

HlyB purification will be identically described and published in Reimann et al. 2015 (under revision). *E. coli* BL21 (DE3) was transformed with pBADHlyB and exposed on selective agar plates containing 100 µg mL^{-1} ampicillin. An overnight culture was inoculated with a single *E. coli* colony and incubated for 16 h at 37 °C and vigorously shaking at 200 rpm. A main culture with selective 2YT medium was inoculated from the overnight culture and grown to an OD_{600} of 4.0 before expression was started by adding 10 mM arabinose. After 2 h of protein expression, cells were harvested by centrifugation and resuspended in buffer A (25 mM NaH_2PO_4, 100 mM KCl, 20 % glycerol, pH 8). Bacteria were disrupted by a cell disrupter (Constant Systems) at 2.5 kbar. Homogenisate was centrifuged at 12 000 g and the supernatant was centrifuged again at 120 000 g. The pellet containing cell membranes was resuspended in buffer A, solubilized with 1 % Fos Cholin 14 at 4 °C for 1 h and centrifuged again at 120 000 g for 30 min. The supernatant was loaded on a metal ion affinity chromatography (IMAC) column (5 mL HiTrap Chelating HP column, GE Healthcare, loaded with $ZnSO_4$) and washed with buffer A, including 0.02 % lauryl maltose neopentyl glycol (LMNG). Unspecifically bound protein was removed by washing with buffer A including 40 mM histidine and HlyB was eluted with buffer A including 150 mM histidine. HlyB containing fractions were pooled and concentrated by ultrafiltration using an Amicon Ultra Centrifugal Filterunit (100,000 MWCO, Merck Millipore). To increase protein purity and to change the buffer, a size exclusion chromatography was performed using a Superdex 200 10/300 GL (GE Healthcare) using buffer B (10 mM CAPS, 20 % glycerol, pH 10.4) including 0.02 % LMNG. HlyB containing fractions were flash-frozen in liquid nitrogen and stored at −80 °C until further use.

Acknowledgment

We would like to thank Iris Fey, Protein Production Facility, Heinrich-Heine-Universitaet, for technical support. We thank Sven Reimann, Sandra Peherstorfer and Kerstin Kanonen-

berg for providing us with the purified proteins HlyB, HlyA and HlyAc. We thank all members of the Institute of Biochemistry, Heinrich-Heine-Universitaet Düsseldorf, for helpful and very fruitful discussions. We gratefully acknowledge support (and training) from the International NRW Research School BioStruct, granted by the Ministry of Innovation, Science and Research of the State North Rhine-Westphalia, the Heinrich-Heine-Universitaet Duesseldorf, and the Entrepreneur Foundation at the Heinrich-Heine-Universitaet of Duesseldorf.

References

[Bakkes et al., 2010] Bakkes, P. J., Jenewein, S., Smits, S. H. J., Holland, I. B. and Schmitt, L. (2010). The rate of folding dictates substrate secretion by the Escherichia coli hemolysin type 1 secretion system. J Biol Chem *285*, 40573–80.

[Delepelaire, 2004] Delepelaire, P. (2004). Type I secretion in gram-negative bacteria. Biochim Biophys Acta *1694*, 149–61.

[Dong et al., 2004] Dong, X., Stothard, P., Forsythe, I. J. and Wishart, D. S. (2004). PlasMapper: a web server for drawing and auto-annotating plasmid maps. Nucleic Acids Res *32*, W660–4.

[Evdokimov et al., 2006] Evdokimov, A. G., Pokross, M. E., Egorov, N. S., Zaraisky, A. G., Yampolsky, I. V., Merzlyak, E. M., Shkoporov, A. N., Sander, I., Lukyanov, K. A. and Chudakov, D. M. (2006). Structural basis for the fast maturation of Arthropoda green fluorescent protein. EMBO Rep *7*, 1006–12.

[Famulla, 2007] Famulla, S. (2007). Analyse der periplasmatischen Domäne des Membranfusionsproteins HlyD. Heinrich Heine Universität Düsseldorf *Diploma thesis*.

[Ghigo and Wandersman, 1994] Ghigo, J. M. and Wandersman, C. (1994). A carboxyl-terminal four-amino acid motif is required for secretion of the metalloprotease PrtG through the Erwinia chrysanthemi protease secretion pathway. J Biol Chem *269*, 8979–85.

[Gray et al., 1986] Gray, L., Mackman, N., Nicaud, J. M. and Holland, I. B. (1986). The carboxy-terminal region of haemolysin 2001 is required for secretion of the toxin from Escherichia coli. Mol Gen Genet *205*, 127–33.

[Hinsa et al., 2003] Hinsa, S. M., Espinosa-Urgel, M., Ramos, J. L. and O'Toole, G. A. (2003). Transition from reversible to irreversible attachment during biofilm formation by Pseudomonas fluorescens WCS365 requires an ABC transporter and a large secreted protein. Mol Microbiol *49*, 905–18.

[Hussmann, 2013] Hussmann, L. (2013). Charakterisierung des Memrbanfusionproteins Hämolysin D. Heinrich Heine Universität Düsseldorf *Bachelor thesis*.

[Jarchau et al., 1994] Jarchau, T., Chakraborty, T., Garcia, F. and Goebel, W. (1994). Selection for transport competence of C-terminal polypeptides derived from Escherichia coli hemolysin: the shortest peptide capable of autonomous HlyB/HlyD-dependent secretion comprises the C-terminal 62 amino acids of HlyA. Mol Gen Genet *245*, 53–60.

[Jones et al., 1999] Jones, H. E., Holland, I. B., Baker, H. L. and Campbell, A. K. (1999). Slow changes in cytosolic free Ca2+ in Escherichia coli highlight two putative influx mechanisms in response to changes in extracellular calcium. Cell Calcium *25*, 265–74.

[Kenny et al., 1994] Kenny, B., Chervaux, C. and Holland, I. B. (1994). Evidence that residues -15 to -46 of the haemolysin secretion signal are involved in early steps in secretion, leading to recognition of the translocator. Mol Microbiol *11*, 99–109.

[Koronakis et al., 1991] Koronakis, V., Hughes, C. and Koronakis, E. (1991). Energetically distinct early and late stages of HlyB/HlyD-dependent secretion across both Escherichia coli membranes. EMBO J *10*, 3263–72.

[Koronakis et al., 1989] Koronakis, V., Koronakis, E. and Hughes, C. (1989). Isolation and analysis of the C-terminal signal directing export of Escherichia coli hemolysin protein across both bacterial membranes. EMBO J *8*, 595–605.

[Lecher et al., 2012] Lecher, J., Schwarz, C. K. W., Stoldt, M., Smits, S. H. J., Willbold, D. and Schmitt, L. (2012). An RTX transporter tethers its unfolded substrate during secretion via a unique N-terminal domain. Structure *20*, 1778–87.

[Lenders et al., 2013] Lenders, M. H. H., Reimann, S., Smits, S. H. J. and Schmitt, L. (2013). Molecular insights into type I secretion systems. Biol Chem *394*, 1371–84.

[Lenders et al., 2015] Lenders, M. H. H., Weidtkamp-Peters, S., Kleinschrodt, D., Jaeger, K.-E., Smits, S. H. J. and Schmitt, L. (2015). Directionality of substrate translocation of the hemolysin A Type I secretion system. Sci Rep *5*, 12470.

[Létoffé et al., 1996] Létoffé, S., Delepelaire, P. and Wandersman, C. (1996). Protein secretion in gram-negative bacteria: assembly of the three components of ABC protein-mediated exporters is ordered and promoted by substrate binding. EMBO J *15*, 5804–11.

[Létoffé et al., 1994] Létoffé, S., Ghigo, J. M. and Wandersman, C. (1994). Secretion of the Serratia marcescens HasA protein by an ABC transporter. J Bacteriol *176*, 5372–7.

[Linhartová et al., 2010] Linhartová, I., Bumba, L., Mašín, J., Basler, M., Osička, R., Kamanová, J., Procházková, K., Adkins, I., Hejnová-Holubová, J., Sadílková, L., Morová, J. and Sebo, P. (2010). RTX proteins: a highly diverse family secreted by a common mechanism. FEMS Microbiol Rev *34*, 1076–112.

[Nicaud et al., 1986] Nicaud, J. M., Mackman, N., Gray, L. and Holland, I. B. (1986). The C-terminal, 23 kDa peptide of E. coli haemolysin 2001 contains all the information necessary for its secretion by the haemolysin (Hly) export machinery. FEBS Lett *204*, 331–5.

[Omori et al., 2001] Omori, K., Idei, A. and Akatsuka, H. (2001). Serratia ATP-binding cassette protein exporter, Lip, recognizes a protein region upstream of the C terminus for specific secretion. J Biol Chem *276*, 27111–9.

[Radics et al., 2014] Radics, J., Königsmaier, L. and Marlovits, T. C. (2014). Structure of a pathogenic type 3 secretion system in action. Nat Struct Mol Biol *21*, 82–7.

[Renn, 2013] Renn, A. (2013). Analyse des Membranfusionsproteins HlyD. Heinrich Heine Universität Düsseldorf *Bachelor thesis*.

[Rhodes et al., 2001] Rhodes, C. R., Gray, M. C., Watson, J. M., Muratore, T. L., Kim, S. B., Hewlett, E. L. and Grisham, C. M. (2001). Structural consequences of divalent metal binding by the adenylyl cyclase toxin of Bordetella pertussis. Arch Biochem Biophys *395*, 169–76.

[Richter, 2012] Richter, D. (2012). Analyse der Interaktionspartner von HlyD. Heinrich Heine Universität Düsseldorf *Bachelor thesis*.

[Robson et al., 2009] Robson, A., Gold, V. A. M., Hodson, S., Clarke, A. R. and Collinson, I. (2009). Energy transduction in protein transport and the ATP hydrolytic cycle of SecA. Proc Natl Acad Sci U S A *106*, 5111–6.

[Rose et al., 1995] Rose, T., Sebo, P., Bellalou, J. and Ladant, D. (1995). Interaction of calcium with Bordetella pertussis adenylate cyclase toxin. Characterization of multiple calcium-binding sites and calcium-induced conformational changes. J Biol Chem *270*, 26370–6.

[Schlumberger et al., 2005] Schlumberger, M. C., Müller, A. J., Ehrbar, K., Winnen, B., Duss, I., Stecher, B. and Hardt, W.-D. (2005). Real-time imaging of type III secretion: Salmonella SipA injection into host cells. Proc Natl Acad Sci U S A *102*, 12548–53.

[Schwarz et al., 2012] Schwarz, C. K. W., Landsberg, C. D., Lenders, M. H. H., Smits, S. H. J. and Schmitt, L. (2012). Using an E. coli Type 1 secretion system to secrete the mammalian, intracellular protein IFABP in its active form. J Biotechnol *159*, 155–61.

[Sebo and Ladant, 1993] Sebo, P. and Ladant, D. (1993). Repeat sequences in the Bordetella pertussis adenylate cyclase toxin can be recognized as alternative carboxy-proximal secretion signals by the Escherichia coli alpha-haemolysin translocator. Mol Microbiol *9*, 999–1009.

[Stanley et al., 1991] Stanley, P., Koronakis, V. and Hughes, C. (1991). Mutational analysis supports a role for multiple structural features in the C-terminal secretion signal of Escherichia coli haemolysin. Mol Microbiol *5*, 2391–403.

[Thanabalu et al., 1998] Thanabalu, T., Koronakis, E., Hughes, C. and Koronakis, V. (1998). Substrate-induced assembly of a contiguous channel for protein export from E.coli: reversible bridging of an inner-membrane translocase to an outer membrane exit pore. EMBO J *17*, 6487–96.

[Thomas et al., 2014] Thomas, S., Bakkes, P. J., Smits, S. H. J. and Schmitt, L. (2014). Equilibrium folding of pro-HlyA from Escherichia coli reveals a stable calcium ion dependent folding intermediate. Biochim Biophys Acta *1844*, 1500–10.

[Zaitseva et al., 2005] Zaitseva, J., Jenewein, S., Jumpertz, T., Holland, I. B. and Schmitt, L. (2005). H662 is the linchpin of ATP hydrolysis in the nucleotide-binding domain of the ABC transporter HlyB. EMBO J *24*, 1901–10.

Supplementary

Table 1: **Number of T1SS**

	Transporter
by fluorometry	3170
	5840
by western blot	6010
	5075
Mean	5024 ± 1301

Table 2: **Values for HlyAc transport rate calculation with different calcium concentration**

Condition	#	Secreted HlyAc after		Secreted HlyAc	Cell growth	Rate
		2 h [mol]	4 h [mol]	[mol min^{-1}]	[cells min^{-1}]	[T1SS^{-1} s^{-1}]
0.00 mM	1	5.4×10^{-11}	7.0×10^{-11}	4.8×10^{-13}	1.23×10^{7}	17.0 aa
$CaCl_2$	2	4.7×10^{-11}	4.4×10^{-11}	4.4×10^{-13}	1.15×10^{7}	18.8 aa
	3	3.7×10^{-11}	4.5×10^{-11}	2.8×10^{-13}	1.17×10^{7}	10.7 aa
0.05 mM	1	5.0×10^{-11}	6.5×10^{-11}	5.5×10^{-13}	1.45×10^{7}	16.6 aa
$CaCl_2$	2	4.0×10^{-11}	5.6×10^{-11}	4.6×10^{-13}	1.53×10^{7}	13.0 aa
	3	3.6×10^{-11}	4.6×10^{-11}	5.2×10^{-13}	1.53×10^{7}	14.9 aa
0.10 mM	1	4.4×10^{-11}	6.9×10^{-11}	5.7×10^{-13}	1.47×10^{7}	17.0 aa
$CaCl_2$	2	4.3×10^{-11}	6.2×10^{-11}	5.0×10^{-13}	1.45×10^{7}	15.2 aa
	3	4.9×10^{-11}	7.1×10^{-11}	5.2×10^{-13}	1.39×10^{7}	16.2 aa
0.15 mM	1	3.9×10^{-11}	5.5×10^{-11}	5.3×10^{-13}	1.43×10^{7}	16.1 aa
$CaCl_2$	2	4.3×10^{-11}	1.0×10^{-10}	5.0×10^{-13}	1.48×10^{7}	14.9 aa
	3	3.4×10^{-11}	8.8×10^{-11}	4.6×10^{-13}	1.48×10^{7}	13.5 aa
0.25 mM	1	4.7×10^{-11}	1.1×10^{-10}	5.5×10^{-13}	1.49×10^{7}	16.0 aa
$CaCl_2$	2	6.0×10^{-11}	1.2×10^{-10}	5.8×10^{-13}	1.49×10^{7}	16.9 aa
	3	6.0×10^{-11}	1.1×10^{-10}	4.9×10^{-13}	1.49×10^{7}	14.4 aa
0.45 mM	1	4.1×10^{-11}	9.5×10^{-11}	3.8×10^{-13}	1.52×10^{7}	10.9 aa
$CaCl_2$	2	3.6×10^{-11}	8.4×10^{-11}	4.2×10^{-13}	1.51×10^{7}	12.2 aa
	3	2.7×10^{-11}	8.0×10^{-11}	4.0×10^{-13}	1.51×10^{7}	11.5 aa
0.65 mM	1	5.4×10^{-11}	1.3×10^{-10}	6.7×10^{-13}	1.61×10^{7}	18.3 aa

$CaCl_2$	2	3.8×10^{-11}	1.0×10^{-10}	5.6×10^{-13}	1.44×10^{7}	16.9 aa
5.00 mM	1	4.4×10^{-11}	1.1×10^{-10}	5.3×10^{-13}	1.45×10^{7}	16.0 aa
$CaCl_2$	2	3.7×10^{-11}	9.6×10^{-11}	4.9×10^{-13}	1.41×10^{7}	15.4 aa
	3	4.4×10^{-11}	9.8×10^{-11}	4.9×10^{-13}	1.41×10^{7}	15.1 aa

Table 3: **Values for HlyA transport rate calculation with different calcium concentration**

Condition	#	Secreted HlyA after		Secreted HlyA	Cell growth	Rate
		2 h [mol]	4 h [mol]	[mol min^{-1}]	[cells min^{-1}]	[T1SS^{-1} s^{-1}]
0.00 mM	1	5.2×10^{-12}	9.9×10^{-12}	8.1×10^{-14}	9.80×10^{6}	16.9 aa
$CaCl_2$	2	4.4×10^{-12}	8.0×10^{-12}	6.8×10^{-14}	1.03×10^{7}	13.6 aa
0.05 mM	1	6.8×10^{-12}	1.7×10^{-11}	9.1×10^{-14}	1.11×10^{7}	16.8 aa
$CaCl_2$	2	6.4×10^{-12}	1.7×10^{-11}	9.1×10^{-14}	1.24×10^{7}	15.1 aa
	3	6.1×10^{-12}	1.6×10^{-11}	8.6×10^{-14}	1.31×10^{7}	13.4 aa
0.10 mM	1	5.5×10^{-12}	1.8×10^{-11}	9.6×10^{-14}	1.38×10^{7}	14.2 aa
$CaCl_2$	2	5.5×10^{-12}	2.1×10^{-11}	9.1×10^{-14}	1.38×10^{7}	13.5 aa
0.15 mM	1	9.6×10^{-12}	2.8×10^{-11}	1.5×10^{-13}	1.95×10^{7}	15.4 aa
$CaCl_2$	2	7.5×10^{-12}	2.0×10^{-11}	1.1×10^{-13}	1.84×10^{7}	11.8 aa
0.25 mM	1	6.3×10^{-12}	2.0×10^{-11}	1.1×10^{-13}	1.56×10^{7}	14.4 aa
$CaCl_2$	2	5.1×10^{-12}	2.1×10^{-11}	8.5×10^{-14}	1.45×10^{7}	11.9 aa
	3	6.5×10^{-12}	1.9×10^{-11}	9.8×10^{-14}	1.58×10^{7}	12.7 aa
0.45 mM	1	7.9×10^{-12}	2.1×10^{-11}	1.1×10^{-13}	1.49×10^{7}	14.9 aa
$CaCl_2$	2	7.2×10^{-12}	2.2×10^{-11}	1.1×10^{-13}	1.71×10^{7}	13.7 aa
	3	7.4×10^{-12}	1.7×10^{-11}	8.9×10^{-14}	1.50×10^{7}	12.2 aa
0.65 mM	1	5.8×10^{-12}	1.8×10^{-11}	9.6×10^{-14}	1.36×10^{7}	14.4 aa
$CaCl_2$	2	6.1×10^{-12}	2.1×10^{-11}	1.1×10^{-13}	1.59×10^{7}	14.6 aa
	3	8.2×10^{-12}	2.3×10^{-11}	1.2×10^{-13}	1.37×10^{7}	17.6 aa
5.00 mM	1	9.6×10^{-12}	2.5×10^{-11}	1.3×10^{-13}	2.01×10^{7}	13.0 aa
$CaCl_2$	2	9.7×10^{-12}	2.4×10^{-11}	1.27×10^{-13}	2.04×10^{7}	12.7 aa
	3	9.3×10^{-12}	2.5×10^{-11}	1.3×10^{-13}	2.04×10^{7}	12.9 aa

Table 4: **Primers used in this study**

Name	Sequence
H662A-5for-B-NBD	5'-CGGTTATAATCATTGCTGCGCGTCTGTCTACAGTAA-3'
H662A-3rev-B-NBD	5'-TTACTGTAGACAGACGCGCAGCAATGATTATAACCG-3'

Table 5: **Plasmids used in this study**

Name	Description	Referenz
pK184-HlyB	Plasmid encoding hlyB and hlyD	[Bakkes et al., 2010]
pK184-HlyB-H662A-HlyD	Plasmid pK184-HlyB with a base pair substitution to generate *hlyB-H662A* via site-directed mutagenesis; encodes for *hlyB-H662A* and *hlyD*	This study
pSU-*hlyA*	Plasmid encoding *hlyA*	[Thomas et al., 2014]
pSU-*hlyA1*	Plasmid encoding *hlyAc*	[Lecher et al., 2012]
pSOI-eGFP-HlyAc	Plasmid encoding *eGFP-hlyAc*	[Lenders et al., 2015]
pSOI-eGFP-HlyA	Plasmid encoding *eGFP-hlyA*	[Lenders et al., 2015]

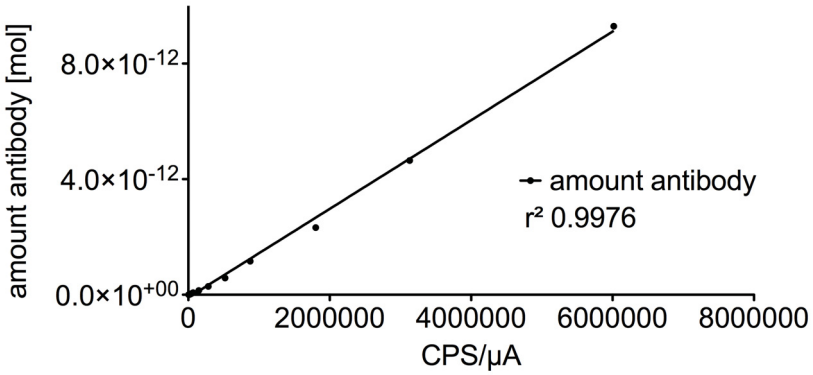

Figure 1: **Cy3 fluorescence regression curve for free secondary antibody.** Shown is the determined Cy3 fluorescence in CPS μA^{-1} depending on the amount of applied antibody in mol.

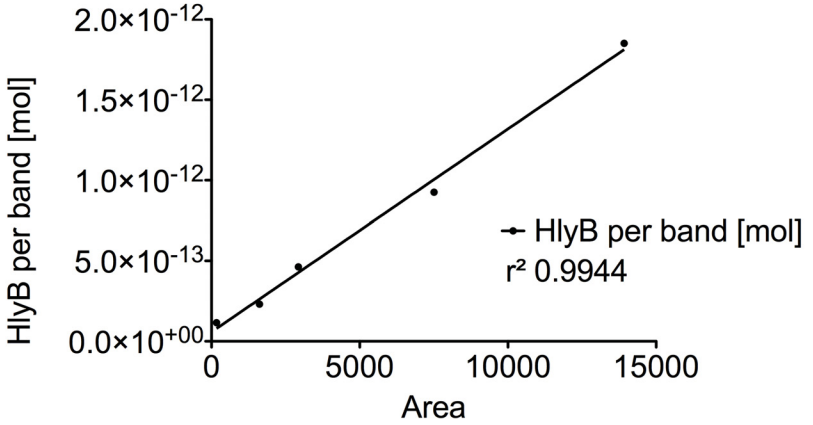

Figure 2: **Integrated area respectively integral density of the HlyB western blot signals for purified HlyB.** Shown is the integral density of the HlyB western blot signals depending on the amount of purified HlyB in mol.

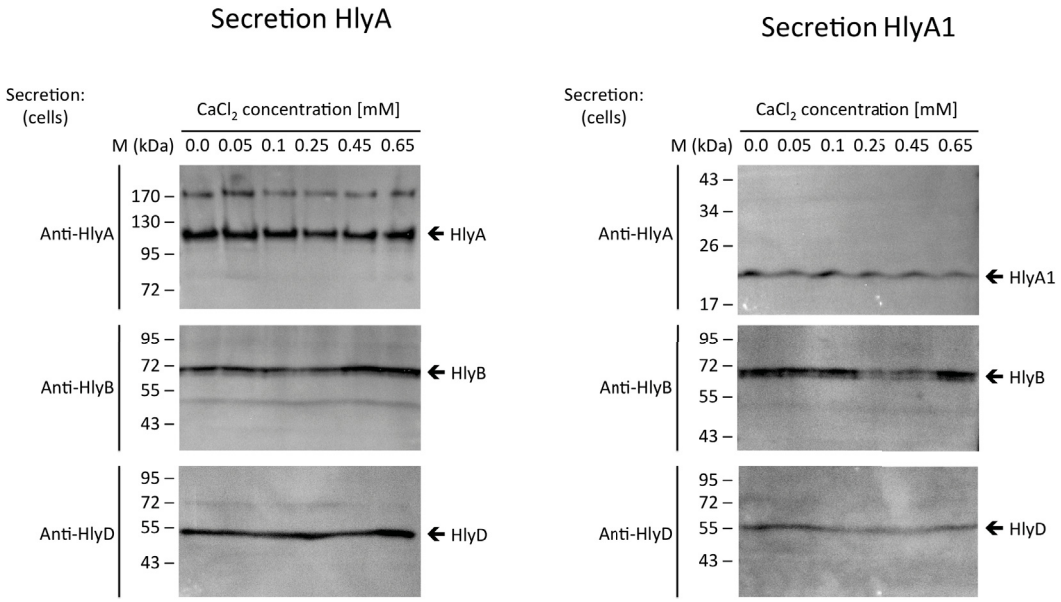

Figure 3: **Western blot analysis of total cells content after** 2 h **of secretion rate analyst cells for different Ca^{2+} concentration.** HlyA respectively HlyAc, HlyB and HlyD are only present if the corresponding promotors were induced and their total amount is equal during expression and secretion with different Ca^{2+} concentration.

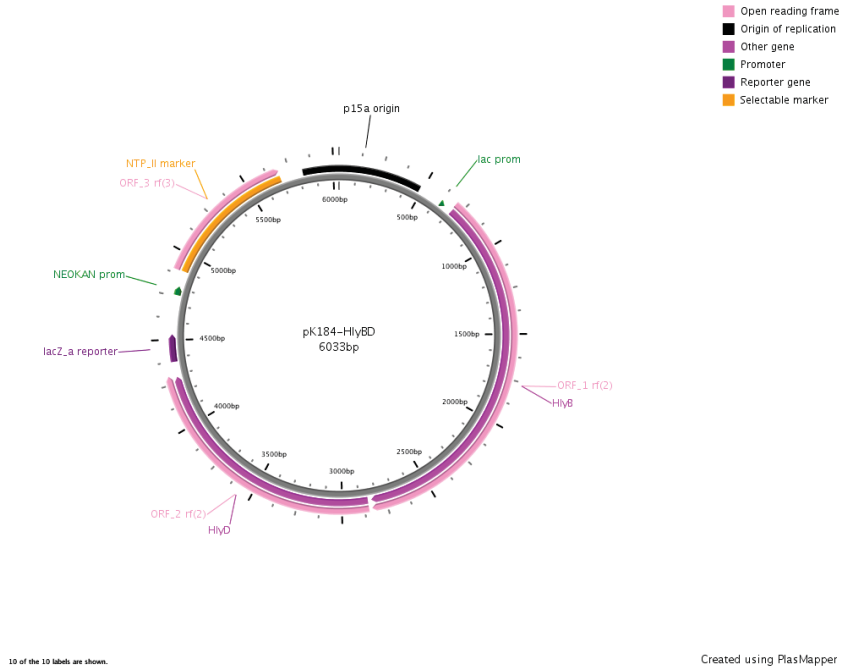

Figure 4: **Plasmid map pK184-HlyBD.** The map was created using the PlasMapper web server [Dong et al., 2004].

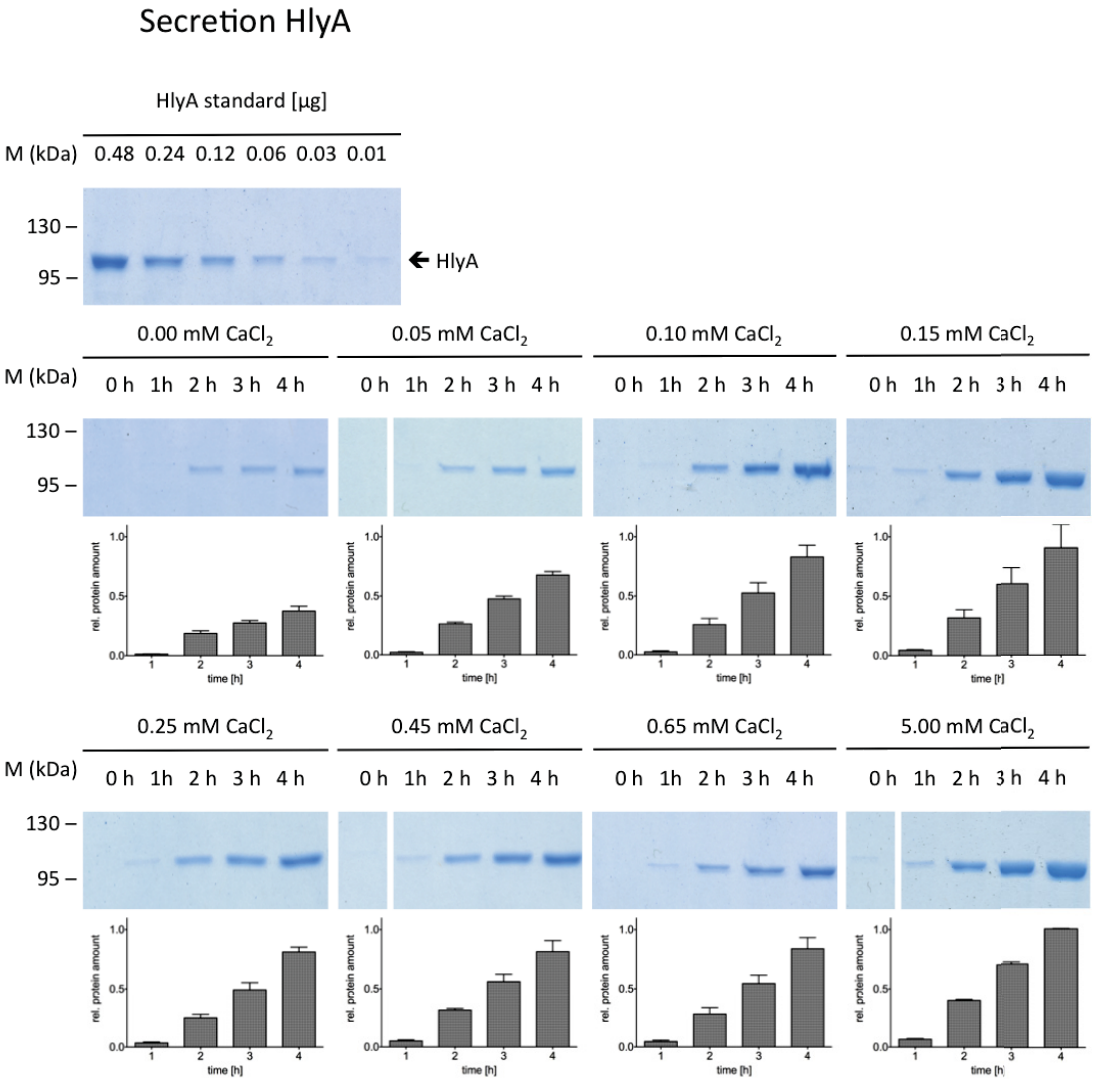

Figure 5: **Secretion level of HlyA in presence of different extracellular Ca^{2+} concentration.** SDS-PAGE analysis of the HlyA secretion level in the culture supernatant over a four-hour time period. Upper SDS-PAGE represent the concentration series of purified HlyA. The used amounts are mentioned above the gel. Middle and lower SDS-PAGEs show the HlyA secretion level after every hour. Different extracellular Ca^{2+} concentration are highlighted above the gels. Bar diagrams below the SGS-PAGEs show the relative intensity of the SDS-PAGE bands. Bands are normalized on the highest mean value of secreted HlyA after 4 h secretion time. Error bars represent the standard deviation.

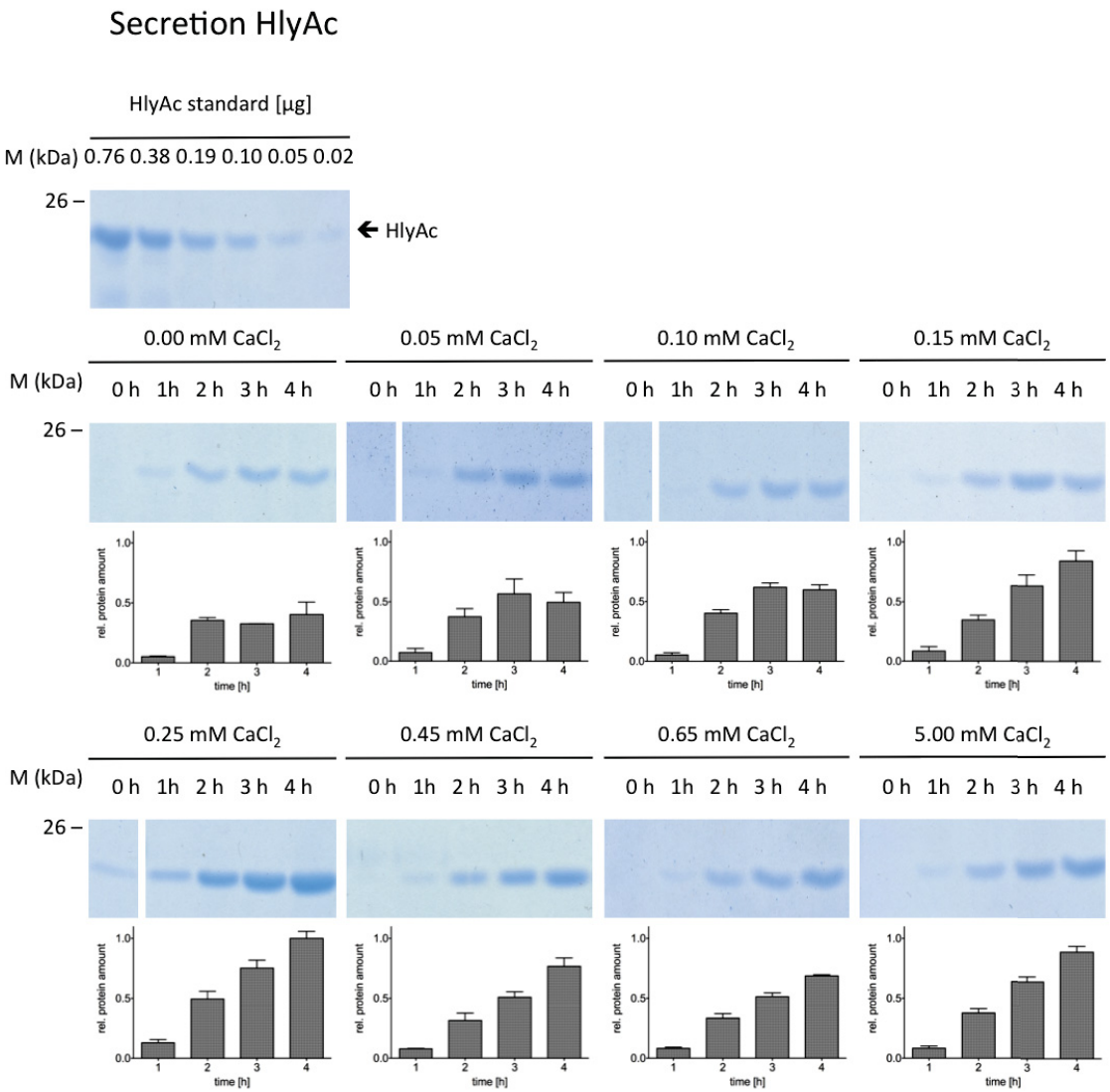

Figure 6: **Secretion level of HlyAc in presence of different extracellular Ca^{2+} concentration.** SDS-PAGE analysis of the HlyAc secretion level in the culture supernatant over a four-hour time period. Upper SDS-PAGE represent the concentration series of purified HlyAc. The used amounts are mentioned above the gel. Middle and lower SDS-PAGEs show the HlyAc secretion level after every hour. Different extracellular Ca^{2+} concentration are highlighted above the gels. Bar diagrams below the SGS-PAGEs show the relative intensity of the SDS-PAGE bands. Bands are normalized on the highest mean value of secreted HlyAc after 4 h secretion time. Error bars represent the standard deviation.

3.7. Chapter VII - Characterization of the membrane fusion protein hemolysin D

Title Characterization of the membrane fusion protein hemolysin D

Authors Michael H.H. Lenders, Sander H.J. Smits and Lutz Schmitt

In Preparation

Own proportion of this work 60 %;
Construction of the plasmids, purification of the different constructs, circular dichroism spectroscopy, crystallization trials, homology model simulations, writing of the manuscript.

Characterization of the membrane fusion protein HlyD

Michael H.H. Lenders, Sander H.J. Smits and Lutz Schmitt*

Institute of Biochemistry, Heinrich-Heine-Universität,
40225 Düsseldorf, Germany

Abstract

Type I secretion system (T1SS) consists of an ABC transporter and a membrane fusion protein (MFP). The ABC transporter HlyB secretes the 110 kDa toxin HlyA in one step from the cytoplasm directly into the extracellular space. To achieve this a complex with the MFP HlyD and the outer membrane protein TolC is formed. HlyD is a single-spanning membrane protein. The N-terminal 62 residues are located in the cytosol which adopt an unknown function and a single α-helix predicted to contain twenty amino acids spans the inner membrane. The remaining 396 residues reside in the periplasmic space forming a domain, which closes the gap between TolC and HlyB. So far, no structural information of HlyD is known. The oligomeric state of HlyD is currently unknown but thought to be hexameric, which bridges a dimeric HlyB with the trimeric TolC. To answer these questions, different tagged and untagged protein variants were designed and purification strategies were established. We are able to purify high homogeneous amounts of full-length HlyD and of the periplasmic HlyD fragment, which show monomeric and oligomeric states in solution. Blue native PAGE and multi angle light scattering indicate a trimer as well as a hexamer. Further, initial crystalisation trails were tested.

*To whom correspondence should be addressed: Lutz.Schmitt@hhu.de,
Tel. +49 211 81-10773, Fax +49 211 81-15310, Universitätsstraße 1, 40225 Düsseldorf, Germany

Introduction

Bacterial type I secretion system (T1SS) allow the transport of a broad range of substrate from the cytoplasm into the extracellular space [Delepelaire, 2004]. The transport of the substrate occurs unfolded without any periplasmic intermediate [Thanassi and Hultgren, 2000, Debarbieux and Wandersman, 2001, Bakkes et al., 2010, Schwarz et al., 2012].

A prominent example for an *Escherichia coli* T1SS is the hemolysin A (HlyA) secretion system. It consist of three different kinds of membrane proteins that build up a continuous channel across both membranes to allow translocation of the 110 kDa toxin HlyA. The inner membrane localized ABC transporter hemolysin B (HlyB) recognizes the substrate and enables secretion whereas the outer membrane protein (OMP) TolC builds a pore through the outer membrane [Thanabalu et al., 1998, Koronakis et al., 2000, Benabdelhak et al., 2003]. The periplasmic gap between both proteins is bridged by the membrane fusion protein (MFP) hemolysin D (HlyD) that is essential for recruiting the whole HlyA T1SS [Thanabalu et al., 1998]. Further, HlyD is involved in substrate recognition, coupled with TolC recruitment [Thanabalu et al., 1998, Balakrishnan et al., 2001].

The structure of HlyD is unknown. Hydrophilicity plots indicate a single transmembrane helix between amino acids 60 to 79 [Johnson and Church, 1999, Zgurskaya et al., 2009]. The small cytosolic domain (first 59 amino acids) is involved in substrate recognition and essential for TolC recruitment [Balakrishnan et al., 2001] whereas the large periplasmic domain (amino acids 80 to 478) is important for direct TolC interaction and the proper secretion of HlyA [Pimenta et al., 2005, Lee et al., 2012]. Crystal structures of other MFPs that are involved in resistance-nodulation-division (RND) efflux pumps [Higgins et al., 2004, Yum et al., 2009, Su et al., 2009, Akama et al., 2004] indicate that the periplasmic part of the proteins harbors two highly conserved lipoyl half-motifs that are connected by an α-helical domain with an α-hairpin [Johnson and Church, 1999, Zgurskaya et al., 2009]. This α-helical domain can vary in size from 20 Å in case of CusB to 127 Å for EmrA [Su et al., 2009, Hinchliffe et al., 2014]. Biochemical studies of this proteins show that they drive only OMP recruitment but are not mediating direct substrate interaction like HlyD [Balakrishnan et al., 2001, Kim et al., 2010, Xu et al., 2010].

The oligomeric state of MFPs differs dramatically in different secretion systems [Tikhonova et al., 2009]. In case of AcrA, a hexameric state could be determined as the active protein conformation [Xu et al., 2011] whereas a trimer is assumed to be the active state for EmrA [Borges-Walmsley et al., 2003]. For HlyD, dimers and trimers

could be detected [Thanabalu et al., 1998]. Nevertheless, the crystal structure for the HlyB NBDs show a dimer whereas TolC is characterized as a trimer [Koronakis et al., 2000, Zaitseva et al., 2006]. A hexameric state of HlyD could bridge both proteins.

For that purpose, the structure of HlyD could answer the questions how HlyD-HlyA interaction mediates TolC recruitment, how the periplasmic part of the MFP interacts with the OMP and HlyA during secretion and how HlyD manage to bridge HlyB and TolC. We tired to crystallized HlyD and perform cross-linking to answer this questions.

Results

Purification of HlyD-His

Many structures of MFPs could be solved during the last years [Akama et al., 2004, Higgins et al., 2004, Su et al., 2009, Yum et al., 2009]. Nevertheless, the structures of MFPs that are involved in T1SS and that are important for substrate recognition and OMP recruitment are unknown [Thanabalu et al., 1998, Balakrishnan et al., 2001]. For that purpose, initial trials for purifying HlyD with an affinity tag were done and will be described in more detail.

The HlyB and HlyD producing pK184 plasmid was transformed to *E. coli* BL21 (DE3) cells. The P_{lac} promoter controlled production of HlyB and HlyD was induced by IPTG. HlyD harbors a C-terminal deca-histidine-tag, which is linked to the protein by a Xa-cleavage site (called HlyD-His). The tag allows the purification of the solubilized HlyD-His out of the cell crowd extract via an immobilized metal ion affinity chromatography (IMAC; see Figure 1a). Gradual increase of imidazole to a concentration of 500 mM resulted in elution of HlyD-His in highly pure form. Protein purity was confirmed by SDS-PAGE analysis with Coomassie blue staining (see Figure 1b). Eluate was concentrated with an Amicon Ultracentrifugation unit and underwent a gel filtration to remove imidazole and to determine the homogeneity of the protein. Size exclusion chromatography of HlyD-His highlighted that the protein is very inhomogeneous and aggregating (see Figure 1c P1) during concentration respectively during gel filtration (see Figure 1c). SDS-PAGE analysis confirm that all protein peaks and shoulders of the gel filtration represent HlyD-His (see Figure 1d). Detergent switch during IMAC or alternative detergent usage during solubilization did not result in a homogeneous HlyD-His gel filtration distribution [Richter, 2012]. Further, the usage of a HlyD construct with N-terminal localized histidine-tag did not increase the homogeneity and stability of the protein [Richter, 2012].

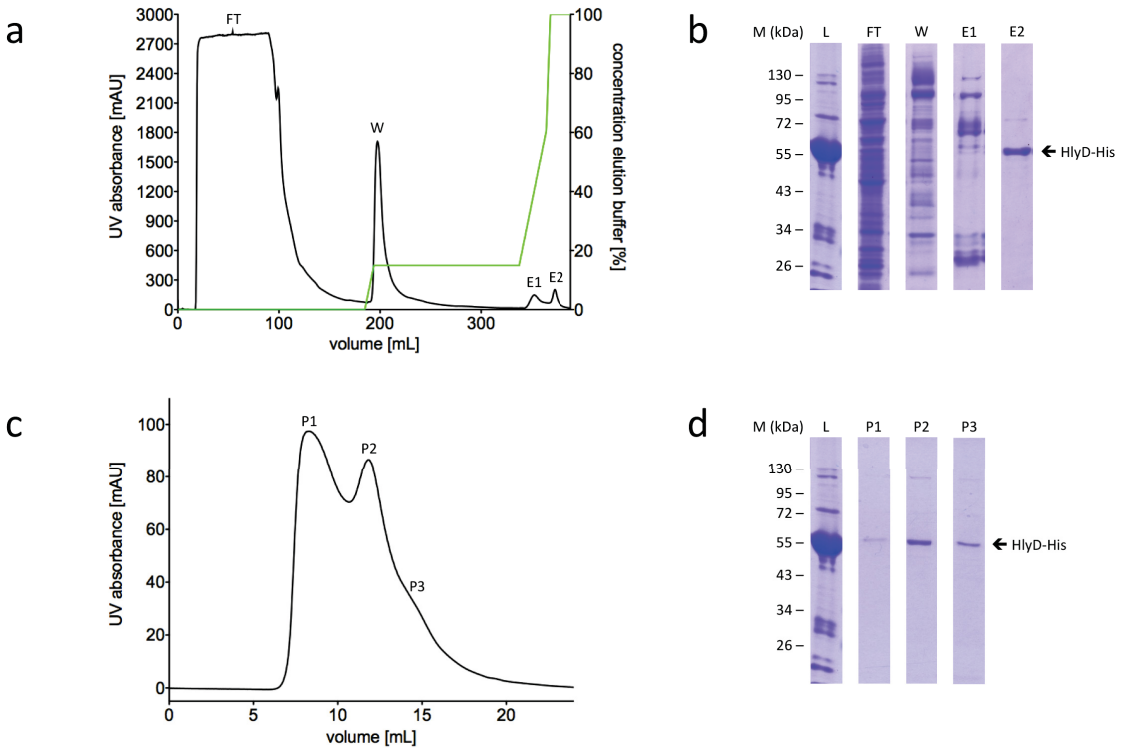

Figure 1: **Purification of HlyD-His**
(**a**) IMAC of HlyD-His with a 1 mL HiTrap^{TM} Chelating HP column loaded with Zn^{2+}. Left ordinate represents the UV absorbance (black graph) whereas the right ordinate show the changes in elution buffer concentration (green graph). Different peaks are abbreviated as follows: FT, flow through; W, wash fraction; E1, elution peak 1; E2, elution peak 2. (**b**) SDS- PAGE analysis (with Coomassie blue staining) of the HlyD-His IMAC from (a). Different lanes represent the different peaks of (a) using the same abbreviations. Load is abbreviated with L. HlyD-His is indicated by an arrow on the right site. (**c**) Gel filtration of concentrated IMAC eluate E2 with a Superdex^{TM} 200 HR 10/30 column. Different peaks are abbreviated as follows: P1, peak 1; P2, peak 2; P3, peak 3. (**d**) SDS- PAGE analysis (with Coomassie blue staining) of the HlyD-His gel filtration from (c). Different lanes represent the different peaks of (c) with the same abbreviations. Load of the concentrated IMAC eluate E2 is abbreviated with L. HlyD-His is indicated with an arrow on the right site.

In summary, full length HlyD with its single transmembrane helix was to unstable for crystallization usage.

Purification of HisTEV-HlyD-80-478

Most of the crystallized MFPs consisting only of a periplasmic domain that is anchored to the inner membrane by an uncleavable signal peptide or by a lipid moiety [Lewis, 2000, Putman et al., 2000, Yum et al., 2009]. None of them is crystallized with a transmembrane helix.

According to this, we create a HlyD construct laking the first 79 amino acids. This sequence includes the cytoplasmic domain of HlyD as well as its proposed transmembrane helix. The new construct harbors a N-terminal hexa-histidine-tag followed by a TEV protease cleavage site and the HlyD amino acids 80 to 478 (called HisTEV-HlyD-80-478). The protein was soluble expressed in *E. coli* BL21 (DE3) cells and could be isolated using its affinity tag by IMAC out of the cell extract (see Figure 2a). Further, the protein was eluted via an imidazole gradient up to 500 mM. SDS-PAGE analysis with Coomassie blue staining confirmed that HisTEV-HlyD-80-478 was pure and showed no contamination (see Figure 2b). Concentrating of the IMAC eluate was only possible to a concentration of $4\,\mathrm{mg\,mL^{-1}}$. Higher concentration results in protein aggregation. Gel filtration chromatography highlighted that most of the loaded protein eluted in the void volume at 8 mL and in two distinct peaks (labeled with P1 and P2; see Figure 2c). The molecular mass of the proteins of the elution peaks could not be determined but SDS-Page analysis confirm that both peaks contained pure HisTEV-HlyD-80-478 (see Figure 2d). The eluate of the gel filtration was unstable and could not be concentrated to sufficient amounts for crystallization.

Purification of HlyD-80-478

The previous chapter showed that the periplasmic part of HlyD with a N-terminal tag was not stable enough for concentrating and for crystallization. According to this, we created a tag-free version of the periplasmic part of HlyD (called HlyD-80-478) and purified it out of inclusion bodies to get a more native protein version [Famulla, 2007].

HlyD-80-478 could be purified out of inclusion bodies in high yields. The isolated protein is pure and natively foldable. HlyD-80-478 could be isolated from contamination by ion exchange (see Figure 3a) and eluted from the affinity column via a salt gradient up to 500 mM NaCl. SDS-PAGE analysis with Coomassie blue staining confirmed the protein purity (see Figure 3b). Eluate could be concentrated up to $30\,\mathrm{mg\,mL^{-1}}$.

Size-exclusion chromatography coupled with MALS analysis indicate a single homogeneous protein species with a molecular mass of 44 ± 0.9 kDa that fits to the theoretical mass of 45 kDa of HlyD-80-478 (see Figure 3c). SDS-Page analysis confirm that

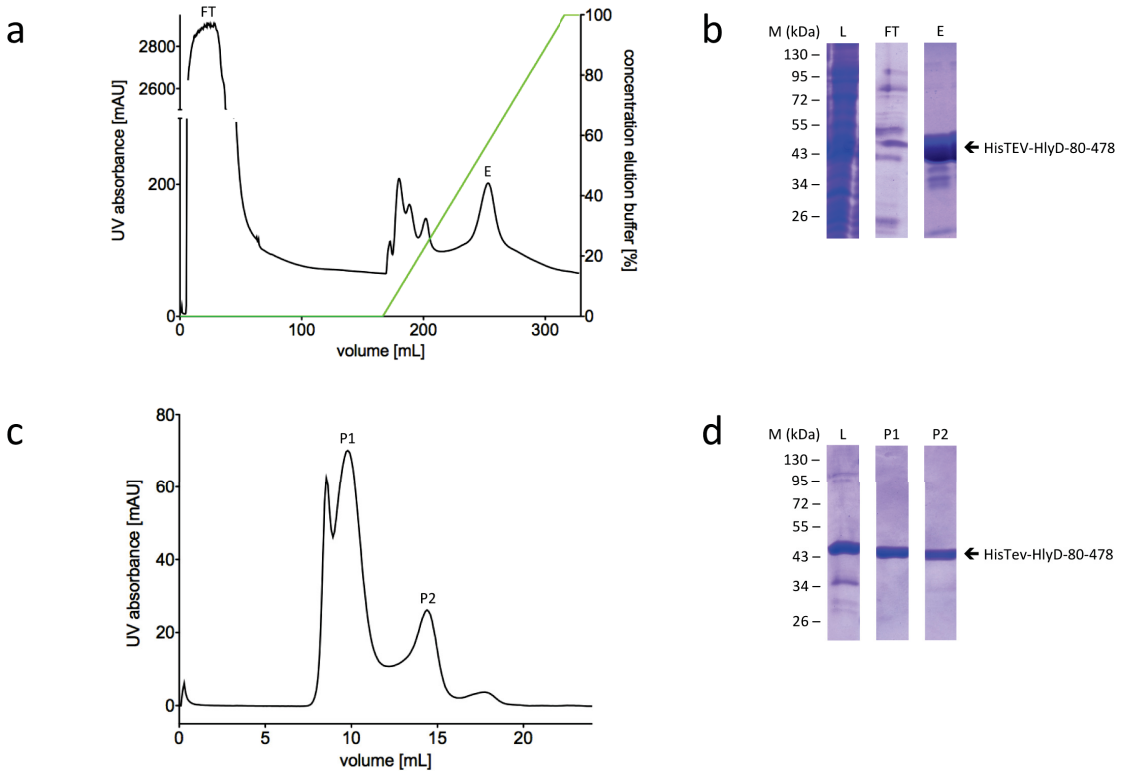

Figure 2: **Purification of HisTEV-HlyD-80-478**
(**a**) IMAC of HisTEV-HlyD-80-478 with a 1 mL HiTrap^{TM} Chelating HP column loaded with Zn^{2+}. Left ordinate represents the UV absorbance (black graph) whereas the right ordinate show the changes in elution buffer concentration (green graph). Different peaks are abbreviated as follows: FT, flow through; E, elution peak. (**b**) SDS- PAGE analysis (with Coomassie blue staining) of the HisTEV-HlyD-80-478 IMAC from (a). Different lanes represent the different peaks of (a) with the same abbreviations. Load is abbreviated with L. HisTEV-HlyD-80-478 is indicated with an arrow on the right site. (**c**) Gel filtration of concentrated IMAC eluate with a Superdex^{TM} 200 HR 10/30 column. Different peaks are abbreviated as follows: P1, peak 1; P2, peak 2. (**d**) SDS-PAGE analysis (with Coomassie blue staining) of the HisTEV-HlyD-80-478 gel filtration from (c). Different lanes represent the different peaks of (c) with the same abbreviations. Load of the concentrated IMAC eluate is abbreviated with L. HisTEV-HlyD-80-478 is indicated with an arrow on the right site.

the size-exclusion chromatography peak contained pure HlyD-80-478 (see Figure 3d). To confirm that refolded HlyD-80-478 had the same secondary structure like soluble expressed HisTEV-HlyD-80-478, circular dichroism (CD) spectroscopy of both variants were performed. Figure 4 highlights that the secondary structures of both molecules are nearly identical and that refolded HlyD-80-478 can use for crystallization of a native

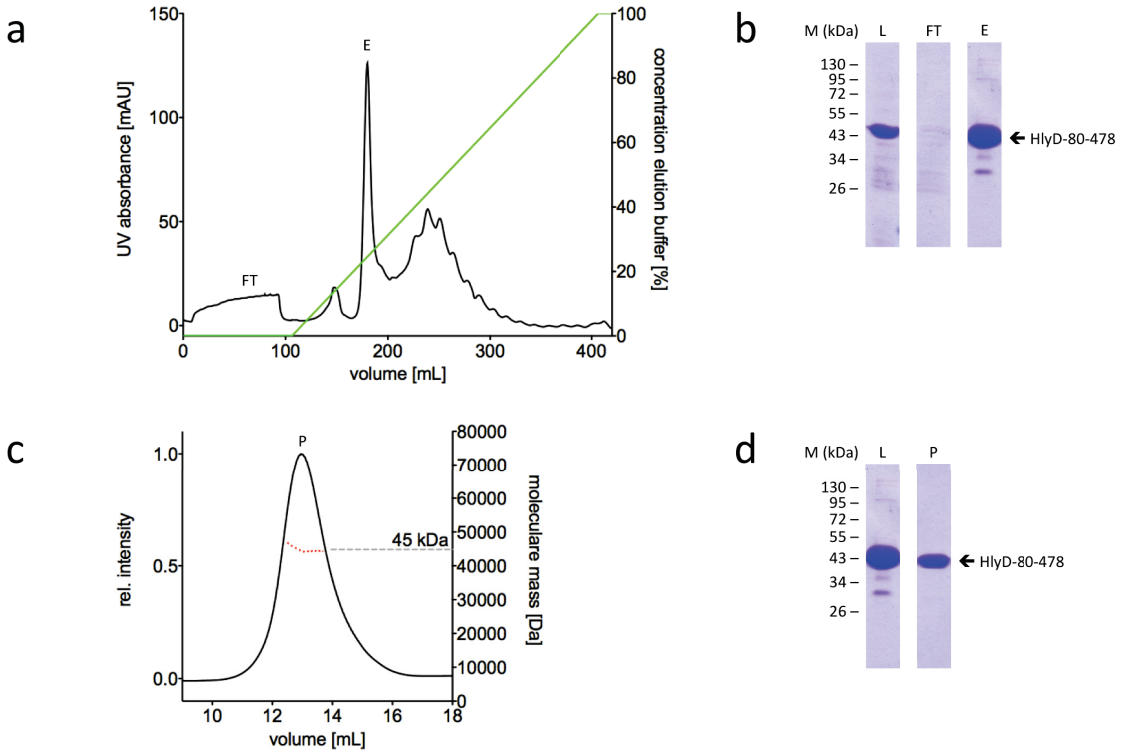

Figure 3: **Purification of HlyD-80-478**
(**a**) Ion exchange of HlyD-80-478 with a 5 mL HiTrap^{TM} Q HP column. Left ordinate represents the UV absorbance (black graph) whereas the right ordinate show the changes in elution buffer concentration (green graph). Different peaks are abbreviated as follows: FT, flow through; E, elution peak. (**b**) SDS- PAGE analysis (with Coomassie blue staining) of the HlyD-80-478 ion exchange from (a). Different lanes represent the different peaks of (a) with the same abbreviations. Load is abbreviated with L. HlyD-80-478 is indicated with an arrow on the right site. (**c**) Gel filtration of non concentrated ion exchange eluate in combination with MALS analysis with a Superdex^{TM} 200 HR 10/30 column. Left ordinate represents the relative signal intensity (black graph) whereas the right ordinate show the calculated molecular mass (red dotted line). Peak is abbreviated with P. (**d**) SDS- PAGE analysis (with Coomassie blue staining) of the HlyD-80-478 gel filtration from (c). Different lanes represent the load and peak of (c) with the same abbreviations. Load of non concentrated ion exchange eluate is abbreviated with L. HlyD-80-478 is indicated with an arrow on the right site.

periplasmic protein fragment.

Size-exclusion chromatography and MALS analysis showed that HlyD-80-478 is a homogeneous monomer. Additionally, a blue native PAGE of HlyD-80-478 was performed. The PAGE indicate that HlyD-80-478 occupied also different oligomeric states

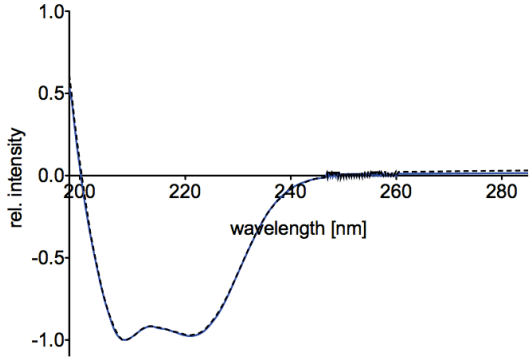

Figure 4: **CD spectra of HlyD-80-478** Shown are the CD spectra of HisTEV-HlyD-80-478 purified out of the cytoplasm (black broken graph) and of refolded HlyD-80-478 purified from inclusion bodies (blue unbroken graph). Congruent graphs reveal an identical secondary structure of both constructs.

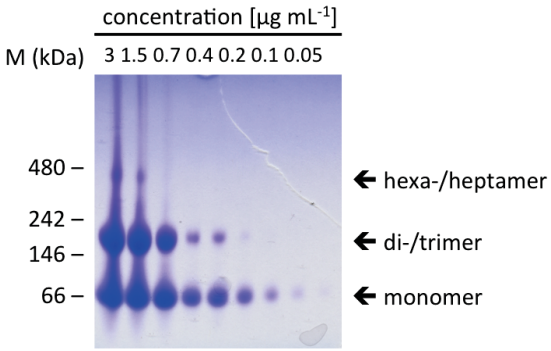

Figure 5: **Blue native PAGE of different concentrated HlyD-80-478** Shown is a blue native PAGE of different concentrated HlyD-80-478 purified from inclusion bodies. Proposed concentration induced oligomeric states of HlyD-80-478 are labeled on the right site.

in solution (see Figure 5). Two higher states are preferred and this states seems to be concentration dependent. Concentration dependency of this states could be shown by lowering the protein concentration, which resulted in disappearing of the corresponding blue native PAGE bands by deceed a specific concentration.

Purified HlyD-80-478 was used for crystallization trials (see Table 1). Unfortunately, the trials did not provide any usable crystallization condition.

Table 1: **Crystallization trials for HlyD-80-478**

Screen	Protein buffer	Protein conc. [mg mL^{-1}]	Drop [µL]	Temp. [°C]	Time [d]	Hits
Mol. Dimensions MIDAS	150 mM NaCl, 20 mM Tris/HCl, pH 7.5	5, 10	1.0	4 12 25	300	0
Mol. Dimensions MemGold	150 mM NaCl, 20 mM Tris/HCl, pH 7.5	5, 10	1.0	4 12 25	300	0
Mol. Dimensions MemGold2	150 mM NaCl, 20 mM Tris/HCl,	5, 10	1.0	4 12	300	0

	pH 7.5			25		
NeXtal Classics Suite	150 mM NaCl, 20 mM Tris/HCl, pH 7.5	5, 10	1.0	4 12 25	300	0
NeXtal Classics II Suite	150 mM NaCl, 20 mM Tris/HCl, pH 7.5	5, 10	1.0	4 12 25	300	0
NeXtal ComPAS Suite	150 mM NaCl, 20 mM Tris/HCl, pH 7.5	5, 10	1.0	4 12 25	300	0
NeXtal Cryos Suite	150 mM NaCl, 20 mM Tris/HCl, pH 7.5	5, 10	1.0	4 12 25	300	0
NeXtal JCSG Core Suite I	150 mM NaCl, 20 mM Tris/HCl, pH 7.5	5, 10	1.0	4 12 25	300	0
NeXtal JCSG Core Suite I	150 mM NaCl, 20 mM Tris/HCl, 20 % Glycerol, pH 7.5	5, 10, 20	0.2	4 12	300	0
NeXtal JCSG Core Suite II	150 mM NaCl, 20 mM Tris/HCl, pH 7.5	5, 10	1.0	4 12 25	300	0
NeXtal JCSG Core Suite III	150 mM NaCl, 20 mM Tris/HCl, pH 7.5	5, 10	1.0	4 12 25	300	0
NeXtal JCSG Core Suite IV	150 mM NaCl, 20 mM Tris/HCl, pH 7.5	5, 10	1.0	4 12 25	300	0
NeXtal MPD Suite	150 mM NaCl, 20 mM Tris/HCl, pH 7.5	5, 10	1.0	4 12 25	300	0
NeXtal PACT Suite	150 mM NaCl, 20 mM Tris/HCl, pH 7.5	5, 10	1.0	4 12 25	300	0

NeXtal PEGs Suite	150 mM NaCl, 20 mM Tris/HCl, pH 7.5	5, 10	1.0	4 12 25	300	0
NeXtal PEGs II Suite	150 mM NaCl, 20 mM Tris/HCl, pH 7.5	5, 10	1.0	4 12 25	300	0
Protein Complex Suite	150 mM NaCl, 20 mM Tris/HCl, pH 7.5	5, 10	1.0	4 12 25	300	0

Identifying HlyD-80-453 and HlyD-80-458

Due to the fact that crystallization trials of purified HlyD-80-478 did not result in diffracting protein crystals, alternative constructs were designed. According to this, a limited proteolytic trypsin digest of HlyD-80-478 was performed to identify the most stable protein fragments. Trypsin cleaves peptide bounds after the basic amino acids arginine and lysine which are randomly distributed in the HlyD sequence. For that purpose, trypsin will first cleave easier accessible peptide bounds whereas the more difficult accessible fragments will be cleaved at last. The trypsin digest of HlyD-80-478 was stopped after different time intervals and analysed via SDS-PAGE (see Figure 6). The PAGE highlights two prominent bands that resisted trypsin digest for at least 10 min. The first band is located close to the HlyD-80-478 band at 45 kDa and could be identified by mass spectrometry as the HlyD-80-453 fragment whereas the other band at 30 kDa was not analyzed (see Figure 6). We decided to crystallize the HlyD-80-453 fragment.

Furthermore, a homology model of HlyD was designed using the Phyre2 web portal [Kelley et al., 2015]. The model base on the *E. coli* MacA crystal structure [Yum et al., 2009]. 260 residues of the 478 HlyD amino acids (54 % of your sequence) could been modeled and fitted with 100 % confidence to the MacA template. The model includes amino acids 80 to 458 (see Figure 7a). According to this, a construct was designed reaching from amino acid 80 to 458 (called HlyD-80-458). The model includes the MFP specific β-barrel domain and the lipoyl-half motifs that are separated by the α-helical hairpin (see Figure 7a). MacA could be crystallized as a hexamer [Yum et al., 2009]. As mentioned above, a hexameric state for HlyD is also highly likely for bridging the dimeric and trimeric oligomerization state of HlyB and TolC. According to this, the

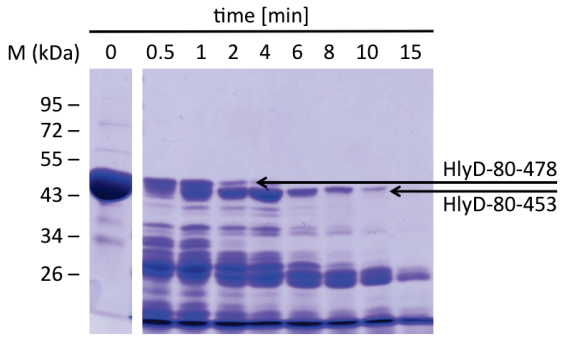

Figure 6: **Limited proteolytic trypsin digest of HlyD-80-478**
SDS-PAGE analysis of a limited proteolytic trypsin digest of HlyD-80-478. Different lanes indicate the different time point after trypsin digest was stopped. Most prominent band is labeled with HlyD-80-453. The identity was verified by MS analysis.

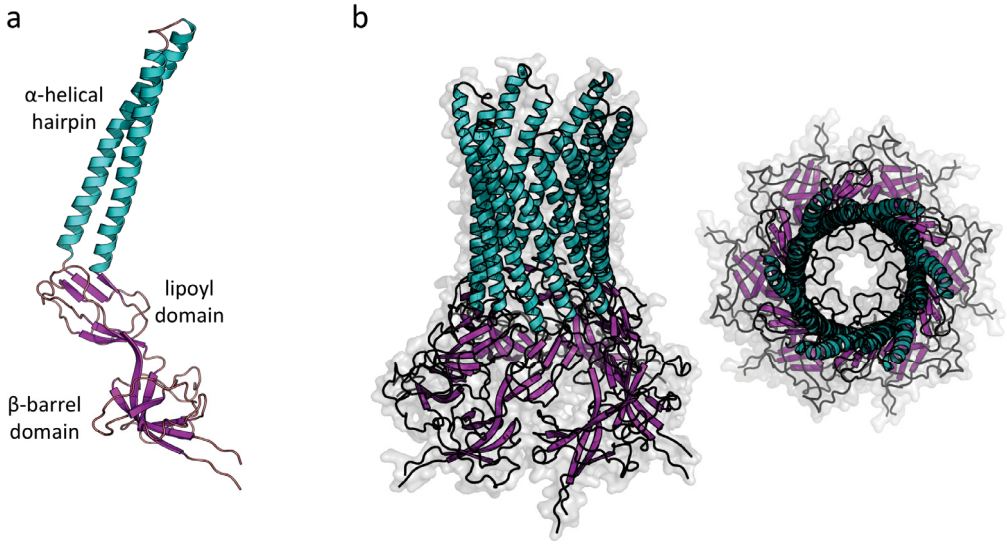

Figure 7: **Homology model of the periplasmic part of HlyD**
(**a**) Homology model was prepared by using the Phyre2 web portal [Kelley et al., 2015]. Model based on crystal structure of *E. coli* MacA (pdb file 3FPP) and reaches from amino acid 80 to 458 of HlyD. Marked are the specific domains (α-helical hairpin, lipoyl domain and β-barrel domain) of MFPs (**b**) Alignment of the HlyD homology model on the hexametric crystal package of MacA. Shown is the side and top view of the channel like assembly. α-helices are indicated in cyan and β-strands in pink.

HlyD homology model was aligned to the hexameric MacA crystal structure (see Figure 7b and 7c). The α-helical domain of the periplasmic part of HlyD build a cylindrical structure with an internal diameter of 40 Å. This is broad enough to allow passage of

unfolded or partially folded substrates.

Purification of HlyD-80-458

HlyD-80-458 could be expressed in inclusion bodies in high yields like HlyD-80-478. Refolding was carried out as described in Methods. The isolate was pure and natively folded.

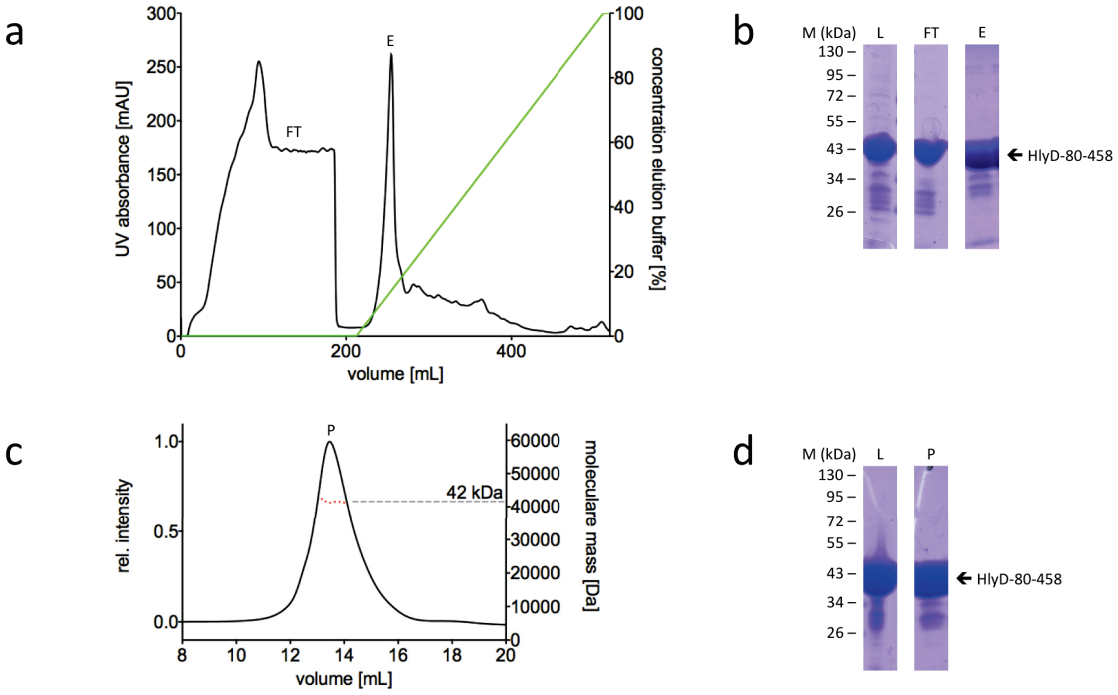

Figure 8: **Purification of HlyD-80-458**
(**a**) Ion exchange of HlyD-80-458 with a 5 mL HiTrap^{TM} Q HP column. Left ordinate represents the UV absorbance (black graph) whereas the right ordinate show the changes in elution buffer concentration (green graph). Different peaks are abbreviated as follows: FT, flow through; E, elution peak. (**b**) SDS- PAGE analysis (with Coomassie blue staining) of the HlyD-80-458 ion exchange from (a). Different lanes represent the different peaks of (a) with the same abbreviations. Load is abbreviated with L. HlyD-80-458 is indicated with an arrow on the right site. (**c**) Gel filtration of non concentrated ion exchange eluate in combination with MALS analysis with a Superdex^{TM} 200 HR 10/30 column. Left ordinate represents the relative signal intensity (black graph) whereas the right ordinate show the calculated molecular mass (red dotted line). Peak is abbreviated with P. (**d**) SDS- PAGE analysis (with Coomassie blue staining) of the HlyD-80-458 gel filtration from (c). Different lanes represent the load and peak of (c) with the same abbreviations. Load of non concentrated ion exchange eluate is abbreviated with L. HlyD-80-458 is indicated with an arrow on the right site.

Contaminations were separated from the target protein by ion exchange (see Figure 8a) and eluted from the affinity column via a salt gradient up to 500 mM NaCl. SDS-PAGE analysis with Coomassie blue staining confirmed the protein purity (see Figure 8b). Eluate could be concentrated up to 50 mg mL^{-1}. Size-exclusion chromatography coupled with MALS analysis indicate a single homogeneous protein species with a molecular mass of around 42 kDa that fits to the theoretical mass of 43 kDa of HlyD-80-458 (see Figure 8c). SDS-Page analysis confirm that the size-exclusion chromatography peak contained pure HlyD-80-458 (see Figure 8d).

Size-exclusion chromatography and MALS analysis showed that HlyD-80-458 is a homogeneous monomer. Additionally, cross-linking studies of HlyD-80-458 were performed. For that purpose, HlyD-80-458 was treated with different DTBP cross-linker concentration and visualized by SDS-PAGE (see Figure 9). The PAGE showed that even in presents of low cross-linker different oligomeric species of HlyD-80-458 are fixed. The trimeric oligomer seems to be favorable. A trimer could also observed in additional studies [Thanabalu et al., 1998]. Further, dimers, pentamers and hexamers are detectable (see Figure 9).

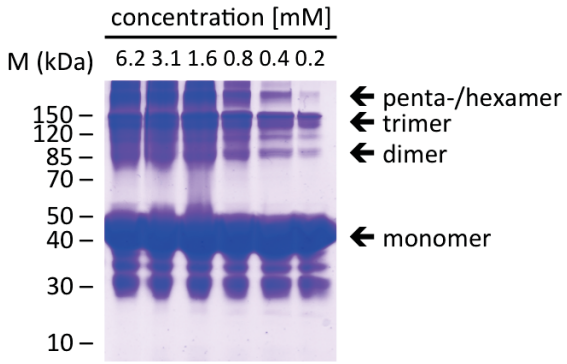

Figure 9: **Cross-linking of HlyD-80-458**
SDS-PAGE analysis of cross-linked HlyD-80-458. Different lanes indicate different concentration of cross-linker. Most prominent bands represent HlyD-80-458 oligomers and are labeled on the right site.

Purified HlyD-80-458 was used for crystallization trials (see Table 2). Unfortunately, the trials did not provide any usable crystallization condition.

Table 2: **Crystallization trials for HlyD-80-458**

Screen	Protein buffer	Protein conc. [mg mL^{-1}]	Drop [µL]	Temp. [°C]	Time [d]	Hits
Mol. Dimensions MemGold	150 mM NaCl, 20 mM Tris/HCl, pH 9.5	10, 20, 50	0.2	4 12 25	300 12 25	0
Mol. Dimensions MemGold2	150 mM NaCl, 20 mM Tris/HCl, pH 9.5	10, 20, 50	0.2	4 12 25	300	0
NeXtal Classics Suite	150 mM NaCl, 20 mM Tris/HCl, pH 9.5	10, 20, 50	0.2	4 12 25	300	0
NeXtal JCSG Core Suite I	150 mM NaCl, 20 mM Tris/HCl, pH 9.5	10, 20, 50	0.2	4 12 25	300	0
NeXtal JCSG Core Suite I	150 mM NaCl, 20 mM Tris/HCl, 0.001 % DDM, pH 9.5	10, 20	0.2	4 12 25	300	0
NeXtal JCSG Core Suite I	150 mM NaCl, 20 mM Tris/HCl, 0.01 % DDM, pH 9.5	10, 20	0.2	4 12 25	300	0
NeXtal JCSG Core Suite I	150 mM NaCl, 20 mM Tris/HCl, 0.1 % DDM, pH 9.5	10, 20	0.2	4 12 25	300	0
NeXtal PEGs Suite	150 mM NaCl, 20 mM Tris/HCl, pH 9.5	10, 20, 50	0.2	4 12 25	300	0
NeXtal PEGs II Suite	150 mM NaCl, 20 mM Tris/HCl, pH 9.5	10, 20, 50	0.2	4 12 25	300	0

Purification of HlyD-80-453

As shown by limited proteolytic digest (see Figure 6), HlyD-80-453 could be identified as a stable HlyD fragment.

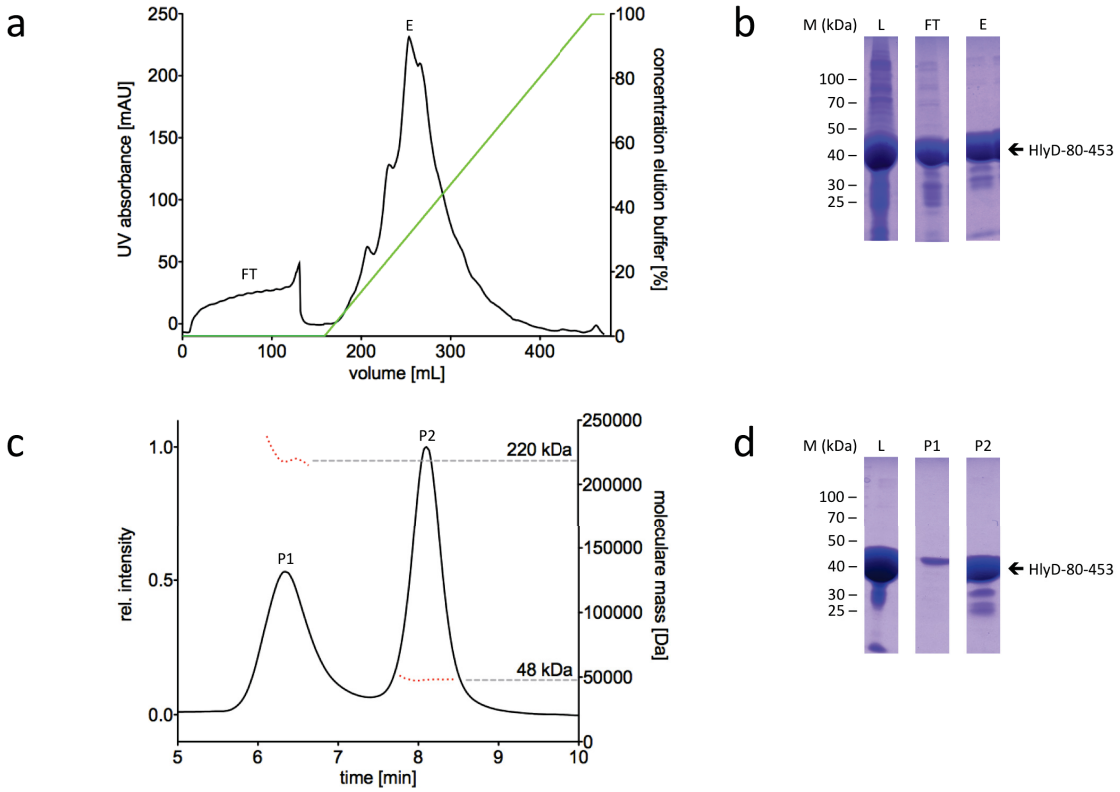

Figure 10: **Purification of HlyD-80-453**
(**a**) Ion exchange of HlyD-80-453 with a 5 mL HiTrap^{TM} Q HP column. Left ordinate represents the UV absorbance (black graph) whereas the right ordinate show the changes in elution buffer concentration (green graph). Different peaks are abbreviated as follows: FT, flow through; E, elution peak. (**b**) SDS- PAGE analysis (with Coomassie blue staining) of the HlyD-80-453 ion exchange from (a). Different lanes represent the different peaks of (a) with the same abbreviations. Load is abbreviated with L. HlyD-80-453 is indicated with an arrow on the right site. (**c**) HPLC of concentrated ion exchange eluate in combination with MALS analysis with a Bio SEC-5 column. Left ordinate represents the relative signal intensity (black graph) whereas the right ordinate show the calculated molecular mass (red dotted line) of both species. Different peaks are abbreviated as follows: P1, peak 1; P2, peak 2. (**d**) SDS- PAGE analysis (with Coomassie blue staining) of the HlyD-80-453 HPLC from (c). Different lanes represent the different peaks of (c) with the same abbreviations. Load of concentrated ion exchange eluate is abbreviated with L. HlyD-80-453 is indicated with an arrow on the right site.

Similar to the purification of HlyD-80-478 and HlyD-80-458, the fragment could be expressed in inclusion bodies in high yields. The protein is separated from contaminations by ion exchange (see Figure 10a) and eluted from the affinity column via a salt gradient up to 500 mM NaCl. SDS-PAGE analysis with Coomassie blue staining confirmed the protein purity (see Figure 10b). Eluate could be concentrated up to $20\,\mathrm{mg\,mL^{-1}}$. Size-exclusion chromatography coupled with MALS analysis indicate two homogeneous protein species. The first one has a molecular mass of around 220 kDa whereas the second one has a molecular mass of around 48 kDa (see Figure 10c). The theoretical mass of HlyD-80-453 is 42 kDa. Both peaks were not completely base line separated from each other during the MALS analysis. According to this, the determined mass of the first peak is slightly reduced by the mass of the second peak whereas the mass of the second peak is increased by the first peak. SDS-Page analysis confirm that both peaks contained pure HlyD-80-453 (see Figure 10d).

Purified HlyD-80-453 was used for crystallization trials (see Table 3). Unfortunately, the trials did not provide any usable crystallization condition.

Table 3: **Crystallization trials for HlyD-80-453**

Screen	Protein buffer	Protein conc. [$\mathrm{mg\,mL^{-1}}$]	Drop [µL]	Temp. [°C]	Time [d]	Hits
Mol. Dimensions MemGold	150 mM NaCl, 20 mM Tris/HCl, pH 7.5	10, 20	0.2	12	300	0
Mol. Dimensions MemGold2	150 mM NaCl, 20 mM Tris/HCl, pH 7.5	10, 20	0.2	12	300	0
NeXtal Classics Suite	150 mM NaCl, 20 mM Tris/HCl, pH 7.5	10, 20	0.2	12	300	0
NeXtal Classics II Suite	150 mM NaCl, 20 mM Tris/HCl, pH 7.5	10, 20	0.2	12	300	0
NeXtal ComPAS Suite	150 mM NaCl, 20 mM Tris/HCl, pH 7.5	10, 20	0.2	12	300	0
NeXtal	150 mM NaCl,	10, 20	0.2	12	300	0

Cryos Suite	20 mM Tris/HCl, pH 7.5					
NeXtal JCSG Core Suite I	150 mM NaCl, 20 mM Tris/HCl, pH 7.5	10, 20	0.2	12	300	0
NeXtal JCSG Core Suite II	150 mM NaCl, 20 mM Tris/HCl, pH 7.5	10, 20	0.2	12	300	0
NeXtal JCSG Core Suite III	150 mM NaCl, 20 mM Tris/HCl, pH 7.5	10, 20	0.2	12	300	0
NeXtal JCSG Core Suite IV	150 mM NaCl, 20 mM Tris/HCl, pH 7.5	10, 20	0.2	12	300	0
NeXtal MPD Suite	150 mM NaCl, 20 mM Tris/HCl, pH 7.5	10, 20	0.2	12	300	0
NeXtal PACT Suite	150 mM NaCl, 20 mM Tris/HCl, pH 7.5	10, 20	0.2	12	300	0
NeXtal PEGs Suite	150 mM NaCl, 20 mM Tris/HCl, pH 7.5	10, 20	0.2	12	300	0
NeXtal PEGs II Suite	150 mM NaCl, 20 mM Tris/HCl, pH 7.5	10, 20	0.2	12	300	0

Discussion

Biochemical studies of HlyD showed that it has an important function for translocator assembly and substrate secretion [Thanabalu et al., 1998, Pimenta et al., 2005]. For that purpose, we tried to crystallize the protein.

Full length HlyD (HlyD-His) as well as the tagged periplasmic part of HlyD (HisTEV-HlyD-80-478) could purified to high purity but not homogeneously. In case of HlyD-His,

the single transmembrane helix seems to destabilize the protein. Further, the detergent micelle around the HlyD membrane helix impeded a proper crystallization. In case of HisTEV-HlyD-80-478, the His-tag followed by a TEV protease cleavage site seems to decrease protein stability drastically. Cleaving efficiency of the tag was very low and resulted only in very low amounts of cleaved protein. Nevertheless, purification on the untagged HlyD-80-478 increased protein stability drastically and resulted in a homogeneous monomeric protein species. This implied that the tag was responsible for the protein instability. If we compare this with crystallization trials of other crystallized MFPs, like MacA the corresponding tag was also removed to facilitate crystallization [Yum et al., 2009]. CD spectroscopy measurements show that the secondary structure of HisTEV-HlyD-80-478 and HlyD-80-478 was identical. Unfortunately, even the crystallization trials of HlyD-80-478 did not result in diffracting crystals. All MFP structure show no electron density of the C-terminus [Akama et al., 2004, Mikolosko et al., 2006, Yum et al., 2009]. The C-terminus of MFPs is essential for the protein function and highly conserved in the protein family [Zgurskaya et al., 2009]. For that purpose, we designed additional HlyD constructs lacking this domain. The length of this construct were defined by limited proteolytic trypsin digest (resulting in HlyD-80-453) and by a homology model (resulting in HlyD-80-458). Both constructs could be purified in high yields and without any contaminations. Both showed high homogeneity and stability and were used for crystallization trials. Unfortunately, the did not result in refracting crystals so far. More crystal conditions has to be tested and are under research.

The second topic of this work was an analyzing of the bridging function of HlyD. Cross-linking studies as well as blue native PAGE and MALS analysis were performed to answer this question. Blue native PAGE experiments could demonstrate that a concentration dependent oligomerization of the periplasmic HlyD domain appears. According to the migration behavior of HlyD-80-478 and the marker bands it can be assumed that monomers and di-/trimers are the preferred HlyD-80-478 species. Higher oligomers appeared only at higher protein concentration. It is discussable if these bands really represent higher oligomers or only dimers of di-/trimers. Nevertheless, this oligomers were only detectable by blue native page and did not appear during MALS analysis. Further, cross-linking experiments of isolated HlyD-80-458 indicate a trimer as the preferred oligomeric state. Even at low cross-linker concentration the trimer appeared as the favorite oligomeric species. Only at higher cross-linker, other oligomeric species of HlyD-80-458 like dimers or higher oligomers are detectable. Unfortunately, MALS analysis detect only the monomer. Only in case of HlyD-80-453, MALS analysis could detect a higher oligomeric species thats ranged between the molecular mass of a pentamer or

hexamer. It could be possible, that the deletion of the last 25 amino acids resulted in an increased interaction contact surface of the periplasmic part.

In summary, we were able to purify different variants of the periplasmic part of HlyD in high yields and purity but crystallization of this part needs further investigation. Furthermore, we could show that the trimeric oligomer of HlyD is the favorite species. We are in line with this results with cross-linking experiments of full length HlyD *in vivo* [Thanabalu et al., 1998]. Nevertheless, higher oligomeric states of HlyD like in the case of AcrA or MacA could not completely excluded [Yum et al., 2009, Xu et al., 2011]. According to this, the question how HlyD manage to bridge HlyB and TolC could not completely answered and the crystal structure would help to characterize the protein function in more detail.

Methods

Bacterial strains and plasmids

E. coli strain DH5α was used for all cloning procedures. The pK184 plasmid was used for HlyD-His production under the control of a P_{lac} promoter, inducible with IPTG (isopropyl β-D-1-thiogalactopyranoside) [Bakkes et al., 2010]. For that purpose, the sequence of a C-terminal deca-histidine-tag, which is linked to the protein by a Xa-cleavage site, was cloned into the vector [Jenewein, 2008].

pET28-HisTEV-HlyD-80-478 vector was used for HisTEV-HlyD-80-478 expression under the control of a IPTG inducible P_{lac} promoter. The In-Fusion®Advantage PCR Cloning Kit (ClonTech) was used for cloning. For that purpose, the primer pair (5'-TAACAAGCTTGCGGCCGCACTC-3') and (5'-GCCCTGAAAATAAAGATTCTCGC TATGGTGATG-3') was used for linearizing the pET28b vector. The insert was amplified by PCR using the pK184 plasmid as template. The forward (5'-CTTTATTTTCAG GGCGTGGAAATTGTTGCCACTGCAAATGGG-3') and reverse primer (5'-GCCGCA AGCTTGTTAACGCTCATGTAAACTTTCTGTTACAGAC-3') were used. The In-Fusion reaction was carried out after the manufacture protocol and results in successful insertion of the *hlyD-80-478* sequence into the pET28b vector.

Cloning of the HlyD-80-478 construct were done by deleting the base pairs encoding for the histidine-tag and the TEV protease cleavage site. The forward primer (5'-GTGGAAATTGTTGCCACTGCAAATGGGAAATTAACACTAAGTGG-3') and the reverse primer (5'-CATGGTATATCTCCTTCTTAAAGTTAAAC-3') were used.

pET28-HlyD-80-458 and pET28-HlyD-80-453 were cloned by introducing stop-codons

via site directed mutagenesis at amino acid positions 459 and 454. Primer pairs (5'-A TGCGAAGCTGAATCAGCTATC-3') and (5'-GATAGCTGATTCAGCTTCGCAT-3') respectively (5'-GAAATAAAGTGAGGAATGCGAAGC-3') and (5'-GCTTCGCATTC CTCACTTTATTTC-3') were applied.

Cell cultivation and protein expression

Chemically competent *E. coli* BL21 (DE3) cells were transformed with pK184-HlyD-His, pET28-HisTEV-HlyD-80-478, pET28-HlyD-80-478, pET28-HlyD-80-458 or pET28-HlyD-80-453 and grown on LB agar plates supplemented with 30 µg mL^{-1} kanamycin. Overnight cultures of single colonies were used to inoculate 10 L 2 YT medium supplemented with 30 µg mL^{-1} kanamycin at an OD_{600} of 0.1.

In case of HlyD-His expression, cells were grown at 37 °C to an OD_{600} of 1.0 in a 15 L table-top glass fermentor (Applikon Biotechnology). Aeration was kept at 30 % and cells were stirred with 500 rpm. The expression of HlyD-His was induced with 1 mM IPTG at an OD_{600} of 1.0 and cells were grown for additional 1.5 h. Afterwards, cells were harvested by centrifugation and stored at −20 °C.

Cells harboring the pET28-HisTEV-HlyD-80-478 vector were grown at 37 °C and 160 rpm in 5 L flasks with baffles to an OD_{600} of 0.6-0.8. After reaching the OD_{600} of 0.6-0.8, cells were cooled down on ice (4 °C) for 15 min. Afterwards, HisTEV-HlyD-80-478 expression was induced with 0.1 mM IPTG and cells were grown additional 4.5 h at 25 °C and 160 rpm. Cells were harvested by centrifugation and stored at −20 °C.

Cells expressing HlyD-80-478, HlyD-80-458 or HlyD-80-453 were grown at 37 °C and 160 rpm in 5 L flasks with baffles. Protein expression was induced with 1 mM IPTG at an OD_{600} of 0.6-0.8. After induction, cells were grown additional 4 h under the same condition, harvested by centrifugation and stored at −20 °C.

Membrane preparation of HlyD-His

HlyD-His expressing *E. coli* BL21 (DE3) cells were resuspended in buffer A1 (150 mM NaCl, 100 mM HEPES, pH 8.0) and broken by three passages through a cell disrupter (Constant Systems) at 2.5 kbar. Lysate was centrifuged for 30 min at 18 000 xg. Afterwards, supernatant was again centrifuged for 90 min at 200 000 xg. Pelleted membranes were resolved and homogenized in buffer A2 (150 mM NaCl, 100 mM HEPES, 10 % (w/v) glycerol, pH 8.0). Membranes were adjusted with buffer A2 to 10 mg mL^{-1}, shock frosted in liquid nitrogen and stored at −80 °C.

Purification of HlyD-His

HlyD-His were solubilized out of the homogenized *E. coli* membrane by incubating for 1 h with 1 % (w/v) n-Dodecyl-β-D-maltopyranoside (DDM). Afterwards, homogenizate was centrifuged for 1 h at 200 000 xg and supernatant was diluted one to one with buffer A3 (250 mM NaCl, 100 mM HEPES, 10 mM imidzole, pH 8.0). The diluted supernatant was applied to an IMAC column (1 mL HiTrap^{TM} Chelating HP column, GE Healthcare) that is loaded with $ZnCl_2$ and equilibrated in buffer A3. After loading of the supernatant, column is washed with 5 column volume (CV) buffer A3 that contained 0.05 % (w/v) DDM. Contaminations were washed of the column by increasing the concentration of buffer A4 (250 mM NaCl, 100 mM HEPES, 250 mM imidzole, 0.05 % (w/v) DDM, pH 8.0) to 15 %. HlyD-His was eluted by a linear gradient from 47.5 to 250 mM imidazole. Before loading onto a Size exclusion chromatography (SEC), eluted HlyD-His were concentrated by Amicon Ultracentrifugation unit (30 kDa cut off) to 0.5 mL. The concentrated is loaded on a Superdex^{TM} 200 HR 10/30 column (GE Healthcare) that is equilibrated with buffer A5 (100 mM NaCl, 20 mM HEPES, 0.02 % (w/v) DDM, pH 8.0). HlyD-His elution fractions were pooled and tried to concentrate via Amicon Ultracentrifugation unit (30 kDa cut off) to 10 mg mL^{-1}. IMAC and SEC elution fractions were analyzed by SDS-PAGE and western blot against a specific polyclonal HlyD antibody.

Purification of HisTEV-HlyD-80-478

HisTEV-HlyD-80-478 containing *E. coli* BL21 (DE3) cells were resuspended in buffer B1 (250 mM NaCl, 100 mM Tris/HCl, 10 mM imidzole, pH 8.0) and broken by three passages through a cell disrupter (Constant Systems) at 2.5 kbar. Lysate was centrifuged for 45 min at 200 000 xg. The supernatant was applied to an IMAC column (5 mL HiTrap^{TM} Chelating HP column,GE Healthcare) that is loaded with $ZnCl_2$ and equilibrated in buffer B1. HisTEV-HlyD-80-478 was eluted by a linear gradient over 30 CV with buffer B2 (250 mM NaCl, 100 mM Tris/HCl, 250 mM imidzole, pH 8.0) from 10 to 250 mM imidazole. Eluate was concentrated via Ultracentrifugation units (30 kDa cut off) to 0.2 mL. Afterwards, concentrate was loaded on a Superdex^{TM} 200 HR 10/30 column (GE Healthcare) that is equilibrated with buffer B3 (150 mM NaCl, 20 mM Tris/HCl, pH 8.0). HisTEV-HlyD-80-478 elution fractions were pooled and tried to concentrate via Ultracentrifugation unit (30 kDa cut off) to 10 mg mL^{-1}. IMAC and SEC elution fractions were analyzed by SDS-PAGE and western blot against a specific polyclonal HlyD antibody.

Inclusion bodies preparation of HlyD-80-478, HlyD-80-458 and HlyD-80-453

HlyD-80-478, HlyD-80-458 or HlyD-80-453 containing *E. coli* BL21 (DE3) cells were resuspended in buffer C1 (50 mM NaCl, 50 mM Tris/HCl, 50 mM EDTA, pH 8.0) and broken by three passages through a cell disrupter (Constant Systems) at 2.5 kbar. Lysate was centrifuged for 30 min at 26 000 xg. Pellet was resuspended in buffer C2 (50 mM NaCl, 50 mM Tris/HCl, 50 mM EDTA, 1 % (w/v) Triton X-100, pH 8.0) and centrifuged again for 30 min at 26 000 xg. Afterwards, pellet was resuspended in buffer C3 (1 M NaCl, 50 mM Tris/HCl, pH 8.0) and one more time centrifuged for 30 min at 26 000 xg. The resulting pellet was incubated under stirring for 3 to 4 h at 4 °C in buffer C4 (6 M guanidine hydrochloride, 50 mM NaCl, 50 mM Tris/HCl, pH 8.0). After incubation, solvate was centrifuged for 15 min at 6000 xg. Supernatant was stored at −20 °C.

Purification of HlyD-80-478, HlyD-80-458 and HlyD-80-453

50 mL of unfolded HlyD-80-478, HlyD-80-458 or HlyD-80-453 (ajusted to 3 mg mL^{-1}) in buffer C4 was dialyzed for 8 to 12 h at 4 °C against 5 L buffer C5 (100 mM NaCl, 50 mM Tris/HCl, 1 mM EDTA, pH 8.0). Dialysate was centrifuged for 30 min at 20 000 xg and supernatant was diluted four times in buffer C6 (20 mM Tris/HCl, pH 7.5). Supernatant was applied to an ion exchange column (5 mL HiTrap^{TM} Q HP column, GE Healthcare). Column is equilibrated with buffer C6 and a linear gradient over 60 CV with buffer C7 (500 mM NaCl, 20 mM Tris/HCl, pH 7.5) from 0 to 500 mM NaCl eluted HlyD-80-478, HlyD-80-458 respectively HlyD-80-453. Eluted proteins were pooled and concentrated by Amicon Ultracentrifugation unit (30 kDa cut off) to 0.5 mL. The concentrated is loaded on a Superdex^{TM} 200 HR 10/30 column (GE Healthcare) that is equilibrated with buffer C8 (150 mM NaCl, 20 mM Tris/HCl, pH 7.5). Purity of elution fractions were analyzed by SDS-PAGE and western blot against a specific polyclonal HlyD antibody.

Proteins were concentrated using Amicon Ultracentrifugation units to their final concentration and used for crystallization trials, CD and MALS analysis, Blue native PAGE, cross-linking or limited proteolytic trypsin digest.

Crystallization of HlyD-80-478, HlyD-80-458 and HlyD-80-453

Crystallization trials for HlyD-80-478, HlyD-80-458 and HlyD-80-453 were performed using the sitting-drop vapor diffusion method at different temperatures (4, 12 and 25 °C). 0.5 µL or 0.1 µL of homogeneous protein solution (concentration 10 to 50 mg mL^{-1}) was mixed with 0.5 µL or 0.1 µL reservoir solution of the listed crystallization screens (see

Table 1, 2 and 3). Reservoir size was 400 µL respectively 50 µL. Crystal growth was observed for 300 d. After 1, 2, 3, 7, 14, 30, 60, 120 and 300 d, crystallization progress of the different conditions were checked.

SEC and HPLC coupled multi angle light scattering (MALS) of HlyD-80-478, HlyD-80-458 and HlyD-80-453

Size-exclusion chromatography (SEC) respectively high performance liquid chromatography (HPLC) coupled to multi angle light scattering detection (SEC-/HPLC-MALS) was used to determine the molecular mass and the oligomeric state of HlyD-80-478, HlyD-80-458 and HlyD-80-453. SEC was performed with a Superdex^{TM}200 HR 10/30 column (GE Healthcare) and HPLC was performed with a Bio SEC-5 HPLC column (Agilent Technologies Deutschland GmbH, Böblingen, Germany) with a pore size of 300 Å. Columns were equilibrated in 150 mM NaCl, 20 mM Tris/HCl, pH 7.5 containing buffer. Runs were performed int he same buffer. SEC (GE Healthcare) and HPLC system (Agilent Technologies) was connected with a triple-angle light-scattering detector (miniDAWN TREOS, Wyatt Technology Europe GmbH, Dernbach, Germany) followed by a differential refractive index detector (OPTILab T-rEX, Wyatt Technology). 100 µL of purified HlyD-80-478, HlyD-80-458 or HlyD-80-453 (concentration 4 mg mL^{-1}) was loaded onto the columns, and the obtained data were analyzed with the ASTRA software package (Wyatt Technology).

Circular dichroism (CD) spectroscopy of HlyD-80-478 and HisTEV-HlyD-80-478

A J-715 spectropolarimeter from Jasco was used to obtain the CD spectra of HlyD-80-478. A 0.1 cm quartz cuvette was used at room temperature. Scanning speed was 20 nm min^{-1} with a step size of 0.5 nm. For HisTEV-HlyD-80-478 respectively refolded HlyD-80-478 from inclusion bodies, 10 spectra were accumulated between 190 and 260 nm. Protein concentration were 310 µg mL^{-1} and used buffer contain 150 mM NaCl and 20 mM Tris/HCl, pH 7.5. 200 µL protein solution was used per sample and the buffer spectra were subtracted from the respective protein spectra.

Limited proteolytic trypsin digest of HlyD-80-478

HlyD-80-478 (concentration 0.7 mg mL^{-1}) was incubated together with trypsin (final concentration 0.175 mg mL^{-1}) at 25 °C. Reaction buffer was 150 mM NaCl and 20 mM Tris/HCl, pH 7.5. After 0.5 min, 1 min, 2 min, 4 min, 6 min, 8 min, 10 min and 15 min,

reaction was stopped by adding Laemmli sample buffer and directly shock frosting in liquid nitrogen. Samples were analyzed via SDS-PAGE and protein bands of interest were analyzed by mass spectrometry.

Cross-linking of HlyD-80-478

Dimethyl-dithiobispropionimidate (DTBP) was used as cross-linking reagent. Reaction was done in 150 mM NaCl and 100 mM triethanolamin, pH 8.0. One volume cross-linker (concentration 6.2, 3.1, 1.6, 0.8, 0.4 and 0.2 mM) was added to three volumes of protein solution (concentration 30 mg mL^{-1}) and incubated for 1 h at room temperature. Reaction was stopped by adding 20 to 50 mM Tris/HCl, pH 8.0. Finally, reaction composites were diluted four times with water and analyzed via SDS-PAGE.

Homology modeling of HlyD

The homology model was prepared by using the Phyre2 web portal [Kelley et al., 2015]. Resulting model shows the HlyD target sequence (UniProtKB - O08269) basing on the crystal structure of *E. coli* MacA (pdb file 3FPP) as template [Yum et al., 2009]. 260 residues (54 % of your sequence) have been modelled with 100 % confidence by the template.

Acknowledgment

We thank all members of the Institute of Biochemistry, Heinrich-Heine-Universität Düsseldorf, for helpful and very fruitful discussions. We gratefully acknowledge support (and training) from the International NRW Research School BioStruct, granted by the Ministry of Innovation, Science and Research of the State North Rhine-Westphalia, the Heinrich-Heine-Universität Düsseldorf, and the Entrepreneur Foundation at the Heinrich-Heine-Universität of Düsseldorf.

References

[Akama et al., 2004] Akama, H., Matsuura, T., Kashiwagi, S., Yoneyama, H., Narita, S.-I., Tsukihara, T., Nakagawa, A. and Nakae, T. (2004). Crystal structure of the membrane fusion protein, MexA, of the multidrug transporter in Pseudomonas aeruginosa. J Biol Chem *279*, 25939–42.

[Bakkes et al., 2010] Bakkes, P. J., Jenewein, S., Smits, S. H. J., Holland, I. B. and Schmitt, L. (2010). The rate of folding dictates substrate secretion by the Escherichia coli hemolysin type 1 secretion system. J Biol Chem *285*, 40573–80.

[Balakrishnan et al., 2001] Balakrishnan, L., Hughes, C. and Koronakis, V. (2001). Substrate-triggered recruitment of the TolC channel-tunnel during type I export of hemolysin by Escherichia coli. J Mol Biol *313*, 501–10.

[Benabdelhak et al., 2003] Benabdelhak, H., Kiontke, S., Horn, C., Ernst, R., Blight, M. A., Holland, I. B. and Schmitt, L. (2003). A specific interaction between the NBD of the ABC-transporter HlyB and a C-terminal fragment of its transport substrate haemolysin A. J Mol Biol *327*, 1169–79.

[Borges-Walmsley et al., 2003] Borges-Walmsley, M. I., Beauchamp, J., Kelly, S. M., Jumel, K., Candlish, D., Harding, S. E., Price, N. C. and Walmsley, A. R. (2003). Identification of oligomerization and drug-binding domains of the membrane fusion protein EmrA. J Biol Chem *278*, 12903–12.

[Debarbieux and Wandersman, 2001] Debarbieux, L. and Wandersman, C. (2001). Folded HasA inhibits its own secretion through its ABC exporter. EMBO J *20*, 4657–63.

[Delepelaire, 2004] Delepelaire, P. (2004). Type I secretion in gram-negative bacteria. Biochim Biophys Acta *1694*, 149–61.

[Famulla, 2007] Famulla, S. (2007). Analyse der periplasmatischen Domäne des Membranfusionsproteins HlyD. Heinrich Heine Universität Düsseldorf *Diploma thesis*.

[Higgins et al., 2004] Higgins, M. K., Bokma, E., Koronakis, E., Hughes, C. and Koronakis, V. (2004). Structure of the periplasmic component of a bacterial drug efflux pump. Proc Natl Acad Sci U S A *101*, 9994–9.

[Hinchliffe et al., 2014] Hinchliffe, P., Greene, N. P., Paterson, N. G., Crow, A., Hughes, C. and Koronakis, V. (2014). Structure of the periplasmic adaptor protein from a major facilitator superfamily (MFS) multidrug efflux pump. FEBS Lett *588*, 3147–53.

[Hussmann, 2013] Hussmann, L. (2013). Charakterisierung des Memrbanfusionproteins Hämolysin D. Heinrich Heine Universität Düsseldorf *Bachelor thesis*.

[Jenewein, 2008] Jenewein, S. (2008). The Escherichia coli haemolysin transporter - A paradigm for Type I secretion. Heinrich Heine Universität Düsseldorf *PhD thesis*.

[Johnson and Church, 1999] Johnson, J. M. and Church, G. M. (1999). Alignment and structure prediction of divergent protein families: periplasmic and outer membrane proteins of bacterial efflux pumps. J Mol Biol *287*, 695–715.

[Kelley et al., 2015] Kelley, L. A., Mezulis, S., Yates, C. M., Wass, M. N. and Sternberg, M. J. E. (2015). The Phyre2 web portal for protein modeling, prediction and analysis. Nat Protoc *10*, 845–58.

[Kim et al., 2010] Kim, H.-M., Xu, Y., Lee, M., Piao, S., Sim, S.-H., Ha, N.-C. and Lee, K. (2010). Functional relationships between the AcrA hairpin tip region and the TolC aperture tip region for the formation of the bacterial tripartite efflux pump AcrAB-TolC. J Bacteriol *192*, 4498–503.

[Koronakis et al., 2000] Koronakis, V., Sharff, A., Koronakis, E., Luisi, B. and Hughes, C. (2000). Crystal structure of the bacterial membrane protein TolC central to multidrug efflux and protein export. Nature *405*, 914–9.

[Lee et al., 2012] Lee, M., Jun, S.-Y., Yoon, B.-Y., Song, S., Lee, K. and Ha, N.-C. (2012). Membrane fusion proteins of type I secretion system and tripartite efflux pumps share a binding motif for TolC in gram-negative bacteria. PLoS One *7*, e40460.

[Lewis, 2000] Lewis, K. (2000). Translocases: a bacterial tunnel for drugs and proteins. Curr Biol *10*, R678–81.

[Mikolosko et al., 2006] Mikolosko, J., Bobyk, K., Zgurskaya, H. I. and Ghosh, P. (2006). Conformational flexibility in the multidrug efflux system protein AcrA. Structure *14*, 577–87.

[Pimenta et al., 2005] Pimenta, A. L., Racher, K., Jamieson, L., Blight, M. A. and Holland, I. B. (2005). Mutations in HlyD, part of the type 1 translocator for hemolysin secretion, affect the folding of the secreted toxin. J Bacteriol *187*, 7471–80.

[Putman et al., 2000] Putman, M., van Veen, H. W. and Konings, W. N. (2000). Molecular properties of bacterial multidrug transporters. Microbiol Mol Biol Rev *64*, 672–93.

[Renn, 2013] Renn, A. (2013). Analyse des Membranfusionsproteins HlyD. Heinrich Heine Universität Düsseldorf *Bachelor thesis*.

[Richter, 2012] Richter, D. (2012). Analyse der Interaktionspartner von HlyD. Heinrich Heine Universität Düsseldorf *Bachelor thesis*.

[Schwarz et al., 2012] Schwarz, C. K. W., Landsberg, C. D., Lenders, M. H. H., Smits, S. H. J. and Schmitt, L. (2012). Using an E. coli Type 1 secretion system to secrete the mammalian, intracellular protein IFABP in its active form. J Biotechnol *159*, 155–61.

[Su et al., 2009] Su, C.-C., Yang, F., Long, F., Reyon, D., Routh, M. D., Kuo, D. W., Mokhtari, A. K., Van Ornam, J. D., Rabe, K. L., Hoy, J. A., Lee, Y. J., Rajashankar, K. R. and Yu, E. W. (2009). Crystal structure of the membrane fusion protein CusB from Escherichia coli. J Mol Biol *393*, 342–55.

[Thanabalu et al., 1998] Thanabalu, T., Koronakis, E., Hughes, C. and Koronakis, V. (1998). Substrate-induced assembly of a contiguous channel for protein export from E.coli: reversible bridging of an inner-membrane translocase to an outer membrane exit pore. EMBO J *17*, 6487–96.

[Thanassi and Hultgren, 2000] Thanassi, D. G. and Hultgren, S. J. (2000). Multiple pathways allow protein secretion across the bacterial outer membrane. Curr Opin Cell Biol *12*, 420–30.

[Tikhonova et al., 2009] Tikhonova, E. B., Dastidar, V., Rybenkov, V. V. and Zgurskaya, H. I. (2009). Kinetic control of TolC recruitment by multidrug efflux complexes. Proc Natl Acad Sci U S A *106*, 16416–21.

[Xu et al., 2011] Xu, Y., Lee, M., Moeller, A., Song, S., Yoon, B.-Y., Kim, H.-M., Jun, S.-Y., Lee, K. and Ha, N.-C. (2011). Funnel-like hexameric assembly of the periplasmic adapter protein in the tripartite multidrug efflux pump in gram-negative bacteria. J Biol Chem *286*, 17910–20.

[Xu et al., 2010] Xu, Y., Sim, S.-H., Song, S., Piao, S., Kim, H.-M., Jin, X. L., Lee, K. and Ha, N.-C. (2010). The tip region of the MacA alpha-hairpin is important for the binding to TolC to the Escherichia coli MacAB-TolC pump. Biochem Biophys Res Commun *394*, 962–5.

[Yum et al., 2009] Yum, S., Xu, Y., Piao, S., Sim, S.-H., Kim, H.-M., Jo, W.-S., Kim, K.-J., Kweon, H.-S., Jeong, M.-H., Jeon, H., Lee, K. and Ha, N.-C. (2009). Crystal

structure of the periplasmic component of a tripartite macrolide-specific efflux pump. J Mol Biol *387*, 1286–97.

[Zaitseva et al., 2006] Zaitseva, J., Oswald, C., Jumpertz, T., Jenewein, S., Wiedenmann, A., Holland, I. B. and Schmitt, L. (2006). A structural analysis of asymmetry required for catalytic activity of an ABC-ATPase domain dimer. EMBO J *25*, 3432–43.

[Zgurskaya et al., 2009] Zgurskaya, H. I., Yamada, Y., Tikhonova, E. B., Ge, Q. and Krishnamoorthy, G. (2009). Structural and functional diversity of bacterial membrane fusion proteins. Biochim Biophys Acta *1794*, 794–807.

3.8. Chapter VIII - Isolation of the hemolysin A Type I secretion system in action

Title Isolation of the hemolysin A Type I secretion system in action

Authors Michael H.H. Lenders, Tobias Beer, Sander H.J. Smits and Lutz Schmitt

In Preparation

Own proportion of this work 30 %;
Construction of the plasmids, initial purification of the used constructs, writing of the manuscript.

Isolation of the hemolysin A Type I secretion system in action

Michael H.H. Lenders[*], Tobias Beer[*], Sander H.J. Smits and Lutz Schmitt[†]

Institute of Biochemistry, Heinrich-Heine-Universität,
40225 Düsseldorf, Germany

Abstract

Gram-negativ bacteria possess a broad range of membrane localized nanomachineries. Type I secretion system (T1SS) are one of the essential secretion systems. They transport a broad range of unfolded substrates across both cell membranes. The hemolysin A (HlyA) T1SS from *E. coli* is a well characterized example and secrets the 110 kDa toxin HlyA in one step from the cytoplasm directly into the extracellular space without any periplasmic intermediate. The inner membrane embedded ABC transporter hemolysin B (HlyB) and the membrane fusion protein (MFP) hemolysin D (HlyD) as well as the outer membrane factor (OMF) TolC catalyze this reaction and build a continuous channel across the membranes. However, the stoichiometry of the assembling proteins is unknown as well as any structural information about the associated T1SS. To address this question, we use an eGFP-HlyA fusion protein to stall the HlyA T1SS. *E. coli* membranes with the intact stalled complex could be isolated and initial solubilization trials suggest that an isolating of the stalled system out off the crowd membranes is possible.

[*]Authors contributed equally to this article.

[†]To whom correspondence should be addressed: Lutz.Schmitt@hhu.de
Tel. +49 211 81-10773, Fax +49 211 81-15310,
Universitätsstraße 1, 40225 Düsseldorf, Germany

Introduction

Gram-negative bacteria harbor a broad range of nanomachineries that enables substrate transport across both cell membranes into the extracellular space or into a host cell [Costa et al., 2015]. This nanomachineries are called secretion systems and can be divided in subgroups ranging from type I secretion systems (T1SS) up to type VII. They transport various substrates, ranging from small molecules, proteins and deoxyribonucleic acid [Costa et al., 2015]. In case of the T1SS, the substrate is secreted out of the cytoplasm directly into the extracellular space. This kind of one-step secretion occurs for type III, IV and VI secretions systems, too. Only type II and V secretion systems have a preliminary substrate translocation into the periplasm whereas the secretion occurs over the outer membrane [Costa et al., 2015].

T1SS are prominent examples for transport systems that are able to transport a great variety of substrates like toxins, hemophores, adenylate cyclases, lipases, proteases, nodulation or adhesion factors [Delepelaire, 2004]. The size of the substrates various between 19 kDa in the case of the hemophore HasA from *Serratia marcescens* and over 900 kDa for the surface layer proteins LapA from *Pseudomonas fluorescens* [Arnoux et al., 1999, Hinsa et al., 2003]. All substrates in common is the unfolded respectively partially folded secretion [Debarbieux and Wandersman, 2001, Bakkes et al., 2010].

One of the best characterized T1SS, is the hemolysin A (HlyA) secretion system. It consists out of the ABC transporter hemolysin B (HlyB) and the membrane fusion protein (MFP) hemolysin D (HlyD) [Thanabalu et al., 1998]. Both proteins are located in the inner membrane. Together with the outer membrane factor (OMP) TolC, they build up the fully assembled HlyA T1SS that creates a continuous channel across both membranes and allows substrate secretion in one step from the cytoplasm directly into the extracellular space [Thanabalu et al., 1998]. Secretion of the 110 kDa repeats in toxin (RTX) protein HlyA occurs without any periplasmic intermediate [Delepelaire, 2004]. Further, the C-terminal localized HlyA secretion signal that contains all necessary and sufficient information for secretion is not cleaved during or after secretion [Koronakis et al., 1989, Jarchau et al., 1994].

Many biochemical information about the HlyA T1SS are available. For example, the role of the secretion signal, the substrate orientation during secretion and interaction studies between the translocator building proteins as well as their interaction with the substrate [Thanabalu et al., 1998, Balakrishnan et al., 2001, Lee et al., 2012, Lenders et al., 2015]. Nevertheless, structurally the system is barely understood. Only structural information about TolC and the HlyB NBD and CLD are available [Koronakis et al.,

2000, Zaitseva et al., 2005, Lecher et al., 2011]. The translocator stoichiometry is unknown so far. Further, nearly nothing is known about structural changes of the different T1SS components during secretion [Thanabalu et al., 1998].

For that purpose, we use an eGFP-HlyA fusion protein to stall the HlyA T1SS [Lenders et al., 2015]. *E. coli* membranes with the intact stalled complex could be isolated and initial solubilization trials suggest that an isolating of the stalled system out off the crowd membranes is possible.

Results

Membrane preparation of the stalled HlyA T1SS

Previous studies could show that the HlyA T1SS can be stalled by an eGFP-HlyA fusion protein [Lenders et al., 2015]. Co-expression of HlyAc and eGFP-HlyAc leaded to completely abolished secretion of HlyAc within the first two hours. The fast folded eGFP could not pass the translocator and remained inside the translocator whereas the unfolded HlyA part entered the T1SS and reached the extracellular surface [Evdokimov et al., 2006, Lenders et al., 2015]. A similar behavior could also observed for the injectisome of *Salmonella enterica* serovar Typhimurium [Radics et al., 2014]. Here, tandemly repeated effector domains of the natural substrate SptP were fused to GFP to stall the injectisome. The stalled injectisome could be purified and structurally analysted by cryo-EM [Radics et al., 2014].

According to this, we started initial trials to purify the eGFP-HlyA stalled HlyA T1SS. Cells were disrupted by sonification and membranes were prepared. If the eGFP-HlyA T1SS interaction is strong enough, immunofluorescence signals of TolC, HlyB, HlyD and eGFP-HlyA should be detectable in the prepared membranes. If the complex did not stick together, only the signals of the membrane proteins TolC, HlyB and HlyD would be detectable but not the signal of the soluble protein eGFP-HlyA. Free expressed eGFP-HlyA is not interacting with the membrane and would not appear in the immunofluorescence of the membrane preparation.

Immunofluorescence analysis of the prepared membranes highlighted the presence of TolC, HlyB, HlyD and eGFP-HlyA inside the membranes (see Figure 1). These results indicated that the stalled translocator is still assembled and could be used for further purification and analyzation steps.

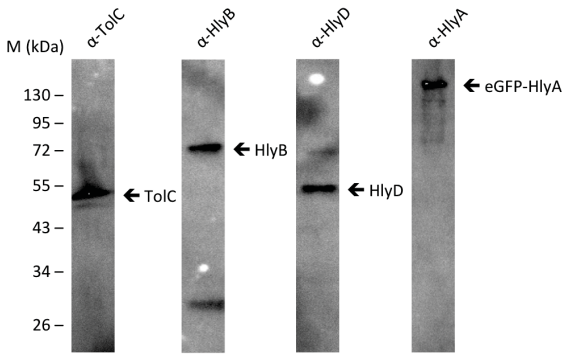

Figure 1: **Western blot analysis of purified *Escherichia coli* membranes with eGFP-HlyA stalled translocator**
Western blots show that all parts of the HlyA T1SS including the fusion protein eGFP-HlyA are present in the purified membranes. Immunofluorescence labeling was mediated by antibodies that are mentioned above the corresponding blots. Specific bands of eGFP-HlyA, HlyB, HlyD and TolC are labeled by arrows.

Solubilization screen of the stalled HlyA T1SS

In a next step, the stalled complex had to be isolated throughout the membrane. For that purpose, different detergents and their solubilization efficiency for the translocator were analyzed. The dot blot technique was used to identify promising candidate for solubilization of the trapped T1SS. Only detergents with a positiv immunofluorescence signal for TolC, HlyB, HlyD and eGFP-HlyA were used for further purification. Positiv signals for all of these proteins indicated a proper solubilization throughout the membrane. If only one of the proteins is detectable by immunofluorescence, it could be that the complex collapsed during solubilization.

The solubilization screen indicated that especially the zwitterionic Fos-Cholines®-14, 15 and 16 and Cyclofos^{TM}-5 showed a very efficient solubilization behavior (see Figure 2). Further, the non-ionic pyranoside n-Dodecyl-β-D-maltopyranoside and n-Dodecyl-β-D-thiomaltopyranoside as well as digitonin seemed to be prominent candidates for solubilization (see Figure 2).

Discussion

Our results could clearly demonstrate that a T1SS can be stalled *in vivo* [Lenders et al., 2015]. It is the first time that membranes of a stalled T1SS can be isolated and enables further steps for purification of the complex. Only separated parts of the HlyA T1SS are structurally characterized like the HlyB NBDs or CLDs [Zaitseva et al., 2005, Lecher

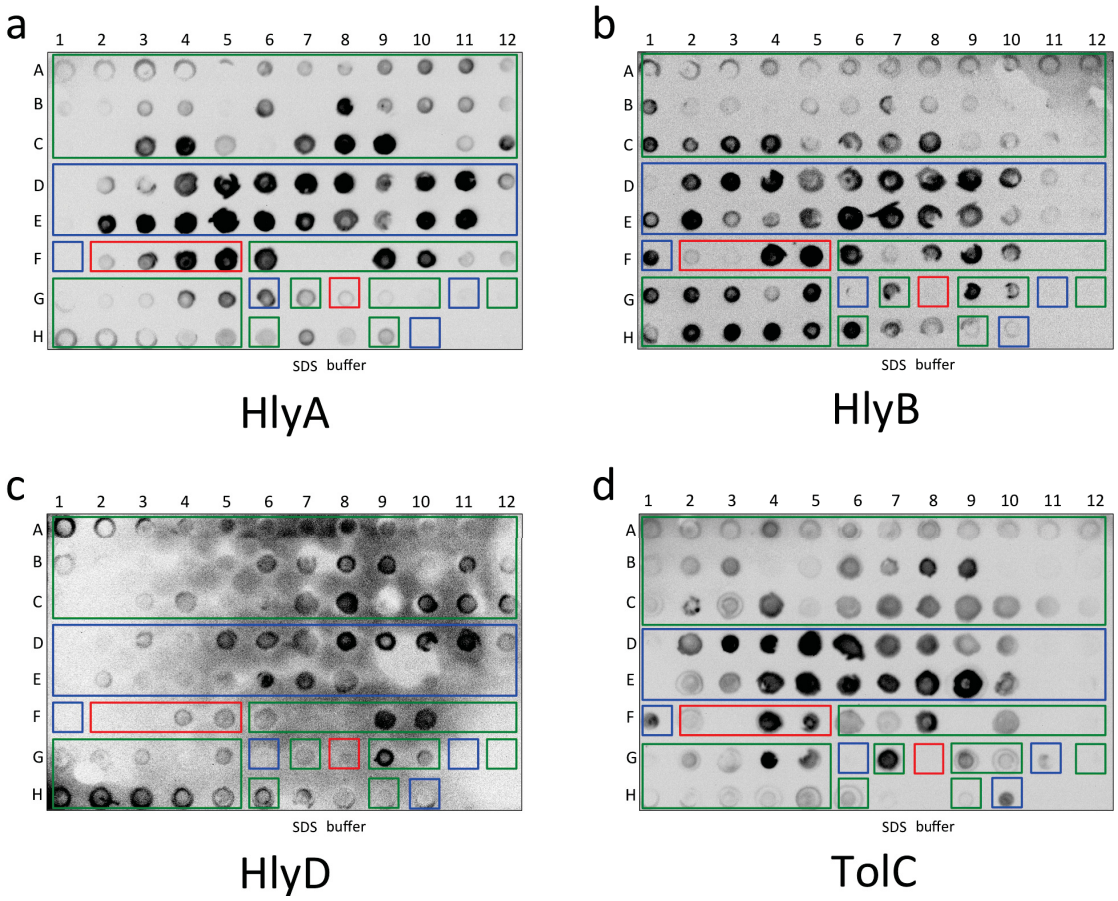

Figure 2: **Solubilization screen of the eGFP-HlyA trapped HlyA T1SS** Solubilization screen of *Escherichia coli* membranes containing eGFP-HlyA trapped HlyA T1SS. Solubilization efficacy of the complex was analyzed with 92 different different detergents. The solubilized complex was spotted onto a nitrocellulose membrane and examined via dot blotting with (**a**) HlyA, (**a**) HlyB, (**c**) HlyD and (**d**) TolC specific antibodies. Non-ionic detergents are marked by green boxes, zwitterionic detergents are marked by blue boxes and anionic detergents are marked by red boxes. SDS and buffer controls are in line H7 and H8 and labeled below. Table 1 lists all used detergents.

et al., 2011]. The whole T1SS in action is not understood and characterized so far. The stalled T1SS gave us now the opportunity to characterize the complete system in action. For that purpose, the membrane preparation of the intact complex was a first step in this direction. Western blot analysis demonstrated that all involved proteins like eGFP-HlyA, HlyB, HlyD and TolC were present in the purified membranes.

According to this, the solubilization screen gave us a first hint how the stalled HlyA T1SS could be isolated out off the membrane. The zwitterionic Fos-Cholines®-

14, 15 and 16 and Cyclofos^{TM}-5 as well as the non-ionic pyranosides n-Dodecyl-β-D-maltopyranoside and n-Dodecyl-β-D-thiomaltopyranoside and digitonin seemed to be goo candidates to reach this ambition. Nevertheless, a positiv fluorescence signal of eGFP-HlyA, HlyB, HlyD and TolC during this solubilization screen gave only a first hint if the solubilization is working but not if the protein complex is still intact. To verify this, density gradient centrifugation would be the method of choice. Only if eGFP-HlyA, HlyB, HlyD and TolC are co-localized within the same layer, the complex is still assembled. This strategies are still ongoing and need further investigations. Further, the solubilization screen have to be repeated with proper working controls for SDS for 100 % solubilization efficiency and for buffer for 0 % solubilization. Only with this controls, a quantification of the solubilization efficiency of the other detergents can be defined.

In summary, we were able to isolate membranes with eGFP-HlyA stalled HlyA T1SS and to define first detergent candidates for complex isolation out off the membrane.

Methods

Bacterial strains and plasmids

E. coli BL21 (DE3) cells were used for protein expression. The eGFP-HlyA expressing plasmid pSOI-eGFP-HlyA were generated as previous described [Lenders et al., 2015]. Protein expression is under the control of a P_{BAD} promoter. HlyB and HlyD expression were done by using the pK184 plasmid that is under the control of a P_{lac} promoter, inducible with IPTG (isopropyl β-D-1-thiogalactopyranoside) [Bakkes et al., 2010].

Cell cultivation and protein expression

Chemically competent cells were transformed with pK184-HlyBD and pSOI-eGFP-HlyA and grown on LB agar plates supplemented with 100 µg mL^{-1} ampicillin and 30 µg mL^{-1} kanamycin.

Overnight cultures of single colonies were used to inoculate 10 L 2 YT medium supplemented with 100 µg mL^{-1} ampicillin and 30 µg mL^{-1} kanamycin at an OD_{600} of 0.1. Cells were grown at 37 °C and 160 rpm in 5 L flasks with baffles to an OD_{600} of 0.6-0.8. Protein expression was induced with 10 mM arabinose and 1 mM IPTG. Additionally, 5 mM $CaCl_2$ was added to the cell culture. After induction, cells were grown additional 2 h under the same condition, harvested by centrifugation and stored at −20 °C.

Membrane preparation of the stalled HlyA T1SS

Complex expressing *E. coli* BL21 (DE3) cells were resuspended in buffer A1 (150 mM NaCl, 100 mM HEPES, 5 mM $CaCl_2$, pH 8.0). Cell were disrupted by sonication (Bandelin Sonopuls HD 2200). They were broken by five 1 min cycles at 4 °C, 20 kHz and an amplitude at 50 %, interrupted by 1 min breaks. Lysate was centrifuged for 30 min at 18 000 xg. Resulting supernatant was again centrifuged for 90 min at 200 000 xg. Pelleted membranes were resolved and homogenized in buffer A2 (250 mM NaCl, 100 mM HEPES, 5 mM $CaCl_2$, 10 % (w/v) glycerol, pH 8.0). Membranes were adjusted with buffer A2 to 10 mg mL^{-1}, shock frosted in liquid nitrogen and stored at −80 °C.

Solubilization screen via the dot blot technique

Membranes were solubilized in buffer A2 and adjusted to 10 mg mL^{-1}. Detergents were used at a concentration of 1 or 2 % according to their critical micellar concentration (see Table 1 for used concentration). Samples were solubilized for 1 h at 4 °C and shook at 750 rpm. Afterwards, solubilized samples were centrifuged for 30 min at 120 000 xg. Supernatant was supplemented with SDS sample buffer and 3 µL samples were spotted onto a dry nitrocellulose membrane. Membranes were dried over night and than blocked for an additional night in TBS-T with 5 % (w/v) milk powder. Blocked dot blots were incubated for 3 h in the corresponding primary rabbit antibody solutions (Dilution 1:8000 for anti-HlyA, anti-HlyB and anti-TolC antibody and dilution 1:4000 for anti-HlyD antibody). Afterwards, blots were washed three times in TBS-T buffer and incubated 1 h in a HRP-conjugated, secondary antibody solution. Incubated blots were again washed two times in TBS-T and one time in TBS buffer. The ECL advance kit (GE Healthcare) was used for the visualization of the protein signals. Signal intensity of dot blots were quantified by using the program ImageJ.

Table 1: **Detergents of the solubilization screen**

Number	Detergent	Used [%]	Nature
A1	Anameg®-7	1 %	N
A2	Anapoe®-20	1 %	N
A3	Anapoe®-35	1 %	N
A4	Anapoe®-58	1 %	N
A5	Anapoe®-80	1 %	N
A6	Anapoe®-C10E6	1 %	N
A7	Anapoe®-C10E9	1 %	N

A8	Anapoe®-C12E8	1 %	N
A9	Anapoe®-C12E9	1 %	N
A10	Anapoe®-C12E10	1 %	N
A11	Anapoe®-C13E8	1 %	N
A12	Anapoe®-X-100	1 %	N
B1	Anapoe®-X-114	1 %	N
B2	Anapoe®-X-305	1 %	N
B3	Anapoe®-X-405	1 %	N
B4	Big CHAP	1 %	N
B5	Big CHAP deoxy	1 %	N
B6	CYGLU®-3	2 %	N
B7	CYMAL®-1	2 %	N
B8	CYMAL®-2	2 %	N
B9	CYMAL®-3	1 %	N
B10	2,6-Dimethyl-4-heptyl-β-D-maltopyranoside	2 %	N
B11	n-Decyl-α-D-maltopyranoside	2 %	N
B12	n-Decyl-β-D-maltopyranoside	2 %	N
C1	n-Decyl-β-D-thiomaltopyranosid	2 %	N
C2	n-Decyl-N,N-Dimethylglycin	2 %	N
C3	n-Dodecyl-α-D-maltopyranoside	1 %	N
C4	n-Dodecyl-β-D-maltopyranoside	1 %	N
C5	n-Heptyl-β-D-thioglucopyranoside	2 %	N
C6	n-Heptyl-β-D-Glucopyranoside	2 %	N
C7	n-Nonyl-β-D-thiomaltopyranoside	1 %	N
C8	n-Dodecyl-β-D-thiomaltopyranoside	1 %	N
C9	CYMAL 4	2 %	N
C10	CYMAL®-5	2 %	N
C11	CYMAL 6	1 %	N
C12	CYMAL 7	1 %	N
D1	Anzergent 3-8	2 %	Z
D2	Anzergent®3-10	2 %	Z
D3	Anzergent®3-12	1 %	Z
D4	Anzergent®3-14	1 %	Z
D5	CHAPS	2 %	Z
D6	CHAPSO	2 %	Z
D7	Cyclofos^{TM}-4	2 %	Z

D8	Cyclofos™-5	1 %	Z
D9	Cyclofos™-6	1 %	Z
D10	Cyclofos™-7	1 %	Z
D11	Fos-Choline®-9	2 %	Z
D12	Fos-Choline-10	2 %	Z
E1	Cyclofos™-3	2 %	Z
E2	Fos-Choline®-11	1 %	Z
E3	Fos-Choline®-12	1 %	Z
E4	Fos-Choline®-13	1 %	Z
E5	Fos-Choline®-14	1 %	Z
E6	Fos-Choline®-15	1 %	Z
E7	Fos-Choline®-16	1 %	Z
E8	Fos-Choline®-Iso-9	2 %	Z
E9	Fos-Choline®-Iso-11	2 %	Z
E10	Fos-Choline®-Unisat-11-10	1 %	Z
E11	Fos-Choline®-8	2 %	Z
E12	n-Dodecyl-N,N-dimethylglycine	1 %	Z
F1	n-Dodecyl-N,N-dimethylamine-N-oxide (DDAO)	1 %	Z
F2	Cholic acid, sodium salt	1 %	A
F3	Deoxycholic acid, sodium salt	1 %	A
F4	Fosmea-8	1 %	A
F5	Fosmea®-10	1 %	A
F6	Hexaethylene Glycol Monooctyl Ether (C8E6)	1 %	N
F7	n-Hexyl-β-D-Glucopyranoside	2 %	N
F8	n-Hexyl-β-D-Maltopyranoside	2 %	N
F9	n-Nonyl-β-D- Glucopyranoside	1 %	N
F10	n-Nonyl-β-D-Maltopyranoside	1 %	N
F11	n-Nonyl-β-D-Thiomaltopyranoside	1 %	N
F12	Octaethylene Glycol Monodecyl Ether (C12E8)	1 %	N
G1	n-Octyl-β-D-Glucopyranoside	1 %	N
G2	n-Octyl-β-D-Thiomaltopyranoside	1 %	N
G3	n-Octyl-β-D-Maltopyranoside	2 %	N
G4	Pentaethylene Glycol Monodecyl Ether (C10E5)	1 %	N
G5	PMAL-C8	1 %	N
G6	Hexaethylene Glycol Monooctyl Ether (C8E6)	1 %	Z

G7	2-Propyl-1-Pentyl Maltopyranoside	2 %	N
G8	Sodium Dodecanoyl Sarcosine	1 %	A
G9	Sucrose Monododecanoate	1 %	N
G10	n-Tetradecyl-β-D-Maltopyranoside	1 %	N
G11	n-Tetradecyl-N,N-Dimethylamine-N-Oxide (TDAO)	1 %	Z
G12	Tetraethylene Glycol Monooctyl Ether (C8E4)	1 %	N
H1	n-Tridecyl-β-D-Maltopyranoside	1 %	N
H2	n-Undecyl-β-D-Maltopyranoside	1 %	N
H3	n-Undecyl-β-D-Maltopyranoside	1 %	N
H4	n-Undecyl-β-D-Thiomaltopyranoside	1 %	N
H5	Digitonin	1 %	N
H6	propyl(bi)cyclohexyl-α-maltoside (PCC-α-M)	1 %	N
H7	sodium dodecyl sulfate (SDS)	1 %	A
H8	buffer		
H9	MEGA-8	2 %	N
H10	Cyclofos^{TM}-2	1 %	Z

Column number highlights the position of the used detergent in the solubilization screen (see Figure 2), whereas nature described the overall charge of the detergent (N, non-ionic; Z, zwitterionic and A, anionic).

Acknowledgment

We thank all members of the Institute of Biochemistry, Heinrich-Heine-Universität Düsseldorf, for helpful and very fruitful discussions. We gratefully acknowledge support (and training) from the International NRW Research School BioStruct, granted by the Ministry of Innovation, Science and Research of the State North Rhine-Westphalia, the Heinrich-Heine-Universität Düsseldorf, and the Entrepreneur Foundation at the Heinrich-Heine-Universität of Düsseldorf.

References

[Arnoux et al., 1999] Arnoux, P., Haser, R., Izadi, N., Lecroisey, A., Delepierre, M., Wandersman, C. and Czjzek, M. (1999). The crystal structure of HasA, a hemophore secreted by Serratia marcescens. Nat Struct Biol *6*, 516–20.

[Bakkes et al., 2010] Bakkes, P. J., Jenewein, S., Smits, S. H. J., Holland, I. B. and Schmitt, L. (2010). The rate of folding dictates substrate secretion by the Escherichia coli hemolysin type 1 secretion system. J Biol Chem *285*, 40573–80.

[Balakrishnan et al., 2001] Balakrishnan, L., Hughes, C. and Koronakis, V. (2001). Substrate-triggered recruitment of the TolC channel-tunnel during type I export of hemolysin by Escherichia coli. J Mol Biol *313*, 501–10.

[Costa et al., 2015] Costa, T. R. D., Felisberto-Rodrigues, C., Meir, A., Prevost, M. S., Redzej, A., Trokter, M. and Waksman, G. (2015). Secretion systems in Gram-negative bacteria: structural and mechanistic insights. Nat Rev Microbiol *13*, 343–59.

[Debarbieux and Wandersman, 2001] Debarbieux, L. and Wandersman, C. (2001). Folded HasA inhibits its own secretion through its ABC exporter. EMBO J *20*, 4657–63.

[Delepelaire, 2004] Delepelaire, P. (2004). Type I secretion in gram-negative bacteria. Biochim Biophys Acta *1694*, 149–61.

[Evdokimov et al., 2006] Evdokimov, A. G., Pokross, M. E., Egorov, N. S., Zaraisky, A. G., Yampolsky, I. V., Merzlyak, E. M., Shkoporov, A. N., Sander, I., Lukyanov, K. A. and Chudakov, D. M. (2006). Structural basis for the fast maturation of Arthropoda green fluorescent protein. EMBO Rep *7*, 1006–12.

[Hinsa et al., 2003] Hinsa, S. M., Espinosa-Urgel, M., Ramos, J. L. and O'Toole, G. A. (2003). Transition from reversible to irreversible attachment during biofilm formation by Pseudomonas fluorescens WCS365 requires an ABC transporter and a large secreted protein. Mol Microbiol *49*, 905–18.

[Jarchau et al., 1994] Jarchau, T., Chakraborty, T., Garcia, F. and Goebel, W. (1994). Selection for transport competence of C-terminal polypeptides derived from Escherichia coli hemolysin: the shortest peptide capable of autonomous HlyB/HlyD-dependent secretion comprises the C-terminal 62 amino acids of HlyA. Mol Gen Genet *245*, 53–60.

[Koronakis et al., 1989] Koronakis, V., Koronakis, E. and Hughes, C. (1989). Isolation and analysis of the C-terminal signal directing export of Escherichia coli hemolysin protein across both bacterial membranes. EMBO J *8*, 595–605.

[Koronakis et al., 2000] Koronakis, V., Sharff, A., Koronakis, E., Luisi, B. and Hughes, C. (2000). Crystal structure of the bacterial membrane protein TolC central to multidrug efflux and protein export. Nature *405*, 914–9.

[Lecher et al., 2011] Lecher, J., Stoldt, M., Schwarz, C. K. W., Smits, S. H. J., Schmitt, L. and Willbold, D. (2011). 1H, 15N and 13C resonance assignment of the N-terminal C39 peptidase-like domain of the ABC transporter Haemolysin B (HlyB). Biomol NMR Assign *5*, 199–201.

[Lee et al., 2012] Lee, M., Jun, S.-Y., Yoon, B.-Y., Song, S., Lee, K. and Ha, N.-C. (2012). Membrane fusion proteins of type I secretion system and tripartite efflux pumps share a binding motif for TolC in gram-negative bacteria. PLoS One *7*, e40460.

[Lenders et al., 2015] Lenders, M. H. H., Weidtkamp-Peters, S., Kleinschrodt, D., Jaeger, K.-E., Smits, S. H. J. and Schmitt, L. (2015). Directionality of substrate translocation of the hemolysin A Type I secretion system. Sci Rep *5*, 12470.

[Radics et al., 2014] Radics, J., Königsmaier, L. and Marlovits, T. C. (2014). Structure of a pathogenic type 3 secretion system in action. Nat Struct Mol Biol *21*, 82–7.

[Thanabalu et al., 1998] Thanabalu, T., Koronakis, E., Hughes, C. and Koronakis, V. (1998). Substrate-induced assembly of a contiguous channel for protein export from E.coli: reversible bridging of an inner-membrane translocase to an outer membrane exit pore. EMBO J *17*, 6487–96.

[Zaitseva et al., 2005] Zaitseva, J., Jenewein, S., Wiedenmann, A., Benabdelhak, H., Holland, I. B. and Schmitt, L. (2005). Functional characterization and ATP-induced dimerization of the isolated ABC-domain of the haemolysin B transporter. Biochemistry *44*, 9680–90.

4. Discussion

This dissertation discusses four major questions about the function and mechanism of the HlyA T1SS (see Chapter 2). First, the directionality of secretion was analyzed to find out whether the N- or C-terminus of HlyA is translocated first. Second, the role of the secretion signal for initiating secretion was investigated in more detail. The third question deals with the secretion rate of HlyA and how it is influenced by the protein length, by the number of GG repeats of the protein and by external calcium ion concentration. Fourth, the role of different states of the ATP consumption cycle for the HlyA secretion process was analyzed.

4.1. The secretion signal threads the substrate into the translocator

Many publications in the last thirty years highlight the importance of the HlyA secretion signal for successful substrate secretion [Gray et al., 1986, Stanley et al., 1991, Kenny et al., 1994]. Substrates without secretion signal are not secreted but the exact roll of the secretion signal was not clearly characterized. It is known that the secretion signal interacts with the HlyB NBDs and that the substrate presence is essential for TolC recruitment [Thanabalu et al., 1998, Benabdelhak et al., 2003].

Fusion proteins of MBP or IFABP the HlyAc fragment are not secreting, but slow folding variants of MBP- or IFABP-HlyAc fused to fusions are secreting by the HlyA T1SS [Bakkes et al., 2010, Schwarz et al., 2012a]. Thereby, the question arises, if the not secreted fusion proteins are still interacting with the transporter and if HlyAc is still threaded into the translocator. The competition experiments with HlyAc and an eGFP-HlyAc fusion protein show that the HlyAc secretion is reduced to 30 % by eGFP-HlyAc co-expression (see Chapter 3.5, Figure 2b). In this case, HlyAc is competing with the fusion protein for the free T1SS. HlyAc can pass the membrane whereas the fusion protein eGFP-HlyAc can not pass the translocator due to the folded globular shape of eGFP that can not fit in the secretion pore. After one hour nearly all T1SS are blocked by eGFP-HlyAc and HlyAc can not secreted anymore. From this point the HlyAc level

in the medium remains constant over time and the supernatant contains only HlyAc that was secreted within the first hour. The same effect could be observed for an MBP-HlyAc fusion protein that was co-expressed with HlyAc. Here, all transporters are also blocked after an hour of co-expression and HlyAc secretion is also reduced. This data confirm that any kind of globular plug at the HlyAc N-terminus results in blocking of the translocator. Further, translocator blocking by folding of the substrate could also observed in other T1SS. Folded HasA leads to an inhibition of its own secretion by its T1SS in *Serratia marcescens* [Debarbieux and Wandersman, 2001].

Deletion of the last 60 C-terminal amino acids from eGFP-HlyAc (respectively MBP-HlyAc) abolished blocking of the HlyA T1SS in competition experiments. HlyAc is secreted in the same amount with and without co-expression of eGFP-HlyAc. This results indicates that the secretion signal is essential for threading the substrate into the translocator. Even without the secretion signal, the substrate is still recognized by the GG repeats by the HlyB CLDs [Lecher et al., 2012] but translocation of the substrate into the T1SS is not initiated. These results are in line with previous published data. SPR experiments show that the secretion signal of HlyA is interacting with the HlyB NBDs [Benabdelhak et al., 2003]. It is assumable that the substrate is stabilized by the CLD and the GG repeats (and maybe by the cytoplasmic part of HlyD that is also interacting with HlyA [Balakrishnan et al., 2001]) and that this interaction leads to complex assembly whereas the binding of the secretion signal initiates the translocation process. After NBD interaction, the secretion signal can pass on the TMD of HlyB (interaction areas could be identified between the secretion signal and the HlyB TMDs [Zhang et al., 1993]) and leads from there the way into the translocator. Such a kind of mechanism indicates secretion of the substrate with the C-terminus ahead as could be shown by confocal laser scanning microscopy (CLSM) (see Chapter 3.5). The N-terminal eGFP of the fusion proteins remain located inside the cytoplasm. The fluorescence images confirm that the eGFP has to be in a folded conformation, otherwise no specific eGFP fluorescence would appear inside the cytoplasm. Due to the fact that folded globular eGFP can not pass the translocator, this results confirm that the T1SS is stalled via blocking the pore by the fusion protein.

4.2. The substrate is secreted with its C-terminus first

Secretion experiments with HlyAc fused to slow folding mutants of MBP or IFABP demonstrates that the substrate for the HlyA T1SS is secreted unfolded [Bakkes et al., 2010, Schwarz et al., 2012a]. This matches with the inner diameter of TolC which is

only 20 Å [Koronakis et al., 2004] too tight to allow the passage of folded proteins. The average diameter of an α-helix is 12 Å. Consequently, the substrate can only enter the translocator unfolded or partly folded with one terminus first. A hairpin insertion is highly unlikely. Confocal laser scanning microscopy images of the stalled complex by eGFP-HlyAc respectively eGFP-HlyA demonstrate that the C-terminal parts of the fusion proteins are exposed at the cell surface. A secretion with the C-terminus ahead can therefore be assumed.

According to a secretion with the C-terminus ahead, an activating model is highly presumable for the HlyA T1SS. In case of an activating model, the C-terminus respectively the secretion signal initiates the transport process via binding to the HlyB NBDs [Benabdelhak et al., 2003]. This can be simultaneous with the GG repeat interaction to the HlyB CLDs [Lecher et al., 2012]. Secretion signal binding induces NBD dimerization and TolC recruitment to assemble the full translocator. In a next step, conformational changes of the ABC transporter could initiate the transfer of the secretion signal from the NBDs to the TMDs whereas conformational changes of the TMDs leads to pathway opening. Thereby, the substrate is threaded with the C-terminus ahead into and through the transenvelope channel [Lenders et al., 2015]. Full substrate translocation could than leads to the disassemble of the T1SS and to a reset of HlyB (probably HlyD, too) into its initial state to allow new substrate translocation.

One has to discuss, if the C-terminal initiated secretion by the HlyA T1SS is a general feature of type I secretion. The ABC transporter of T1SS can be classified into three subgroups. The ABC transporter of the first group harbors a N-terminal fully active C39 peptidase, the second group contains a N-terminal CLD, whereas the third group harbors no additional domain. Transporter with a C39 peptidase transport small substrates (<10 kDa). The substrates belong mainly to the bacteriocin family and contain a cleavable N-terminal leader peptide for secretion (see Figure 1.4). Due to the fact that this class is also found in Gram-positive bacteria and that they have a N-terminal cleavable leader sequence, this group can be excluded from general C-terminal initiated secretion. Transporters that contain a N-terminal CLD mainly transport larger substrates (>55 kDa) that are all member of the RTX protein family (see Figure 1.4). The substrates harbor a C-terminal secretion signal (last 50-60 amino acids) which is not cleaved during or after secretion. Further, they contain GG repeats that are located in front of the secretion signal. HlyA belongs to this substrates. It is proposed that the CLD stabilizes the substrate [Lecher et al., 2012] and leads to an orientation of the C-terminus near to the ABC transporter entrance. This could promote a C-terminal secretion. Additionally, C-terminal initiated secretion leads to an early translocation of

the GG repeats that promote the active folding of the secreted protein by binding of calcium ions in the extracellular medium. This results in an early stabilization of the substrate during secretion [Rhodes et al., 2001]. It is favorable that C-terminal initiated secretion works in general for T1SS with ABC transporter harboring a CLD. Secretion systems with transporter without any additional domain like the HasA T1SS from *Serratia marcescens* transport substrates with a C-terminal secretion signal [Létoffé et al., 1996, Masi and Wandersman, 2010]. The signal is not cleaved during or after translocation. HasA contain primary recognition sites throughout the protein and a secretion dependency on SecB that could not found for RTX protein substrates [Delepelaire and Wandersman, 1998, Bakkes et al., 2010, Masi and Wandersman, 2010].

Furthermore, the fluorescence images allow a localization of the HlyA T1SS on the cell envelope. A majority of the images indicate a helical-like localization of the secretion systems over the whole cell reaching from one pole to the other. A similar localization could be observed for the rod shape-determining protein MreB and the cell wall synthetic machinery from *Escherichia coli* and *Bacillus subtilis* [Garner et al., 2011, van Teeffelen et al., 2011, Govindarajan et al., 2012]. This gives rise to a chiral insertion of peptidoglycan into the cell wall and causes the cell to twist during elongation growth [Govindarajan et al., 2012, Wang et al., 2012]. It is possible that the HlyA T1SS is coupled to the cell wall synthetic machinery due to the fact that the secretion system has to pass the peptidoglycan at some point. Nevertheless, this assumption is only speculative and needs further investigation.

4.3. Secretion rate is independent of various factors

Competition experiments with HlyAc and the eGFP-HlyAc fusion protein confirm that after 1 h of co-expression all functional formed T1SS are blocked (see Chapter 3.5). Fluorescence images of cells expressing eGFP-HlyAc confirm that the HlyAc fragment is exposed at the cell surface and is accessible for antibody binding (see Chapter 3.5). Due to the results that show that HlyA T1SS substrates are secreted unfolded, the HlyAc part of the fusion protein has to be unfolded or only partly folded inside the translocator [Bakkes et al., 2010]. The fragment has a size of 218 amino acids which is approximately 788.4 Å. Although, the structure and the size of the HlyA T1SS is unknown, the cryo-EM images of the RND efflux pump AcrAB-TolC indicate that the length of the complex is approximately 320 Å. Taken into account that the ABC transporter of the HlyA T1SS is enlarged by 45 Å into the cytoplasm due to the NBD, only 425.6 Å of fully elongated HlyAc (represents 118 amino acids) can face the cell surface. The last 60 C-terminal

amino acids show a low antibody binding affinity. Further, the exposed fragment will start folding at the extracellular surface. A folded fragment will only have a 40-50 Å globular surface that is accessible for antibody interaction. The binding groove of an antibody (pdb file 1MEL) is only 20-40 Å in size. Thus, only one or maximal two antibody can bind per active T1SS. Together with the assumption that quantum yields of bound and free antibody are identical, an amount of approximately 5000 active T1SS per cell could be determined. Western blot quantification of the cellular HlyB amount confirm this value.

The defined number of T1SS allow the quantification of the secreted rate of HlyA per T1SS. HlyA and HlyAc secretion are with 15.2 ± 1.7 and 14.1 ± 1.0 translocated amino acids per sec and T1SS identical. The protein length of the substrate is not important for the secretion velocity. Moreover, the GG repeat/protein length ratio has no influence on the secretion rate. HlyA is 4.7 times longer than HlyAc but have only twice the amount of GG repeats. HlyAc has a higher GG repeat/protein length ratio than HlyA but both proteins secrete with the same rate.

It could be shown that the GG repeats bind Ca^{2+} ions with a high affinity (K_D of 100 µM) [Thomas et al., 2014a]. Binding appears only at the extracellular surface due to the higher calcium ion concentration [Jones et al., 1999]. As mentioned before, the C-terminus is secreted first. According to this, the GG repeats that are located in front of the secretion signal reaches the cell surface in an early stage of secretion. Ca^{2+} binding of the GG repeats induces protein folding [Rhodes et al., 2001, Linhartová et al., 2010]. The induced folding could promote an inherent driving force that 'pulls' the protein, e.g. HlyA out of the translocator [Linhartová et al., 2010]. To determine if such a folding induced driving force energizes the HlyA T1SS, secretion rates in presence of different extracellular calcium ion concentration were prepared. The results indicate that such a 'pulling' mechanism does not exist because HlyA and HlyAc secretion rate is similar even by deceeding the K_D of the GG repeats for Ca^{2+} binding. The results demonstrate that the GG repeats of HlyA and HlyAc are only important for protein stability and protein folding but not for creating a driving force for the translocation process.

4.4. ATP hydrolysis threads the substrate into the translocator

The role and amount of ATP hydrolyzes for the HlyA translocation cycle is currently unknown. The exact number of ATP for completing one secretion cycle is highly speculative. It was assumed that only two ATP are needed for completing one translocation cycle like in the case of OpuA from *Lactococcus lactis* or in the case of the maltose or

glycine-betaine import system of *Escherichia coli* [Mimmack et al., 1989, Patzlaff et al., 2003]. Further, an iterative mechanism where a distinct number of ATP is consumed per translocated amino acid is possible. Such a mechanism was observed for the Sec pathway. Here, one ATP is consumed per 20-30 transported amino acids [Schiebel et al., 1991, Uchida et al., 1995]. Due to the fact that HlyA has a size of 1024 amino acids it seems unlikely that only one or two ATP are used for a full translocation process. Energizing of the secretion via a 'pulling' mechanism or via the PMF in late stages of secretion could be excluded [Koronakis et al., 1991].

Secretion experiments with the ATP hydrolyzing deficient HlyB-H662A variant show that HlyA and HlyAc secretion is completely abolished. The mutant is still able to bind ATP and leads to dimerization of the NBDs [Zaitseva et al., 2005]. Western blots confirm that expression of HlyB wild type and HlyB-H662A are equal. Previous studies indicate that ATP hydrolyzing deficient variants still results in a full assemble HlyA T1SS [Thanabalu et al., 1998]. Fluorescence images show that in case of co-expression of eGFP-HlyA, HlyB-H662A and HlyD the HlyA part of the substrate is not reaching the cell surface (see Chapter 3.6). This indicates that ATP hydrolyzes is necessary for threading the substrate into the translocation pore. This results indicate two possibilities how ATP hydrolysis is involved in HlyA secretion. First, ATP can energize the translocation process in an iterative way. Therefore, a distinct number of ATP is consumed per translocated amino acid. Or second, ATP hydrolysis can be involved in some gating activity. Therefore, the HlyA T1SS works as an ATP hydrolysis gated channel, where a first ATP hydrolysis step is necessary for initiating transport and channel opening whereas a second ATP hydrolysis step terminates the transport process and results in channel closing.

ATPase data of the HlyB-NBDs mutants R611A and D551A show *in vitro* a dramatical decrease in the ATPase activity [Zaitseva et al., 2006]. The two amino acids form a salt bridge that is proposed to act as a gate to close or open the phosphate exit tunnel in the HlyB NBD structure [Zaitseva et al., 2006]. Secretion of HlyAc in presence of HlyB-R611A results in wild type secretion levels whereas HlyB-D551A results in a four fold reduced secretion rate (see Figure 4.1). Expression rates of all HlyB variants are identical. The results indicate that the ATPase activity of the NBDs have a directly influence on the secretion rate but that ATP hydrolysis seems to be not the time limiting factor for secretion. In case of HlyB-R611A, the ATPase activity is 10 fold reduced but results in the same secretion rate whereas the ATPase activity of HlyB-D551A is 15 fold reduced and the secretion rate drops by a factor of four. Also, it is not known how far the *in vitro* ATPase data of the isolated NBDs can be transferred on the *in vivo*

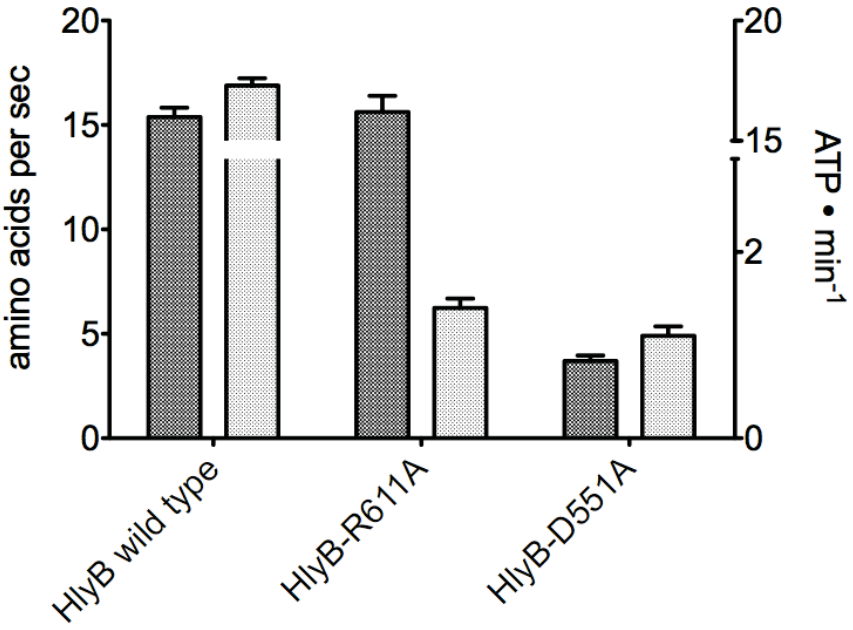

Figure 4.1.: **Secretion rate of HlyAc with different HlyB variants and corresponding NBD ATPase activity**
Secretion rate of HlyAc (dark grey bars) in presence of different HlyB variants. Secretion rate is measured in secreted amino acids per second and T1SS (left ordinate). Measured ATPase activity of the isolated and purified HlyB-NBD variants is highlighted as light grey bars. Activity is represented by the turnover number in hydrolyzed ATP per minute and NBD (right ordinate). ATPase activity determination was performed in *vitro* [Zaitseva et al., 2006].

situation. To answer this question, this topic requires further investigation.

4.5. Proposed translocation mechanism for the HlyA T1SS

The described observations indicate that an 'activating' model with C-terminal initiated secretion is favorable for the HlyA T1SS. Even in absence of the substrate, the IM compounds HlyB and HlyD are assembled [Thanabalu et al., 1998]. In a first step, HlyA interaction with HlyB and HlyD results in TolC recruitment (see Figure 4.2, step 1). As mentioned, it is assumed that the GG repeats interact with the CLD of HlyB whereas the secretion signal interacts with the HlyB NBDs [Benabdelhak et al., 2003, Lecher et al., 2012]. Further, the cytoplasmic part of HlyD is interacting with HlyA via its potential amphiphatic helix and its charged amino acid cluster [Balakrishnan et al., 2001].The

exact motif of HlyA for HlyD interaction is unknown yet but the substrate interaction with both IM compounds is essential for TolC recruitment. TolC is recruited by the periplasmic part of HlyD [Lee et al., 2012]. Direct interaction between TolC and the ABC transporter could not be observed [Thanabalu et al., 1998]. HlyA interaction with the substrate is assumed to stabilized the protein in an unfolded conformation [Lecher et al., 2012]. If this process occurs co- or post-translational for HlyA, is unknown so far and needs further investigation.

In a next step, the secretion signal initiates the translocation process and threads the substrate into the translocator. This thesis could clearly demonstrate that the secretion signal is essential for threading the substrate into the translocator and that the C-terminus leads the way throughout the translocation pore [Lenders et al., 2015] (see Figure 4.2, step 2). In this state, the dimerization of the HlyB NBDs have to take place. It could be shown that substrate presence results in stimulation of the HlyB ATPase activity i*n vitro*. For that purpose, the NBDs have to dimerize to build a full and active ATP binding site [Zaitseva et al., 2005, Zaitseva et al., 2006]. Dimerization will result in drastically conformational changes of the ABC transporter due to the coupling helices that link the NBDs and the TMDs [Dawson and Locher, 2006]. It is supposed that the secretion signal is interaction with the TMDs of HlyB [Zhang et al., 1993]. The conformational changes of the transporter can result in transfer of the secretion signal to the TMDs of HlyB. If the GG repeats are still interacting with the CLD during that time is unknown.

Afterwards, the substrate has to be secreted in some way. It could be shown that ATP hydrolysis is necessary for completing substrate translocation [Thanabalu et al., 1998]. Our results demonstrate that ATP hydrolysis is necessary for the transport process itself. Without hydrolysis, the substrate is not reaching the cell surface. This leads to two possible explanations how ATP hydrolysis is involved in substrate translocation. The first explanation could be that the HlyA T1SS works in an iterative way like the Sec pathway (see Figure 4.2, step 3). Here, a distinct number of ATP are consumed per translocated amino acid. The secretion rate experiments show that HlyA and HlyAc are secreted with the same rate. This indicates that a distinct number of ATP are consumed per translocated amino acid. Nevertheless, secretion rate experiments in presence of slow ATP hydrolyzing HlyB mutants results not always in a reduced secretion rate but this could also due to the fact that ATP hydrolysis is not the limiting factor or that the *in vitro* measured ATPase data do not reflect the *in vivo* situation. An other explanation can be that the HlyA T1SS work like an ATP hydrolysis gated channel. For that purpose, hydrolysis of one or two ATP leads to channel opening by conformational

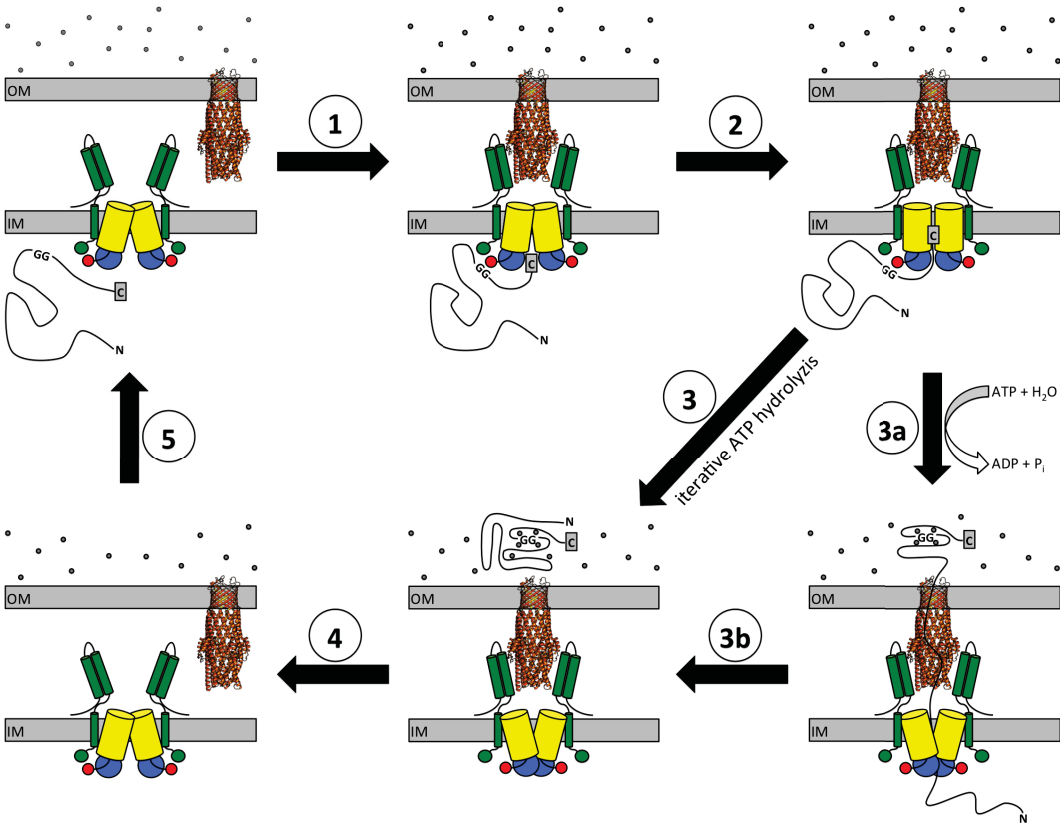

Figure 4.2.: **Possible steps of the HlyA T1SS**
Cross section of the *Escherichia coli* IM and OM with a HlyA T1SS. Membranes are represented by grey bars. Dimeric HlyB (TMDs in yellow, NBDs in blue and CLDs in red) and oligomeric HlyD (in green) are located in the IM whereas TolC (in orange; pdb file 1EK9) is located in the OM. Grey dots represent extracellular Ca^{2+} and black twisted line the substrate HlyA where GG stands for the GG repeats, N for the N-terminus and grey boxed C for the C-terminus with the secretion signal. Numbers indicate the different proposed steps of the mechanism. (1) Synthesized HlyA binds to the IM components over the GG repeats, the secretion signal and further regions. Leads to TolC recruiting and NBD dimerizing. (2) Secretion signal is transferred to the TMDs and leads to conformational changes of HlyB. (3) Iterative ATP hydrolysis leads to full substrate translocation. Extracellular folding of HlyA by Ca^{2+} binding to GG repeats. (3a) ATP hydrolysis gated channel opening leads to substrate translocation into the translocation pore. (3b) An unknown inherent driving force complete substrate translocation. Extracellular folding of HlyA by Ca^{2+} binding to GG repeats. (4) Completed substrate translocation is recognized by the T1SS, leads to its disassembly and to HlyB reset into the initial state. (5) IM compounds are ready for new substrate recognition and for repeating the translocation cycle.

changes of HlyB and to substrate translocation to the cell surface (see Figure 4.2, step 3a). At the cell surface, substrate binding is induced by extracellular Ca^{2+} binding to the GG repeats. If this assumption is true, the driving force for the remaining substrate translocation is unknown. In case of an iterative translocation, ATP hydrolysis energizes the transport process. In case of an ligand gated channel the energy has to be provided by something different. Only two ATP molecules for translocation of 1024 amino acid for HlyA are highly unlikely. A 'pulling' mechanism by Ca^{2+} induced protein folding could be excluded by our experiments as well as an influence of the GG repeats on the secretion speed. Furthermore, the PMF as the inherent driving force could be excluded in late stages for HlyA secretion [Koronakis et al., 1991]. Only diffusion along a concentration and electrostatic gradient of HlyA and the PMF in early stages of secretion can energize and complete the secretion process (see Figure 4.2, step 3b). Nevertheless, substrate translocation will be completed and HlyA folds into its active form in the extracellular space by Ca^{2+} binding.

Completion of the secretion process have to be recognized by the translocator in some way. This recognition can be mediated by the absence of the substrate or by other signals that could not be determined yet. Finally this leads to the disassembly of the T1SS and to a reset of the ABC transporter into its initial state (see Figure 4.2, step 4). The transporter is now able to bind a new cytosolic unfolded HlyA molecule and to start a new translocation cycle 4.2, step 5). How far the first translocation cycle has to be completed before a new cycle can be initiated is also only speculative. It could be that during translocation of the substrate the free CLD of HlyB can interact with a new HlyA molecule and leads to a first reorientation and to a movement of the new substrate into the initial position. According to this, a new translocation cycle could start immediately.

List of Abbreviations

ABC ATP binding cassette

acyl-ACP acylated acyl carrier protein

ADP Adenosine diphosphate

ATP Adenosine triphosphate

CCCP carbonylcyanide m-chlorophenylhy-drazone

CLD C39-like domain

CLSM confocal laser scanning microscopy

DAUDA 11-(Dansylamino)undecanoic acid

DNA deoxyribonucleic acid

eGFP enhanced Green Fluorescence Protein

cryo-EM Cryo-electron microscopy

GG repeats glycine-rich repeats

HlyA hemolysin A

HlyAc C-terminal 218 amino acids of HlyA

HlyB hemolysin B

HlyC hemolysin C

HlyD hemolysin D

IFABP intestinal fatty acid binding protein

IM inner membrane

MBP maltose binding protein

MD Molecular dynamic

MFP membrane fusion protein

NBD nucleotide binding domain

NMR nuclear magnetic resonance

OM outer membrane

OMP outer membrane protein

pdb Protein Data Bank

PMF proton motive force

RND resistance-nodulation-division

pro-HlyA non-toxic pre-protein

RTX repeats in toxin

Sec general secretory

SPR Surface plasmon resonance

T1SS Type I secretion system

T2SS Type II secretion system

T3SS Type III secretion system

T4SS Type IV secretion system

T5SS Type V secretion system

T6SS Type VI secretion system

T7SS Type VII secretion system

Tat twin arginine translocation

TMD transmembrane domain

UPEC uropathogenic *Escherichia coli*

List of Figures

Bibliography

[Akama et al., 2004a] Akama, H., Kanemaki, M., Yoshimura, M., Tsukihara, T., Kashiwagi, T., Yoneyama, H., Narita, S.-i., Nakagawa, A. and Nakae, T. (2004a). Crystal structure of the drug discharge outer membrane protein, OprM, of Pseudomonas aeruginosa: dual modes of membrane anchoring and occluded cavity end. J Biol Chem *279*, 52816–9.

[Akama et al., 2004b] Akama, H., Matsuura, T., Kashiwagi, S., Yoneyama, H., Narita, S.-I., Tsukihara, T., Nakagawa, A. and Nakae, T. (2004b). Crystal structure of the membrane fusion protein, MexA, of the multidrug transporter in Pseudomonas aeruginosa. J Biol Chem *279*, 25939–42.

[Akeda and Galán, 2005] Akeda, Y. and Galán, J. E. (2005). Chaperone release and unfolding of substrates in type III secretion. Nature *437*, 911–5.

[Alvarez-Martinez and Christie, 2009] Alvarez-Martinez, C. E. and Christie, P. J. (2009). Biological diversity of prokaryotic type IV secretion systems. Microbiol Mol Biol Rev *73*, 775–808.

[Ames et al., 1992] Ames, G. F., Mimura, C. S., Holbrook, S. R. and Shyamala, V. (1992). Traffic ATPases: a superfamily of transport proteins operating from Escherichia coli to humans. Adv Enzymol Relat Areas Mol Biol *65*, 1–47.

[Andersen et al., 2002] Andersen, C., Koronakis, E., Bokma, E., Eswaran, J., Humphreys, D., Hughes, C. and Koronakis, V. (2002). Transition to the open state of the TolC periplasmic tunnel entrance. Proc Natl Acad Sci U S A *99*, 11103–8.

[Arnoux et al., 1999] Arnoux, P., Haser, R., Izadi, N., Lecroisey, A., Delepierre, M., Wandersman, C. and Czjzek, M. (1999). The crystal structure of HasA, a hemophore secreted by Serratia marcescens. Nat Struct Biol *6*, 516–20.

[Bakkes et al., 2010] Bakkes, P. J., Jenewein, S., Smits, S. H. J., Holland, I. B. and Schmitt, L. (2010). The rate of folding dictates substrate secretion by the Escherichia coli hemolysin type 1 secretion system. J Biol Chem *285*, 40573–80.

[Balakrishnan et al., 2001] Balakrishnan, L., Hughes, C. and Koronakis, V. (2001). Substrate-triggered recruitment of the TolC channel-tunnel during type I export of hemolysin by Escherichia coli. J Mol Biol *313*, 501–10.

[Balsalobre et al., 2006] Balsalobre, C., Silván, J. M., Berglund, S., Mizunoe, Y., Uhlin, B. E. and Wai, S. N. (2006). Release of the type I secreted alpha-haemolysin via outer membrane vesicles from Escherichia coli. Mol Microbiol *59*, 99–112.

[Basler et al., 2012] Basler, M., Pilhofer, M., Henderson, G. P., Jensen, G. J. and Mekalanos, J. J. (2012). Type VI secretion requires a dynamic contractile phage tail-like structure. Nature *483*, 182–6.

[Bauche et al., 2006] Bauche, C., Chenal, A., Knapp, O., Bodenreider, C., Benz, R., Chaffotte, A. and Ladant, D. (2006). Structural and functional characterization of an essential RTX subdomain of Bordetella pertussis adenylate cyclase toxin. J Biol Chem *281*, 16914–26.

[Baumann et al., 1993] Baumann, U., Wu, S., Flaherty, K. M. and McKay, D. B. (1993). Three-dimensional structure of the alkaline protease of Pseudomonas aeruginosa: a two-domain protein with a calcium binding parallel beta roll motif. EMBO J *12*, 3357–64.

[Bavro et al., 2008] Bavro, V. N., Pietras, Z., Furnham, N., Pérez-Cano, L., Fernández-Recio, J., Pei, X. Y., Misra, R. and Luisi, B. (2008). Assembly and channel opening in a bacterial drug efflux machine. Mol Cell *30*, 114–21.

[Benabdelhak et al., 2003] Benabdelhak, H., Kiontke, S., Horn, C., Ernst, R., Blight, M. A., Holland, I. B. and Schmitt, L. (2003). A specific interaction between the NBD of the ABC-transporter HlyB and a C-terminal fragment of its transport substrate haemolysin A. J Mol Biol *327*, 1169–79.

[Berks et al., 2005] Berks, B. C., Palmer, T. and Sargent, F. (2005). Protein targeting by the bacterial twin-arginine translocation (Tat) pathway. Curr Opin Microbiol *8*, 174–81.

[Beveridge, 1999] Beveridge, T. J. (1999). Structures of gram-negative cell walls and their derived membrane vesicles. J Bacteriol *181*, 4725–33.

[Bhakdi et al., 1986] Bhakdi, S., Mackman, N., Nicaud, J. M. and Holland, I. B. (1986). Escherichia coli hemolysin may damage target cell membranes by generating transmembrane pores. Infect Immun *52*, 63–9.

[Binet and Wandersman, 1995] Binet, R. and Wandersman, C. (1995). Protein secretion by hybrid bacterial ABC-transporters: specific functions of the membrane ATPase and the membrane fusion protein. EMBO J *14*, 2298–306.

[Blight and Holland, 1994] Blight, M. A. and Holland, I. B. (1994). Heterologous protein secretion and the versatile Escherichia coli haemolysin translocator. Trends Biotechnol *12*, 450–5.

[Boehm et al., 1990] Boehm, D. F., Welch, R. A. and Snyder, I. S. (1990). Calcium is required for binding of Escherichia coli hemolysin (HlyA) to erythrocyte membranes. Infect Immun *58*, 1951–8.

[Boyer et al., 2009] Boyer, F., Fichant, G., Berthod, J., Vandenbrouck, Y. and Attree, I. (2009). Dissecting the bacterial type VI secretion system by a genome wide in silico analysis: what can be learned from available microbial genomic resources? BMC Genomics *10*, 104.

[Boyer, 1997] Boyer, P. D. (1997). The ATP synthase–a splendid molecular machine. Annu Rev Biochem *66*, 717–49.

[Bradley, 1980] Bradley, D. E. (1980). Morphological and serological relationships of conjugative pili. Plasmid *4*, 155–69.

[Brinker et al., 2001] Brinker, A., Pfeifer, G., Kerner, M. J., Naylor, D. J., Hartl, F. U. and Hayer-Hartl, M. (2001). Dual function of protein confinement in chaperonin-assisted protein folding. Cell *107*, 223–33.

[Brooks et al., 1980] Brooks, H. J., O'Grady, F., McSherry, M. A. and Cattell, W. R. (1980). Uropathogenic properties of Escherichia coli in recurrent urinary-tract infection. J Med Microbiol *13*, 57–68.

[Brunet et al., 2014] Brunet, Y. R., Hénin, J., Celia, H. and Cascales, E. (2014). Type VI secretion and bacteriophage tail tubes share a common assembly pathway. EMBO Rep *15*, 315–21.

[Büttner, 2012] Büttner, D. (2012). Protein export according to schedule: architecture, assembly, and regulation of type III secretion systems from plant- and animal-pathogenic bacteria. Microbiol Mol Biol Rev *76*, 262–310.

[Campos et al., 2010] Campos, M., Nilges, M., Cisneros, D. A. and Francetic, O. (2010). Detailed structural and assembly model of the type II secretion pilus from sparse data. Proc Natl Acad Sci U S A *107*, 13081–6.

[Carrier et al., 2007] Carrier, I., Urbatsch, I. L., Senior, A. E. and Gros, P. (2007). Mutational analysis of conserved aromatic residues in the A-loop of the ABC transporter ABCB1A (mouse Mdr3). FEBS Lett *581*, 301–8.

[Cascales and Christie, 2004] Cascales, E. and Christie, P. J. (2004). Agrobacterium VirB10, an ATP energy sensor required for type IV secretion. Proc Natl Acad Sci U S A *101*, 17228–33.

[Cescau et al., 2007] Cescau, S., Debarbieux, L. and Wandersman, C. (2007). Probing the in vivo dynamics of type I protein secretion complex association through sensitivity to detergents. J Bacteriol *189*, 1496–504.

[Chandran et al., 2009] Chandran, V., Fronzes, R., Duquerroy, S., Cronin, N., Navaza, J. and Waksman, G. (2009). Structure of the outer membrane complex of a type IV secretion system. Nature *462*, 1011–5.

[Chen et al., 2003] Chen, J., Lu, G., Lin, J., Davidson, A. L. and Quiocho, F. A. (2003). A tweezers-like motion of the ATP-binding cassette dimer in an ABC transport cycle. Mol Cell *12*, 651–61.

[Christie et al., 2014] Christie, P. J., Whitaker, N. and González-Rivera, C. (2014). Mechanism and structure of the bacterial type IV secretion systems. Biochim Biophys Acta *1843*, 1578–91.

[Clantin et al., 2007] Clantin, B., Delattre, A.-S., Rucktooa, P., Saint, N., Méli, A. C., Locht, C., Jacob-Dubuisson, F. and Villeret, V. (2007). Structure of the membrane protein FhaC: a member of the Omp85-TpsB transporter superfamily. Science *317*, 957–61.

[Cornelis, 2006] Cornelis, G. R. (2006). The type III secretion injectisome. Nat Rev Microbiol *4*, 811–25.

[Costa et al., 2015] Costa, T. R. D., Felisberto-Rodrigues, C., Meir, A., Prevost, M. S., Redzej, A., Trokter, M. and Waksman, G. (2015). Secretion systems in Gram-negative bacteria: structural and mechanistic insights. Nat Rev Microbiol *13*, 343–59.

[Cotter et al., 2005] Cotter, S. E., Surana, N. K. and St Geme, 3rd, J. W. (2005). Trimeric autotransporters: a distinct subfamily of autotransporter proteins. Trends Microbiol *13*, 199–205.

[Dawson and Locher, 2006] Dawson, R. J. P. and Locher, K. P. (2006). Structure of a bacterial multidrug ABC transporter. Nature *443*, 180–5.

[Debarbieux and Wandersman, 2001] Debarbieux, L. and Wandersman, C. (2001). Folded HasA inhibits its own secretion through its ABC exporter. EMBO J *20*, 4657–63.

[DeBoy et al., 1980] DeBoy, 2nd, J. M., Wachsmuth, I. K. and Davis, B. R. (1980). Hemolytic activity in enterotoxigenic and non-enterotoxigenic strains of Escherichia coli. J Clin Microbiol *12*, 193–8.

[Delepelaire, 1994] Delepelaire, P. (1994). PrtD, the integral membrane ATP-binding cassette component of the Erwinia chrysanthemi metalloprotease secretion system, exhibits a secretion signal-regulated ATPase activity. J Biol Chem *269*, 27952–7.

[Delepelaire, 2004] Delepelaire, P. (2004). Type I secretion in gram-negative bacteria. Biochim Biophys Acta *1694*, 149–61.

[Delepelaire and Wandersman, 1998] Delepelaire, P. and Wandersman, C. (1998). The SecB chaperone is involved in the secretion of the Serratia marcescens HasA protein through an ABC transporter. EMBO J *17*, 936–44.

[Desvaux et al., 2009] Desvaux, M., Hébraud, M., Talon, R. and Henderson, I. R. (2009). Secretion and subcellular localizations of bacterial proteins: a semantic awareness issue. Trends Microbiol *17*, 139–45.

[Dirix et al., 2004] Dirix, G., Monsieurs, P., Dombrecht, B., Daniels, R., Marchal, K., Vanderleyden, J. and Michiels, J. (2004). Peptide signal molecules and bacteriocins in Gram-negative bacteria: a genome-wide in silico screening for peptides containing a double-glycine leader sequence and their cognate transporters. Peptides *25*, 1425–40.

[Du et al., 2014] Du, D., Wang, Z., James, N. R., Voss, J. E., Klimont, E., Ohene-Agyei, T., Venter, H., Chiu, W. and Luisi, B. F. (2014). Structure of the AcrAB-TolC multidrug efflux pump. Nature *509*, 512–5.

[Dürrenberger et al., 1991] Dürrenberger, M. B., Villiger, W. and Bächi, T. (1991). Conjugational junctions: morphology of specific contacts in conjugating Escherichia coli bacteria. J Struct Biol *107*, 146–56.

[Eichelberg et al., 1994] Eichelberg, K., Ginocchio, C. C. and Galán, J. E. (1994). Molecular and functional characterization of the Salmonella typhimurium invasion genes invB and invC: homology of InvC to the F0F1 ATPase family of proteins. J Bacteriol *176*, 4501–10.

[Eswaran et al., 2003] Eswaran, J., Hughes, C. and Koronakis, V. (2003). Locking TolC entrance helices to prevent protein translocation by the bacterial type I export apparatus. J Mol Biol *327*, 309–15.

[Finnie et al., 1998] Finnie, C., Zorreguieta, A., Hartley, N. M. and Downie, J. A. (1998). Characterization of Rhizobium leguminosarum exopolysaccharide glycanases that are secreted via a type I exporter and have a novel heptapeptide repeat motif. J Bacteriol *180*, 1691–9.

[Fronzes et al., 2009] Fronzes, R., Schäfer, E., Wang, L., Saibil, H. R., Orlova, E. V. and Waksman, G. (2009). Structure of a type IV secretion system core complex. Science *323*, 266–8.

[Galán et al., 2014] Galán, J. E., Lara-Tejero, M., Marlovits, T. C. and Wagner, S. (2014). Bacterial type III secretion systems: specialized nanomachines for protein delivery into target cells. Annu Rev Microbiol *68*, 415–38.

[Gangola and Rosen, 1987] Gangola, P. and Rosen, B. P. (1987). Maintenance of intracellular calcium in Escherichia coli. J Biol Chem *262*, 12570–4.

[Garner et al., 2011] Garner, E. C., Bernard, R., Wang, W., Zhuang, X., Rudner, D. Z. and Mitchison, T. (2011). Coupled, circumferential motions of the cell wall synthesis machinery and MreB filaments in B. subtilis. Science *333*, 222–5.

[Gawarzewski et al., 2014] Gawarzewski, I., DiMaio, F., Winterer, E., Tschapek, B., Smits, S. H. J., Jose, J. and Schmitt, L. (2014). Crystal structure of the transport unit of the autotransporter adhesin involved in diffuse adherence from Escherichia coli. J Struct Biol *187*, 20–9.

[Gawarzewski et al., 2013] Gawarzewski, I., Smits, S. H. J., Schmitt, L. and Jose, J. (2013). Structural comparison of the transport units of type V secretion systems. Biol Chem *394*, 1385–98.

[Ge et al., 2009] Ge, Q., Yamada, Y. and Zgurskaya, H. (2009). The C-terminal domain of AcrA is essential for the assembly and function of the multidrug efflux pump AcrAB-TolC. J Bacteriol *191*, 4365–71.

[Gentschev et al., 2002] Gentschev, I., Dietrich, G. and Goebel, W. (2002). The E. coli alpha-hemolysin secretion system and its use in vaccine development. Trends Microbiol *10*, 39–45.

[Gerlach and Hensel, 2007] Gerlach, R. G. and Hensel, M. (2007). Protein secretion systems and adhesins: the molecular armory of Gram-negative pathogens. Int J Med Microbiol *297*, 401–15.

[Gouaux and Mackinnon, 2005] Gouaux, E. and Mackinnon, R. (2005). Principles of selective ion transport in channels and pumps. Science *310*, 1461–5.

[Govindarajan et al., 2012] Govindarajan, S., Nevo-Dinur, K. and Amster-Choder, O. (2012). Compartmentalization and spatiotemporal organization of macromolecules in bacteria. FEMS Microbiol Rev *36*, 1005–22.

[Goyal et al., 2014] Goyal, P., Krasteva, P. V., Van Gerven, N., Gubellini, F., Van den Broeck, I., Troupiotis-Tsaïlaki, A., Jonckheere, W., Péhau-Arnaudet, G., Pinkner, J. S., Chapman, M. R., Hultgren, S. J., Howorka, S., Fronzes, R. and Remaut, H. (2014). Structural and mechanistic insights into the bacterial amyloid secretion channel CsgG. Nature *516*, 250–3.

[Gray et al., 1986] Gray, L., Mackman, N., Nicaud, J. M. and Holland, I. B. (1986). The carboxy-terminal region of haemolysin 2001 is required for secretion of the toxin from Escherichia coli. Mol Gen Genet *205*, 127–33.

[Gray et al., 2011] Gray, M. D., Bagdasarian, M., Hol, W. G. J. and Sandkvist, M. (2011). In vivo cross-linking of EpsG to EpsL suggests a role for EpsL as an ATPase-pseudopilin coupling protein in the Type II secretion system of Vibrio cholerae. Mol Microbiol *79*, 786–98.

[Greene et al., 2015] Greene, N. P., Crow, A., Hughes, C. and Koronakis, V. (2015). Structure of a bacterial toxin-activating acyltransferase. Proc Natl Acad Sci U S A *112*, E3058–66.

[Gruss et al., 2013] Gruss, F., Zähringer, F., Jakob, R. P., Burmann, B. M., Hiller, S. and Maier, T. (2013). The structural basis of autotransporter translocation by TamA. Nat Struct Mol Biol *20*, 1318–20.

[Guzmán-Verri et al., 1997] Guzmán-Verri, C., García, F. and Arvidson, S. (1997). Incomplete activation of Escherichia coli hemolysin (HlyA) due to mutations in the 3' region of hlyC. J Bacteriol *179*, 5959–62.

[Hagan et al., 2010] Hagan, C. L., Kim, S. and Kahne, D. (2010). Reconstitution of outer membrane protein assembly from purified components. Science *328*, 890–2.

[Hammar et al., 1995] Hammar, M., Arnqvist, A., Bian, Z., Olsén, A. and Normark, S. (1995). Expression of two csg operons is required for production of fibronectin- and congo red-binding curli polymers in Escherichia coli K-12. Mol Microbiol *18*, 661–70.

[Hammer et al., 2012] Hammer, N. D., McGuffie, B. A., Zhou, Y., Badtke, M. P., Reinke, A. A., Brännström, K., Gestwicki, J. E., Olofsson, A., Almqvist, F. and Chapman, M. R. (2012). The C-terminal repeating units of CsgB direct bacterial functional amyloid nucleation. J Mol Biol *422*, 376–89.

[Hardie et al., 1991] Hardie, K. R., Issartel, J. P., Koronakis, E., Hughes, C. and Koronakis, V. (1991). In vitro activation of Escherichia coli prohaemolysin to the mature membrane-targeted toxin requires HlyC and a low molecular-weight cytosolic polypeptide. Mol Microbiol *5*, 1669–79.

[Håvarstein et al., 1995] Håvarstein, L. S., Diep, D. B. and Nes, I. F. (1995). A family of bacteriocin ABC transporters carry out proteolytic processing of their substrates concomitant with export. Mol Microbiol *16*, 229–40.

[Higgins et al., 2004] Higgins, M. K., Bokma, E., Koronakis, E., Hughes, C. and Koronakis, V. (2004). Structure of the periplasmic component of a bacterial drug efflux pump. Proc Natl Acad Sci U S A *101*, 9994–9.

[Hinchliffe et al., 2014] Hinchliffe, P., Greene, N. P., Paterson, N. G., Crow, A., Hughes, C. and Koronakis, V. (2014). Structure of the periplasmic adaptor protein from a major facilitator superfamily (MFS) multidrug efflux pump. FEBS Lett *588*, 3147–53.

[Hinsa et al., 2003] Hinsa, S. M., Espinosa-Urgel, M., Ramos, J. L. and O'Toole, G. A. (2003). Transition from reversible to irreversible attachment during biofilm formation by Pseudomonas fluorescens WCS365 requires an ABC transporter and a large secreted protein. Mol Microbiol *49*, 905–18.

[Ho et al., 2014] Ho, B. T., Dong, T. G. and Mekalanos, J. J. (2014). A view to a kill: the bacterial type VI secretion system. Cell Host Microbe *15*, 9–21.

[Holland et al., 2005] Holland, I. B., Schmitt, L. and Young, J. (2005). Type 1 protein secretion in bacteria, the ABC-transporter dependent pathway (review). Mol Membr Biol *22*, 29–39.

[Hollenstein et al., 2007] Hollenstein, K., Frei, D. C. and Locher, K. P. (2007). Structure of an ABC transporter in complex with its binding protein. Nature *446*, 213–6.

[Houben et al., 2014] Houben, E. N. G., Korotkov, K. V. and Bitter, W. (2014). Take five - Type VII secretion systems of Mycobacteria. Biochim Biophys Acta *1843*, 1707–16.

[Hu et al., 2015] Hu, B., Morado, D. R., Margolin, W., Rohde, J. R., Arizmendi, O., Picking, W. L., Picking, W. D. and Liu, J. (2015). Visualization of the type III secretion sorting platform of Shigella flexneri. Proc Natl Acad Sci U S A *112*, 1047–52.

[Hughes et al., 1992] Hughes, C., Issartel, J. P., Hardie, K., Stanley, P., Koronakis, E. and Koronakis, V. (1992). Activation of Escherichia coli prohemolysin to the membrane-targetted toxin by HlyC-directed ACP-dependent fatty acylation. FEMS Microbiol Immunol *5*, 37–43.

[Hultgren et al., 1991] Hultgren, S. J., Normark, S. and Abraham, S. N. (1991). Chaperone-assisted assembly and molecular architecture of adhesive pili. Annu Rev Microbiol *45*, 383–415.

[Hwang and Tai, 1999] Hwang, J. and Tai, P. C. (1999). Mutational analysis of CvaA in the highly conserved domain of the membrane fusion protein family. Curr Microbiol *39*, 195–9.

[Ieva and Bernstein, 2009] Ieva, R. and Bernstein, H. D. (2009). Interaction of an autotransporter passenger domain with BamA during its translocation across the bacterial outer membrane. Proc Natl Acad Sci U S A *106*, 19120–5.

[Ieva et al., 2011] Ieva, R., Tian, P., Peterson, J. H. and Bernstein, H. D. (2011). Sequential and spatially restricted interactions of assembly factors with an autotransporter beta domain. Proc Natl Acad Sci U S A *108*, E383–91.

[Ishii et al., 2010] Ishii, S., Yano, T., Ebihara, A., Okamoto, A., Manzoku, M. and Hayashi, H. (2010). Crystal structure of the peptidase domain of Streptococcus ComA, a bifunctional ATP-binding cassette transporter involved in the quorum-sensing pathway. J Biol Chem *285*, 10777–85.

[Issartel et al., 1991] Issartel, J. P., Koronakis, V. and Hughes, C. (1991). Activation of Escherichia coli prohaemolysin to the mature toxin by acyl carrier protein-dependent fatty acylation. Nature *351*, 759–61.

[Jarchau et al., 1994] Jarchau, T., Chakraborty, T., Garcia, F. and Goebel, W. (1994). Selection for transport competence of C-terminal polypeptides derived from Escherichia coli hemolysin: the shortest peptide capable of autonomous HlyB/HlyD-dependent secretion comprises the C-terminal 62 amino acids of HlyA. Mol Gen Genet *245*, 53–60.

[Jardetzky, 1966] Jardetzky, O. (1966). Simple allosteric model for membrane pumps. Nature *211*, 969–70.

[Johnson and Church, 1999] Johnson, J. M. and Church, G. M. (1999). Alignment and structure prediction of divergent protein families: periplasmic and outer membrane proteins of bacterial efflux pumps. J Mol Biol *287*, 695–715.

[Jones et al., 1999] Jones, H. E., Holland, I. B., Baker, H. L. and Campbell, A. K. (1999). Slow changes in cytosolic free Ca2+ in Escherichia coli highlight two putative influx mechanisms in response to changes in extracellular calcium. Cell Calcium *25*, 265–74.

[Jones and George, 1999] Jones, P. M. and George, A. M. (1999). Subunit interactions in ABC transporters: towards a functional architecture. FEMS Microbiol Lett *179*, 187–202.

[Jones et al., 2009] Jones, P. M., O'Mara, M. L. and George, A. M. (2009). ABC transporters: a riddle wrapped in a mystery inside an enigma. Trends Biochem Sci *34*, 520–31.

[Jose et al., 1995] Jose, J., Jähnig, F. and Meyer, T. F. (1995). Common structural features of IgA1 protease-like outer membrane protein autotransporters. Mol Microbiol *18*, 378–80.

[Junker et al., 2009] Junker, M., Besingi, R. N. and Clark, P. L. (2009). Vectorial transport and folding of an autotransporter virulence protein during outer membrane secretion. Mol Microbiol *71*, 1323–32.

[Kadaba et al., 2008] Kadaba, N. S., Kaiser, J. T., Johnson, E., Lee, A. and Rees, D. C. (2008). The high-affinity E. coli methionine ABC transporter: structure and allosteric regulation. Science *321*, 250–3.

[Kanonenberg et al., 2013] Kanonenberg, K., Schwarz, C. K. W. and Schmitt, L. (2013). Type I secretion systems - a story of appendices. Res Microbiol *164*, 596–604.

[Kawamoto et al., 2013] Kawamoto, A., Morimoto, Y. V., Miyata, T., Minamino, T., Hughes, K. T., Kato, T. and Namba, K. (2013). Common and distinct structural features of Salmonella injectisome and flagellar basal body. Sci Rep *3*, 3369.

[Kenny et al., 1994] Kenny, B., Chervaux, C. and Holland, I. B. (1994). Evidence that residues -15 to -46 of the haemolysin secretion signal are involved in early steps in secretion, leading to recognition of the translocator. Mol Microbiol *11*, 99–109.

[Kenny et al., 1991] Kenny, B., Haigh, R. and Holland, I. B. (1991). Analysis of the haemolysin transport process through the secretion from Escherichia coli of PCM, CAT or beta-galactosidase fused to the Hly C-terminal signal domain. Mol Microbiol *5*, 2557–68.

[Kim et al., 2010] Kim, H.-M., Xu, Y., Lee, M., Piao, S., Sim, S.-H., Ha, N.-C. and Lee, K. (2010). Functional relationships between the AcrA hairpin tip region and the TolC aperture tip region for the formation of the bacterial tripartite efflux pump AcrAB-TolC. J Bacteriol *192*, 4498–503.

[Kim et al., 2006] Kim, I.-W., Peng, X.-H., Sauna, Z. E., FitzGerald, P. C., Xia, D., Müller, M., Nandigama, K. and Ambudkar, S. V. (2006). The conserved tyrosine residues 401 and 1044 in ATP sites of human P-glycoprotein are critical for ATP binding and hydrolysis: evidence for a conserved subdomain, the A-loop in the ATP-binding cassette. Biochemistry *45*, 7605–16.

[Kim and Frieden, 1998] Kim, K. and Frieden, C. (1998). Turn scanning by site-directed mutagenesis: application to the protein folding problem using the intestinal fatty acid binding protein. Protein Sci *7*, 1821–8.

[Koronakis et al., 2004] Koronakis, V., Eswaran, J. and Hughes, C. (2004). Structure and function of TolC: the bacterial exit duct for proteins and drugs. Annu Rev Biochem *73*, 467–89.

[Koronakis et al., 1991] Koronakis, V., Hughes, C. and Koronakis, E. (1991). Energetically distinct early and late stages of HlyB/HlyD-dependent secretion across both Escherichia coli membranes. EMBO J *10*, 3263–72.

[Koronakis et al., 2000] Koronakis, V., Sharff, A., Koronakis, E., Luisi, B. and Hughes, C. (2000). Crystal structure of the bacterial membrane protein TolC central to multidrug efflux and protein export. Nature *405*, 914–9.

[Korotkov et al., 2011] Korotkov, K. V., Johnson, T. L., Jobling, M. G., Pruneda, J., Pardon, E., Héroux, A., Turley, S., Steyaert, J., Holmes, R. K., Sandkvist, M. and Hol, W. G. J. (2011). Structural and functional studies on the interaction of GspC and GspD in the type II secretion system. PLoS Pathog *7*, e1002228.

[Korotkov et al., 2012] Korotkov, K. V., Sandkvist, M. and Hol, W. G. J. (2012). The type II secretion system: biogenesis, molecular architecture and mechanism. Nat Rev Microbiol *10*, 336–51.

[Korotkova et al., 2014] Korotkova, N., Freire, D., Phan, T. H., Ummels, R., Creekmore, C. C., Evans, T. J., Wilmanns, M., Bitter, W., Parret, A. H. A., Houben, E. N. G. and Korotkov, K. V. (2014). Structure of the Mycobacterium tuberculosis type VII secretion system chaperone EspG5 in complex with PE25-PPE41 dimer. Mol Microbiol *94*, 367–82.

[Kotake et al., 2008] Kotake, Y., Ishii, S., Yano, T., Katsuoka, Y. and Hayashi, H. (2008). Substrate recognition mechanism of the peptidase domain of the quorum-sensing-signal-producing ABC transporter ComA from Streptococcus. Biochemistry *47*, 2531–8.

[Kube et al., 2014] Kube, S., Kapitein, N., Zimniak, T., Herzog, F., Mogk, A. and Wendler, P. (2014). Structure of the VipA/B type VI secretion complex suggests a contraction-state-specific recycling mechanism. Cell Rep *8*, 20–30.

[Kubori et al., 1998] Kubori, T., Matsushima, Y., Nakamura, D., Uralil, J., Lara-Tejero, M., Sukhan, A., Galán, J. E. and Aizawa, S. I. (1998). Supramolecular structure of the Salmonella typhimurium type III protein secretion system. Science *280*, 602–5.

[Kudryashev et al., 2015] Kudryashev, M., Wang, R. Y.-R., Brackmann, M., Scherer, S., Maier, T., Baker, D., DiMaio, F., Stahlberg, H., Egelman, E. H. and Basler, M. (2015). Structure of the type VI secretion system contractile sheath. Cell *160*, 952–62.

[Lally et al., 1997] Lally, E. T., Kieba, I. R., Sato, A., Green, C. L., Rosenbloom, J., Korostoff, J., Wang, J. F., Shenker, B. J., Ortlepp, S., Robinson, M. K. and Billings, P. C. (1997). RTX toxins recognize a beta2 integrin on the surface of human target cells. J Biol Chem *272*, 30463–9.

[Lanyi, 2004] Lanyi, J. K. (2004). Bacteriorhodopsin. Annu Rev Physiol *66*, 665–88.

[Lara-Tejero et al., 2011] Lara-Tejero, M., Kato, J., Wagner, S., Liu, X. and Galán, J. E. (2011). A sorting platform determines the order of protein secretion in bacterial type III systems. Science *331*, 1188–91.

[Lecher et al., 2012] Lecher, J., Schwarz, C. K. W., Stoldt, M., Smits, S. H. J., Willbold, D. and Schmitt, L. (2012). An RTX transporter tethers its unfolded substrate during secretion via a unique N-terminal domain. Structure *20*, 1778–87.

[Lecher et al., 2011] Lecher, J., Stoldt, M., Schwarz, C. K. W., Smits, S. H. J., Schmitt, L. and Willbold, D. (2011). 1H, 15N and 13C resonance assignment of the N-terminal C39 peptidase-like domain of the ABC transporter Haemolysin B (HlyB). Biomol NMR Assign *5*, 199–201.

[Lee et al., 2012] Lee, M., Jun, S.-Y., Yoon, B.-Y., Song, S., Lee, K. and Ha, N.-C. (2012). Membrane fusion proteins of type I secretion system and tripartite efflux pumps share a binding motif for TolC in gram-negative bacteria. PLoS One *7*, e40460.

[Leiman et al., 2009] Leiman, P. G., Basler, M., Ramagopal, U. A., Bonanno, J. B., Sauder, J. M., Pukatzki, S., Burley, S. K., Almo, S. C. and Mekalanos, J. J. (2009). Type VI secretion apparatus and phage tail-associated protein complexes share a common evolutionary origin. Proc Natl Acad Sci U S A *106*, 4154–9.

[Lenders et al., 2013] Lenders, M. H. H., Reimann, S., Smits, S. H. J. and Schmitt, L. (2013). Molecular insights into type I secretion systems. Biol Chem *394*, 1371–84.

[Lenders et al., 2015] Lenders, M. H. H., Weidtkamp-Peters, S., Kleinschrodt, D., Jaeger, K.-E., Smits, S. H. J. and Schmitt, L. (2015). Directionality of substrate translocation of the hemolysin A Type I secretion system. Sci Rep *5*, 12470.

[Leo et al., 2012] Leo, J. C., Grin, I. and Linke, D. (2012). Type V secretion: mechanism(s) of autotransport through the bacterial outer membrane. Philos Trans R Soc Lond B Biol Sci *367*, 1088–101.

[Létoffé et al., 1996] Létoffé, S., Delepelaire, P. and Wandersman, C. (1996). Protein secretion in gram-negative bacteria: assembly of the three components of ABC protein-mediated exporters is ordered and promoted by substrate binding. EMBO J *15*, 5804–11.

[Leyton et al., 2012] Leyton, D. L., Rossiter, A. E. and Henderson, I. R. (2012). From self sufficiency to dependence: mechanisms and factors important for autotransporter biogenesis. Nat Rev Microbiol *10*, 213–25.

[Lim et al., 2000] Lim, K. B., Walker, C. R., Guo, L., Pellett, S., Shabanowitz, J., Hunt, D. F., Hewlett, E. L., Ludwig, A., Goebel, W., Welch, R. A. and Hackett, M. (2000). Escherichia coli alpha-hemolysin (HlyA) is heterogeneously acylated in vivo with 14-, 15-, and 17-carbon fatty acids. J Biol Chem *275*, 36698–702.

[Linhartová et al., 2010] Linhartová, I., Bumba, L., Mašín, J., Basler, M., Osička, R., Kamanová, J., Procházková, K., Adkins, I., Hejnová-Holubová, J., Sadílková, L., Morová, J. and Sebo, P. (2010). RTX proteins: a highly diverse family secreted by a common mechanism. FEMS Microbiol Rev *34*, 1076–112.

[Locher et al., 2002] Locher, K. P., Lee, A. T. and Rees, D. C. (2002). The E. coli BtuCD structure: a framework for ABC transporter architecture and mechanism. Science *296*, 1091–8.

[Loquet et al., 2012] Loquet, A., Sgourakis, N. G., Gupta, R., Giller, K., Riedel, D., Goosmann, C., Griesinger, C., Kolbe, M., Baker, D., Becker, S. and Lange, A. (2012). Atomic model of the type III secretion system needle. Nature *486*, 276–9.

[Low et al., 2014] Low, H. H., Gubellini, F., Rivera-Calzada, A., Braun, N., Connery, S., Dujeancourt, A., Lu, F., Redzej, A., Fronzes, R., Orlova, E. V. and Waksman, G. (2014). Structure of a type IV secretion system. Nature *508*, 550–3.

[Lu et al., 2013] Lu, C., Turley, S., Marionni, S. T., Park, Y.-J., Lee, K. K., Patrick, M., Shah, R., Sandkvist, M., Bush, M. F. and Hol, W. G. J. (2013). Hexamers of the type II secretion ATPase GspE from Vibrio cholerae with increased ATPase activity. Structure *21*, 1707–17.

[Ludwig et al., 1996] Ludwig, A., Garcia, F., Bauer, S., Jarchau, T., Benz, R., Hoppe, J. and Goebel, W. (1996). Analysis of the in vivo activation of hemolysin (HlyA) from Escherichia coli. J Bacteriol *178*, 5422–30.

[Ludwig et al., 1988] Ludwig, A., Jarchau, T., Benz, R. and Goebel, W. (1988). The repeat domain of Escherichia coli haemolysin (HlyA) is responsible for its Ca2+-dependent binding to erythrocytes. Mol Gen Genet *214*, 553–61.

[Ludwig et al., 1991] Ludwig, A., Schmid, A., Benz, R. and Goebel, W. (1991). Mutations affecting pore formation by haemolysin from Escherichia coli. Mol Gen Genet *226*, 198–208.

[Luo et al., 2015] Luo, J., Li, W., Liu, Z., Guo, Y., Pu, X. and Li, M. (2015). A sequence-based two-level method for the prediction of type I secreted RTX proteins. Analyst *140*, 3048–56.

[Mackman et al., 1987] Mackman, N., Baker, K., Gray, L., Haigh, R., Nicaud, J. M. and Holland, I. B. (1987). Release of a chimeric protein into the medium from Escherichia coli using the C-terminal secretion signal of haemolysin. EMBO J *6*, 2835–41.

[Marlovits et al., 2006] Marlovits, T. C., Kubori, T., Lara-Tejero, M., Thomas, D., Unger, V. M. and Galán, J. E. (2006). Assembly of the inner rod determines needle length in the type III secretion injectisome. Nature *441*, 637–40.

[Marlovits et al., 2004] Marlovits, T. C., Kubori, T., Sukhan, A., Thomas, D. R., Galán, J. E. and Unger, V. M. (2004). Structural insights into the assembly of the type III secretion needle complex. Science *306*, 1040–2.

[Martin et al., 2001] Martin, C., Higgins, C. F. and Callaghan, R. (2001). The vinblastine binding site adopts high- and low-affinity conformations during a transport cycle of P-glycoprotein. Biochemistry *40*, 15733–42.

[Masi and Wandersman, 2010] Masi, M. and Wandersman, C. (2010). Multiple signals direct the assembly and function of a type 1 secretion system. J Bacteriol *192*, 3861–9.

[McLaughlin et al., 2012] McLaughlin, L. S., Haft, R. J. F. and Forest, K. T. (2012). Structural insights into the Type II secretion nanomachine. Curr Opin Struct Biol *22*, 208–16.

[Menestrina et al., 1994] Menestrina, G., Moser, C., Pellet, S. and Welch, R. (1994). Pore-formation by Escherichia coli hemolysin (HlyA) and other members of the RTX toxins family. Toxicology *87*, 249–67.

[Menestrina et al., 1995] Menestrina, G., Ropele, M., Dalla Serra, M., Pederzolli, C., Hugo, F., Pellet, S. and Welch, R. A. (1995). Binding of antibodies to functional epitopes on the pore formed by Escherichia coli hemolysin in cells and model membranes. Biochim Biophys Acta *1238*, 72–80.

[Meng et al., 2006] Meng, G., Surana, N. K., St Geme, 3rd, J. W. and Waksman, G. (2006). Structure of the outer membrane translocator domain of the Haemophilus influenzae Hia trimeric autotransporter. EMBO J *25*, 2297–304.

[Mimmack et al., 1989] Mimmack, M. L., Gallagher, M. P., Pearce, S. R., Hyde, S. C., Booth, I. R. and Higgins, C. F. (1989). Energy coupling to periplasmic binding protein-dependent transport systems: stoichiometry of ATP hydrolysis during transport in vivo. Proc Natl Acad Sci U S A *86*, 8257–61.

[Minshew et al., 1978] Minshew, B. H., Jorgensen, J., Counts, G. W. and Falkow, S. (1978). Association of hemolysin production, hemagglutination of human erythrocytes, and virulence for chicken embryos of extraintestinal Escherichia coli isolates. Infect Immun *20*, 50–4.

[Moayeri and Welch, 1997] Moayeri, M. and Welch, R. A. (1997). Prelytic and lytic conformations of erythrocyte-associated Escherichia coli hemolysin. Infect Immun *65*, 2233–9.

[Nehme and Poole, 2007] Nehme, D. and Poole, K. (2007). Assembly of the MexAB-OprM multidrug pump of Pseudomonas aeruginosa: component interactions defined by the study of pump mutant suppressors. J Bacteriol *189*, 6118–27.

[Nicaud et al., 1985] Nicaud, J. M., Mackman, N., Gray, L. and Holland, I. B. (1985). Characterisation of HlyC and mechanism of activation and secretion of haemolysin from E. coli 2001. FEBS Lett *187*, 339–44.

[Nicaud et al., 1986] Nicaud, J. M., Mackman, N., Gray, L. and Holland, I. B. (1986). The C-terminal, 23 kDa peptide of E. coli haemolysin 2001 contains all the information necessary for its secretion by the haemolysin (Hly) export machinery. FEBS Lett *204*, 331–5.

[Nivaskumar et al., 2014] Nivaskumar, M., Bouvier, G., Campos, M., Nadeau, N., Yu, X., Egelman, E. H., Nilges, M. and Francetic, O. (2014). Distinct docking and stabilization steps of the Pseudopilus conformational transition path suggest rotational assembly of type IV pilus-like fibers. Structure *22*, 685–96.

[Nivaskumar and Francetic, 2014] Nivaskumar, M. and Francetic, O. (2014). Type II secretion system: a magic beanstalk or a protein escalator. Biochim Biophys Acta *1843*, 1568–77.

[Oldham et al., 2007] Oldham, M. L., Khare, D., Quiocho, F. A., Davidson, A. L. and Chen, J. (2007). Crystal structure of a catalytic intermediate of the maltose transporter. Nature *450*, 515–21.

[Olsén et al., 1989] Olsén, A., Jonsson, A. and Normark, S. (1989). Fibronectin binding mediated by a novel class of surface organelles on Escherichia coli. Nature *338*, 652–5.

[Oomen et al., 2004] Oomen, C. J., van Ulsen, P., van Gelder, P., Feijen, M., Tommassen, J. and Gros, P. (2004). Structure of the translocator domain of a bacterial autotransporter. EMBO J *23*, 1257–66.

[Osborne et al., 2005] Osborne, A. R., Rapoport, T. A. and van den Berg, B. (2005). Protein translocation by the Sec61/SecY channel. Annu Rev Cell Dev Biol *21*, 529–50.

[Oswald et al., 2006] Oswald, C., Holland, I. B. and Schmitt, L. (2006). The motor domains of ABC-transporters. What can structures tell us? Naunyn Schmiedebergs Arch Pharmacol *372*, 385–99.

[Parsot et al., 2003] Parsot, C., Hamiaux, C. and Page, A.-L. (2003). The various and varying roles of specific chaperones in type III secretion systems. Curr Opin Microbiol *6*, 7–14.

[Patzlaff et al., 2003] Patzlaff, J. S., van der Heide, T. and Poolman, B. (2003). The ATP/substrate stoichiometry of the ATP-binding cassette (ABC) transporter OpuA. J Biol Chem *278*, 29546–51.

[Pavlova et al., 2013] Pavlova, O., Peterson, J. H., Ieva, R. and Bernstein, H. D. (2013). Mechanistic link between beta-barrel assembly and the initiation of autotransporter secretion. Proc Natl Acad Sci U S A *110*, E938–47.

[Pei et al., 2011] Pei, X.-Y., Hinchliffe, P., Symmons, M. F., Koronakis, E., Benz, R., Hughes, C. and Koronakis, V. (2011). Structures of sequential open states in a symmetrical opening transition of the TolC exit duct. Proc Natl Acad Sci U S A *108*, 2112–7.

[Piddock, 2006] Piddock, L. J. V. (2006). Multidrug-resistance efflux pumps - not just for resistance. Nat Rev Microbiol *4*, 629–36.

[Pimenta et al., 2005] Pimenta, A. L., Racher, K., Jamieson, L., Blight, M. A. and Holland, I. B. (2005). Mutations in HlyD, part of the type 1 translocator for hemolysin secretion, affect the folding of the secreted toxin. J Bacteriol *187*, 7471–80.

[Pinkett et al., 2007] Pinkett, H. W., Lee, A. T., Lum, P., Locher, K. P. and Rees, D. C. (2007). An inward-facing conformation of a putative metal-chelate-type ABC transporter. Science *315*, 373–7.

[Poyraz et al., 2010] Poyraz, O., Schmidt, H., Seidel, K., Delissen, F., Ader, C., Tenenboim, H., Goosmann, C., Laube, B., Thünemann, A. F., Zychlinsky, A., Baldus, M., Lange, A., Griesinger, C. and Kolbe, M. (2010). Protein refolding is required for assembly of the type three secretion needle. Nat Struct Mol Biol *17*, 788–92.

[Py et al., 2001] Py, B., Loiseau, L. and Barras, F. (2001). An inner membrane platform in the type II secretion machinery of Gram-negative bacteria. EMBO Rep *2*, 244–8.

[Radics et al., 2014] Radics, J., Königsmaier, L. and Marlovits, T. C. (2014). Structure of a pathogenic type 3 secretion system in action. Nat Struct Mol Biol *21*, 82–7.

[Reichow et al., 2010] Reichow, S. L., Korotkov, K. V., Hol, W. G. J. and Gonen, T. (2010). Structure of the cholera toxin secretion channel in its closed state. Nat Struct Mol Biol *17*, 1226–32.

[Rennie et al., 1974] Rennie, R. P., Freer, J. H. and Arbuthnott, J. P. (1974). The kinetics of erythrocyte lysis by Escherichia coli haemolysin. J Med Microbiol *7*, 189–95.

[Rhodes et al., 2001] Rhodes, C. R., Gray, M. C., Watson, J. M., Muratore, T. L., Kim, S. B., Hewlett, E. L. and Grisham, C. M. (2001). Structural consequences of divalent metal binding by the adenylyl cyclase toxin of Bordetella pertussis. Arch Biochem Biophys *395*, 169–76.

[Rivera-Calzada et al., 2013] Rivera-Calzada, A., Fronzes, R., Savva, C. G., Chandran, V., Lian, P. W., Laeremans, T., Pardon, E., Steyaert, J., Remaut, H., Waksman, G. and Orlova, E. V. (2013). Structure of a bacterial type IV secretion core complex at subnanometre resolution. EMBO J *32*, 1195–204.

[Robson et al., 2009] Robson, A., Gold, V. A. M., Hodson, S., Clarke, A. R. and Collinson, I. (2009). Energy transduction in protein transport and the ATP hydrolytic cycle of SecA. Proc Natl Acad Sci U S A *106*, 5111–6.

[Roman-Hernandez et al., 2014] Roman-Hernandez, G., Peterson, J. H. and Bernstein, H. D. (2014). Reconstitution of bacterial autotransporter assembly using purified components. Elife *3*, e04234.

[Rose et al., 1995] Rose, T., Sebo, P., Bellalou, J. and Ladant, D. (1995). Interaction of calcium with Bordetella pertussis adenylate cyclase toxin. Characterization of multiple calcium-binding sites and calcium-induced conformational changes. J Biol Chem *270*, 26370–6.

[Sapriel et al., 2003] Sapriel, G., Wandersman, C. and Delepelaire, P. (2003). The SecB chaperone is bifunctional in Serratia marcescens: SecB is involved in the Sec pathway and required for HasA secretion by the ABC transporter. J Bacteriol *185*, 80–8.

[Schatz and Beckwith, 1990] Schatz, P. J. and Beckwith, J. (1990). Genetic analysis of protein export in Escherichia coli. Annu Rev Genet *24*, 215–48.

[Schiebel et al., 1991] Schiebel, E., Driessen, A. J., Hartl, F. U. and Wickner, W. (1991). Delta mu H+ and ATP function at different steps of the catalytic cycle of preprotein translocase. Cell *64*, 927–39.

[Schlumberger et al., 2005] Schlumberger, M. C., Müller, A. J., Ehrbar, K., Winnen, B., Duss, I., Stecher, B. and Hardt, W.-D. (2005). Real-time imaging of type III secretion: Salmonella SipA injection into host cells. Proc Natl Acad Sci U S A *102*, 12548–53.

[Schmitt et al., 2003] Schmitt, L., Benabdelhak, H., Blight, M. A., Holland, I. B. and Stubbs, M. T. (2003). Crystal structure of the nucleotide-binding domain of the ABC-transporter haemolysin B: identification of a variable region within ABC helical domains. J Mol Biol *330*, 333–42.

[Schraidt and Marlovits, 2011] Schraidt, O. and Marlovits, T. C. (2011). Three-dimensional model of Salmonella's needle complex at subnanometer resolution. Science *331*, 1192–5.

[Schwarz et al., 2012a] Schwarz, C. K. W., Landsberg, C. D., Lenders, M. H. H., Smits, S. H. J. and Schmitt, L. (2012a). Using an E. coli Type 1 secretion system to secrete the mammalian, intracellular protein IFABP in its active form. J Biotechnol *159*, 155–61.

[Schwarz et al., 2012b] Schwarz, C. K. W., Lenders, M. H. H., Smits, S. H. J. and Schmitt, L. (2012b). Secretion of slow-folding proteins by a Type 1 secretion system. Bioengineered *3*, 289–92.

[Seeger and van Veen, 2009] Seeger, M. A. and van Veen, H. W. (2009). Molecular basis of multidrug transport by ABC transporters. Biochim Biophys Acta *1794*, 725–37.

[Selkrig et al., 2012] Selkrig, J., Mosbahi, K., Webb, C. T., Belousoff, M. J., Perry, A. J., Wells, T. J., Morris, F., Leyton, D. L., Totsika, M., Phan, M.-D., Celik, N., Kelly, M., Oates, C., Hartland, E. L., Robins-Browne, R. M., Ramarathinam, S. H., Purcell, A. W., Schembri, M. A., Strugnell, R. A., Henderson, I. R., Walker, D. and Lithgow, T. (2012). Discovery of an archetypal protein transport system in bacterial outer membranes. Nat Struct Mol Biol *19*, 506–10, S1.

[Singer and Nicolson, 1972] Singer, S. J. and Nicolson, G. L. (1972). The fluid mosaic model of the structure of cell membranes. Science *175*, 720–31.

[Smith et al., 2002] Smith, P. C., Karpowich, N., Millen, L., Moody, J. E., Rosen, J., Thomas, P. J. and Hunt, J. F. (2002). ATP binding to the motor domain from an ABC transporter drives formation of a nucleotide sandwich dimer. Mol Cell *10*, 139–49.

[Solomonson et al., 2013] Solomonson, M., Huesgen, P. F., Wasney, G. A., Watanabe, N., Gruninger, R. J., Prehna, G., Overall, C. M. and Strynadka, N. C. J. (2013). Structure of the mycosin-1 protease from the mycobacterial ESX-1 protein type VII secretion system. J Biol Chem *288*, 17782–90.

[Stanley et al., 1991] Stanley, P., Koronakis, V. and Hughes, C. (1991). Mutational analysis supports a role for multiple structural features in the C-terminal secretion signal of Escherichia coli haemolysin. Mol Microbiol *5*, 2391–403.

[Stanley et al., 1998] Stanley, P., Koronakis, V. and Hughes, C. (1998). Acylation of Escherichia coli hemolysin: a unique protein lipidation mechanism underlying toxin function. Microbiol Mol Biol Rev *62*, 309–33.

[Stanley et al., 1994] Stanley, P., Packman, L. C., Koronakis, V. and Hughes, C. (1994). Fatty acylation of two internal lysine residues required for the toxic activity of Escherichia coli hemolysin. Science *266*, 1992–6.

[Strathdee and Lo, 1989] Strathdee, C. A. and Lo, R. Y. (1989). Cloning, nucleotide sequence, and characterization of genes encoding the secretion function of the Pasteurella haemolytica leukotoxin determinant. J Bacteriol *171*, 916–28.

[Su et al., 2009] Su, C.-C., Yang, F., Long, F., Reyon, D., Routh, M. D., Kuo, D. W., Mokhtari, A. K., Van Ornam, J. D., Rabe, K. L., Hoy, J. A., Lee, Y. J., Rajashankar, K. R. and Yu, E. W. (2009). Crystal structure of the membrane fusion protein CusB from Escherichia coli. J Mol Biol *393*, 342–55.

[Takagi et al., 2003] Takagi, F., Koga, N. and Takada, S. (2003). How protein thermodynamics and folding mechanisms are altered by the chaperonin cage: molecular simulations. Proc Natl Acad Sci U S A *100*, 11367–72.

[Tamura et al., 2005] Tamura, N., Murakami, S., Oyama, Y., Ishiguro, M. and Yamaguchi, A. (2005). Direct interaction of multidrug efflux transporter AcrB and outer membrane channel TolC detected via site-directed disulfide cross-linking. Biochemistry *44*, 11115–21.

[Thanabalu et al., 1998] Thanabalu, T., Koronakis, E., Hughes, C. and Koronakis, V. (1998). Substrate-induced assembly of a contiguous channel for protein export from E.coli: reversible bridging of an inner-membrane translocase to an outer membrane exit pore. EMBO J *17*, 6487–96.

[Thomas et al., 2014a] Thomas, S., Bakkes, P. J., Smits, S. H. J. and Schmitt, L. (2014a). Equilibrium folding of pro-HlyA from Escherichia coli reveals a stable calcium ion dependent folding intermediate. Biochim Biophys Acta *1844*, 1500–10.

[Thomas et al., 2014b] Thomas, S., Smits, S. H. J. and Schmitt, L. (2014b). A simple in vitro acylation assay based on optimized HlyA and HlyC purification. Anal Biochem *464*, 17–23.

[Tikhonova et al., 2009] Tikhonova, E. B., Dastidar, V., Rybenkov, V. V. and Zgurskaya, H. I. (2009). Kinetic control of TolC recruitment by multidrug efflux complexes. Proc Natl Acad Sci U S A *106*, 16416–21.

[Trent et al., 1999a] Trent, M. S., Worsham, L. M. and Ernst-Fonberg, M. L. (1999a). HlyC, the internal protein acyltransferase that activates hemolysin toxin: roles of various conserved residues in enzymatic activity as probed by site-directed mutagenesis. Biochemistry *38*, 9541–8.

[Trent et al., 1999b] Trent, M. S., Worsham, L. M. and Ernst-Fonberg, M. L. (1999b). HlyC, the internal protein acyltransferase that activates hemolysin toxin: role of conserved histidine, serine, and cysteine residues in enzymatic activity as probed by chemical modification and site-directed mutagenesis. Biochemistry *38*, 3433–9.

[Trent et al., 1999c] Trent, M. S., Worsham, L. M. and Ernst-Fonberg, M. L. (1999c). HlyC, the internal protein acyltransferase that activates hemolysin toxin: the role of conserved tyrosine and arginine residues in enzymatic activity as probed by chemical modification and site-directed mutagenesis. Biochemistry *38*, 8831–8.

[Trokter et al., 2014] Trokter, M., Felisberto-Rodrigues, C., Christie, P. J. and Waksman, G. (2014). Recent advances in the structural and molecular biology of type IV secretion systems. Curr Opin Struct Biol *27*, 16–23.

[Uchida et al., 1995] Uchida, K., Mori, H. and Mizushima, S. (1995). Stepwise movement of preproteins in the process of translocation across the cytoplasmic membrane of Escherichia coli. J Biol Chem *270*, 30862–8.

[Vaccaro et al., 2008] Vaccaro, L., Scott, K. A. and Sansom, M. S. P. (2008). Gating at both ends and breathing in the middle: conformational dynamics of TolC. Biophys J *95*, 5681–91.

[Vakharia et al., 2001] Vakharia, H., German, G. J. and Misra, R. (2001). Isolation and characterization of Escherichia coli tolC mutants defective in secreting enzymatically active alpha-hemolysin. J Bacteriol *183*, 6908–16.

[van den Berg, 2010] van den Berg, B. (2010). Crystal structure of a full-length autotransporter. J Mol Biol *396*, 627–33.

[van Teeffelen et al., 2011] van Teeffelen, S., Wang, S., Furchtgott, L., Huang, K. C., Wingreen, N. S., Shaevitz, J. W. and Gitai, Z. (2011). The bacterial actin MreB rotates, and rotation depends on cell-wall assembly. Proc Natl Acad Sci U S A *108*, 15822–7.

[Vetsch et al., 2004] Vetsch, M., Puorger, C., Spirig, T., Grauschopf, U., Weber-Ban, E. U. and Glockshuber, R. (2004). Pilus chaperones represent a new type of protein-folding catalyst. Nature *431*, 329–33.

[Voulhoux et al., 2003] Voulhoux, R., Bos, M. P., Geurtsen, J., Mols, M. and Tommassen, J. (2003). Role of a highly conserved bacterial protein in outer membrane protein assembly. Science *299*, 262–5.

[Wai et al., 2003] Wai, S. N., Lindmark, B., Söderblom, T., Takade, A., Westermark, M., Oscarsson, J., Jass, J., Richter-Dahlfors, A., Mizunoe, Y. and Uhlin, B. E. (2003). Vesicle-mediated export and assembly of pore-forming oligomers of the enterobacterial ClyA cytotoxin. Cell *115*, 25–35.

[Walker et al., 1982] Walker, J. E., Saraste, M., Runswick, M. J. and Gay, N. J. (1982). Distantly related sequences in the alpha- and beta-subunits of ATP synthase, myosin, kinases and other ATP-requiring enzymes and a common nucleotide binding fold. EMBO J *1*, 945–51.

[Wang et al., 2012] Wang, S., Furchtgott, L., Huang, K. C. and Shaevitz, J. W. (2012). Helical insertion of peptidoglycan produces chiral ordering of the bacterial cell wall. Proc Natl Acad Sci U S A *109*, E595–604.

[Welch et al., 1992] Welch, R. A., Forestier, C., Lobo, A., Pellett, S., Thomas, Jr, W. and Rowe, G. (1992). The synthesis and function of the Escherichia coli hemolysin and related RTX exotoxins. FEMS Microbiol Immunol *5*, 29–36.

[Wickner et al., 1991] Wickner, W., Driessen, A. J. and Hartl, F. U. (1991). The enzymology of protein translocation across the Escherichia coli plasma membrane. Annu Rev Biochem *60*, 101–24.

[Wolff et al., 1994] Wolff, N., Ghigo, J. M., Delepelaire, P., Wandersman, C. and Delepierre, M. (1994). C-terminal secretion signal of an Erwinia chrysanthemi protease secreted by a signal peptide-independent pathway: proton NMR and CD conformational studies in membrane-mimetic environments. Biochemistry *33*, 6792–801.

[Wolff et al., 2003] Wolff, N., Sapriel, G., Bodenreider, C., Chaffotte, A. and Delepelaire, P. (2003). Antifolding activity of the SecB chaperone is essential for secretion of HasA, a quickly folding ABC pathway substrate. J Biol Chem *278*, 38247–53.

[Worsham et al., 2001] Worsham, L. M., Trent, M. S., Earls, L., Jolly, C. and Ernst-Fonberg, M. L. (2001). Insights into the catalytic mechanism of HlyC, the internal protein acyltransferase that activates Escherichia coli hemolysin toxin. Biochemistry *40*, 13607–16.

[Worsham et al., 2005] Worsham, L. M. S., Langston, K. G. and Ernst-Fonberg, M. L. (2005). Thermodynamics of a protein acylation: activation of Escherichia coli hemolysin toxin. Biochemistry *44*, 1329–37.

[Wright et al., 2007] Wright, K. J., Seed, P. C. and Hultgren, S. J. (2007). Development of intracellular bacterial communities of uropathogenic Escherichia coli depends on type 1 pili. Cell Microbiol *9*, 2230–41.

[Wu and Tai, 2004] Wu, K.-H. and Tai, P. C. (2004). Cys32 and His105 are the critical residues for the calcium-dependent cysteine proteolytic activity of CvaB, an ATP-binding cassette transporter. J Biol Chem *279*, 901–9.

[Wu et al., 2005] Wu, T., Malinverni, J., Ruiz, N., Kim, S., Silhavy, T. J. and Kahne, D. (2005). Identification of a multicomponent complex required for outer membrane biogenesis in Escherichia coli. Cell *121*, 235–45.

[Xu et al., 2011] Xu, Y., Lee, M., Moeller, A., Song, S., Yoon, B.-Y., Kim, H.-M., Jun, S.-Y., Lee, K. and Ha, N.-C. (2011). Funnel-like hexameric assembly of the periplasmic adapter protein in the tripartite multidrug efflux pump in gram-negative bacteria. J Biol Chem *286*, 17910–20.

[Xu et al., 2010] Xu, Y., Sim, S.-H., Song, S., Piao, S., Kim, H.-M., Jin, X. L., Lee, K. and Ha, N.-C. (2010). The tip region of the MacA alpha-hairpin is important for the binding to TolC to the Escherichia coli MacAB-TolC pump. Biochem Biophys Res Commun *394*, 962–5.

[Yip et al., 2005] Yip, C. K., Kimbrough, T. G., Felise, H. B., Vuckovic, M., Thomas, N. A., Pfuetzner, R. A., Frey, E. A., Finlay, B. B., Miller, S. I. and Strynadka, N. C. J. (2005). Structural characterization of the molecular platform for type III secretion system assembly. Nature *435*, 702–7.

[Yum et al., 2009] Yum, S., Xu, Y., Piao, S., Sim, S.-H., Kim, H.-M., Jo, W.-S., Kim, K.-J., Kweon, H.-S., Jeong, M.-H., Jeon, H., Lee, K. and Ha, N.-C. (2009). Crystal structure of the periplasmic component of a tripartite macrolide-specific efflux pump. J Mol Biol *387*, 1286–97.

[Zaitseva et al., 2005] Zaitseva, J., Jenewein, S., Jumpertz, T., Holland, I. B. and Schmitt, L. (2005). H662 is the linchpin of ATP hydrolysis in the nucleotide-binding domain of the ABC transporter HlyB. EMBO J *24*, 1901–10.

[Zaitseva et al., 2006] Zaitseva, J., Oswald, C., Jumpertz, T., Jenewein, S., Wiedenmann, A., Holland, I. B. and Schmitt, L. (2006). A structural analysis of asymmetry required for catalytic activity of an ABC-ATPase domain dimer. EMBO J *25*, 3432–43.

[Zgurskaya and Nikaido, 2000] Zgurskaya, H. I. and Nikaido, H. (2000). Cross-linked complex between oligomeric periplasmic lipoprotein AcrA and the inner-membrane-associated multidrug efflux pump AcrB from Escherichia coli. J Bacteriol *182*, 4264–7.

[Zgurskaya et al., 2009] Zgurskaya, H. I., Yamada, Y., Tikhonova, E. B., Ge, Q. and Krishnamoorthy, G. (2009). Structural and functional diversity of bacterial membrane fusion proteins. Biochim Biophys Acta *1794*, 794–807.

[Zhang et al., 1993] Zhang, F., Sheps, J. A. and Ling, V. (1993). Complementation of transport-deficient mutants of Escherichia coli alpha-hemolysin by second-site mutations in the transporter hemolysin B. J Biol Chem *268*, 19889–95.

[Zhang et al., 1995] Zhang, F., Yin, Y., Arrowsmith, C. H. and Ling, V. (1995). Secretion and circular dichroism analysis of the C-terminal signal peptides of HlyA and LktA. Biochemistry *34*, 4193–201.

[Zheng and Leung, 2007] Zheng, J. and Leung, K. Y. (2007). Dissection of a type VI secretion system in Edwardsiella tarda. Mol Microbiol *66*, 1192–206.

[Zolnerciks et al., 2011] Zolnerciks, J. K., Andress, E. J., Nicolaou, M. and Linton, K. J. (2011). Structure of ABC transporters. Essays Biochem *50*, 43–61.

[Zoued et al., 2014] Zoued, A., Brunet, Y. R., Durand, E., Aschtgen, M.-S., Logger, L., Douzi, B., Journet, L., Cambillau, C. and Cascales, E. (2014). Architecture and assembly of the Type VI secretion system. Biochim Biophys Acta *1843*, 1664–73.

A. Acknowledgment/Danksagung

Mein erstes Dankeschön gilt meinen Doktorvater Prof. Dr. Lutz Schmitt. Danke Lutz für eine wirklich tolle Doktorandenzeit und das coolste Projekt, was ich mir nur hätte wünschen können. Danke für die tolle Arbeitsatmosphäre, für deine Ideen, für deine Unterstützung und für den Enthusiasmus und die Leidenschaft, die du mit mir für das Projekt geteilt hast. Keiner brüllt mir meinen Namen auf den Gang so schön hinterher wie du, wenn dir mal wieder eine gute Idee in den Sinn gekommen ist.

Sander, dir danke ich für die tolle Betreuung während meiner gesamten Doktorandenzeit. Ohne dich hätte ich manchmal wirklich den Kopf verloren. Danke für die inspirierenden Kaffee-Pausen und dein offenes Ohr, ob es nun um wissenschaftliche oder private Dinge ging. Vielen Dank für deine Ruhe und Geduld, wenn ich mal wieder nicht auf den Punkt kommen wollte.

Hiermit möchte ich mich auch bei Prof. Dr. Karl-Erich Jaeger für die freundliche Übernahme des Korreferats bedanken.

Mein größter Dank geht an Christina, meiner geliebten Frau. Ohne dich wäre diese Promotion nicht möglich gewesen. Du hast mir den Rücken gestärkt, wann immer ich halt brauchte. Du hast mich ertragen, wann immer ich ertragen werden musste und du hast mich aufgemuntert, wann immer ich Aufmunterung bedurfte. Deine Liebe hat mir jeden schweren Arbeitstag erleichtert und ich freue mich auf die neuen Herausforderungen, die vor uns liegen und denen wir gemeinsam begegnen.

Ein nicht minder großes Dankeschön geht an meine Eltern Michael und Heidi, so wie an meine Großmutter Hannelore, die mich während meines Studiums und meiner Promotion in jeglicher Hinsicht unterstützt haben. Ob es nun mit guten Ratschlägen, finanzieller Hilfe oder einfach nur mit eurer Zeit für ein gutes Gespräch war, ihr wart und seid immer an meiner Seite und dafür Danke ich euch von ganzen Herzen.

Ein herzliches Dankeschön geht auch an Stefanie Weidtkamp-Peters vom Center for Advanced Imaging (CAi) für die tolle Betreuung bei den Mikroskopen und eine wunderbare Einführung in die Fluoreszenzmikroskopie. Dank dir hab ich bei den ganzen Leuchten den Durchblick behalten.

Ulrich, dir danke ich für die hervorragende Betreuung während und nach dem Studium, ohne die ich nicht so reibungslos durch den Studiengang gekommen wäre und das eine oder andere Mal bestimmte Fristen nicht hätte einhalten können. Vielen Dank.

Sven, mein guter Freund, Kollege und meine Arbeitsehefrau. Dir danke ich für die schöne Zeit im Labor und Privat. Unsere Diskussionen und die kritische Auseinandersetzung mit meinen verrückten Ideen haben mich mehr als einmal vor Monaten der vergeudeten Arbeit bewahrt. Ich danke dir für die netten Späße zwischendurch, die Entspannungspausen mit Kaffee, Witz und Sonne und einen unvergleichbaren Junggesellenabschied.

Marcel, meinen schwarzen Bruder, Tobias, meinen Masterstudenten, und Manuel, unseren Lab29 Adoptivsohn, danke ich für einen schönen Laboralltag mit viel Spaß und Spannung und Schokolade. Nun kann ich euch am Ende der Promotion nur noch mit einen großväterlichen Rat zur Seite stehen. Marcel auch deine Wacht geht bald zu Ende, Tobias, nur der Schüler kann den Meister übertreffen und Manuel, wo Rauch ist, ist auch ein Feuerball, Junge! Ihr seid super. Vielen Dank!

Rebecca und Katja, danke für die sehr lustigen und informativen Gespräche im Büro. Ohne euch wären die Pausen und die Mittagszeit in der Mensa langweilig geworden. Ich werde die Pferde- und Hexengeschichten vermissen.

Mein Dank gilt natürlich auch Jens und Martina. Jens dir danke ich für die technische Unterstützung in Labor, so wie bei der Bekämpfung meiner cholerischen Anfälle. Martina, dir danke ich für die Unterstützung beim Bestellen und deine meditative Art, mit der du mich öfters von 180 °C zurück auf Raumtemperatur gebracht hast.

Many thanks to Sakshi and Eleanor for good times in the lab and funny heart attack moments for you and me. Our trip to the Harry Potter exhibition was fantastic as well as the restaurant visits. Both I will never forget. In this sense the Hogwarts express is waiting for us.

Ein weiterer Dank geht an meine Pflanzenmädels, Kalpana und Katharina. Ich möchte euch für viele lustige Momente bei der Arbeit danken. Niemand sagt so schon “Och Michael” wie ihr beide. Danke für viele nette Momente und damit einhergehendes Erschrecken ;-)

Sandra und Kerstin, danke ich für viele gute Diskussionen rund um das Typ 1 Sekretionssystems. Mit eurer Hilfe habe ich des öfteren einen Ganz neuen Blickwinkel auf das Projekt gewonnen. Ohne euren Input wäre ich des öfteren auf der Stelle getreten.

Susanne danke ich für viel wissenschaftliche Hilfe und schöne Diskussionen über die Targaryen, Baratheon und Stark. Der Eiserne Thron gehört dir, ergreife ihn!

Meinen beiden DNA Feen, Diana und Iris, danke ich für die wunderbare Unterstützung beim Klonieren. Ohne euch wäre so manches Konstrukt nicht rechtzeitig fertig geworden. Des weiteren danke ich euch für viele tolle Diskussionen rund um Superhelden und Kindheitserinnerungen. Für mich seit ihr DNA-Woman und Cloning-Girl. Ich wünsche euch viel Glück und Erfolg beruflich und Privat und wünsche dir Diana gute Nerven mit deinen kleinen Würmchen.

Christian und Romy danke ich, für die tolle Unterstützung und dem wissenschaftlichen Input bei meinen Projekt. Ohne dich Christian hätte ich so manches Plasmid noch einmal klonieren müssen.

Ein großes Dankeschön geht auch an Astrid, Steffi und Franziska von der Crystal farm and X-ray Facility. Auch wenn es leider mit den HlyD Kristallen nicht geklappt hat, habt ihr mehr doch sehr geholfen und mir wirklich viel über das Kristallisieren beigebracht. Dafür vielen Dank!

Mein weiterer Dank geht an Frau Rasid für ihre unterstützende Hilfe im Labor. Ohne ihre Unterstützung würden wir ganz schön Probleme haben.

Vielen Dank auch an Frau Blum und an Frau Simons für die administrative Betreuung während meiner Promotion.

Des weiteren danke ich meinen ehemaligen Kollegen Jan und Philipp, sowie Ricarda, André und Sabrina. Das Arbeiten mit euch hat viel Spaß gemacht und war immer wieder

für eine Überraschung gut.

Cordula Kruse danke ich für die tolle Betreuung im Rahmen des BioStruct-Stipendiums und motivierenden Gespräche, auch wenn ich sie manchmal mit meinen Witzen zur Weißglut getrieben habe.

Ich möchte mich auch bei meinen Bachelorstudentinnen Daniela, Andrea und Larissa bedanken. Es hat Spaß gemacht euch zu betreuen und ich hab dabei wahrscheinlich genau so viel gelernt, wie ihr von mir.

Mein Dank gilt der Internationalen NRW Forschungsschule BioStruct vom Ministerium für Innovation, Wissenschaft und Forschung des Landes Nordrhein-Westfalen, der Heinrich-Heine-Universität Düsseldorf und der Entrepreneur-Stiftung der Heinrich-Heine-Universität Düsseldorf für die finanzielle Unterstützung und Ausbildung im Rahmen meines Stipendiums.

Ins fernen Campen in Ostfriesland sende ich meinen Dank an meine zweite Familie, die ich durch meine Frau hinzugewonnen habe. Insbesondere gilt hier mein Dank Bernhard und Gudrun für die tollen Ratschläge und die moralische Unterstützung. Eure Motivation hat auch zum gelingen dieser Arbeit beigetragen. Nicht minder danke ich Familie Arends, Merker und Lomscher junior für die tolle Unterstützung.

Ein herzliches Dankeschön geht auch an meine besten Freunde Daniel, Lisa und Philipp für die tolle moralische Unterstützung während der gesamten Promotion. Ohne eure Freundschaft, Rückhalt und natürlich den tollen Aktionen an den Wochenenden, hätte ich diese Herausforderung nicht durchgehalten.

Zu guter Letzt danke ich allen Leuten, die hier zwar nicht namentlich erwähnt wurden, aber trotzdem zum Gelingen dieser Arbeit beigetragen haben!

B. Curriculum vitae

Personal data

Date of birth	07^{th} August 1987, Düsseldorf
Adress	Volmerswerther Straße 276, 40221 Düsseldorf
Mobile	+49 (0) 171 / 7873010
Phone	+49 (0) 211 / 31111881
e-Mail	Michael.Lenders@uni-duesseldorf.de
Family status	married, no children

Doctorate

since 03.2012	at the Heinrich-Heine-University Düsseldorf
12.2015	Doctor rerum naturalium (Dr.rer.nat.)
PhD thesis	*Mechanisms for hemolysin A type I secretion in E. coli*
First examiner	Univ. Prof. Dr. Lutz Schmitt, Institute for Biochemistry, Heinrich-Heine-University Düsseldorf
Second examiner	Prof. Dr. Karl-Erich Jaeger, Institute for Molecular Enzyme Technology, Heinrich-Heine-University Düsseldorf

Studies

Master of Science "Biochemistry"

10.2010 - 02.2012	at the Heinrich-Heine-University Düsseldorf, *Overall grade: 1,5*
21.02.2012	Master of Science (M.Sc.)
Master thesis	*Characterization of self-inserting membrane proteins by atomic force microscopy*

First examiner	Prof. Dr. Daniel Müller, Department of Biosystems Science and Engineering, Swiss Federal Institute of Technology Zurich
Second examiner	Univ. Prof. Dr. Lutz Schmitt, Institute for Biochemistry, Heinrich-Heine-University Düsseldorf

Bachelor of Science "Biochemistry"

10.2007 - 09.2010	at the Heinrich-Heine-University Düsseldorf, *Overall grade: 1,6*
22.06.2010	Bachelor of Science (B.Sc.)
Bachelor thesis	*Analysis of a type I secretion system*
First examiner	Univ. Prof. Dr. Lutz Schmitt, Institute for Biochemistry, Heinrich-Heine-University Düsseldorf
Second examiner	PD Dr. Ulrich Schulte, Institute for Biochemistry, Heinrich-Heine-University Düsseldorf

Scholarships

03.2012 - 09.2013	PhD bursary of the international NRW Research School BioStruct, granted by the Ministry of Innovation, Science and Research of the State North Rhine-Westphalia, the Heinrich-Heine-University Düsseldorf, and the Entrepreneur Foundation at the Heinrich-Heine-University of Düsseldorf
09.2011 - 02.2012	Full study grant of the Wolters-Vollhardt-Foundation for students of life sciences

Publications

1	**Lenders, M. H. H.**, Weidtkamp-Peters, S., Kleinschrodt, D., Jaeger, K.-E., Smits, S. H. J., and Schmitt, L. (2015). Directionality of substrate translocation of the hemolysin a type i secretion system. Sci. Rep. 5.
2	Höppner, A., Widderich, N., **Lenders, M.**, Bremer, E. and Smits, S. H. J. (2014). Crystal structure of the ectoine hydroxylase, a snapshot of the active site. J Biol Chem 289, 29570-83.

3	**Lenders, M. H. H.**, Reimann, S., Smits, S. H. J. and Schmitt, L. (2013). Molecular insights into type I secretion systems. Biol Chem 394, 1371-84.
4	Schwarz, C. K. W., Landsberg, C. D., **Lenders, M. H. H.**, Smits, S. H. J. and Schmitt, L. (2012). Using an E. coli Type 1 secretion system to secrete the mammalian, intracellular protein IFABP in its active form. J Biotechnol 159, 155-61.
5	Schwarz, C. K. W., **Lenders, M. H. H.**, Smits, S. H. J. and Schmitt, L. (2012). Secretion of slow-folding proteins by a Type 1 secretion sys- tem. Bioengineered 3, 289-92.

Participation at scientific conferences

10.2014	Association for General and Applied Microbiology (VAAM) 2014 Poster Presentation: Michael H H Lenders, Stefanie Weidtkamp-Peters, Sander H J Smits and Lutz Schmitt. "What goes out first": Substrate orientation during type I secretion in*Escherichia coli*. (Düsseldorf/Germany)
10.2013	Molecular Life Sciences 2013: International Symposium of the German Society for Biochemistry and Molecular Biology (GBM), Frankfurt am Main, Germany Poster Presentation: Michael H H Lenders, Sander H J Smits and Lutz Schmitt. Approach in characterization of the membrane fusion protein HlyD. (Düsseldorf/Germany)

School education

2004 - 2007	**Abitur**: Städtisches Comenius-Gymnasium in Düsseldorf, *Overall grade: 1,4*
1998 - 2004	**Ordinary level**: Städtische Realschule in Osterath

C. Erklärung

Hiermit erkläre ich, dass ich die heute eingereichte Doktorarbeit selbständig verfasst und keine anderen als die angegebenen Quellen und Hilfsmittel benutzt sowie Zitate kenntlich gemacht habe. Bei der vorliegenden Doktorarbeit handelt es sich um in Wort und Bild völlig übereinstimmende Exemplare.

Weiterhin erkläre ich, dass digitale Abbildungen nur die originalen Daten enthalten und in keinem Fall inhaltsverändernde Bildbearbeitung vorgenommen wurde.

Ort, Datum	Michael Lenders